

**Leaf Senescence in *Arabidopsis thaliana* and
Brassica napus: From Molecular Regulation to
Nutrient Remobilization Processes**

Dissertation

der Mathematisch-Naturwissenschaftlichen Fakultät

der Eberhard Karls Universität Tübingen

zur Erlangung des Grades eines

Doktors der Naturwissenschaften

(Dr. rer. nat.)

vorgelegt von

Lena Maria Riester

aus Tübingen

Tübingen

2019

Gedruckt mit Genehmigung der Mathematisch-Naturwissenschaftlichen Fakultät der Eberhard Karls Universität Tübingen.

Tag der mündlichen Qualifikation:	18.11.2019
Dekan:	Prof. Dr. Wolfgang Rosenstiel
1. Berichterstatter:	Prof. Dr. Ulrike Zentgraf
2. Berichterstatter:	Prof. Dr. Klaus Harter

Für Julius, Gero und meine Eltern

*In der Wissenschaft gleichen wir alle nur den Kindern, die am Rande des Wissens
hie und da einen Kiesel aufheben, während sich der weite Ozean des Unbekannten
vor unseren Augen erstreckt.*

Sir Isaac Newton

Table of Contents

Eidesstattliche Versicherung	xi
List of Major Abbreviations	xii
Summary	xv
Zusammenfassung	xvii
List of Publications.....	xix
Personal Contributions	xx
1 Introduction.....	1
1.1 What Is Senescence?.....	1
1.2 Leaf Senescence.....	3
1.2.1 Changes in Cell Structure	3
1.2.2 Changes in Biochemistry of the Cell	5
1.3 Hydrogen Peroxide as Signaling Molecule in Leaf Senescence.....	6
1.4 Molecular Regulation of Leaf Senescence	8
1.4.1 Transcriptional Regulation of Leaf Senescence.....	9
1.5 Nutrient Recycling as Biological “Purpose” of Senescence: Remobilization and Storage of Nitrogen in Seed Storage Proteins in <i>Brassica napus</i> L.	13
2 Objectives.....	15
3 Results and Discussion	16
3.1 Overview	16
3.2 Part A: Transcription Factors in Arabidopsis Leaf Senescence	18
3.2.1 Ethylene Response Factor 4 (ERF4) in Senescence Regulation.....	18
3.2.2 Regulation of <i>WRKY53</i> Expression	24
3.3 Part B: Senescence-Related Seed Storage Protein Expression in Rapeseed Leaves	31
4 Conclusions.....	34

5	Future Perspectives.....	42
6	References	47
7	Danksagung	61
8	Appendix	62

Eidesstattliche Versicherung

Ich versichere hiermit, dass ich

- die vorliegende Arbeit selbstständig verfasst habe,
- keine anderen als die angegebenen Quellen benutzt und alle wörtlich oder sinngemäß aus anderen Werken übernommenen Aussagen als solche gekennzeichnet habe,
- und dass die eingereichte Arbeit weder vollständig noch in wesentlichen Teilen Gegenstand eines anderen Prüfungsverfahrens gewesen ist.


Statement of Authorship

I hereby certify that

- I have composed this thesis by myself,
- all references and verbatim extracts have been quoted, and all sources of information have been specifically acknowledged
- this thesis has not been accepted in any previous application for a degree, neither in total nor in substantial parts.

Tübingen, 2. November 2019

Ort, Datum/ Place, Date



Unterschrift/ Signature

List of Major Abbreviations

$^1\text{O}_2$	singlet oxygen
ABA	abscisic acid
APA	alternative polyadenylation
AS	alternative splicing
ATAF	<i>Arabidopsis</i> transcription activation factor
NH_3	ammonia
AP2/ERF	APETALA2/ETHYLENE RESPONSE FACTOR
<i>A. thaliana</i>	<i>Arabidopsis thaliana</i>
APX1	ASCORBATE PEROXIDASE 1
ASC	ascorbic acid
ACA	automated colorimetric assay
ATG	autophagy-related
avr	avirulence
BiFC	bimolecular fluorescence complementation
<i>B. napus</i>	<i>Brassica napus</i>
CAT	CATALASE
CAB	chlorophyll a/b binding protein
Chip-seq	Chromatin immunoprecipitation sequencing
CK	cytokinins
Co-IP	co-immunoprecipitation
<i>Col-0</i>	<i>Columbia 0</i>
CBF2	C-REPEAT/ DEHYDRATION RESPONSIBLE ELEMENT BINDING FACTOR 2
CUC	cup-shaped cotyledone
DAS	days after sowing
DNA	desoxyribonucleic acid
DAB	diaminobenzidine
H_2DCFDA	di-hydro-di-carboxy-hydro-fluorescein-di-acetate
EAR motif	ERF-associated amphiphilic repression motif
ELF3	EARLY FLOWERING 3

<i>E. coli</i>	<i>Escherichia coli</i>
ERF	ethylene response factor
EC	evening complex
FRET-FLIM	förster resonance energy transfer-fluorescence lifetime imaging microscopy
FAA	free amino acids
GBF1	G-box binding factor 1
GA	giberellic acid
GSH	glutathione
GSSG	glutathione disulphide
GR	glutathione reductase
GFP	green fluorescent protein
ha	hectare
H ₂ O ₂	hydrogen peroxide
OH-	hydroxyl radical
JA	jasmonic acid
JUB1	jungbrunnen 1
kg	kilogram
NL	low nitrogen
MA	microarray
MAP kinase	mitogen activated protein kinase
NAC	NAM/ ATAF and CUC
NAM	no apical meristem
nm	nanometer
NADH	nicotinamide adenine dinucleotide
NADPH	nicotinamide adenine dinucleotide phosphate
NO ₃ ⁻	nitrate
NH ₄ ⁺	nitrite
N	nitrogen
OSR	oilseed rape
NO	optimal nitrogen
ORE1	oresara 1
<i>O. sativa</i>	<i>Oriza sativa</i>

POX	Peroxidase
PRXRs	Peroxiredoxins
PS	Photosystem
PCD	programmed cell death
REV	REVOLUTA
ROS	reactive oxygen species
roGFP	reduction-oxidation sensitive green fluorescent protein
RAV1	RELATED TP ABI3/ VP1
RNA	ribonucleic acid
Rubisco	ribulose-1,5-bisphosphate carboxylase/ oxygenase
RNA-seq	RNA sequencing
SA	salicylic acid
SSP	seed storage protein
SAG	senescence associated gene
SDG	senescence down-regulated gene
SIRK	senescence-induced receptor like kinase
SPAD	Soil-plant analysis development
S	Sulfur
O ₂ ⁻	Superoxide
SOD	superoxide dismutase
TF	transcription factors
VPE	vacuolar processing enzyme
VSP	vegetative storage protein
Y1H	Yeast-one-hybrid
Y2H	Yeast-two-hybrid

Summary

Leaf senescence is the final stage of leaf development and guarantees successful survival of a plant and its progeny. It follows a coordinated, genetically encoded program, which involves the differential expression of thousands of genes as basis of an ordered execution of events. The aim of senescence is the degradation of macromolecules so that released nutrients can be reallocated to storage organs or developing parts of the plant. Transcription factors (TFs) are generally accepted as crucial elements in senescence regulation and coordination. Ethylene response factors (ERFs) as well as WRKY TFs are superfamilies of TFs that are overrepresented in the senescence transcriptome. Furthermore, the role of hydrogen peroxide (H_2O_2) as signaling molecule in senescence has often been demonstrated and it induces the expression of many senescence associated genes (SAGs), amongst them *WRKY53*, which is a central player in senescence regulation.

We identified a small sub-network between *WRKY18*, *WRKY25* and *WRKY53*, in which *WRKY25* is a positive and *WRKY18* is a negative regulator of *WRKY53* expression. All three WRKY factors are influencing senescence and moreover, H_2O_2 treatment enhanced expression of all three factors. In DPI-ELISAs we showed that binding of *WRKY25* to the *WRKY53* promoter is redox-sensitive. However, even though *WRKY25* is a positive regulator of *WRKY53*, it is a negative regulator of leaf senescence, pointing to a more complex regulatory network with more and still unknown factors. Furthermore, the mitogen-activated kinase kinase kinase 1 (MEKK1) was found to bind to the promoter of *WRKY53* and influence its expression most likely via phosphorylation of WRKY proteins. By reporter gene assays I confirmed that MEKK1 increased the effect of *WRKY53* protein on the promoter activity of its own gene and I could show that MEKK1 also enhanced the positive effect of *WRKY25* protein on *WRKY53* driven gene expression. Moreover, MEKK1 turned the negative effect of *WRKY18* on *WRKY53* expression into a positive one. Taken together, this indicates that MEKK1 does not specifically interact with *WRKY53* but also with other WRKY proteins. It is noteworthy, that it exhibited a positive effect on the expression of all three WRKYs. By characterizing an inducible knockdown line for *MEKK1*, a clear role of MEKK1 in senescence regulation was observed.

ERF4 exists in two different isoforms due to alternative polyadenylation: ERF4-R, which contains an ERF-associated amphiphilic repression (EAR) motif and ERF4-A, which lacks this motif. By a reverse genetics approach, in which I analyzed the phenotype, I could show that *ERF4* isoforms are both involved in leaf senescence regulation. By subsequent molecular and biochemical assays, I gained an understanding of the mode of action of ERF4 isoforms and how they possibly affect leaf senescence. Both isoforms bind to the promoter of the *CATALASE3* (*CAT3*) gene and have antagonistic effects on *CAT3* gene expression. The ratio of ERF4-A to ERF4-R changed over time. Together with visualization of CAT3 activity on native gels, this hints at a function of the ERF4 isoforms as an activator of *CAT3* in earlier and as a repressor of *CAT3* expression in later stages. This could foster an increase of H₂O₂ in later stages, which induces expression of many SAGs and contributes to degradation processes.

Lastly, by analysis of transcriptome data, seed storage proteins (SSPs) were found to be expressed in vegetative tissues of *Brassica napus* L. (cv. Mozart). I confirmed *NAPIN* and *CRUCIFERIN* expression in leaves via quantitative real-time PCR and found a correlation between intracellular H₂O₂ and SSP accumulation. Moreover, their expression depended on the nitrogen (N)-supply. In addition, N-starvation induced senescence differed from developmental senescence, since H₂O₂ levels were not increased but reduced in these plants.

This work reveals new insights in senescence regulation. It contributes to the general endeavor, to gain an understanding of the complex molecular network underlying leaf senescence regulation.

Zusammenfassung

Das finale Stadium in der Blattentwicklung ist die Blattseneszenz. Sie basiert auf einer genetisch festgelegten Abfolge von Prozessen, die die Grundlage zu einem erfolgreichen Überleben der Pflanze und deren Nachkommen bilden. Tausende von Genen werden differenziell exprimiert, was die Voraussetzung zum Abbau von Makromolekülen schafft. Die so freigesetzten Nährstoffe werden zu Speichergeweben oder zu Pflanzenorganen transportiert, die sich noch in der Entwicklung befinden. Transkriptionsfaktoren (TFs) spielen in der Regulation und Koordination der Seneszenz eine zentrale Rolle. Ethylen-Response-Faktoren (ERFs) und WRKYs sind zwei Familien von TFs, die im Seneszenztranskriptom überrepräsentiert sind. Außerdem hat Wasserstoffperoxid (H_2O_2) in der Seneszenzregulation eine wichtige Funktion als Signalmolekül, und es wurde schon mehrfach demonstriert, dass H_2O_2 die Expression vieler Seneszenz-assoziiierter Gene (SAGs) induziert, unter anderem auch die von *WRKY53*, einem zentralen Faktor in der Seneszenz Regulation.

Wir beschrieben ein Sub-Netzwerk, bestehend aus *WRKY18*, *WRKY53* und *WRKY25*, in welchem *WRKY25* als positiver und *WRKY18* als negativer Regulator der *WRKY53* Expression agiert. Wir konnten zeigen, dass die Bindung von *WRKY25* an den *WRKY53* Promotor redox-sensitiv ist. H_2O_2 hingegen, induzierte die Expression aller drei Faktoren. Außerdem wurde die mitogen-aktivierte Kinase Kinase Kinase 1 (MEKK1) als Protein identifiziert, das an den Promotor von *WRKY53* bindet und dessen Expression beeinflusst, vermutlich mittels Phosphorylierung von WRKY Proteinen. Ich konnte bestätigen, dass MEKK1 den Effekt steigerte, den *WRKY53* Proteine auf die Promotoraktivität ihres eigenen Genes ausübten und des Weiteren konnte ich zeigen, dass MEKK1 auch den positiven Effekt steigerte, den *WRKY25* Proteine auf die *WRKY53* Genexpression hatten. Zudem verkehrte MEKK1 den negativen Effekt von *WRKY18* auf die *WRKY53* Genexpression in einen Positiven. Das deutet darauf hin, dass MEKK1 nicht spezifisch mit *WRKY53* interagiert, sondern auch mit anderen WRKY Proteinen, und dass es immer einen positiven Effekt auf ihre Expression hat. Alle drei Faktoren beeinflussen Seneszenz, jedoch, obschon *WRKY25* ein positiver Regulator von *WRKY53* ist, ist es ein negativer Regulator der Blattseneszenz, was auf ein komplexeres Netzwerk hindeutet. Durch die

Charakterisierung einer induzierbaren *MEKK1* knockdown Linie, konnte ich eine eindeutige Rolle von MEKK1 in der Seneszenzregulation beobachten.

ERF4 existiert in zwei verschiedenen Isoformen, die aufgrund von alternativer Polyadenylierung entstehen. ERF4-R enthält ein ERF-assoziiertes repressions (EAR) Motiv, bei ERF4-A fehlt dieses Motiv. Einem Ansatz der reversen Genetik folgend, analysierte ich den Phänotyp von *erf4* Mutanten und ERF4 Überexpressionslinien und konnte zeigen, dass beide Isoformen an der Regulation der Seneszenz beteiligt sind. In darauffolgenden molekularen und biochemischen Experimenten näherte ich mich einem Verständnis der Bedeutung und Funktion von ERF4 Isoformen und ihrem Einfluss auf Blattseneszenz. Ich bestätigte die Bindung beider Isoformen an den *CATALASE3* (*CAT3*) Promotor und zeigte, dass beide Isoformen antagonistische Effekte auf die Genexpression unter diesem Promotor haben. Das Verhältnis von ERF4-A zu ERF4-R veränderte sich im Laufe der Seneszenz. Dies und die Visualisierung von CAT3 Enzymaktivität auf nativen Gelen führte zu der Schlussfolgerung, dass ERF4 in frühen Seneszenz Stadien als Aktivator und in späten Stadien als Repressor der *CAT3* fungiert. Das fördert den Anstieg von H₂O₂ in späten Stadien, was die Expression von SAGs induziert und bei Abbauprozessen eine wesentliche Rolle spielt.

Durch die Analyse von Transkriptom-Daten sind wir auf die Expression von Samen-Speicherproteinen (SSPs) in vegetativem Pflanzengewebe in *Brassica napus* L. (cv. Mozart) gestoßen. Ich habe die Expression von CRUCIFERIN und NAPIN mittels quantitativer Echtzeit PCR in Blättern nachgewiesen und eine Korrelation zwischen der Menge an intrazellulärem H₂O₂ und der Akkumulation von SSP gezeigt. Außerdem konnten wir nachweisen, dass die Expression von SSPs von der Versorgung der Pflanze mit Stickstoff (N) abhängt. Überdies zeigten wir, dass das durch N-Entzug ausgelöste Seneszenz Programm von der entwicklungsabhängigen Seneszenz zumindest teilweise divergiert, da diese Pflanzen eine reduzierte intrazelluläre Akkumulation von H₂O₂ aufwiesen.

Die vorliegende Arbeit eröffnet neue Einblicke in die Regulation der Blattseneszenz und trägt so dazu bei, einem Verständnis der Zusammenhänge im komplexen molekularen Netzwerk der Seneszenzregulation näher zu kommen.

List of Publications

This thesis is based on the following research articles, referred to by Roman numbers in the text:

Published research articles

- I. Impact of Alternatively Polyadenylated Isoforms of ETHYLENE RESPONSE FACTOR 4 with Activator and Repressor Function on Senescence in *Arabidopsis thaliana* L.**

L. Riester, S. Köster-Hofmann, J. Doll, K.W. Berendzen and U. Zentgraf
Genes; January 2019

- II. Nitrogen Supply Drives Senescence-Related Seed Storage Protein Expression in Rapeseed Leaves**

S. Bieker, L. Riester, J. Doll, J. Franzaring, A. Fangmeier and U. Zentgraf
Genes; January 2019

Unpublished research article

- III. WRKY25: A negative Senescence-Regulator with a Redox-state dependent Regulation of *WRKY53*.**

J. Doll*, M. Muth*, L. Riester, K. W. Berendzen, J. Bresson, U. Zentgraf
Unpublished, *shared first author

Published review article

- IV. A guideline for leaf senescence analyses: from quantification to physiological and molecular investigations**

J. Bresson*, S. Bieker*, L. Riester*, J. Doll* and U. Zentgraf
Journal of Experimental Botany; February 2018, *shared first author

Published Spotlight

- V. Live and Let Die: The core circadian oscillator coordinates life history of plants and pilots leaf senescence**

U. Zentgraf, J. Doll, L. Riester
Molecular Plant; March 2018

Personal Contributions

Published research articles

Impact of Alternatively Polyadenylated Isoforms of ETHYLENE RESPONSE FACTOR 4 with Activator and Repressor Function on Senescence in *Arabidopsis thaliana* L. (Riester et al., 2019)

This article describes the involvement of Ethylene Response Factor 4 (ERF4) isoforms in the regulation of *CATALASE3* (CAT3) and their effect on leaf senescence in *Arabidopsis*.

I was involved in the initial planning, performed the experiments, analyzed the data, did the statistical analysis and prepared all figures except for supplemental figure S5 A and B (the Western blot and the zymogram) I supervised and assisted repetitions of the experiments and I wrote the first draft of the manuscript and took part in revision processes.

Nitrogen Supply Drives Senescence-Related Seed Storage Protein Expression in Rapeseed Leaves (Bieker et al., 2019)

In this research article, we investigated the expression of seed storage proteins (SSPs) in vegetative tissues during senescence of *B. napus*.

I grew and sampled plants and performed gene expression analysis of *CRUCIFERINS* and *NAPINS* and H₂O₂ measurements shown in Fig. 2 A, B and C.

Unpublished research article

WRKY25: A negative Senescence-Regulator with a Redox-state dependent Regulation of *WRKY53* (Doll et al., unpublished)

This article describes WRKY25 as redox-sensitive upstream regulator of *WRKY53* expression and its impact on leaf senescence in *Arabidopsis*.

For this article, I contributed the reporter gene assays shown in Fig. 3C and S4A. Furthermore, I did the phenotyping experiments of the amiRNA_{MEKK1} line, which

included growing and sampling plants, as well as taking pictures, shown in Fig. S4B and performing Fv/Fm measurements, shown in Fig. S4D. Furthermore, I tested β -estradiol induction via GFP fluorescence (Fig. S4C). I conducted the following data analysis and contributed to the figure preparation.

Published review article

A guideline for leaf senescence analyses: from quantification to physiological and molecular investigations (Bresson et al., 2018)

In this article, we provided a guideline for leaf senescence analysis, including the respective protocols and example data.

I was involved in growing and sampling of the plants and I performed the following experiments: H₂O₂ measurement (Fig. 5B), DAB-staining (Fig. 5C), qRT-PCR of key senescence marker genes (Fig. 6 A-J) and electrolyte leakage (Fig. 7A), including data analysis. I took part in the initial planning and the writing of the manuscript. I reviewed the manuscript during preparation and wrote the supplemental protocols S1 and S7.

Published Spotlight

Live and Let Die: The core circadian oscillator coordinates life history of plants and pilots leaf senescence (Zentgraf et al., 2018)

This article describes how circadian regulatory circuits are involved in senescence regulation.

I was involved in preparation of the overview-figure and reviewing of the manuscript.

1 Introduction

1.1 What Is Senescence?

Linguistically, senescence has its origin in the Latin word *senescere*, which means “to grow old”. With the passage of time, all organisms age and finally enter the stage of senescence, followed by death. This topic has always been of interest for us humans, since it enters the realm of our experience early in childhood. We see people and animals grow old, and we wait for our food crops to have filled grains in order to supply us with food. Therefore, how and when living beings senesce and die are central questions in the field of biology, and many aspects are still unanswered. This thesis contributes to enlighten senescence processes in plants.

First, I would like to introduce the two concepts “senescence” and “programmed cell death” (PCD). Depending on author or scientific field, both terms will be interpreted differently. In general, the term PCD summarizes different forms of genetically encoded, intracellular programs, which lead to the elimination of damaged, no longer needed or harmful cells. Senescence is often used to describe deteriorative processes, in which organs or whole organisms age and die. However, Thomas et al. (2003) argued for example, that leaf senescence in plants has a set of defining characteristics, which clearly distinguishes it from PCD, such as reversibility. Since - at least during early senescence stages - yellow leaves has been shown to regreen again, senescence does not necessarily lead to cell death. But there is also a line of argumentation, which says that PCD as well is reversible (Lockshin and Zakeri, 2004). Van Doorn and Woltering (2004) gave an overview of all the different arguments, which either see senescence and PCD to be the same, or to be different processes or to occur in sequential order. To date, there is no general agreement upon these definitions. Boundaries and overlaps between senescence, PCD, aging, dying, necrosis, hypersensitive response (HR) and similar processes exist, and thus it is difficult to distinguish exactly between them. Throughout this thesis I will use the term senescence, sticking to the definition of Lim and coworkers, who define senescence in

Introduction

plants as the genetically programmed degradation process of cells, tissues, organs or whole organisms, which eventually leads to death (Lim et al., 2007).

Second, I would like to shortly describe the relevance of senescence for plants. Senescence in plants is not a chaotic breakdown but an ordered, highly regulated and sequential process, in which cellular components are broken down and the released nutrients are translocated to and re-used in developing parts of the plant (Gan and Amasino, 1997; Lim et al., 2007). In order to have an optimal nutrient use efficiency, the timing is crucial. The decisions when and how to die are essential for plant fitness. Senescence has evolved as a flexible and dynamic process, which underlies a tight regulation by a complex genetic program. Under optimal conditions, the onset of senescence occurs in an age-dependent manner. However, unable to escape the habitat in which they grow, plants must be able to deal with adverse conditions. Under stress for instance, senescence is induced prematurely as an exit strategy in favor of the offspring. To ensure an optimal timing of onset and progression of senescence, the permanent integration of endogenous and exogenous signals is crucial (Buchanan-Wollaston et al., 2003; Lim et al., 2007; Thomas and Stoddart, 1980). This requires efficient signal transduction, which comprises many factors, such as plant hormones, nitrogen (N) and sugar compounds, calcium, reactive oxygen species (ROS) and most likely further substances. The plasticity of senescence is an evolutionary advantage for plants, since it ensures the plant's survival and that of its progeny. Moreover, it is also a big issue in agriculture. Premature senescence leads to crop losses, decreases grain filling and biomass yield. So far, many molecular mechanisms of plant senescence are still unknown, probably partly due to their high complexity. One part of this thesis (research article I and III) focuses on molecular mechanisms in senescing *Arabidopsis thaliana*. *Arabidopsis* is not considered a crop species, on the contrary, it is seen as a weed. However, studying senescence in *Arabidopsis* provides valuable insights and hopefully a deeper understanding of fundamental aspects of senescence regulation. These findings can be utilized and transferred to important crop plants to improve agronomic traits like seed yield, increased biomass or post-harvest quality. The other part of this thesis (research article II) focuses on N-remobilization in the agriculturally important plant species *Brassica napus* L. (cv. Mozart).

1.2 Leaf Senescence

Plants are autotroph organisms and the leaves are the primary site for harvesting the energy of the sunlight, which is then converted into chemical energy. This is the process, which enables them to fix carbon. In the course of senescence, leaves lose their photosynthetic capacity. Nevertheless, the leaf still functions as source, since the nutrients and metabolites are then translocated to other parts of the plant (Guiboileau et al., 2010). Therefore, senescence is an important phase, because it is not mere deterioration; instead it is often described as a recycling program (Lim et al., 2007). To avoid a highly uneconomic loss of nutrients – mostly N, but also minerals and stored energy – plants recycle these resources through nutrient redistribution from the dying leaves (source) to developing organs (sink), for example siliques, seeds, storage tissues, flowers or newly expanding leaves. In order to support developing parts of the plant or the progeny in the best possible way, cell death is actively delayed until the nutrients have been remobilized (Buchanan-Wollaston et al., 2003). The death of older leaves during vegetative growth is termed sequential leaf senescence and occurs before anthesis. During this phase, nutrients from older leaves are repartitioned to developing non-reproductive organs. Monocarpic plants flower only once, set seed and then die. Reproduction triggers senescence in these plants and therefore monocarpic leaf senescence, which occurs after anthesis, leads to nutrient reallocation to the now developing reproductive organs. This process is critical for yield quality and quantity.

1.2.1 Changes in Cell Structure

Senescence leads to massive physiological changes in leaf cells, which include the transition from catabolism to anabolism (reviewed in Lim et al. 2007). This transition from carbon assimilation to nutrient remobilization is associated with disintegration of cellular components like chloroplasts and a massive but selective degradation of macromolecules such as proteins, membrane lipids and RNA. The disintegration of cellular structures happens in a highly coordinated and sequential manner:

The first and most significant step is the breakdown of chloroplasts, which are the plant's characteristic organelles and main energy suppliers. During vegetative growth, they are the site for crucial biochemical processes, such as photosynthesis, the

Introduction

assimilation of nutrients and the biosynthesis of many metabolites, such as amino acids, purine and pyrimidine bases, fatty acids, pigments and hormones (Jarvis and López-Juez, 2013). Most of plant N and other nutrients can be found in expanding and mature leaves (Makino et al., 1997; Schulze et al., 2006). During senescence, chloroplasts undergo destruction and finally collapse. This involves dramatic changes in the thylakoids (summarized in Lundquist et al. 2012) and finally the membrane system disappears because of the degradation of membrane constituents such as lipids, proteins and chlorophyll (Hörtensteiner and Kräutler, 2011). As the constituents of the chloroplasts are dismantled, they gradually shrink and are transformed into what is called “gerontoplasts” (Parthier, 1988), which have the potential to be converted into chloroplasts again. The first visible sign of senescence is the leaf yellowing, which is due to chloroplast dismantling and chlorophyll catabolism (Gan and Amasino, 1997; Thomas and Stoddart, 1980). The characteristic leaf yellowing is often used as a phenotypic marker to determine the status and progression of senescence and there are several recent publications about newly developed methods for computational image color analysis (for example review article IV; Czedik-Eysenberg et al. 2018; Veley et al. 2018). A further parameter to describe senescence is the loss of the photosynthetic efficiency (Fv/Fm) of photosystem II since the senescence-induced damage of the photosynthetic apparatus leads to a reduction of Fv/Fm values (Johnson and Maxwell, 2000).

Peroxisomes play a central role in the balance of reactive oxygen species (ROS). They are involved in oxidative metabolic processes that generate ROS and additionally, they contain enzymes for ROS detoxification, such as catalases, superoxide dismutases or ascorbate peroxidases (Palma et al., 2009). During senescence, peroxisomes are converted into glyoxysomes, which contain enzymes for the β -oxidation of fatty acids and which thus enables the transformation of the thylakoids into sugars (del Río et al., 1998).

Nucleus and mitochondria stay undamaged until the last stages of senescence (Smart, 1994; Zentgraf and Hemleben, 2008). Thus, gene expression and energy supply were preserved until very late in the senescence process. This is necessary for the efficient translocation and recycling of nutrients, which is the main purpose of leaf senescence. In the last stage of leaf senescence, visible disintegration of the plasma membranes

and vacuolar membranes appear. This finally causes the break-down of cellular homeostasis, which means the end of the cell's life.

1.2.2 Changes in Biochemistry of the Cell

Already in early senescence, leaves show biochemical changes, which go together with a reduced anabolism. The amounts of polysomes and ribosomes decrease, which consequently leads to a decrease in protein biosynthesis. Total RNA levels are rapidly reduced and the activity of several RNases is increased at the same time (Taylor et al., 1993). All the processes in the senescent cell aim at nutrient salvage. Macromolecules are degraded and the released nutrients are remobilized, which is regulated by a complex interplay of different metabolic pathways (Guiboileau et al., 2010). Proteins are degraded into free amino acids by endo- and exopeptidases and by degrading enzymes, which accumulate in the vacuole, such as cysteine proteases (Martínez et al., 2008; Otegui, 2018; Roberts et al., 2012). Cellular proteostasis is a key determinant of senescence and a dysfunction is often related to premature senescence and disease (Riera et al., 2016). Therefore, protein degradation systems are in place to maintain proteostasis. The ubiquitin proteasome pathway plays an important role in cytosolic protein breakdown during senescence (Buchanan-Wollaston et al., 2003; Guo et al., 2004). Beside the canonical autophagy pathway, which is involved in nutrient recycling in plants (Anne et al., 2012), very recently, a new and autophagy-independent pathway has been described, which involves ATG8-ABS3 interaction at the late endosome. Under nutrient deprivation or when autophagy is blocked, this interaction promotes ABS3 trafficking, which is a putative transport protein, to the vacuole. This could trigger the senescence program in a nutrient-dependent manner (Jia et al., 2019). Chloroplast degeneration leads to a loss of chloroplast proteins, like the very abundant ribulose-1,5-bisphosphate carboxylase/oxygenase (Rubisco) and chlorophyll a/b binding protein (CAB). Lipid-degrading enzymes destabilize membranes and fatty acids are either oxidized to provide energy or converted to α -ketoglutarate, which is either involved in mobilizing amino acids, or it could be metabolized into phloem-mobile sugars (Thompson et al. 1998; for review of senescence processes see Lim et al. 2007, Thomas & Stoddart 1980).

1.3 Hydrogen Peroxide as Signaling Molecule in Leaf Senescence

Reactive oxygen species (ROS) are defined as oxygen-containing molecules with a higher chemical reactivity than O_2 . Therefore, they have a high potential for causing cellular damage. The major ROS-forms in plants are singlet oxygen (1O_2), the superoxide anion (O_2^-), hydrogen peroxide (H_2O_2) and the hydroxyl radical ($HO\cdot$). Amongst the ROS, H_2O_2 is a rather stable molecule, with a moderate *in vivo* half-life of milliseconds to seconds. Thus it can accumulate transiently and form intracellular gradients (Marinho et al., 2014). Like water, it is relatively poor at permeating membranes; however diffusion through membranes is facilitated by aquaporins (Bienert et al., 2007). Moreover, if its production accelerates, it is scavenged by the antioxidative system. These characteristics render it useful as signaling molecule and indeed, it cannot only induce cellular damage by oxidation of proteins, it has been shown to induce changes in gene expression in plants (for review see He et al. 2018). Furthermore, it is involved in the response to different kinds of stresses and it participates in the regulation of leaf senescence. Despite this wide range of action, the signal transduction mechanisms, especially in plants, are poorly understood. However, it is generally agreed upon, that important effects of ROS are not mediated through causing damage, but through their function as signaling molecules.

In recent years, much research was dedicated to find ROS sensing mechanisms and it seems likely that the oxidative properties of ROS are the basis of ROS signaling (Waszczak et al., 2018). H_2O_2 oxidizes specific cysteine residues of target proteins. This modification could initiate thiol-based redox relays and modify target enzymes, receptor kinases and transcription factors (reviewed in He et al. 2018; Smirnov & Arnaud 2019), which could change protein conformation and function.

Because of the high reactivity as well as the function as signaling molecule, a fine-tuned balance between production and scavenging of H_2O_2 is required. Indeed, plants have evolved numerous enzymatic and non-enzymatic scavenging mechanisms to protect macromolecules from oxidative damage. Key enzymes, which buffer the local

Introduction

redox environment, are on the one hand haem peroxidases, such as catalases (CATs) and ascorbate peroxidases (APXs) and on the other hand peroxiredoxins (PRXs), which use thiol-based catalytic mechanisms. Moreover, the ascorbate-glutathione cycle is a major antioxidant system, which consists of several enzymes. This work focuses on catalases, and specifically on the senescence specific regulation of *CAT3* expression by ethylene response factor 4 (ERF4), a transcription factor, that will be introduced in the following section. Catalases are H₂O₂ decomposing enzymes and have been described as peroxisomal “redox guardians” (Mhamdi et al., 2012). Peroxisomes are a major site for H₂O₂ production, and H₂O₂ that results from peroxisomal photorespiration is estimated to account for about 70 % of the total H₂O₂ formed (Noctor et al., 2002). In Arabidopsis, there are three catalase isoforms, all of which display a senescence-associated expression and activity pattern: *CAT2* is down-regulated, whereas *CAT3* is up-regulated during early senescence. *CAT1* is up-regulated during late senescence. A complex regulatory circuit, in which catalases play an important role, leads to the characteristic changes in H₂O₂ levels in the progression of senescence. The onset of leaf senescence coincides with a peak in the intracellular H₂O₂ concentration, which is a result of the fine-tuned regulatory-loop between the H₂O₂ scavenging enzymes *CAT2* and ASCORBATE PEROXIDASE 1 (APX1) (Zimmermann and Zentgraf, 2005; Zimmermann et al., 2006): The increase of H₂O₂ at this moment mainly results from the decrease of *CAT2* activity and expression. Furthermore, ASCORBATE PEROXIDASE 1 (APX1) appears to be down-regulated on the posttranscriptional level in leaf tissue at the same time. This is the phase where plants go through the transition from vegetative to reproductive growth and the H₂O₂ burst was interpreted as an internal signal to induce senescence-associated gene expression (Bieker et al., 2012; Zimmermann et al., 2006). The increased H₂O₂ levels lead to the induction of *CAT3* expression and activity. Consequently, H₂O₂ levels are lowered again and APX1 activity is restored. In this thesis, ERF4 is described as a further player in the network that seems to act as an activator of *CAT3* expression in early and as a repressor in later stages of leaf development.

1.4 Molecular Regulation of Leaf Senescence

On the molecular level, leaf senescence underlies a multi-layered regulation, including key regulatory molecules such as ROS, calcium or peptides, chromatin-modifying factors, receptors and signaling components for hormones and stress responses, transcriptional regulation, post-transcriptional, translational and post-translational regulation, as well as metabolism regulating factors (summarized in Woo et al. 2013; Kim et al. 2016; Kim et al. 2017). Recently, transcriptomic and metabolomic analyses revealed a distinctive chronological order of senescence processes (Breeze et al., 2011; Kim et al., 2016; Watanabe et al., 2013). With the possibilities of high throughput studies and extensive research, our knowledge of the molecular regulation underlying senescence processes has greatly expanded during the past twenty years. The identification and characterization of specific transporters, transcription factors, signaling and hormone pathways, as well as the connection between metabolic processes and cellular pathways have been studied (Breeze et al., 2011; Buchanan-Wollaston et al., 2005; van der Graaff et al., 2006; Zentgraf et al., 2004). Many senescence-associated-genes (SAGs) have been characterized, such as the senescence delaying *ore* mutants and their involvement in ROS metabolism (Woo et al., 2004). Plant hormones and their role in senescence have also been studied (van der Graaff et al., 2006). The plant hormone ethylene is well known as an accelerator of senescence, however, it is not essential for the onset and progression of senescence (Grbic and Bleek, 1995; Jing et al., 2002). Abscisic acid (ABA) and jasmonic acid (JA) are known to enhance senescence, whereas cytokinins (CK) delay it. Auxins interestingly, have been reported to have the potential for both: positive as well as negative regulation of senescence (Khan et al., 2013; Wojciechowska et al., 2018). However, many fundamental questions remain unanswered. This work contributes to elucidate part of the transcriptional regulation by functionally characterizing the transcription factor ERF4, the MAP kinase kinase kinase 1 (MEKK1) and their interplay with selected members of the WRKY transcription factor family in leaf senescence.

1.4.1 Transcriptional Regulation of Leaf Senescence

Many of the genes expressed in developing, green leaves, such as genes related to photosynthesis, are down-regulated in senescence (senescence down-regulated genes, SDGs), whereas other genes, which are involved in the senescence recycling program, are up-regulated in the course of senescence (senescence-associated genes, SAGs) (Breeze et al., 2011). Therefore, transcriptional control mechanisms, which lead to differential gene expression, are generally believed to play a central role in the regulation of leaf senescence. Transcription Factors (TFs) regulate the rate of gene expression by binding to specific DNA sequences (cis-elements), generally located in the 5' upstream regulatory regions of their target genes. They lead to activation and/ or suppression of gene expression. Indeed, TFs have been identified as a sizable fraction of SAGs.

The major families of senescence-regulated TFs belong to the NAC, WRKY, MYB, C2H2 zinc-finger, bZIP and AP2/ERF families (Balazadeh et al., 2008; Breeze et al., 2011; Buchanan-Wollaston et al., 2005; Guo et al., 2004). Many senescence-activated and senescence down-regulated TF genes have been discovered using qRT-PCR or microarray-based expression profiling, as performed in Breeze et al. (2011). The NAC family was found to be the largest group of TFs of the senescence transcriptome. Many members of this family show an overrepresentation already at an early time point, about 19-21 days after sowing (DAS) and more than 30 members displayed an altered expression at various times during senescence. Other families show up-regulated transcription later in the course of senescence. The WRKY TF family is also overrepresented, with many members being up-regulated from around 25 DAS. This is followed by the upregulation of the large APETALA2/ETHYLENE RESPONSE FACTOR (AP2/ERF) family, which becomes overrepresented around 27 DAS (Breeze et al. 2011). The upregulation of WRKYs and ERFs occurred after flowering (around 21 DAS) and before the leaves started to show yellowing (31 DAS).

The NAC TFs are involved in a diverse range of developmental and physiological processes, such as senescence, defense, biotic and abiotic stress (summarized in Olsen et al. 2005). My work focuses on the WRKY and the AP2/ERF families, which are described in more detail in the following paragraphs.

Introduction

The WRKY family expanded in the plant kingdom and is the second largest group of TFs up-regulated in the senescence transcriptome (Breeze et al., 2011; Guo et al., 2004). They form a superfamily of zinc-finger-type TFs with 75 members in *Arabidopsis*, named after the highly conserved WRKYGQK DNA-binding motif, which can be found in their 60 amino acid DNA-binding domain. According to their protein motifs, they can be subdivided into three groups (Rushton et al., 2010). Almost all WRKYs contain one or more W-boxes in their promoters, which are the consensus binding motifs (TTGACC/T) of their target genes. This strongly suggests that they regulate each other in a transcriptional network. Moreover, they can act together and form heterodimers, which changes their DNA-binding properties (Xu et al., 2006).

Previous studies have shown the involvement of WRKYs in diverse physiological processes, including environmental stress responses and developmental processes (Wang et al. 2010; Rushton et al. 2010; Jiang et al. 2014; Chen et al. 2013). Furthermore, they play an important role in pathogen response; it has been shown in *Arabidopsis*, that around 70 % of the WRKY genes were differentially expressed after infection with the bacterial pathogen *Pseudomonas syringae* (Dong et al., 2003). Moreover, several WRKY factors have been associated with senescence and many of them react to ROS, SA and JA, which hints at a cross-talk between senescence and stress-response (Besseau et al., 2012; Potschin et al., 2014; Zentgraf et al., 2010; Zhou et al., 2011, research article III).

WRKY53 is a positive senescence regulator acting in early senescence. At the onset of leaf senescence, the *WRKY53* gene locus is activated by H3K4me2 and H3K4me3 histone methylation (Ay et al., 2009; Bruslan et al., 2012). It is a central hub in the WRKY-senescence-network and it acts upstream of many other WRKY factors (Ay et al., 2009; Miao et al., 2004; Potschin et al., 2014; Xie et al., 2014). Additionally, it exhibits an interesting senescence related expression pattern, with a switch from leaf age to plant age specific expression (Hinderhofer and Zentgraf, 2001), which is likely caused by increasing H₂O₂ levels at this time point (Bieker et al., 2012; Miao et al., 2004). It underlies a tight and complex control with regard to gene expression, activity and protein stability (Zentgraf et al., 2010). At least 12, probably more (so far unknown) proteins can bind to the promoter and affect the expression of *WRKY53*, among them are WRKY53 itself, several other WRKYs and MEKK1 (Miao et al., 2004, 2007;

Introduction

Potschin et al., 2014; Xie et al., 2014). Out of the WRKYs tested, WRKY18 was identified as the strongest negative and WRKY25 as the strongest positive regulator of *WRKY53* expression (Potschin et al. 2014, research article III). In addition, H₂O₂ induces *WRKY53* expression and on top of that, it up-regulates the expression of its upstream regulator MEKK1 (Miao et al., 2007). Besides, the WRKY25 protein contains two zinc-finger DNA binding domains. Zinc-finger domains are in general potentially redox-sensitive (Kretz-Remy and Arrigo, 2002), which makes WRKY25 an excellent candidate for direct redox-regulation. This work contributes to depict the redox-dependent action of WRKY25 on *WRKY53* expression.

Searching for regulatory proteins of *WRKY53* expression, MEKK1 was identified as a bifunctional protein: surprisingly, it directly binds to the *WRKY53* promoter and additionally, it interacts with the *WRKY53* protein and can phosphorylate it *in vitro*, thereby enhancing its DNA-binding activity (Miao et al., 2007).

Beside the WRKYs, many members of the AP2/ERF family are regulated in a senescence-dependent manner (Breeze et al., 2011; Buchanan-Wollaston et al., 2005; Lin and Wu, 2004). Its 147 representatives in Arabidopsis (Nakano et al., 2006; Riechmann et al., 2000) form one superfamily that is involved in a number of stress responses and developmental processes (Licausi et al., 2013). Some AP2/ERFs are involved in the responses to components of stress signal transduction, like for example ROS, ethylene, jasmonic acid (JA), abscisic acid (ABA) and cytokinins (Mizoi et al., 2012; Nakano et al., 2006). All of these signaling molecules are also important in senescence-associated signaling. Moreover, their involvement in leaf senescence has been shown: RELATED TP ABI3/ VP1 (RAV1) has been characterized as positive, and C-REPEAT/ DEHYDRATION RESPONSIBLE ELEMENT BINDING FACTOR 2 (CBF2) as negative regulator. Koyama and coworkers have worked out that ERF4 and ERF8 act together as positive regulators of leaf senescence. They function as repressors of the EPITHIOSPECIFYING SENESCENCE REGULATOR (ESP/ESR), which is a negative regulator of *WRKY53* activity at the transcriptional and posttranslational levels (Koyama et al., 2013; Miao and Zentgraf, 2007). Furthermore, we characterized ERF4 as a regulator of *CAT3*, and thus showed a second pathway of how ERF4 could influence leaf senescence (research article I).

Introduction

One subfamily of the AP2/ERF genes are the ERFs with 122 members in Arabidopsis. Their distinguishing feature is the possession of one AP2/ERF domain (Nakano et al., 2006; Riechmann et al., 2000). On the basis of their genome wide phylogenetic analysis of the ERF gene-family in Arabidopsis and rice, Nakano et al. 2006 suggested a classification of the ERFs into 12 subgroups, according to conserved amino acid motifs. In this classification, *AtERF4* is grouped in the VIIIa ERFs, which have an ERF-associated amphiphilic repression (EAR) motif that makes them act as transcriptional repressors. *AtERF4* is a complex candidate gene, since it can result in more than one protein through alternative splicing (AS). AS plays a crucial role in gene regulation. It enables one single gene to code for multiple proteins by including or excluding certain exons from the final, processed mRNA. Many transcription factors have been reported to be products of alternative splicing events (Barbazuk et al., 2008; Li et al., 2012; Lyons et al., 2013; Mastrangelo et al., 2012; Severing et al., 2012). This opens up a further layer of complexity underlying the ERF-mediated gene regulation, because *ERF4* pre-mRNA can be translated into two different, oppositional protein isoforms: One can act as a transcriptional activator (ERF4-A), because due to alternative polyadenylation (APA), the EAR motif is spliced out. The other variant, ERF4-R, contains the EAR motif and acts as transcriptional repressor (Lyons et al., 2013). To date, the role of AS in leaf senescence has not been studied extensively. This thesis contributes to analyze the role of AS and polyadenylation of ERF4 in senescence.

Functional studies on the molecular mode of action and the crosstalk between senescence-regulated TF genes are limited. Therefore, a global study of the dynamic changes in transcript levels is – without any doubt – important to achieve an understanding of the system in its entirety. However, the in-depth analyses of smaller parts and subnetworks give us important hints about the identity and biological function of master-regulators and their position within molecular networks. I contributed to this task by characterizing single players in the transcriptional network around, ERF4, WRKY53 and MEKK1.

1.5 Nutrient Recycling as Biological “Purpose” of Senescence: Remobilization and Storage of Nitrogen in Seed Storage Proteins in *Brassica napus* L.

One central feature during senescence is the reallocation of nutrients, especially N. The degradation of chloroplastic proteins plays a critical role, since the majority (up to 80 %) of N is localized in the chloroplasts (Makino and Osmond, 1991) and up to 50 % of the total N amount in C3 plants is found in ribulose-1,5-bisphosphat carboxylase/oxygenase (Rubisco) (Evans, 1989). N is an essential nutrient, which the plant needs for growth and development. Land plants need N for seed production, since the N-content of the seed influences the germination efficiency rates and the survival of the plant's progeny (Masclaux-Daubresse et al., 2010).

N is taken up by plants from the soil mainly as inorganic nitrate and ammonium, but in some soils, environments and plant species also in the form of amino acids or other organic N compounds (Bloom, 2015; Tegeder and Rentsch, 2010). Only legumes can fix atmospheric N₂ with the help of symbiotic bacteria in root nodules. After uptake, it is transported in the xylem from roots to shoots, along with assimilates, other nutrients and water. This movement is driven by transpiration at the leaf surface, causing a hydrostatic pressure gradient in the xylem. Therefore, the N compounds are usually transported to photosynthetically active leaves. Further N-partitioning from source to sink occurs in the phloem. During the vegetative phase, developing roots and leaves are the main N sinks. This changes during the reproductive stage, when flowers, fruits and seeds are the dominant N-importing sinks (Masclaux-Daubresse et al., 2010). N compounds in the source leaves can have different fates: they are either used for leaf function, transported in the phloem to sinks or moved into leaf N-storage pools. Indeed, high amounts of N accumulates in short- or long-term storage pools. Type and amount of N compounds, which are stored in source organs, tissues or cell compartments have a big impact on N transport and partitioning to sinks (Tegeder and Masclaux-Daubresse, 2018). N could be stored as nitrate, ammonium or free amino acids; but the largest N-pools in all plant tissues are proteins. In C3 plants, approximately 80 % of the total leaf N is bound and stored in chloroplasts primarily in photosynthetic

Introduction

proteins (Makino and Osmond, 1991). The extremely abundant carbon-fixing enzyme Rubisco contains 10–30 % of the leaf N (Evans, 1989; Makino et al., 2003). Moreover, vegetative storage proteins (VSPs) are important N-storing molecules in all plant species in vegetative tissues. As nitrate fertilizers are often applied early during growth phase and are likely to be depleted by the reproductive stage, plants very likely rely on remobilization of N-storage pools in leaves or stems to provide reproductive tissues with N nutrition.

We analyzed transcriptome data of *B. napus* L., produced by Safavi-Rizi et al. (2018), for expression of genes involved in N-remobilization and metabolism. Interestingly, we found the two main families of seed storage proteins (SSPs), CRUCIFERINS and NAPINS, to be expressed in leaf tissue, as well as in stem tissue and pod walls (research article II), suggesting a function as an interim N-storage during N-remobilization. SSPs – as indicated by their name – accumulate mainly in developing seeds and there they serve as a storage reserve for N, but also carbon and sulfur. These proteins play an important role for the growing seedlings, as they are their major source of N.

N fertilizer is among the most added fertilizers world-wide and one of the most expensive nutrients to supply. The application of N fertilizers averages at 74 kg/ha/year worldwide, in China even at 305 kg/ha/year (Cui et al., 2018). There are serious concerns regarding N overload in the field. It causes acidification of soil and groundwater pollution and contributes to the general disturbance of our ecosystems. Oilseed Rape (OSR) is in general good in acquiring N, however with regard to N-remobilization during leaf senescence, its performance is rather inefficient (Rossato et al., 2001). One strategy to tackle the problem is the development of crops that are efficient in acquiring and using N, which comprises N-uptake, remobilization and utilization. Therefore, research, which aims at understanding and improving N use efficiency specifically during senescence processes, is important for an efficient agriculture as well as for our ecosystems and their stability. This work tries to shed light on the N-remobilization under different N-regimes in *B. napus* by analyzing expression patterns of seed storage proteins (CRUCIFERINS and NAPINS), which interestingly appear in leaf tissue.

2 Objectives

The differential expression of almost 6500 genes (Breeze et al., 2011) has been identified as the basis of the genetic program, which contributes to the sequential succession of events in leaf senescence in *Arabidopsis*. Central components of the senescence regulatory network are transcription factors (TFs). The superfamily of WRKY TFs is amongst the major TFs up-regulated in the senescence transcriptome. WRKY53 has been identified as a central hub in the WRKY network (Miao et al., 2004); however, the knowledge about upstream regulators is still incomplete. The TF Ethylene Response Factor 4 (ERF4) is one of these factors and part of this regulatory network (Koyama et al., 2013). Interestingly, it was shown that ERF4 pre-mRNA can be alternatively polyadenylated, resulting in two oppositional isoforms. First, my work had the aim to enlighten the involvement of alternative polyadenylation and splicing of ERF4 in leaf senescence regulation.

Moreover, mitogen activated protein kinase kinase kinase 1 (MEKK1) and another member of the WRKY family, WRKY25 have been shown to act upstream of WRKY53. The second objective of this work was, to generally understand the impact of MEKK1 and redox-conditions on WRKY25 and its downstream target *WRKY53*. As *mekk1* mutants die shortly after germination, I used an inducible amiRNA system to evaluate the impact of MEKK1 on senescence.

A major aspect of senescence is the salvage of nutrients, especially of nitrogen (N). The third aim of this work was to obtain a deeper understanding of N remobilization processes in the agronomical relevant species *Brassica napus L.* (cv. Mozart). Therefore, I analyzed the expression pattern of seed storage proteins (SSPs), which were found to be expressed in vegetative tissues. They serve most likely as an interim storage for nitrogen and appear to be controlled by intracellular hydrogen peroxide (H₂O₂) levels.

3 Results and Discussion

3.1 Overview

The list of publications (see page xviii) comprises two published research articles (research article I and II), one unpublished manuscript (research article III) and additionally one review article and one spotlight. This part focuses on the research articles. The main aspects of my work can be situated at the intersection between leaf senescence and transcription factors, hydrogen peroxide (H₂O₂) and nitrogen (N) remobilization (Fig. 1).

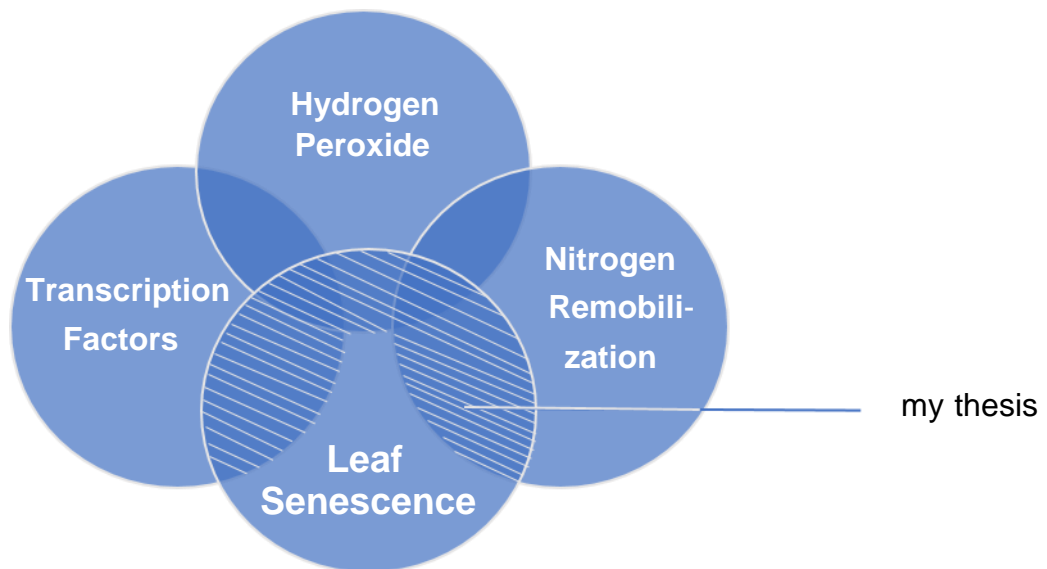


Figure 1: Venn-diagram representing the content of this thesis. This work comprises topics, which are all related to leaf senescence. The shaded area (white lines on the dark blue overlapping parts) is the intersection of the respective topics, which constitute this work.

Already in the introduction, leaf senescence was described as a complex process, which leads to structural and biochemical changes in cells, with the aim of macromolecule breakdown and nutrient remobilization to developing parts of the plant. To ensure an optimal progression of senescence, complex regulatory mechanisms have to be in place: The decision when and how to die is based on a multitude of different input signals, comprising genetic, developmental and environmental factors

Results and Discussion

(Jansson and Thomas, 2008). The different internal and environmental signals are constantly integrated in order to allow the plant to make the best choice between leaf senescence initiation occurring too early, which might lead to reduced carbon assimilation and nitrogen uptake, or occurring too late, which could result in incomplete remobilization of nutrients. (Masclaux-Daubresse, 2010; Malagoli, 2004) .Therefore, an optimal timing is not only crucial for the plant's fitness, but first and foremost for the survival of the plant's progeny. Therefore, studying senescence builds the foundation for future modifications of plant productivity that fits the needs of agriculture in times of a growing world population and climate change.

Part A focuses on transcriptional regulation and the impact of the signaling molecule H_2O_2 on leaf senescence. I will first discuss the role of alternative polyadenylation and splicing of ERF4 in senescence regulation and then go into detail about WRKY25 and the MAP kinase kinase kinase 1 (MEKK1). All these factors can be linked to WRKY53, a central hub in the WRKY senescence network, and interconnected in different ways to H_2O_2 as signaling molecule in senescence. In part B, I will discuss the role of seed storage proteins (SSPs) expression in leaves, their relation to H_2O_2 and their role in N-remobilization, a process, which is of central importance for plants during leaf senescence in order to efficiently support their progeny.

3.2 Part A: Transcription Factors in Arabidopsis Leaf Senescence

3.2.1 Ethylene Response Factor 4 (ERF4) in Senescence Regulation

In young leaves, senescence cannot be observed, indicating that repressors act to suppress cell degradation processes during early leaf development. When leaves age, metabolism has to be switched from anabolism to catabolism and degradation processes are activated. This switch has to be adjusted to environmental conditions and thus demands a massive regulatory network, in which TFs act as central elements (Balazadeh et al., 2008; Breeze et al., 2011). One of these transcription factors is ERF4 (Koyama et al. 2013; research article I, Fig. 1). ERF4 belongs to the VIIIa subgroup of ERFs (Nakano et al., 2006), which is characterized through the ERF-associated amphiphilic repression (EAR) motif that renders them transcriptional repressors. ERF4 pre-mRNA, however, is subject to alternative polyadenylation, which leads to two different protein isoforms: one of them containing the EAR motif (ERF4-R), one of them lacking it (ERF4-A) (research article I, Fig. 2A; Lyons et al. 2013). To understand how ERF4 is involved in the regulation of senescence, I performed phenotyping experiments as well as molecular and biochemical experiments. I assessed changes in mRNA abundance over development in correlation to ERF4 protein stability over time. I analyzed the activity pattern of CATALASE 3 (CAT3), which is a target gene of ERF4. Moreover, I investigated the interaction of the ERF4 isoforms on protein level and had a look at expression and effect of the RNA-binding protein FPA on senescence. In the following section, the relevant results, which describe the age and context dependent function of the two ERF4 isoforms in senescence will be presented.

Effect of ERF4 on Senescence – The Phenotype

To achieve a general understanding of the biological function of ERF4 isoforms in plant senescence, I followed a reverse genetics approach. Hence, I analyzed the *erf4* knock-out plants as well as this line complemented with the coding sequences of the single ERF4 isoforms (lines are named cERF4-A and cERF4-R in the following). There are various ways for conducting senescence phenotyping experiments and consequently

Results and Discussion

there is low comparability of plant lines and experiments. Therefore, we proposed and described a guideline, consisting of a complete set of methods to analyze senescence at physiological, biochemical and molecular levels in review article IV. I designed the experiments according to this set of standardized and complementary analyses to gain reproducible results. The phenotype of the cERF4-A and cERF4-R lines showed that both isoforms were able to complement the delayed senescence phenotype of *erf4* mutant plants (research article I, Fig. 3). These results suggest indeed that both ERF4 isoforms can substitute each other and have identical functions during senescence. However, it is well known, that functional redundancy within multigene families very often complicates attempts to characterize the effect of individual members (Bouché and Bouchez, 2001). Robatzek and Somssich for instance faced this situation with WRKY6, since the knock-out did not lead to a senescence phenotype. However, it resulted in altered gene expression profiles, indicating that functional redundancy might not be complete but nevertheless, the differences do not manifest themselves in phenotypic changes (Robatzek and Somssich, 2002). For the cERF4-A and cERF4-R lines the situation could be similar, which means that the absence of one isoform could result in changes in senescence-associated gene expression, but the partly overlapping functions suffice to almost restore the wildtype phenotype. A transcriptome analysis could give insights in differences between the two isoforms, such as specific target genes, and should be subject of further research.

Microarray experiments revealed that many WRKY transcription factors involved in senescence-regulation are downstream targets of ERF4 (Koyama *et al.*, 2013). Since WRKYs act in a complex network (Potschin *et al.*, 2014; Zentgraf *et al.*, 2010), the outcome on senescence is hard to predict; it is a long way until we will have identified all the important factors and fully understand their interactions. Influencing the expression of one *WRKY* gene could lead to an imbalance of the whole network.

In the reporter gene assays, I could show, that both ERF4 isoforms affected *WRKY53* expression in the same direction: be it either direct or indirect, both isoforms had an activating effect (research article I, Fig. 4). Koyama and coworkers showed in a ChIP experiment that the EPITHIOSPECIFIER PROTEIN/ EPITHIOSPECIFYING SENESCENCE REGULATOR (*ESP/ESR*) is a direct target gene of ERF4. More precisely, ERF4-R acts as a repressor on *ESP/ESR* expression (Koyama *et al.*, 2013).

Results and Discussion

ESP/ESR in turn is a repressor of *WKRY53* (Miao and Zentgraf, 2007), and by repressing a repressor, ERF4 is indirectly a positive regulator of *WKRY53*. Interestingly, in *esp/esr* knock-out plants, I could still see an activating effect of ERF4 on *WKRY53* expression, indicating that there is also an ESP/ESR-independent pathway. Further research is necessary to find out, whether this might be a direct regulation. Since an *in silico* analysis of the *WKRY53* 1-kbp upstream region revealed at least four ethylene responsive *cis*-elements and a DRE element, a direct interaction appears to be possible. These two independent ways of influencing *WKRY53* expression could also add to the effect, that the phenotype of the ERF4 complementation lines differ less than expected. The molecular regulation of *WRKY53* expression is discussed in more detail in chapter 3.2.2.

Due to the inconclusive results of the phenotyping experiments of the complementation lines, I additionally characterized overexpression lines of the ERF4 isoforms. Here, both isoforms had a different and even opposing impact on senescence: 35S:*ERF4-R* plants showed an accelerated senescence phenotype, whereas 35S:*ERF4-A* plants were slightly delayed (research article I, Fig. 1). This suggests that both isoforms have different target genes and are likely to be involved in different pathways. Further evidence for this assumption is provided by differences between the complementation lines. ERF4-A appears to be more involved in regulating intracellular H₂O₂ concentration (research article I, Fig. 3C) and the cERF4-R shows a later increase in electrolyte leakage (EL), which indicates that it is involved in promoting membrane integrity (research article I, Fig. 3E).

In conclusion, two ERF4 isoforms with opposing characteristics exist *in planta* with a different effect on senescence regulation. Furthermore, this implies that alternative polyadenylation has an impact on regulation of senescence and adds a further layer of complexity to it. In order to get a better idea about the function of each isoform, a molecular characterization of the ERF4 mode of action was performed.

Results and Discussion

Both ERF4 Isoforms Are Present Throughout Senescence

According to its gene expression profile, ERF4 plays a role throughout senescence. Over the period that I assessed (31-46 DAS), the mRNA of both ERF4 isoforms could be detected and their expression increased with age. The ERF4-A isoform was always less abundant, however, the ratio between the two isoforms changed. At 31 DAS the A:R ratio was highest, which leads to the conclusion, that ERF4-A is more important at early stages of senescence. Furthermore, I could show in an *in vitro* protein degradation experiment, that ERF4-A was more stable than ERF4-R. The higher ERF4-A protein stability counterbalanced the lower expression level (research article I, Fig. 2). The consequential next step would be to check not only mRNA but also protein abundance *in planta*. To get a first hint, I analyzed protein expression of N-terminal epitope tagged ERF4, since the alternative polyadenylation and splicing occurs at the 3' end. However, this did not lead to any results, since on the Western blot the much higher expression of ERF4-R would always outshine a faint ERF4-A band. Nevertheless, I could see that both isoforms, expressed separately in a protoplast system, resulted in ERF4-A and ERF4-R proteins (research article I, Fig. S6), indicating that the mRNA of both proteins is translated into a protein *in planta*.

CATALASE 3 Is a Target Gene of ERF4 Isoforms

In a yeast-1-hybrid (Y1H) screen, ERF4 could bind to the promoter of *CAT3* (research article I, Fig. 5A) indicating that *CAT3* could be a direct target gene of ERF4. I performed an *in silico* analysis of the 149 bp fragment used for the Y1H of *CAT3* in order to find potential ERF4 binding motifs. DNA-binding of members of the ERF family is not restricted to a single motif. Some ERFs have been shown to bind *in vitro* to an AGCCGCC motif (GCC-box) (Welsch et al., 2007), while others have been reported to bind DRE elements (Wang et al., 2009), or even novel DNA elements (Shaikhali et al., 2008). The *CAT3* promoter contains a DRE motif and I confirmed binding of both protein isoforms ERF4-R and ERF4-A to a fragment containing this motif by DPI-ELISA (research article I, Fig. 5B). Using transient reporter gene expression assays in protoplasts, I analyzed the influence, which each isoform has on the expression controlled by the *CAT3* promoter. As expected, the ERF4-R isoform, containing the

Results and Discussion

EAR-motif, had a repressing effect. In contrast, the ERF4-A isoform, which does not contain the EAR-motif, activated *CAT3* driven reporter gene expression in leaf protoplasts (research article I, Fig. 5C). The ERF4 gene has a conserved motif with acidic residues at the N-terminal part (research article I, Fig. S8), which is known to act as activating domain of plant transcription factor proteins. In line with this, the N-terminal part of tobacco ERF4 has been reported to function as transcriptional activator (Ohta et al., 2000). Thus, in the absence of the EAR motif, the activating domain seems to turn the protein into a transcriptional activator of *CAT3* expression. Moreover, ERF4-A has been characterized in other contexts as transcriptional activator before. Lyons and coworkers showed the transcriptional activation of ERF4-A on a GAL4-GCC promoter and *PDF1.2* expression (Lyons et al., 2013). In summary, my experiments suggest that by binding to a DRE motif in the promoter region of *CAT3*, ERF4-A activated and ERF4-R repressed *CAT3* expression.

Catalases are H₂O₂ decomposing enzymes, which makes them interesting target genes for a senescence-regulating TF. As H₂O₂ is a signaling molecule, which induces the expression of many senescence-associated TFs and SAGs, a tight control is a prerequisite for the coordinated progression of leaf senescence. Catalases are known to be important “redox guardians” (Mhamdi et al., 2012). All three *Arabidopsis* catalases show a senescence-associated activity pattern: *CAT2* expression and activity is down-regulated early during senescence, *CAT3* expression and activity is up-regulated while senescence progresses and finally, during late senescence, *CAT1* is up-regulated. In the phenotyping experiments I could show that *CAT3* activity increased with age in Col-0 plants (research article I, Fig. 5D and S5B). Interestingly, the *erf4* mutants showed an intricate activity pattern: in younger plants, *CAT3* activity is lower compared to wildtype. This indicates the absence of an activating factor, and it suggests that ERF4-A has a higher impact at early senescence stages. In older plants, *CAT3* activity is higher in the mutant compared to Col-0 plants. This hints at the absence of a repressing factor, and hence, ERF4-R seems to be dominant at late senescence stages. These results are in line with the highest A:R ratio in early development (research article I, Fig. 7B). Furthermore, these results are consistent with the increase in *FPA* expression with plant age (research article I, Fig. 7A). *FPA* is an RNA-binding protein, which has been shown to inhibit the alternative

Results and Discussion

polyadenylation, that leads to the ERF4-A formation (Lyons et al., 2013). Interestingly, in *erf4* mutant plants, the increase in FPA expression is lower at later stages. This could be due to delayed senescence, or to a feedback regulation of ERF4 on *FPA*. In order to obtain a hint, whether FPA is involved in senescence regulation via influencing ERF4 alternative polyadenylation, I assessed the phenotype of *fpa* mutant plants (research article I, Fig. 7C-E). However, it is difficult to compare senescence progression with Col-0 plants, as FPA is also involved in controlling FLOWERING LOCUS C expression (Koornneef et al., 1991). The mutants showed a strong delay in reproductive development. They produced more than 30 leaves without bolting and flowering, whereas Col-0 plants developed only 13 leaves in average and had already flowers and siliques, when *fpa* mutants still were in the phase of vegetative growth. Yet, if the first 13 leaves within the rosette of plants with the same age are compared, *fpa* mutants show an accelerated senescence phenotype in these leaves. However, this phenotype is doubtful, because *fpa* plants clearly have higher expression levels of ERF4-A and thus should resemble the 35S:*ERF4-A* overexpressing line. This line was only slightly accelerated in senescence at 41 DAS, in later stages, it rather appears to be delayed. These results indicate that FPA is likely to be involved in the regulation of polyadenylation of more target genes, which are involved in senescence. This could be subject for further investigations. Nevertheless, the regulation of ERF4-A formation by FPA is an interesting fact, as FPA is also involved in flowering and pathogen response, two processes, which have overlapping gene expression patterns with senescence; and this suggests, that alternative polyadenylation is a way for cross-talk between the three processes.

Moreover it should be mentioned, that ERFs bind to a GCC box, a DNA-sequence involved in the ethylene-responsive transcription of genes (Ohme-takagi and Shinshi, 1995). Yang and coworkers conducted a study, which suggests that ERF4 in *Arabidopsis* is a negative regulator of the abscisic acid and the ethylene responsive pathways (Yang et al., 2005). ERF4 is involved in hormone signaling, therefore it could be involved in the regulation of leaf senescence via the ethylene and the abscisic acid pathway.

An interesting point is also the fact that ERF4 could regulate senescence progression also by controlling H₂O₂ concentrations through activation or repression of *CAT3*

expression. The expression of *CAT3* is in general induced by high H_2O_2 contents; but, during senescence, this substrate responsivity is blocked, while other stress responses, like response to water stress, induced by flooding of detached leaves or heat stress, are still running (Orendi et al., 2001). Possibly, ERF4-R might be involved in preventing the *CAT3* induction by H_2O_2 , which contributes to an increase in reactive oxygen species (ROS) with senescence. A comparison of protein amount and activity of *CAT3* over time reveals an increasing protein amount as well as increasing enzyme activity of *CAT3* with age in the wildtype (research article I, Fig. S5). In the *erf4* mutant, there was a stronger increase in protein amount as well as enzyme activity with age compared to wildtype. This suggests a dominance of ERF4-R in later stages of senescence, which appears to be involved in the repression of *CAT3*. This could foster the increase in ROS, especially H_2O_2 , which in later stages is also important for the disintegration of membranes and degradation of macromolecules. In earlier stages, H_2O_2 is involved in the induction of the expression of many SAGs and transcription factors, such as *WRKY53*. Furthermore, many TFs function in a redox-dependent manner, for instance *WRKY25*, which is described in the next sub-chapter.

3.2.2 Regulation of *WRKY53* Expression

WRKY53 Is a Central Hub in the *WRKY* Senescence Network

WRKY53 expression, activity and degradation have been analyzed in detail and this revealed that *WRKY53* is very tightly regulated on all three levels and appears to be one of the important players in the senescence regulatory network. It shows a characteristic senescence specific expression pattern (Hinderhofer and Zentgraf, 2001) and it can influence its own expression in a feedback loop (Miao et al., 2004; Potschin et al., 2014). Moreover, it has an important and central position within the *WRKY* senescence network (Ay et al., 2009; Miao and Zentgraf, 2007; Miao et al., 2004) and it displays a clear senescence phenotype as positive regulator of leaf senescence (Miao et al., 2004). To fully understand its complex regulation and its role within the *WRKY* senescence regulatory network, cross-regulation between different *WRKY* factors which are expressed during senescence must be characterized in detail. This work contributes to unravel the functional relation within a small subnetwork

consisting of WRKY18, WRKY25 and WRKY53 in leaf senescence, in which WRKY18 was already characterized as upstream regulator, downstream target and protein interaction partner of WRKY53 (Potschin et al., 2014). In this part, the role of WRKY25 as key regulator of WRKY53 expression and activity and, in addition, the influence of MEKK1 on WRKY25 protein function is discussed.

Redox-Sensitive Action of WRKY25

ROS, especially H₂O₂, do not only play a deteriorative role during senescence, they also function as signaling molecules. An important and yet unanswered question is how this signal is perceived and transmitted in order to influence senescence onset and progression. As massive changes in the transcriptome occur in the course of senescence, transcription factors would be perfect candidates to receive ROS signals. Furthermore, it is known that H₂O₂-treatment in *Arabidopsis* triggers an increase in the expression of many SAGs and TFs including WRKYs (Chen et al., 2010). However, there is still a long way until ROS signaling, which comprises perception, transduction and transcription, is fully understood. Redox-conditions could influence gene expression through TFs in various ways, such as changing DNA-binding activity, intracellular localization, changing protein-protein interactions or proteolytic degradation (reviewed extensively in He et al., 2018). Indeed, a redox-sensitive action has been reported for some TF families, for instance for the G-group of basic region leucine zipper (bZIP) (Shaikhali et al., 2012) and for the class I TCP family (Viola et al., 2013), to give just two examples. To date, our knowledge of redox-sensitive or redox-responsive transcriptional regulators is still limited. Our research contributed to expand the current knowledge in this field. In research article III, we identified WRKY25 DNA-binding activity to a W-box of the *WRKY53* promoter to be redox-sensitive and we could show that the redox-sensitive changes are reversible depending on the redox-conditions (research article III, Fig. 2). WRKY25 binds selectively to a specific W-box in the promoter of *WRKY53* and it positively regulates its expression (research article III, Fig. 1 and 3). Moreover, under oxidizing conditions, the activation of *WRKY53* expression by WRKY25 was dampened in a protoplast system (research article III, Fig. 3B). Taken together, binding and transactivation is lower under oxidizing conditions,

Results and Discussion

but nevertheless WRKY25 is still involved in the response of the *WRKY53* promoter to oxidizing conditions *in planta*, as the response of *WRKY53* to H₂O₂ was lower in the *wrky25* mutants than in WT, especially in later stages. *WRKY53* as well as *WRKY25* gene expression are up-regulated with increasing H₂O₂ levels.

Surprisingly, the senescence phenotype of plants with ectopic *WRKY25* overexpression and *wrky25* mutant or knock-down lines turned out to be exactly the opposite of the expected phenotype (research article III, Fig. 4). However, we could show that WRKY25 lowers intracellular H₂O₂ contents, especially in later stages of leaf senescence (research article III, Fig. 6). The lower H₂O₂ levels in *WRKY25* overexpressing plants are in line with the delayed senescence phenotype. In the same line of evidence, the *wrky25* mutant or knock-down plants displayed higher levels of H₂O₂ than wildtype and are accelerated in senescence. High H₂O₂ contents in late stages of leaf development are thought to be involved in membrane deterioration and lipid peroxidation processes.

WRKY25 appears to function as a kind of “buffer”, which levels out a too excessive reaction to oxidizing conditions by three different negative feedback loops: it is involved in the down-regulation of intracellular H₂O₂ contents, it negatively regulates its own expression and is restricted in its action by forming heterodimers with its target factor WRKY53. This is consistent with the finding, that it also appears to dampen the activation of the H₂O₂ induced expression of the transcription factors *ZAT12* and *ANAC92* in young leaves (research article III, Fig. 6 and 7).

Furthermore, WRKY25 and WRKY53 are part of a complex regulatory network, in which many other members of the WRKY TF family are involved and which shows multilayered feedback regulations. Therefore, the whole network might be disturbed if one player is knocked out, making it yet impossible to predict the phenotype. More research has to be done, to unveil further interaction partners and their hierarchy and to get a more thorough picture of the WRKY network.

MEKK1 in Leaf Senescence

MAPK cascades transduce a variety of extracellular stimuli into intracellular responses. Therefore, the activation of MAPK cascades is an important mechanism for stress adaptation via the control of gene expression not only in plants, but also in mammals

Results and Discussion

and yeast. Indeed, MAPK cascades have been reported to be involved in senescence regulation. Zhou and coworkers for instance reported that MPK6 is a direct downstream target of MKK9 and that this cascade positively regulates leaf senescence in *Arabidopsis* (Zhou et al. 2009). MAPKKK18 was found to influence the timing of senescence via its protein kinase activity by having an impact on ABA signaling (Matsuoka et al., 2015). Moreover, WRKY factors have been shown to be targets of MAPK signaling or to play a role in transducing the signal from the MAPK cascade to downstream genes (Asai et al., 2002; Wan et al., 2004). Previous work in our laboratory identified MEKK1 as another MAP kinase kinase kinase that is involved in the regulation of WRKYs and senescence (Miao et al., 2007). In a yeast-one-hybrid (Y1H) screen MEKK1 was found as a DNA-binding protein of the *WRKY53* promoter. The function of the DNA-binding activity of MEKK1, as well as the mechanism is still unclear, since it is not a TF *per se*. MAPK pathways are known to regulate gene expression by phosphorylating TFs or other DNA-binding proteins. However, MAPKs have been reported to be associated with chromatin in mammals. In pancreatic β -cells, MEK1/2 was found to bind to the target gene promoter in complexes with its protein substrate, probably to modulate transcription *in situ* in direct response to newly incoming signals (Lawrence et al., 2008). Another example is the stress activated protein kinase (SAPK) p38 in mammals, which is also recruited to chromatin via its interaction with TFs (Ferreiro et al., 2010). In yeast, MAP kinases are frequently physically associated with promoter regions of target genes that they regulate in a kinase cascade dependent manner. Nevertheless, in *Arabidopsis*, to our knowledge, none of the MAPKKKs contains a characterized DNA-binding domain, except for MEKK4 (MAPK Group 2002). The DNA motif for MEKK1 binding was narrowed down to a small 6 bp motif, which appears to be related to the binding motif of Myc-like TFs (CANNTG) and it is present in various promoters. In addition, the kinase activity of MEKK1 also seems to be involved in the regulation of *WRKY53* expression. MEKK1 also interacts with *WRKY53* on protein level and phosphorylates *WRKY53*, at least *in vitro*, and thereby increases the DNA-binding affinity of the TF (Miao *et al.*, 2007).

So far, MEKK1 was characterized to play a role in stress responses to biotic and abiotic stress. In order to get a hint about the role of MEKK1 in leaf senescence, I intended to analyze *mekk1* mutants. However, homozygous knock-out of the *MEKK1* gene is lethal

Results and Discussion

and seedlings die shortly after germination, thus I characterized an inducible amiRNA_{MEKK1} line (Li et al. 2013). *MEKK1* appeared to be a negative regulator of senescence (research article III, Fig. S4B,D), which was surprising, since in addition to and in line with Miao and coworkers, I could show in reporter gene assays, that *MEKK1* is a positive regulator of *WRKY53* expression, which is a positive regulator of senescence. Moreover, the activating effect, which 35S:*WRKY25* overexpression had on *WRKY53* gene expression, was enhanced by co-expressing a 35S:*MEKK1* construct (research article III, Fig. 3C), indicating that *MEKK1* action is most likely not restricted on *WRKY53*. In addition, the repressing effect of *WRKY18* on *WRKY53* expression was reversed to an activating effect (research article III, Fig. S4A). Whether this is due to direct phosphorylation of the *WRKYs* or due to classical MAPK signaling, is subject for further studies. However, *MEKK1* seems to decelerate leaf senescence, since in the absence of *MEKK1*, leaves senesce faster. This is in line with findings of other groups, which characterized the *mekk1* phenotype in seedlings and found dwarfed, infertile plants, with curled, prematurely senescing leaves and stubby root hairs. These plants do not reach maturity and show constitutive expression of pathogenesis-associated genes (Ichimura et al., 2006; Qiu et al., 2008; Suarez-Rodriguez et al., 2006). This pleiotropic phenotype suggests multiple interaction partners and signaling pathways of *MEKK1*.

Forde and coworkers showed that *mekk1/2/3* mutants had an impairment in lateral root growth, which could be rescued by a construct carrying the *MEKK1* gene (Forde et al., 2013). They did not analyze older plants, but it is likely that the impairment in root growth has a negative impact on plant development. Besides, the growth arrest phenotype could be fostered by the constitutive defense responses in *mekk1* mutant plants. Ichimura and coworkers plausibly explained, that *MEKK1* negatively regulates cell death pathways, which are activated by certain resistance (R) proteins, which are temperature sensitive (Ichimura et al., 2006). Thus, the senescence phenotype of the amiR_{MEKK1} line could be explained by a dampened inhibition of cell death pathways in the absence of *MEKK1*. Furthermore, it explains, why *mekk1* plants are able to grow at elevated temperatures (more than 28 °C), whereas they die at moderate temperatures (around 20 °C). The R proteins in question are unstable at high temperatures (for further details see Ichimura et al. 2006 and references therein). The

Results and Discussion

involvement of MEKK1 in plant defense gene expression via MAPK signaling has already been studied. MEKK1 is involved in the regulation of defense genes, such as *PR1*, *PR2* and *PR5* and it is also involved in flg22-triggered activation of MPK4 (Asai et al., 2002; Suarez-Rodriguez et al., 2006).

Furthermore, we saw in a split ubiquitin system, that MEKK1 can interact with many WRKY factors on protein level (Fig. 2 unpublished data), which makes its involvement in the WKRY regulatory network rather complex.

	W6	W13	W15	W18	W22	W25	W29	W30	W33	W38	W40	W53	W60	W62	W70
MEKK1	✓	✓	—	✓	✓	✓	—	✓	✓	✓	✓	✓	✓	✓	✓

Figure 2. Positive interactions of MEKK1 with WRKY proteins in a split ubiquitin system are indicated by ticks. MEKK1 and 15 WRKYs were used both as prey and bait. All 30 combinations were transformed into yeast 4 times independently and plated on three different selection media, respectively (Diplomarbeit Silke Schlienger, 2013).

MEKK1 is also connected to the WKRY network via Arabidopsis MPK4, which functions as a regulator of pathogen defense responses, since it is involved in the repression of salicylic acid (SA) dependent resistance and in the activation of jasmonate (JA) dependent defense gene expression. In brief, MEKK1 is essential for activation of MPK4, which negatively regulates systemic acquired resistance. MPK4 is mainly localized in nuclei where it phosphorylates its substrate protein MKS1. Yeast-two-hybrid (Y2H) screens showed, that MKS1 interacts with WRKY25 and WRKY33 and in this way, MKS1 could direct MAP kinase activity towards specific transcription factors. Both WRKYs turned out to be indeed substrates of MPK4 *in vitro* (Andreasson et al., 2005). For WRKY33 it is known that upon MEKK1 and MKK1/2 signaling, MKS1 is phosphorylated by MPK4 and WRKY33 is released from MPK4 interaction. Thereafter, WRKY33 can activate expression of its downstream genes, such as *PAD3*, which is required for antimicrobial camalexin production (Qiu et al., 2008). Both WRKYs, WRKY25 and WRKY33, are most likely involved in the regulation of gene expression in pathogen response (Zheng et al., 2006, 2007), which might be a link to defense and stress related senescence processes.

Results and Discussion

Additionally, *mekk1* plants have been shown to have an enhanced accumulation of H₂O₂ in leaves (Nakagami et al., 2006), which matches the chlorotic phenotype of leaves of the amiR_{MEKK1} plants (research article III, Fig. S7B). Furthermore, MEKK1 transcript levels (Miao et al., 2007) and protein amounts (Nakagami et al., 2006) have been shown to increase upon H₂O₂ treatment, which strongly suggests that *MEKK1* is regulated by oxidative stress. Additionally, H₂O₂ induced the activation of MEKK1 kinase activity and led to a proteasome-dependent stabilization of MEKK1 protein (Nakagami et al., 2006). Consistently, *MEKK1* gene expression levels increase at the onset of senescence in parallel to the increase of *WRKY53* expression (Miao et al., 2007). Furthermore, MEKK1 activates MPK4 in response to H₂O₂ treatment in protoplasts (Nakagami et al., 2006). All these findings indicate that MEKK1 plays a role in redox-signaling and the transactivation activity of MEKK1 on *WKRY25* expression provides another link to the activation of redox-dependent gene expression.

3.3 Part B: Senescence-Related Seed Storage Protein Expression in Rapeseed Leaves

The generation and redistribution of N-rich compounds is generally seen as a crucial outcome and aim of leaf senescence processes. We were interested to investigate N-remobilization during leaf senescence in *Brassica napus L.*, since it is believed to be rather inefficient (Rossato et al., 2001). Microarrays were performed with plants grown under different N regimes to analyze the genome wide expression of oilseed rape (OSR) genes during senescence (Safavi-Rizi et al., 2018). We analyzed this dataset for genes involved in N-remobilization and N-storage, which parallel the H₂O₂ profiles in their expression patterns. My work contributed to the interesting finding that transcripts of seed storage proteins (SSPs), which were formerly believed to occur exclusively in seed tissue, were identified in leaves (research article II, Fig. 1). We detected *NAPIN* and *CRUCIFERIN* mRNAs in leaves at different canopies and moreover, not only the transcripts but also the proteins were present in leaf tissue (research article II, Fig. 2 and 3). Interestingly, the accumulation of SSPs appeared in a certain pattern: The accumulation started in the oldest leaves early in plant development. When these leaves started to senesce, N was translocated to younger leaves; it literally “climbed up” the plant before the older, lower leaves where shed. However, a residual SSP content remained in the terminal leaf. Furthermore, we could also detect SSP accumulation in shoots and pods (research article II, Fig. 3).

The microarray experiments of Safavi-Rizi and coworkers 2018 were carried out under high and low N-supply. Regarding expression levels of the different SSPs, the different N-regimes led to interesting results. Under low N conditions, NAPINS appeared to be higher expressed and under high N-supply, we could detect more CRUCIFERINS. For sulfur (S) a similar mechanism has been observed: low S supply increased the ratio between the S-rich CRUCIFERINS and S-poor NAPINS (Brunel-Muguet et al., 2016). It is still unknown how differential expression of CRUCIFERIN under high and NAPINS under low N supply is regulated. However, these results point towards a function of these SSPs as an N-interim-storage in leaves during N-remobilization processes in senescence. CRUCIFERINS are bigger and can therefore store higher N-amounts

Results and Discussion

than NAPINS. It is consistent that the two classes of SSPs are expressed differently under different N-regimes in leaves. In addition, the fact that they could be detected in stems and pods hints at a function as interim-storage for N in these tissues. Total N in stem and pods declined, when total N in seeds increased (research article II, supplemental Fig. S1 and S3). Wang and Larkins investigated the *opaque-2* mutation in maize, a mutation, which goes along with an increased level of free amino acids (FAA). They suggest that there could be an association between high levels of FAAs and reduced amounts of storage protein synthesis in mature endosperm (Wang and Larkins, 2001). A similar mechanism could be in place in senescing leaves. During monocarpic senescence, N is remobilized from senescing tissues (sources) to developing organs and seeds (sinks). However, in OSR the N-remobilization takes place in a stepwise manner, from lower to upper leaf canopies. This coincides with a wave-like pattern in SSP expression. Through the build-up of SSPs, it can be hypothesized that the level of FAAs could be reduced in leaves. Consequently, the sink to source relationship changes: the sink strength of newly developing organs and seeds increases in relation to the decreased source strength, a process, which could enhance N-remobilization in OSR. How this process is coordinated in OSR is subject for further research. Girondé and coworkers found a similar function for the stem in OSR. They found the stem to be a transient storage organ, which could be a buffer in the case of an asynchronism between massive remobilization of N coming from source leaves and N-demand for seed filling (Girondé et al., 2015). They also defined two main prerequisites for an efficient interim storage, which are an efficient and compact storage and an easy access for remobilization. Both holds true for SSPs in seeds and in leaves. SSP are synthesized in the rough ER and usually stored in protein storage vacuoles (PSVs), assembled in compact protein complexes in seeds. In order to achieve a compact structure, optimized for maximal storage of amino acids within minimal space, vacuolar processing enzymes (VPEs) are necessary. Indeed, under both N-regimes, VPEs were differentially expressed in leaves (research article II, Table S3), which is the prerequisite for a compact structure of SSPs in multimeric form in leaves.

SSPs and Hydrogen Peroxide

Expression and accumulation of CRUCIFERIN and NAPIN coincided with the H₂O₂ peak (research article II, Fig. 2A) that has been described as internal signal for the onset of senescence. This expression pattern of SSPs suggests a correlation with the developmental senescence program, and ROS contents seems to function as connecting factor. However, which role H₂O₂ exactly plays, still needs to be investigated. Interestingly, under complete N-starvation, neither SSP accumulation, nor H₂O₂ accumulation was observed (research article II, Fig. 5 and S2). Nevertheless, these N-conditions provoked premature senescence, which indicates that at least the H₂O₂ related part of the developmental senescence program seems to be suppressed under N-starvation. Then, most likely, a stress induced N-remobilization and senescence program occurs.

There are strong hints that SSPs are coupled to ROS, and results of other researchers support this. Desikan and coworkers found already in 2001 in a cDNA microarray H₂O₂-regulated genes in Arabidopsis, and amongst them there were SSPs (Desikan et al., 2001). Furthermore, *in silico* analyses revealed the presence of *cis* elements in the 3 kbp promoter regions of *CRUCIFERINS* and *NAPINS*, which are known for redox-responsiveness, such as HY5 (research article II, table S4 and S5). This is a basic leucine zipper (bZIP) TF, which has been shown to bind to promoter regions of ROS-responsive genes to achieve a ROS mediated deetiolation of seedlings (Chen et al. 2013). Due to space limitations, not all examples could be mentioned here. For further ROS-responsive elements, found in the SSP promoter regions, see discussion of research article II.

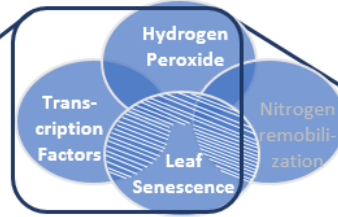
Taken together, the senescence program is controlled by a complex interplay between intracellular H₂O₂ contents and N availability, which also effects N-remobilization through the formation of SSPs. How exactly H₂O₂ influences SSP expression or how expression of SSPs is regulated by the N-status, is still unclear. Further research is necessary to find answers to these questions.

4 Conclusions

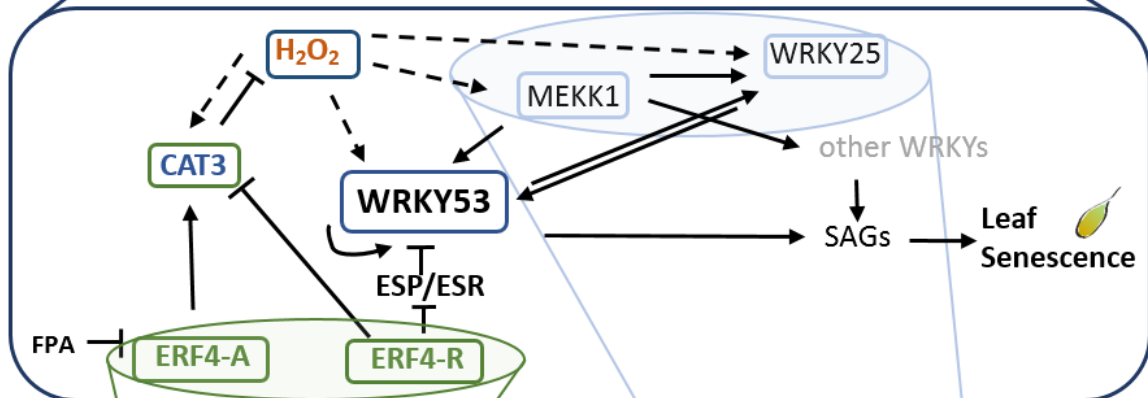
In the first part (summarized in Fig. 3), I have presented and discussed results about the senescence regulatory network around the key regulator *WKRY53* in *Arabidopsis thaliana*. Transcriptional regulation resulting in differential gene expression is the basis for an efficient senescence process, with the final aim of nutrient salvage. My work revealed details about the function of two different variants of ethylene response factor 4 (ERF4), MAP kinase kinase kinase 1 (MEKK1) and WRKY25 in this network and on their interplay with other key elements of senescence regulation, namely CAT3 and hydrogen peroxide (H₂O₂).

Conclusions

Topics Involved in my Work: Part I



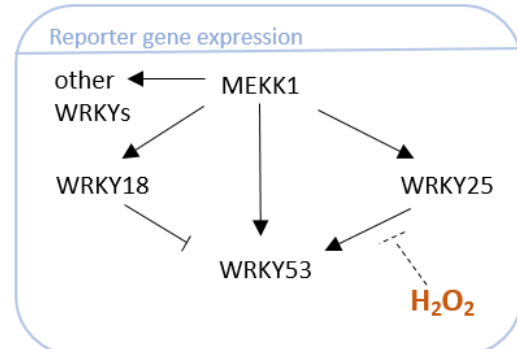
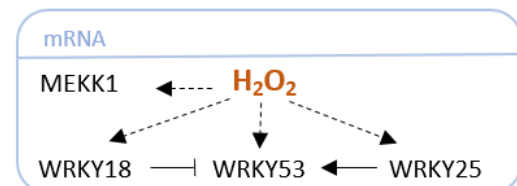
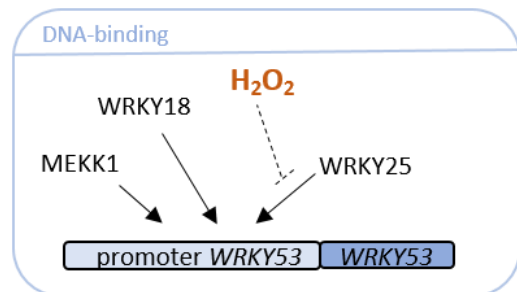
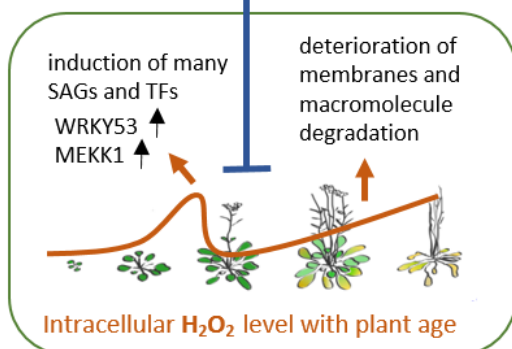
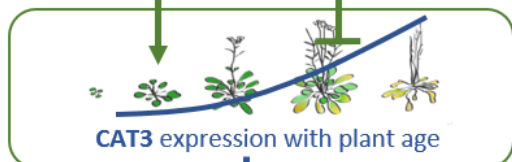
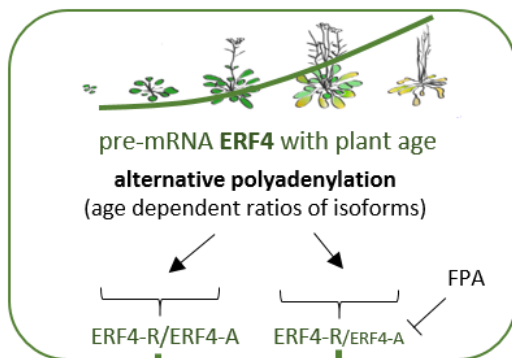
Model of the Senescence Regulation around WRKY53 in Arabidopsis



Main Results

Research article I

Research article III



Conclusions

Figure 3 shows a step-wise zoom-in into the topics of this thesis, their connection with each other and with *WRKY53*. The main results delivered in the research articles I and III are shown, which are details about ethylene response factor 4 (ERF4), *WRKY25* and MAP kinase kinase 1 (MEKK1) in senescence regulation. Research article I describes the involvement of two ERF4 isoforms in senescence regulation. Research article III characterizes *WRKY25* as a redox-dependent regulator of *WRKY53*.

Research article I describes that both ERF4 isoforms are involved in senescence regulation. Alternative polyadenylation, influenced by the RNA-binding protein FPA, changes the ratio of ERF4-R to ERF4-A during senescence. FPA increases with age and leads to a reduced formation of ERF4-A in older plants, which consequently reduces the activation potential of ERF4-A on *CAT3* gene expression in late stages of senescence. This, together with the phenotype of *fpa* mutant plants, suggests that alternative polyadenylation plays a regulatory role, which to our knowledge, has not been described before in the context of senescence. The impact of ERF4 on leaf senescence could result from different pathways. Via the regulation of *CAT3*, ERF4 isoforms are involved in controlling the redox-state of the cell, and therefore they have an impact on redox-signaling. Reactive oxygen species (ROS) and especially H_2O_2 , which is the substrate of *CAT3*, is not only an important signal to induce senescence-associated gene expression. In later stages it is also important for membrane deterioration and degradation of macromolecules. Moreover, in protoplast reporter gene assays both ERF4 isoforms have an activating effect on *WRKY53* expression, a well characterized positive regulator of senescence. My results indicate, that there exists a further pathway, which does not involve the already described pathway via EPITHIOSPECIFIER PROTEIN/ EPITHIOSPECIFYING SENESCENCE REGULATOR (ESP/ESR), since I could also see this effect in *esp/esr* mutant plants.

Furthermore, my work contributed to shed light on the complex involvement of MEKK1 in the *WRKY* senescence network (research article III). It has been shown before that MEKK1 can positively regulate *WRKY53* on transcriptional level by binding to the *WRKY53* promoter as well as on protein level by phosphorylation. We could show that MEKK1 interacts with many other *WRKY* proteins in yeast. MEKK1 action on the *WRKY53* promoter resulted in an increase in *WRKY53* expression. MEKK1 turned the repressor *WRKY18* into a weak activator and it enhanced the activating action of

Conclusions

WRKY25. Thus, MEKK1 can act on *WRKY53* gene expression directly and indirectly through the action of other WRKYs. Phenotyping experiments of an inducible *amiRNA^{MEKK1}* line revealed MEKK1 to be a negative regulator of leaf senescence, which opens up a plethora of questions and ideas for further research, since these results were unexpected. This will be discussed in the next section, “Future Perspectives”.

In addition, we characterized WRKY25 as a redox-sensitive upstream regulator of *WRKY53* expression (research article III). We suggested a model, how WRKY53, WRKY25 and H₂O₂ interplay with each other: Under non-oxidizing conditions, WRKY25 acted as a positive regulator of *WRKY53* expression, whereas oxidizing conditions dampened DNA-binding to the *WRKY53* promoter and the action of WRKY25 on reporter gene expression under the *WRKY53* promoter in a transient expression system in *Arabidopsis* protoplasts. Furthermore, we could see that the intracellular H₂O₂ level in *WRKY25* overexpressing plants is lower than in wildtype and in *wrky25* mutants it is higher. This indicates a role of WRKY25 in controlling the intracellular redox-conditions.

During the last two decades it became clear, that an extremely complex regulatory network controls all aspects and processes of senescence. There is no “master regulator” of senescence, but a network, which is highly responsive to a plethora of signals. This leads to a high plasticity, which enables the plant to react and adapt to changing conditions and various stresses. But at the same time, it requires a high integration capacity. Feedback loops are one element that increase integration capacity, as we could show for WRKY25. WRKY25 positively regulates the expression of WRKY53 and *vice versa*, creating a positive feedback loop. On the other hand, WRKY25 expression is driven by H₂O₂, but at the same time, this TF regulates intracellular H₂O₂ levels and it is itself redox-sensitive, which creates negative feedback loops. High integration capacity is also given by cross-talk, such as between senescence and stress responses. Environmental signals are constantly integrated and if stress conditions produce adverse conditions for the plant, premature senescence is induced as exit-strategy to produce offspring. The signaling molecule H₂O₂ is part of stress- and senescence processes (for review see Smirnov and Arnaud 2019) and it is therefore likely to be involved in cross-talk. There is also evidence that

Conclusions

points to a cross-talk between early and late leaf development, since senescence is affected if early leaf development is perturbed. The transcription factor REVOLUTA (REV) for instance, is involved on the one hand in early developmental processes, such as vascular development, leaf polarity or lateral meristem initiation and on the other hand it is connected to early senescence, since it directly regulates the expression of *WRKY53* in a redox-dependent manner (Xie et al., 2014). Taken together, our current notion of senescence regulation requires regulatory factors that coordinate environmental signals as well as developmental events throughout the different stages of the plant's life cycle. Different molecular networks with overlapping functions create a highly intricate system, which requires interconnections between different pathways. One such node of convergence seems to be the circadian clock. Circadian regulatory circuits have an influence on leaf senescence, which was pointed out by Zhang and coworkers (2018). Their results revealed a molecular mechanism, in which the circadian evening complex (EC) influences JA-induced leaf senescence in *Arabidopsis* via MYC transcription factors. Furthermore, EARLY FLOWERING 3 (ELF3), which is part of the EC, can affect dark-induced leaf senescence in an EC-independent manner via connecting a clock component and classical light signaling. ELF3, together with phytochrome B, can repress PIF4/PIF5, which are positive senescence regulators (Sakuraba et al., 2014). Senescence and the circadian clock seem to have huge overlaps also with other regulatory circuits, for instance carbohydrate and nitrogen metabolism, as well as ROS and hormone signaling pathways (Sanchez and Kay 2016; spotlight, article V). All these details add to the current understanding of senescence regulation as a complex web of connectivity, which is far from being disentangled.

In the second part (summarized in Fig. 4), I have discussed results we obtained in our research about nitrogen (N)-remobilization in *Brassica napus* L. (cv. Mozart). By having a close look at transcriptome analyses, we identified the major classes of seed storage proteins (SSPs), namely CRUCIFERINS and NAPINS to be expressed in vegetative tissues (research article II). Moreover, their expression correlates with intracellular H₂O₂ contents.

Conclusions

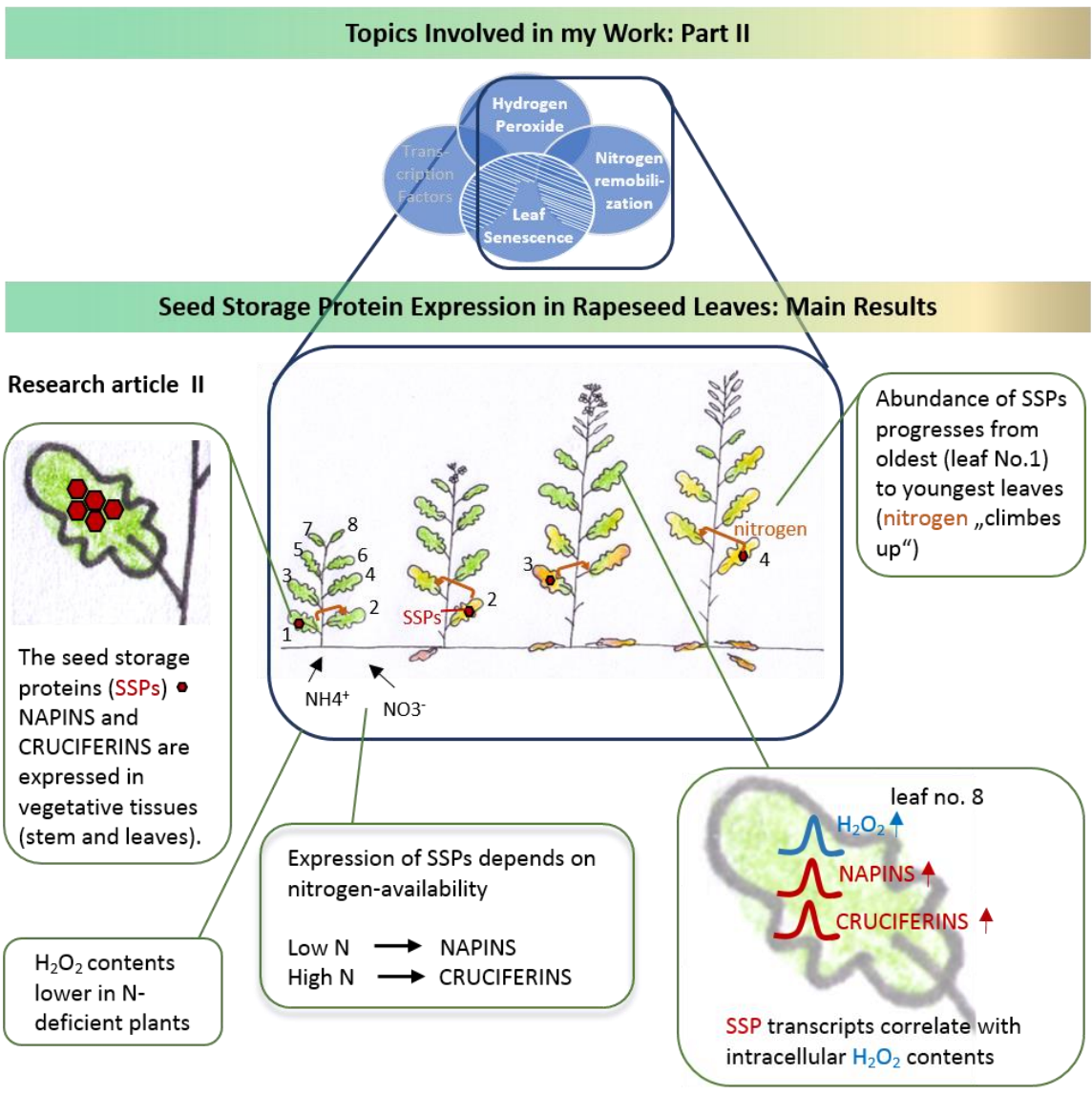


Figure 4 depicts our main findings of research article II. We analyzed the expression of seed storage proteins (SSP) in vegetative tissues of *Brassica napus L.*

We developed the hypothesis that these SSPs in leaves function as interim storage. This is important in OSR, since it is known for an inefficient utilization of applied N fertilizer. Only about 50 % of applied N is recovered in the harvested seeds (Schjoerring et al., 1995). This inefficiency of OSR to remobilize N to harvestable tissues, such as the developing pods, results from loss of leaves with a high N content. The dead leaves on the soil still contain a significant amount of N, usually more than 2

Conclusions

% of the dry weight (Rossato et al., 2001). However, OSR has a high maximum rate of mineral N uptake from the soil compared to other species (Laine et al., 1993), which indicates that the low N harvest index is a result of sink strength limitation rather than N-uptake. Indeed, in OSR, the first leaves senesce before the sink strength of developing seeds is high enough for an efficient remobilization. Therefore, the efficiency, with which leaf N is mobilized out of senescing leaves, might be improved by altering source-sink relationships via transient storage of N in developing leaves, for instance via the accumulation of SSPs. This transient N storage would increase relative sink strength in developing parts and would thereby increase the remobilization efficiency in the senescing leaves. Simultaneously, a transient storage of N in SSPs would allow remobilization to seeds or developing parts at later time points. This efficiency is critical for seed N-content, since most of the N used for grain filling is derived from mobilization of N stored in vegetative tissues and only a minor portion of N is taken up from the soil during seed filling (Rossato et al., 2001). The accumulation of SSPs in leaves progressed from the oldest to the youngest leaves and thus, a stepwise N-remobilization from lower to upper leaf canopies could take place. Moreover, we could see that the expression of SSPs in leaves depends on N-supply, what indicates that the N-storage can be adjusted to N-availability.

Furthermore, we analyzed H₂O₂ levels under complete N-starvation. Even though premature senescence was induced, H₂O₂ levels were lower in these plants than in plants without N-depletion. This indicates that at least the H₂O₂-triggered part of the developmental senescence program seems to be suppressed under N-deficiency, which means that some stress-induced senescence programs might use other signals than developmental senescence. In line with these results, comparative expression analyses have shown strong divergence between stress-induced and developmental senescence programs in early stages, which, however, converge in later stages (Guo and Gan 2012). Most likely, a stress-induced N-remobilization program is executed under N-starvation. This is supported by the fact that the phenylpropanoid pathway is induced. Several studies in different plant species report the induction of this pathway and the production of anthocyanins under N-limitation (Fritz et al., 2006; Peng et al., 2008; Soubeyrand et al., 2014). In accordance with these results, we saw that anthocyanins were present in high amounts under N-starvation. In these plants, we

Conclusions

measured lower H₂O₂ levels and at the same time a reduction of CAT activity. This observation leads to the hypothesis that the anthocyanins scavenge a substantial amount of H₂O₂. Taken together, a complex interplay between intracellular H₂O₂ levels and nitrogen availability seems to pilot the senescence program in OSR.

5 Future Perspectives

The three research articles, which are the basis of this thesis, deliver results and new insights into molecular senescence regulation. This chapter will give room to thoughts and ideas about how to continue with the work that I have presented, and what could be interesting to develop further.

Regulation of WRKY53

Our attempts around disentangling the complex regulation of WRKY53, which is not only important in senescence, but also in biotic and abiotic stress responses, should be pursued in the future. Investigating a complex network, such as the WRKY network, is generally a challenging task. Since there are so many players in the game, with partly even redundant functions, it is hard to predict or define the role of single factors. However, it is worth to analyze central hubs, such as WRKY53, which target many factors in the network. Genome wide analyses, such as RNA-seq or ChIP-seq techniques, can help to identify target genes, which are influenced in their expression by WRKY53. Furthermore, crosslinking and co-immunoprecipitation (Co-IP) *in planta* could help to find protein interaction partners. The newly found interaction partners or target genes could then be subject to thorough molecular and biochemical analyses to reveal their function. An understanding of all factors involved is necessary regarding a future, in which plants can be genetically modified in a way that leads to higher yields. Due to the large number of components and the highly dynamic structure of the WRKY network, in which protein interactions, signaling molecules and expression levels are constantly changing and adjusting to internal and external influences, simulation on the basis of experimentally obtained data would be a helpful tool. It would allow to predict the output of the network and thus the impact on senescence upon changing single components; however, this is a long-term perspective as quantitative and kinetic data are needed for modelling approaches.

We do not know much about the molecular mechanisms, how WKRY specificity is achieved. There are 75 WKRYs in Arabidopsis and it would be interesting to know,

Future Perspectives

what exactly determines activator or repressor function of the different WRKYs. Depending on the promoter context, one and the same WRKY factor can function as activator or repressor. WRKY18, WRKY25 and WRKY53 belong to different subgroups of the WRKY family, which means, besides the conserved WRKY-domain, they possess different protein domains. Domain deletion and domain swapping experiments between WRKY18 (repressor of WRKY53) and WRKY25 (activator of WRKY53) are already on the way, in order to identify the impact of single WRKY-domains on the activator/ repressor function. Moreover, they can form hetero- and homodimers, which changes their DNA-binding activity and specificity (for review see Llorca et al., 2014) and it would be interesting to find out, what exactly determines the interaction partner. Deletion of single domains with subsequent interaction analyses, such as Pull-Down assay, Yeast-Two-Hybrid, BiFC or FRET-FLIM, could shed light on the role of single domains in the determination of interaction-specificity. Moreover, biophysical methods such as microscale thermophoresis (MST) or fluorescence correlation spectroscopy (FCS) could help to test for either DNA-interaction or dimer formation. Surface Plasmon Resonance could give hints about kinetics of WRKY interactions. Furthermore, one of the central questions is, how the redox-signal is perceived. To investigate this, different mutations in possible redox-sensitive sites could be tested for their influence on transactivation or dimerization. Taken together, the experiments suggested here could lead to conclusions about the impact of single protein domains on WRKY function (activator or repressor?) and on their specificity (to which W-boxes do they bind, with which other WRKYs do they interact?) and finally on their role in redox-signaling. Since there are so many WRKYs, and they contain one or many W-boxes in der promoters themselves, and they display a complex network of homo- and heterodimer formation – this is a challenging and very laborious project. But as a starting point, in my opinion, it is worth to take this effort in order to go in detail and deeper analyze the already well characterized subnetwork between WRKY18, 25 and 53.

The Role of MEKK1 in Leaf Senescence

The project around the MAP kinase kinase kinase 1 (MEKK1) could also be a challenging but nevertheless promising project, with many exciting questions to answer. We know from *in vitro* assays, that MEKK1 binds to the *WKRY53* promoter. In the next step, we should confirm this *in vivo*, in a ChiP experiment. ChiP-seq in combination with RNA-seq are great techniques that offer us the possibility to find new target genes and elucidate the effect of MEKK1 on target gene expression. Usually, overexpressing plants are used for this kind of experiments. In fact, in the beginning of my PhD, I tried to create 35S:*MEKK1* overexpressing plants with N and C-terminal GFP fused to it. Transformation of plants only worked for the C-terminal tagged version, which seemed to display no effect on *WRKY53* expression in reporter gene assays. This strongly indicates that this tag renders MEKK1 dysfunctional. Overexpression – like knock-out – seems to be lethal for plants. However, we could use the conditional knock-out line or overexpressing lines in comparison to wild-type, which would surely deliver interesting results.

After analyzing the general DNA-binding activity, we could continue with a “close-up” and focus on a biochemical analysis of MEKK1. It would be interesting to investigate functional domains. Deletion constructs of the protein could help to find out, which protein domains are responsible for DNA-binding and protein binding to WRKY proteins. Is DNA-binding independent of its kinase activity? Moreover, it would be interesting to further biochemically analyze its role in redox-signaling. Mutations of different cysteines in MEKK1 could help to find out, which are important for redox-regulation. Phosphorylation assays and DPI-ELISAs under different redox-conditions could give insights into DNA-binding and kinase activity and their interconnection to hydrogen peroxide (H₂O₂) contents. Finally, reporter gene assays under different redox-conditions could give a hint, whether MEKK1 is involved in the signal transduction from H₂O₂ to *WRKY53*.

Regarding my results, that MEKK1 can affect the action of WRKY25 and WRKY18 on the expression of *WRKY53* in reporter gene assays, we can further investigate, whether the effect is due to phosphorylation and if so, whether it is direct or also via the classical MAPK pathway. The use of knock-out lines of the upstream kinases could

Future Perspectives

give hints. They could be used for example to create protoplasts with a knock-out background or for gene expression analyses.

Alternative Polyadenylation in Leaf Senescence

The involvement of FPA and alternative polyadenylation in senescence regulation opens up a new field, which gives ample room for further projects. In the beginning, there could be an analysis of FPA targets genes. There are different possibilities for finding target sites of RNA-binding proteins. Besides computational techniques, there are two major methods for large-scale assays *in vivo*: Ribonucleoprotein immunoprecipitation (RIP)-based methods, which do not permanently cross-link the RBP to the RNA or cross-linking and immunoprecipitation (CLIP)-based methods. The results could be sorted according to their relevance in senescence regulation and they could be compared to already known genes, which have more than one gene model. Thus, we should come up with a number of alternatively polyadenylated genes that play a role in senescence regulation, which then could be further analyzed.

Seed Storage Protein Expression in Vegetative Tissue

We suggested the formation of SSPs in leaves to be an interim-storage of nitrogen (N), which changes sink to source relation by storing and thereby “shutting away” available N that could be used for later remobilization. This would increase sink strength of developing tissues and thus enhance N-remobilization to these tissues. It would be interesting to prove this hypothesis by further experiments. By knocking out the expression of *CRUCIFERINS* and/ or *NAPINS* in leaves at different developmental stages, we could test efficiency in N-remobilization. That could be achieved by an artificial microRNA expressed under an inducible, leaf specific promoter. This could support our hypothesis that SSPs in leaves increase sink-strength. At the same time, this could show whether N-remobilization is also sink-limited and not only limited by N-uptake capacities. Improving N-use efficiency of crop plants is of central importance for agriculture in order to reduce nitrogenous fertilizers. The detection of the limiting factors that could be manipulated to increase N-use efficiency is a major goal of

Future Perspectives

research and SSPs in vegetative tissues could be one of the parameters. If this holds true, it would be of interest to investigate regulation of SSP expression and thus identify transacting factors.

Long term Perspectives

One of the greatest scientists, Sir Isaac Newton, said:

We are like children playing on the sea shore and diverting ourselves in now and then finding a smoother pebble or a prettier shell than ordinary, whilst the great ocean of truth lay all undiscovered before us.

He compares us to children, who are unable to grasp the essence of reality. However, if we long enough concern ourselves with “shells and pebbles” and have seen enough of them, one day there is the possibility that, as we become more mature, we can look to the horizon and see the ocean. In analogy to that, by elucidating gradually – little by little – key players and their interconnection in the senescence regulatory network, we could one day come closer to an understanding of the system in its entirety; and possibly, we might catch a glimpse of what kept the human mind busy for centuries: the mechanisms that govern the process of growing old. This deeper understanding may provide means to alter leaf senescence and improve agricultural traits of crop plants, which is one of our urgent challenges in times, in which the climate is changing more rapidly than expected.

6 References

- Andreasson, E., Jenkins, T., Brodersen, P., Thorgrimsen, S., Petersen, N.H.T., Zhu, S., Qiu, J.L., Micheelsen, P., Rocher, A., Petersen, M., et al. (2005). The MAP kinase substrate MKS1 is a regulator of plant defense responses. *EMBO J.* *24*, 2579–2589.
- Anne, G., Kohki, Y., Fabienne, S., Marie-Paule, B., Jean-Christophe, A., and Céline, M. (2012). Autophagy machinery controls nitrogen remobilization at the whole-plant level under both limiting and ample nitrate conditions in *Arabidopsis*. *New Phytol.* *194*, 732–740.
- Asai, T., Tena, G., Plotnikova, J., Willmann, M.R., Chiu, W.-L., Gomez-Gomez, L., Boller, T., Ausubel, F.M., and Sheen, J. (2002). MAP kinase signalling cascade in *Arabidopsis* innate immunity. *Nature* *415*, 977–983.
- Ay, N., Irmeler, K., Fischer, A., Uhlemann, R., Reuter, G., and Humbeck, K. (2009). Epigenetic programming via histone methylation at WRKY53 controls leaf senescence in *Arabidopsis thaliana*. *Plant J.* 333–346.
- Balazadeh, S., Riaño-Pachón, D.M., and Mueller-Roeber, B. (2008). Transcription factors regulating leaf senescence in *Arabidopsis thaliana*. *Plant Biol.* *10*, 63–75.
- Barbazuk, W.B., Fu, Y., and Mcginnis, K.M. (2008). Genome-wide analyses of alternative splicing in plants : Opportunities and challenges Genome-wide analyses of alternative splicing in plants : Opportunities and challenges. 1381–1392.
- Besseau, S., Li, J., and Palva, E.T. (2012). WRKY54 and WRKY70 co-operate as negative regulators of leaf senescence in *Arabidopsis thaliana*. *J. Exp. Bot.* *63*, 2667–2679.
- Bieker, S., Riester, L., Stahl, M., Franzaring, J., and Zentgraf, U. (2012). Senescence-specific Alteration of Hydrogen Peroxide Levels in *Arabidopsis thaliana* and Oilseed Rape Spring Variety *Brassica napus* L. cv. Mozart. *J. Integr. Plant Biol.* *54*, 540–554.
- Bienert, G.P., Møller, A.L.B., Kristiansen, K.A., Schulz, A., Møller, I.M., Schjoerring, J.K., and Jahn, T.P. (2007). Specific aquaporins facilitate the diffusion of hydrogen peroxide across membranes. *J. Biol. Chem.* *282*, 1183–1192.

References

- Bloom, A.J. (2015). The increasing importance of distinguishing among plant nitrogen sources. *Curr. Opin. Plant Biol.* 25, 10–16.
- Bouché, N., and Bouchez, D. (2001). Arabidopsis gene knockout: Phenotypes wanted. *Curr. Opin. Plant Biol.* 4, 111–117.
- Breeze, E., Harrison, E., McHattie, S., Hughes, L., Hickman, R., Hill, C., Kiddle, S., Kim, Y., Penfold, C.A., Jenkins, D., et al. (2011). High-Resolution Temporal Profiling of Transcripts during Arabidopsis Leaf Senescence Reveals a Distinct Chronology of Processes and Regulation. *Plant Cell* 23, 873–894.
- Bresson, J., Bieker, S., Riester, L., Doll, J., and Zentgraf, U. (2017). A guideline for leaf senescence analyses: from quantification to physiological and molecular investigations. *J. Exp. Bot.*
- Brunel-Muguet, S., D'Hooghe, P., Bataillé, M.-P., Larré, C., Kim, T.-H., Trouverie, J., Avice, J.-C., Etienne, P., and Dürr, C. (2016). Corrigendum: Heat Stress during Seed Filling Interferes with Sulfur Restriction on Grain Composition and Seed Germination in Oilseed Rape (*Brassica napus* L.). *Front. Plant Sci.* 6, 1–12.
- Brusslan, J.A., Rus Alvarez-Canterbury, A.M., Nair, N.U., Rice, J.C., Hitchler, M.J., and Pellegrini, M. (2012). Genome-wide evaluation of histone methylation changes associated with leaf senescence in Arabidopsis. *PLoS One* 7.
- Buchanan-Wollaston, V., Earl, S., Harrison, E., Mathas, E., Navabpour, S., Page, T., and Pink, D. (2003). The molecular analysis of leaf senescence--a genomics approach. *Plant Biotechnol J* 1, 3–22.
- Buchanan-Wollaston, V., Page, T., Harrison, E., Breeze, E., Pyung, O.L., Hong, G.N., Lin, J.F., Wu, S.H., Swidzinski, J., Ishizaki, K., et al. (2005). Comparative transcriptome analysis reveals significant differences in gene expression and signalling pathways between developmental and dark/starvation-induced senescence in Arabidopsis. *Plant J.* 42, 567–585.
- Chen, D., Xu, G., Tang, W., Jing, Y., Ji, Q., Fei, Z., and Lin, R. (2013a). Antagonistic Basic Helix-Loop-Helix/bZIP Transcription Factors Form Transcriptional Modules That Integrate Light and Reactive Oxygen Species Signaling in Arabidopsis. *Plant Cell* 25, 1657–1673.

References

- Chen, L., Zhang, L., and Yu, D. (2010). Wounding-Induced WRKY8 Is Involved in Basal Defense in Arabidopsis. *Mol. Plant-Microbe Interact.* 23, 558–565.
- Chen, L., Zhang, L., Li, D., Wang, F., and Yu, D. (2013b). WRKY8 transcription factor functions in the TMV-cg defense response by mediating both abscisic acid and ethylene signaling in Arabidopsis. *Proc. Natl. Acad. Sci.* 110, E1963–E1971.
- Chen, X., Lu, L., Mayer, K.S., Scalf, M., Qian, S., Lomax, A., Smith, L.M., and Zhong, X. (2016). POWERDRESS interacts with HISTONE DEACETYLASE 9 to promote aging in Arabidopsis. *Elife* 5, 1–23.
- Cui, Z., Zhang, H., Chen, X., Zhang, C., Ma, W., Huang, C., Zhang, W., Mi, G., Miao, Y., Li, X., et al. (2018). Pursuing sustainable productivity with millions of smallholder farmers. *Nature* 555, 363–366.
- Czedik-Eysenberg, A., Seitner, S., Güldener, U., Koemeda, S., Jez, J., Colombini, M., and Djamei, A. (2018). The “PhenoBox”, a flexible, automated, open-source plant phenotyping solution. *New Phytol.* 219, 808–823.
- Desikan, R., Mackerness, S.A.H., Hancock, J.T., and Neill, S.J. (2001). Regulation of the Arabidopsis Transcriptome by Oxidative Stress. *Plant Physiol.* 127, 159–172.
- Dong, J., Chen, C., and Chen, Z. (2003). Expression profiles of the Arabidopsis WRKY gene superfamily during plant defense response. *Plant Mol. Biol.* 51, 21–37.
- Evans, J.R. (1989). Photosynthesis and nitrogen relationships in leaves of C3 plants. *Oecologia* 78, 9–19.
- Ferreiro, I., Barragan, M., Gubern, A., Ballestar, E., Joaquin, M., and Posas, F. (2010). The p38 SAPK is recruited to chromatin via its interaction with transcription factors. *J. Biol. Chem.* 285, 31819–31828.
- Forde, B.G., Cutler, S.R., Zaman, N., and Krysan, P.J. (2013). Glutamate signalling via a MEKK1 kinase-dependent pathway induces changes in Arabidopsis root architecture. *Plant J.* 75, 1–10.
- Fritz, C., Palacios-Rojas, N., Feil, R., and Stitt, M. (2006). Regulation of secondary metabolism by the carbon-nitrogen status in tobacco: Nitrate inhibits large sectors of phenylpropanoid metabolism. *Plant J.* 46, 533–548.

References

- Gan, S., and Amasino, R.M. (1997). Making Sense of Senescence. *Plant Physiol.* 113, 313–319.
- Girondé, A., Etienne, P., Trouverie, J., Bouchereau, A., Le Cahérec, F., Leport, L., Orsel, M., Niogret, M.F., Nesi, N., Carole, D., et al. (2015). The contrasting N management of two oilseed rape genotypes reveals the mechanisms of proteolysis associated with leaf N remobilization and the respective contributions of leaves and stems to N storage and remobilization during seed filling. *BMC Plant Biol.* 15.
- van der Graaff, E., Schwacke, R., Schneider, A., Desimone, M., Flügge, U.-I., and Kunze, R. (2006). Transcription analysis of arabidopsis membrane transporters and hormone pathways during developmental and induced leaf senescence. *Plant Physiol.* 141, 776–792.
- Grbic, V., and Bleeker, A.B. (1995). Ethylene regulates the timing of leaf senescence in *Arabidopsis*. *Plant J.* 8, 595–602.
- Guiboileau, A., Sormani, R., Meyer, C., and Masclaux-Daubresse, C. (2010). Senescence and death of plant organs: Nutrient recycling and developmental regulation. *Comptes Rendus - Biol.* 333, 382–391.
- Guo, Y., and Gan, S. (2012). Convergence and divergence in gene expression profiles induced by leaf senescence and 27 senescence-promoting hormonal, pathological and environmental stress treatments. *Plant, Cell Environ.* 35, 644–655.
- Guo, Y., Cai, Z., and Gan, S. (2004). Transcriptome of *Arabidopsis* Leaf Senescence. *Plant. Cell Environ.* 27, 521–549.
- He, H., Van Breusegem, F., and Mhamdi, A. (2018). Redox-dependent Control of Nuclear Transcription in Plants. *J. Exp. Bot.* 1–14.
- Hinderhofer, K., and Zentgraf, U. (2001). Identification of a transcription factor specifically expressed at the onset of leaf senescence. *Planta* 213, 469–473.
- Hörtensteiner, S., and Kräutler, B. (2011). Chlorophyll breakdown in higher plants. *Biochim. Biophys. Acta - Bioenerg.* 1807, 977–988.
- Ichimura, K., Shinozaki, K., Tena, G., Sheen, J., Henry, Y., Champion, A., Kreis, M., Zhang, S., Hirt, H., Wilson, C., et al. (2002). Mitogen-activated protein kinase cascades

References

in plants: a new nomenclature. *Trends Plant Sci.* 7, 301–308.

Ichimura, K., Casais, C., Peck, S.C., Shinozaki, K., and Shirasu, K. (2006). MEKK1 is required for MPK4 activation and regulates tissue-specific and temperature-dependent cell death in *Arabidopsis*. *J. Biol. Chem.* 281, 36969–36976.

Jansson, S., and Thomas, H. (2008). Senescence: developmental program or timetable? *New Phytol.* 179, 575–579.

Jarvis, P., and López-Juez, E. (2013). Biogenesis and homeostasis of chloroplasts and other plastids. *Nat. Rev. Mol. Cell Biol.* 14, 787–802.

Jia, M., Liu, X., Xue, H., Wu, Y., Shi, L., Wang, R., Chen, Y., Xu, N., Shao, J., Qi, Y., et al. (2019). Noncanonical ATG8-ABS3 interaction controls senescence in plants. *Nat. Plants* 5, 212–224.

Jiang, Y., Liang, G., Yang, S., and Yu, D. (2014). *Arabidopsis* WRKY57 Functions as a Node of Convergence for Jasmonic Acid- and Auxin-Mediated Signaling in Jasmonic Acid-Induced Leaf Senescence. *Plant Cell* 26, 230–245.

Jing, H.C., Sturre, M.J.G., Hille, J., and Dijkwel, P.P. (2002). *Arabidopsis* onset of leaf death mutants identify a regulatory pathway controlling leaf senescence. *Plant J.* 32, 51–63.

Johnson, G.N., and Maxwell, K. (2000). Chlorophyll fluorescence - a practical guide. *J. Exp. Bot.* 51, 659–668.

Khan, M., Rozhon, W., and Poppenberger, B. (2013). The role of hormones in the aging of plants - A mini-review. *Gerontology* 60, 49–55.

Kim, J., Woo, H.R.R., and Nam, H.G.G. (2016). Toward Systems Understanding of Leaf Senescence: An Integrated Multi-Omics Perspective on Leaf Senescence Research. *Mol. Plant* 9, 813–825.

Kim, J., Kim, J.H., Lyu, J. II, Woo, H.R., and Lim, P.O. (2017). New insights into the regulation of leaf senescence in *Arabidopsis*. *J. Exp. Bot.*

Koornneef, M., Hanhart, C.J., and van der Veen, J.H. (1991). A genetic and physiological analysis of late flowering mutants in *Arabidopsis thaliana*. *MGG Mol. Gen. Genet.* 229, 57–66.

References

- Koyama, T., Nii, H., Mitsuda, N., Ohta, M., Kitajima, S., Ohme-Takagi, M., and Sato, F. (2013). A regulatory cascade involving class II ETHYLENE RESPONSE FACTOR transcriptional repressors operates in the progression of leaf senescence. *Plant Physiol.* *162*, 991–1005.
- Kretz-Remy, C., and Arrigo, A.P. (2002). Gene expression and thiol redox state. *Methods Enzymol.* *348*, 200–215.
- Laine, P., Ourry, A., Macduff, J., Boucaud, J., and Salette, J. (1993). Kinetic parameters of nitrate uptake by different catch crop species: effects of low temperatures or previous nitrate starvation. *Physiol. Plant.* *88*, 85–92.
- Lawrence, M.C., McGlynn, K., Shao, C., Duan, L., Naziruddin, B., Levy, M.F., and Cobb, M.H. (2008). Chromatin-bound mitogen-activated protein kinases transmit dynamic signals in transcription complexes in -cells. *Proc. Natl. Acad. Sci.* *105*, 13315–13320.
- Li, J.-F., Bush, J., Sheen, J., Chung, H.S., Niu, Y., and McCormack, M. (2013). Comprehensive Protein-Based Artificial MicroRNA Screens for Effective Gene Silencing in Plants. *Plant Cell* *25*, 1507–1522.
- Li, Q., Lin, Y.-C., Sun, Y.-H., Song, J., Chen, H., Zhang, X.-H., Sederoff, R.R., and Chiang, V.L. (2012). Splice variant of the SND1 transcription factor is a dominant negative of SND1 members and their regulation in *Populus trichocarpa*. *Proc. Natl. Acad. Sci.* *109*, 14699–14704.
- Licausi, F., Ohme-Takagi, M., and Perata, P. (2013). APETALA2/ethylene responsive factor (AP2/ERF) transcription factors: Mediators of stress responses and developmental programs. *New Phytol.* *199*, 639–649.
- Lim, P.O., Kim, H.J., and Nam, H.G. (2007). Leaf Senescence. In *Annual Review of Plant Biology*, pp. 115–136.
- Lin, J.F., and Wu, S.H. (2004). Molecular events in senescing Arabidopsis leaves. *Plant J.* *39*, 612–628.
- Llorca, C.M., Potschin, M., and Zentgraf, U. (2014). bZIPs and WRKYs: two large transcription factor families executing two different functional strategies. *Front. Plant Sci.* *5*, 1–14.

References

- Lockshin, R.A., and Zakeri, Z. (2004). Apoptosis, autophagy, and more. *Int. J. Biochem. Cell Biol.* 36, 2405–2419.
- Lundquist, P.K., Poliakov, A., Bhuiyan, N.H., Zybailov, B., Sun, Q., and van Wijk, K.J. (2012). The Functional Network of the Arabidopsis Plastoglobule Proteome Based on Quantitative Proteomics and Genome-Wide Coexpression Analysis. *PLANT Physiol.* 158, 1172–1192.
- Lyons, R., Iwase, A., Gänsewig, T., Sherstnev, A., Duc, C., Barton, G.J., Hanada, K., Higuchi-Takeuchi, M., Matsui, M., Sugimoto, K., et al. (2013). The RNA-binding protein FPA regulates flg22-triggered defense responses and transcription factor activity by alternative polyadenylation. *Sci. Rep.* 3, 2866.
- Makino, A., and Osmond, B. (1991). Effects of Nitrogen Nutrition on Nitrogen Partitioning between Chloroplasts and Mitochondria in Pea and Wheat. *PLANT Physiol.* 96, 355–362.
- Makino, A., Sato, T., Nakano, H., and Mae, T. (1997). Leaf photosynthesis, plant growth and nitrogen allocation in rice under different irradiances. *Planta* 203, 397.
- Makino, A., Sakuma, I., Sudo, E., and Mae, T. (2003). Differences between Maize and Rice in N-use Efficiency for Photosynthesis and Protein Allocation. *Plant Cell Physiol.* 44, 952–956.
- Marinho, H.S., Real, C., Cyrne, L., Soares, H., and Antunes, F. (2014). Hydrogen peroxide sensing, signaling and regulation of transcription factors. *Redox Biol.* 2, 535–562.
- Martínez, D.E., Costa, M.L., Gomez, F.M., Otegui, M.S., and Guiamet, J.J. (2008). “Senescence-associated vacuoles” are involved in the degradation of chloroplast proteins in tobacco leaves. *Plant J.* 56, 196–206.
- Masclaux-Daubresse, C., Daniel-Vedele, F., Dechorgnat, J., Chardon, F., Gaufichon, L., and Suzuki, A. (2010). Nitrogen uptake, assimilation and remobilization in plants: Challenges for sustainable and productive agriculture. *Ann. Bot.* 105, 1141–1157.
- Mastrangelo, A.M., Marone, D., Laidò, G., De Leonardis, A.M., and De Vita, P. (2012). Alternative splicing: Enhancing ability to cope with stress via transcriptome plasticity. *Plant Sci.* 185–186, 40–49.

References

- Matsuoka, D., Yasufuku, T., Furuya, T., and Nanmori, T. (2015). An abscisic acid inducible Arabidopsis MAPKKK, MAPKKK18 regulates leaf senescence via its kinase activity. *Plant Mol. Biol.* 87, 565–575.
- Mhamdi, A., Noctor, G., and Baker, A. (2012). Plant catalases: Peroxisomal redox guardians. *Arch. Biochem. Biophys.* 525, 181–194.
- Miao, Y., and Zentgraf, U. (2007). The antagonist function of Arabidopsis WRKY53 and ESR/ESP in leaf senescence is modulated by the jasmonic and salicylic acid equilibrium. *Plant Cell* 19, 819–830.
- Miao, Y., Laun, T., Zimmermann, P., and Zentgraf, U. (2004). Targets of the WRKY53 transcription factor and its role during leaf senescence in Arabidopsis. *Plant Mol. Biol.* 55, 853–867.
- Miao, Y., Laun, T.M., Smykowski, A., and Zentgraf, U. (2007). Arabidopsis MEKK1 can take a short cut: It can directly interact with senescence-related WRKY53 transcription factor on the protein level and can bind to its promoter. *Plant Mol. Biol.* 65, 63–76.
- Mizoi, J., Shinozaki, K., and Yamaguchi-Shinozaki, K. (2012). AP2/ERF family transcription factors in plant abiotic stress responses. *Biochim. Biophys. Acta - Gene Regul. Mech.* 1819, 86–96.
- Nakagami, H., Soukupová, H., Schikora, A., Žárský, V., and Hirt, H. (2006). A mitogen-activated protein kinase kinase kinase mediates reactive oxygen species homeostasis in Arabidopsis. *J. Biol. Chem.* 281, 38697–38704.
- Nakano, T., Suzuki, K., Fujimura, T., and Shinshi, H. (2006). Genome-wide analysis of the ERF Gene Family in Arabidopsis and rice. *Plant Physiol.* 140, 411–432.
- Noctor, G., Veljovic-Jovanovic, S., Driscoll, S., Novitskaya, L., and Foyer, C.H. (2002). Drought and oxidative load in the leaves of C3 plants: A predominant role for photorespiration? *Ann. Bot.* 89, 841–850.
- Ohme-takagi, M., and Shinshi, H. (1995). Ethylene-Inducible DNA Binding Proteins That Interact with an Ethylene-Responsive Element. *Plant Cell* 7, 173–182.
- Ohta, M., Ohme-Takagi, M., and Shinshi, H. (2000). Three ethylene-responsive transcription factors in tobacco with distinct transactivation functions. *Plant J.* 22, 29–

References

38.

Olsen, A.N., Ernst, H.A., Leggio, L. Lo, and Skriver, K. (2005). NAC transcription factors: Structurally distinct, functionally diverse. *Trends Plant Sci.* 10, 79–87.

Orendi, G., Zimmermann, P., Baar, C., and Zentgraf, U. (2001). Loss of stress-induced expression of catalase3 during leaf senescence in *Arabidopsis thaliana* is restricted to oxidative stress. *Plant Sci.* 161, 301–314.

Otegui, M.S. (2018). Vacuolar degradation of chloroplast components: Autophagy and beyond. *J. Exp. Bot.* 69, 741–750.

Palma, J.M., Corpas, F.J., and Del Río, L.A. (2009). Proteome of plant peroxisomes: New perspectives on the role of these organelles in cell biology. *Proteomics* 9, 2301–2312.

Parthier, B. (1988). Gerontoplasts - The Yellow End In The Ontogenesis Of Chloroplasts. *Endocytobiosis Cell Res.* 163–190.

Peng, M., Hudson, D., Schofield, A., Tsao, R., Yang, R., Gu, H., Bi, Y.M., and Rothstein, S.J. (2008). Adaptation of *Arabidopsis* to nitrogen limitation involves induction of anthocyanin synthesis which is controlled by the NLA gene. *J. Exp. Bot.* 59, 2933–2944.

Potschin, M., Schlienger, S., Bieker, S., and Zentgraf, U. (2014). Senescence Networking: WRKY18 is an Upstream Regulator, a Downstream Target Gene, and a Protein Interaction Partner of WRKY53. *J. Plant Growth Regul.* 33, 106–118.

Qiu, J.-L., Zhou, L., Yun, B.-W., Nielsen, H.B., Fiil, B.K., Petersen, K., MacKinlay, J., Loake, G.J., Mundy, J., and Morris, P.C. (2008). *Arabidopsis* Mitogen-Activated Protein Kinase Kinases MKK1 and MKK2 Have Overlapping Functions in Defense Signaling Mediated by MEKK1, MPK4, and MKS1. *PLANT Physiol.* 148, 212–222.

Riechmann, J.L., Heard, J., Martin, G., Reuber, L., -Z., C., Jiang, Keddie, J., Adam, L., Pineda, O., Ratcliffe, O.J., et al. (2000). *Arabidopsis* Transcription Factors: Genome-Wide Comparative Analysis Among Eukaryotes. *Science* (80-.). 290, 2105–2110.

Riera, C.E., Merkwirth, C., De Magalhaes Filho, C.D., and Dillin, A. (2016). Signaling Networks Determining Life Span. *Annu. Rev. Biochem.* 85, 35–64.

References

- del Río, L.A., Corpas, F.J., Hernández, J.A., Pastori, G.M., Jiménez, A., Sevilla, F., López-Huertas, E., Sandalio, L.M., and Palma, J.M. (1998). The Activated Oxygen Role of Peroxisomes in Senescence. *Plant Physiol.* *116*, 1195–1200.
- Robatzek, S., and Somssich, I.E. (2002). Targets of AtWRKY6 regulation during plant senescence and pathogen defense. *Genes Dev.* 1139–1149.
- Roberts, I.N., Caputo, C., Criado, M.V., and Funk, C. (2012). Senescence-associated proteases in plants. *Physiol. Plant.* *145*, 130–139.
- Rossato, L., Lainé, P., and Ourry, A. (2001). Nitrogen storage and remobilization in *Brassica napus* L. during the growth cycle: Nitrogen fluxes within the plant and changes in soluble protein patterns. *J. Exp. Bot.* *52*, 1655–1663.
- Rushton, P.J., Somssich, I.E., Ringler, P., and Shen, Q.J. (2010). WRKY transcription factors. *Trends Plant Sci.* *15*, 247–258.
- Safavi-Rizi, V., Franzaring, J., Fangmeier, A., and Kunze, R. (2018). Divergent N Deficiency-Dependent Senescence and Transcriptome Response in Developmentally Old and Young *Brassica napus* Leaves. *Front. Plant Sci.* *9*, 1–15.
- Sakuraba, Y., Jeong, J., Kang, M.-Y., Kim, J., Paek, N.-C., and Choi, G. (2014). Phytochrome-interacting transcription factors PIF4 and PIF5 induce leaf senescence in *Arabidopsis*. *Nat. Commun.* *5*, 1–13.
- Sanchez, S.E., and Kay, S.A. (2016). The plant circadian clock: From a simple timekeeper to a complex developmental manager. *Cold Spring Harb. Perspect. Biol.* *8*.
- Schjoerring, J.K., Bock, J.G.H., Gammelvind, L., Jensen, C.R., and Mogensen, V.O. (1995). Nitrogen incorporation and remobilization in different shoot components of field-grown winter oilseed rape (*Brassica napus* L.) as affected by rate of nitrogen application and irrigation. *Plant Soil* *177*, 255–264.
- Schulze, W., Schulze, E.-D., Stadler, J., Heilmeyer, H., Stitt, M., and Mooney, H.A. (2006). Growth and reproduction of *Arabidopsis thaliana* in relation to storage of starch and nitrate in the wild-type and in starch-deficient and nitrate-uptake-deficient mutants. *Plant, Cell Environ.* *17*, 795–809.

References

- Severing, E.I., van Dijk, A.D.J., Morabito, G., Busscher-Lange, J., Immink, R.G.H., and van Ham, R.C.H.J. (2012). Predicting the Impact of Alternative Splicing on Plant MADS Domain Protein Function. *PLoS One* 7, e30524.
- Shaikhali, J., Heiber, I., Seidel, T., Ströher, E., Hiltcher, H., Birkmann, S., Dietz, K.J., and Baier, M. (2008). The redox-sensitive transcription factor Rap2.4a controls nuclear expression of 2-Cys peroxiredoxin A and other chloroplast antioxidant enzymes. *BMC Plant Biol.* 8, 1–14.
- Shaikhali, J., Norén, L., De Dios Barajas-López, J., Srivastava, V., König, J., Sauer, U.H., Wingsle, G., Dietz, K.J., and Strand, Å. (2012). Redox-mediated mechanisms regulate DNA binding activity of the G-group of basic region leucine zipper (bZIP) transcription factors in Arabidopsis. *J. Biol. Chem.* 287, 27510–27525.
- Smart, C.M. (1994). Gene expression during leaf senescence. *Tansley Review No . 64. New Phytol.* 126, 419–448.
- Smirnoff, N., and Arnaud, D. (2019). Hydrogen peroxide metabolism and functions in plants. *New Phytol.* 221, 1197–1214.
- Soubeyrand, E., Basteau, C., Hilbert, G., Van Leeuwen, C., Delrot, S., and Gomès, E. (2014). Nitrogen supply affects anthocyanin biosynthetic and regulatory genes in grapevine cv. Cabernet-Sauvignon berries. *Phytochemistry* 103, 38–49.
- Suarez-Rodriguez, M.C., Adams-Phillips, L., Liu, Y., Wang, H., Su, S., Jester, P.J., Zhang, S., Bent, A.F., and Krysan, P.J. (2006). MEKK1 Is Required for flg22-Induced MPK4 Activation in Arabidopsis Plants. *PLANT Physiol.* 143, 661–669.
- Taylor, C.B., Bariola, P.A., DelCardayre, S.B., Raines, R.T., and Green, P.J. (1993). RNS2: a senescence-associated RNase of Arabidopsis that diverged from the S-RNases before speciation. *Proc. Natl. Acad. Sci.* 90, 5118–5122.
- Tegeder, M., and Masclaux-Daubresse, C. (2018). Source and sink mechanisms of nitrogen transport and use. *New Phytol.* 217, 35–53.
- Tegeder, M., and Rentsch, D. (2010). Uptake and partitioning of amino acids and peptides. *Mol. Plant* 3, 997–1011.
- Thomas, H., and Stoddart, J.L. (1980). LEAF SENESCENCE. *Ann. Rev. Plant Physiol*

References

31, 83–111.

Thomas, H., Ougham, H.J., Wagstaff, C., and Stead, A.D. (2003). Defining senescence and death. *J. Exp. Bot.* 54, 1127–1132.

Thompson, J.E., Froese, C.D., Madey, E., Smith, M.D., and Hong, Y. (1998). Lipid metabolism during plant senescence. *Prog. Lipid Res.* 37, 119–141.

Veley, K.M., Berry, J.C., Pokorny, A.A., Bart, R.S., and Fahlgren, N. (2018). An automated, high-throughput method for standardizing image color profiles to improve image-based plant phenotyping. *PeerJ* 6, e5727.

Viola, I.L., Guttlein, L.N., and Gonzalez, D.H. (2013). Redox Modulation of Plant Developmental Regulators from the Class I TCP Transcription Factor Family. *Plant Physiol.* 162, 1434–1447.

Wan, J., Zhang, S., and Stacey, G. (2004). Activation of a mitogen-activated protein kinase pathway in Arabidopsis by chitin. *Mol. Plant Pathol.* 5, 125–135.

Wang, X., and Larkins, B.A. (2001). Genetic Analysis of Amino Acid Accumulation in opaque-2 Maize Endosperm. *Plant Physiol.* 125, 1766–1777.

Wang, H., Avci, U., Nakashima, J., Hahn, M.G., Chen, F., and Dixon, R.A. (2010). Mutation of WRKY transcription factors initiates pith secondary wall formation and increases stem biomass in dicotyledonous plants. *Proc. Natl. Acad. Sci.* 107, 22338–22343.

Wang, X., Yang, S., Wang, S., Hao, D., Liu, X., Yu, Y., and Yue, L. (2009). Four divergent Arabidopsis ethylene-responsive element-binding factor domains bind to a target DNA motif with a universal CG step core recognition and different flanking bases preference. *FEBS J.* 276, 7177–7186.

Waszczak, C., Carmody, M., and Kangasjärvi, J. (2018). Reactive oxygen species in plant signaling. *Annu. Rev. Plant Biol.* 69, 209–236.

Watanabe, M., Balazadeh, S., Tohge, T., Erban, A., Giavalisco, P., Kopka, J., Mueller-Roeber, B., Fernie, A.R., and Hoefgen, R. (2013). Comprehensive Dissection of Spatiotemporal Metabolic Shifts in Primary, Secondary, and Lipid Metabolism during Developmental Senescence in Arabidopsis. *Plant Physiol.* 162, 1290–1310.

References

- Welsch, R., Maass, D., Voegel, T., DellaPenna, D., and Beyer, P. (2007). Transcription Factor RAP2.2 and Its Interacting Partner SINAT2: Stable Elements in the Carotenogenesis of Arabidopsis Leaves. *Plant Physiol.* *145*, 1073–1085.
- Wojciechowska, N., Sobieszczuk-Nowicka, E., and Bagniewska-Zadworna, A. (2018). Plant organ senescence – regulation by manifold pathways. *Plant Biol.* *20*, 167–181.
- Woo, H.R., Kim, J.H., Nam, H.G., and Lim, P.O. (2004). The Delayed Leaf Senescence Mutants of Arabidopsis, *ore1*, *ore3*, and *ore9* are Tolerant to Oxidative Stress. *Plant Cell Physiol.* *45*, 923–932.
- Woo, H.R., Kim, H.J., Nam, H.G., and Lim, P.O. (2013). Plant leaf senescence and death - regulation by multiple layers of control and implications for aging in general. *J. Cell Sci.* *126*, 4823–4833.
- Xie, Y., Huhn, K., Brandt, R., Potschin, M., Bieker, S., Straub, D., Doll, J., Drechsler, T., Zentgraf, U., and Wenkel, S. (2014). REVOLUTA and WRKY53 connect early and late leaf development in Arabidopsis. *Development* *141*, 4772–4783.
- Xu, X., Chen, C., Fan, B., and Chen, Z. (2006). Physical and Functional Interactions between WRKY60 Transcription Factors. *Plant Cell* *18*, 1310–1326.
- Yang, Z., Tian, L., Latoszek-Green, M., Brown, D., and Wu, K. (2005). Arabidopsis ERF4 is a transcriptional repressor capable of modulating ethylene and abscisic acid responses. *Plant Mol. Biol.* *58*, 585–596.
- Zentgraf, U., and Hemleben, V. (2008). Molecular Cell Biology: Are Reactive Oxygen Species Regulators of Leaf Senescence? In *Progress in Botany*, pp. 117–138.
- Zentgraf, U., Jobst, J., Kolb, D., and Rentsch, D. (2004). Senescence-related gene expression profiles of rosette leaves of Arabidopsis thaliana: Leaf age versus plant age. *Plant Biol.* *6*, 178–183.
- Zentgraf, U., Laun, T., and Miao, Y. (2010). The complex regulation of WRKY53 during leaf senescence of Arabidopsis thaliana. *Eur. J. Cell Biol.* *89*, 133–137.
- Zhang, Y., Wang, Y., Wei, H., Li, N., Tian, W., Chong, K., and Wang, L. (2018). Circadian Evening Complex Represses Jasmonate-Induced Leaf Senescence in Arabidopsis. *Mol. Plant* *11*, 326–337.

References

- Zheng, Z., Qamar, S.A., Chen, Z., and Mengiste, T. (2006). Arabidopsis WRKY33 transcription factor is required for resistance to necrotrophic fungal pathogens. *Plant J.* 48, 592–605.
- Zheng, Z., Mosher, S.L., Fan, B., Klessig, D.F., and Chen, Z. (2007). Functional analysis of Arabidopsis WRKY25 transcription factor in plant defense against *Pseudomonas syringae*. *BMC Plant Biol.* 7, 1–13.
- Zhou, C., Cai, Z., Guo, Y., and Gan, S. (2009). An Arabidopsis Mitogen-Activated Protein Kinase Cascade, MKK9-MPK6, Plays a Role in Leaf Senescence. *Plant Physiol.* 150, 167–177.
- Zhou, X., Jiang, Y., and Yu, D. (2011). WRKY22 transcription factor mediates dark-induced leaf senescence in Arabidopsis. *Mol. Cells* 31, 303–313.
- Zimmermann, P., and Zentgraf, U. (2005). The correlation between oxidative stress and senescence during plant development. *Cell. Mol. Biol. Lett.* 10, 515–534.
- Zimmermann, P., Heinlein, C., Orendi, G., and Zentgraf, U. (2006). Senescence-specific regulation of catalases in Arabidopsis thaliana (L.) Heynh. *Plant, Cell Environ.* 29, 1049–1060.

7 Danksagung

An dieser Stelle möchte ich allen danken, die mir die Erstellung dieser Arbeit ermöglicht haben.

Frau Professor Ulrike Zentgraf bin ich zu besonderem Dank verpflichtet. Danke Uli, dass du mir die Möglichkeit eröffnet hast, die Doktorarbeit in deiner Arbeitsgruppe anzufertigen, dass du mich jederzeit mit thematischen und wissenschaftlichen Anregungen unterstützt hast und dass ich während dieser Zeit so viel lernen durfte.

Bei Professor Klaus Harter möchte ich mich für die Bereitschaft bedanken, diese Arbeit zu begutachten. Außerdem möchte ich mich bei Prof. Harter und Prof. Christopher Grefen dafür bedanken, dass sie mich als „Thesis Advisory Commity“ stets mit wertvollem, wissenschaftlichem Rat unterstützt haben.

Herzlich bedanke ich mich bei der AG Zentgraf für die Unterstützung, die nette Zusammenarbeit und nicht zu vergessen, die kulinarischen Highlights bei unseren gemeinsamen Koch-Aktionen. Danke Jasmin, für viele hilfreiche Tipps, deine tatkräftige Unterstützung bei Problemen im Laboralltag und für viele nette Gespräche. Danke Stefan dafür, dass du mir viel gezeigt, geholfen und mich als Student in die Laborarbeit eingewiesen hast. Danke Maren, Carles und Justine für viele Tipps und viele tolle Momente. Danke auch an Gesine und Siliya, die mir bei zahlreichen Phänotypisierungen eine helfende Hand waren.

Des Weiteren möchte ich mich beim gesamten 6. Stock für die schöne Atmosphäre, für viele aufmunternde und kritische Diskussionen bedanken.

Ein besonderer Dank gilt meinen Eltern. Danke für all die Jahre Eures Lebens, die Ihr in mich investiert habt. Danke für die Liebe und Geduld, mit der Ihr mich erzogen habt, und die ungebrochene Unterstützung, die Ihr mir zuteilwerden lasst. Ohne Euch wäre ich nicht der Mensch, der ich heute bin.

Meine tiefste Dankbarkeit möchte ich meinen zwei Liebsten aussprechen. Gero, es ist schön, dich an meiner Seite zu haben; danke dafür, dass du mich in jeder Situation unterstützt und motivierst. Danke Julius, dass du mich täglich aufs Neue daran erinnerst, was wirklich wichtig ist.

8 Appendix

Published research articles

- I. **Impact of Alternatively Polyadenylated Isoforms of ETHYLENE RESPONSE FACTOR 4 with Activator and Repressor Function on Senescence in *Arabidopsis thaliana* L.**

L. Riester, S. Köster-Hofmann, J. Doll, K.W. Berendzen and U. Zentgraf
Genes; January 2019

- II. **Nitrogen Supply Drives Senescence-Related Seed Storage Protein Expression in Rapeseed Leaves**

S. Bieker, L. Riester, J. Doll, J. Franzaring, A. Fangmeier and U. Zentgraf
Genes; January 2019

Unpublished research article

- III. **WRKY25: A negative Senescence-Regulator with a Redox-state dependent Regulation of *WRKY53*.**

J. Doll*, M. Muth*, L. Riester, K. W. Berendzen, J. Bresson, U. Zentgraf
Unpublished, *shared first author

Published review article

- IV. **A guideline for leaf senescence analyses: from quantification to physiological and molecular investigations**

J. Bresson*, S. Bieker*, L. Riester*, J. Doll* and U. Zentgraf
Journal of Experimental Botany; February 2018, *shared first author


Published Spotlight

- V. **Live and Let Die: The core circadian oscillator coordinates life history of plants and pilots leaf senescence**

U. Zentgraf, J. Doll, L. Riester
Molecular Plant; March 2018

Article

Impact of Alternatively Polyadenylated Isoforms of ETHYLENE RESPONSE FACTOR4 with Activator and Repressor Function on Senescence in *Arabidopsis thaliana* L.

Lena Riester, Siliya Köster-Hofmann, Jasmin Doll, Kenneth W. Berendzen 
and Ulrike Zentgraf *

Center for Plant Molecular Biology (ZMBP), University of Tuebingen, 72076 Tuebingen, Germany; lena.riester@zmbp.uni-tuebingen.de (L.R.); hofmann@uni-tuebingen.de (S.K.-H.); jasmin.doll@zmbp.uni-tuebingen.de (J.D.); kenneth.berendzen@zmbp.uni-tuebingen.de (K.W.B.)

* Correspondence: ulrike.zentgraf@zmbp.uni-tuebingen.de

Received: 19 December 2018; Accepted: 22 January 2019; Published: 28 January 2019



Abstract: Leaf senescence is highly regulated by transcriptional reprogramming, implying an important role for transcriptional regulators. ETHYLENE RESPONSE FACTOR4 (ERF4) was shown to be involved in senescence regulation and to exist in two different isoforms due to alternative polyadenylation of its pre-mRNA. One of these isoforms, ERF4-R, contains an ERF-associated amphiphilic repression (EAR) motif and acts as repressor, whereas the other form, ERF4-A, is lacking this motif and acts as activator. Here, we analyzed the impact of these isoforms on senescence. Both isoforms were able to complement the delayed senescence phenotype of the *erf4* mutant with a tendency of ERF4-A for a slightly better complementation. However, overexpression led to accelerated senescence of 35S:*ERF4-R* plants but not of 35S:*ERF4-A* plants. We identified *CATALASE3* (*CAT3*) as direct target gene of ERF4 in a yeast-one-hybrid screen. Both isoforms directly bind to the *CAT3* promoter but have antagonistic effects on gene expression. The ratio of *ERF4-A* to *ERF4-R* mRNA changed during development, leading to a complex age-dependent regulation of *CAT3* activity. The RNA-binding protein FPA shifted the R/A-ratio and *fpa* mutants are pointing towards a role of alternative polyadenylation regulators in senescence.

Keywords: Alternative polyadenylation; ETHYLENE RESPONSE FACTOR4; senescence regulation; *CATALASE3*; FPA; *Arabidopsis*

1. Introduction

At the end of their development, plants lose their photosynthetic capacity and finally shed their leaves. To avoid an uneconomic loss of stored energy, minerals and nutrients through leaf abscission, the leaves undergo leaf senescence before they die. During this process, plants recycle resources and nutrients by relocating them to developing organs. It is a dynamic and highly regulated process driven by a complex genetically encoded program. However, under stress conditions, senescence is induced prematurely as an exit strategy. Therefore, this program requires a high plasticity through constantly integrating endogenous and exogenous signals. Molecules such as plant hormones, nitrogen and sugar compounds, calcium, reactive oxygen species (ROS) and most likely further substances mediate signal transduction [1–5].

In general, ROS act as signaling molecules at their site of production due to their short half-life. Among all ROS, hydrogen peroxide (H₂O₂) is most likely the signaling molecule with the broadest reach, since it is more stable than other ROS and it can pass membranes [6]. Hydrogen peroxide

is involved in many signal transduction pathways spanning from biotic to abiotic stress responses, but also participates in the regulation of senescence processes. The onset of senescence coincides with an increase of intracellular H_2O_2 levels as a result of a coordinated regulation of the H_2O_2 scavenging enzymes catalase and ascorbate peroxidase [7,8]. Many senescence-associated genes and transcription factors are upregulated by ROS. Differential gene expression plays an important role in the coordination of leaf senescence onset and progression [9–12]. Breeze and coworkers [12] suggested that the temporal expression and activation of transcription factors (TFs) is a crucial aspect in the course of leaf senescence. Among others, several members of the APETALA2/ETHYLENE RESPONSE FACTOR (AP2/ERFs) family are regulated in a senescence-dependent manner [9,11,12]. AP2/ERFs form a superfamily of 147 TF genes in Arabidopsis [13,14]. Up to now, a number of AP2/ERFs have been reported to be involved in stress responses and developmental processes [15]. Some AP2/ERF TFs are involved in the responses to components of stress signal transduction pathways, such as ROS, ethylene, jasmonic acid (JA), abscisic acid (ABA) and cytokinin, all of which are also important molecules in senescence-associated signaling [14,16]. During leaf senescence, RELATED TP ABI3/VP1 (RAV1) and C-REPEAT/DEHYDRATION RESPONSIBLE ELEMENT BINDING FACTOR 2 (CBF2) have been reported to be positive and negative regulators, respectively. Moreover, Koyama et al. [17] have shown that ERF4 (At3g15210) and ERF8 (At1g53170) act together as positive regulators of leaf senescence by suppressing the expression of its direct target gene *EPITHIOSPECIFIER PROTEIN/EPITHIOSPECIFYING SENESCENCE REGULATOR (ESP/ESR)* (At1g54040). This protein is a negative regulator of the transcription factor WKRY53 (At4g23810), a positive regulator of leaf senescence [18,19]. WKRY53 turns out to be a central node of a complex regulatory network of leaf senescence and to underlie a tight multi-layer control of expression, activity and protein stability [20–23]. In addition, ERF4 can up-regulate intracellular ROS production, as overexpression of *ERF4* led to higher ROS levels, visualized by Trypan blue and DAB (3,3-diaminobenzidine)-staining [17]. In contrast, *erf4/erf8* double-mutant plants produce fewer amounts of ROS during dark-induced senescence, indicating that ERF4 and/or 8 are themselves involved in regulating intracellular ROS contents [17].

The Arabidopsis *ERF4* belongs to the ERF subfamily containing 122 genes. They only possess one AP2/ERF domain, which is their distinguishing feature [13,14]. They can be further classified into 12 subgroups based on further conserved amino acid motifs [14]. *AtERF4* is a member of the group VIIIa ERFs, characterized by the ERF-associated amphiphilic repression (EAR) motif. This motif allows them to act as transcriptional repressors. They can repress target gene transcription even in the presence of ERF activators in transient reporter gene assays [24–26]. However, due to alternative polyadenylation and splicing, *ERF4* exists in two different protein isoforms, one containing the EAR-motif (*ERF4-R*), one lacking it (*ERF4-A*) [27]. Formation of the *ERF4-A* isoform was shown to be induced by flg22 treatment, a bacterial peptide derived from flagellin, which induces PAMP-triggered immunity and a ROS burst. The plant RNA-binding protein FPA (At2g43410) can inhibit the formation of the *ERF4-A* isoform and the ROS burst. The ability of *ERF4* to switch from a repressor to an activator by alternative splicing and polyadenylation adds an extra layer of complexity to molecular mechanisms underlying the ERF-mediated gene regulation [27].

Alternative splicing (AS) is an important factor in gene regulation. Many transcription factor genes undergo this process, which results in the production of multiple proteins from one single gene [28–31]. It is involved in a variety of plant growth and developmental processes, such as induction of flowering [32], plant responses to changing environmental conditions and pathogen attacks [28]. However, AS in leaf senescence has so far not been studied in detail. This study aims to analyze the role of alternative splicing and polyadenylation of *ERF4* in leaf senescence. By complementation of the *erf4* mutant plants with both isoforms, we provide evidence that both *ERF4* isoforms function in senescence. *ERF4-A* acts as transcriptional activator and *ERF4-R* as repressor of their direct target gene *CATALASE3 (CAT3)*, which we could identify in a yeast-one-hybrid (Y1H) screen. Catalase proteins are important enzymes in catalyzing the decomposition of H_2O_2 to water (H_2O) and oxygen (O_2) and controlling the concentrations of ROS in cells [33,34]. All three Arabidopsis catalases are regulated in

a senescence-associated manner [7,8] and H₂O₂ is used as signaling molecule in senescence. Moreover, we could show that the ratio of ERF4-A and ERF4-R expression changes over development and is influenced by the RNA-binding protein FPA. A complex pattern of activating and repressing activities on CAT3 function became obvious in the *erf4* mutant plants. We provide a model on how the interplay of the different components might be organized.

2. Material and Methods

2.1. Yeast-One-Hybrid System

The Matchmaker yeast-one-hybrid library screening system (ClonTech, Heidelberg, Germany) was used to screen for genes that bind to fragments of the *CAT3* promoter. A 150-bp fragment (pos. -182 to -332) upstream of the linear reporter plasmid was integrated into *Saccharomyces cerevisiae* strain Y187 by recombination. The yeast strain with the integrated *pHISi* plasmid was mated with the yeast strain AH109 carrying a cDNA library, which was prepared from RNA of 7-week-old rosette leaves of *Arabidopsis thaliana* and integrated into the *pGADT7-Rec* vector with the Gal4 activation domain and the *leu2* selection marker. The one-hybrid screenings and assays were performed as described in the manufacturer's protocols. Two independent clones partially coding for *ERF4* clones were found in the screening. Therefore, the full-length cDNA of *ERF4* was cloned into *pGADT7-Rec* vector and transformed again into Y187 cells carrying the *CAT3* driven *HIS3* gene to confirm the interaction.

2.2. Expression and Extraction of Recombinant Proteins for DNA-Protein-Interaction- Enzyme-linked Immunosorbent Assay (DPI-ELISA), Pull-Down Assay and in vitro Protein Degradation Assay

The coding sequences of the two *ERF4* isoforms [27] were cloned into the expression vector pETG-10A with N-terminal hexahistidine-tag (6xHIS-tag) and in the pDEST-15 expression vector with N-terminal Gluthathione-S-Transferase (GST)-tag (for pull-down assay). For protein expression, the *E. coli* strain BL21 Rosetta was used. The transformed cells were grown in 5 ml selective LB (lysogeny broth) medium overnight and the next day a fresh 50 ml culture was inoculated with 500 µL of the overnight culture and grown in selective LB medium until it reached OD₅₉₅ of 0.5. Protein expression was induced by adding IPTG (Isopropyl-β-D-thiogalactopyranoside) to a final concentration of 1 mM. After 4 h of shaking at 30 °C the cells were harvested by centrifugation (4600 rpm, 20 min, 4 °C). The pellet was resuspended in protein extraction buffer (500 mM NaCl, 5 mM Imidazole, 20 mM Tris-HCl, 2 mM sodium azide, pH 7.0, 1 × complete proteinase inhibitor without ethylenediaminetetraacetic acid (Roche, Basel, Switzerland) was added freshly). Proteins were extracted under native conditions by sonicating and the protein concentration was measured in a Bradford assay (Bio-Rad, Munich, Germany).

2.3. DPI-ELISA

Streptavidin-coated, transparent 96-well ELISA plates (Thermo Scientific, Waltham, MA, USA) were used to immobilize double-stranded (ds) oligonucleotides (Biomers, Ulm, Germany). The 5'biotinylated forward and its complementary reverse oligonucleotide were annealed at 95 °C for 5 min, followed by a slow, stepwise cooling down to room temperature. 2 pmol ds oligonucleotides were added per well in a total volume of 60 µL and incubated for 1 h. The liquid was removed after each step. After 1 h of blocking (60 µL Roche blocking solution), 5, 10 and 25 µg of protein crude extracts were diluted with protein dilution buffer (4 mM Hepes pH 7.5, 100 mM KCl, 8% (v/v) glycerol) and the mixture was incubated for 1 h. Two washing steps with 100 µL Qiagen wash buffer were performed, 60 µL of Penta-His-horseradish peroxidase conjugate antibody (Qiagen, Venlo, The Netherlands) was added (diluted 1:1500 in Qiagen wash buffer) and incubated for 1 h. After another two washing steps, the interaction was visualized using the substrate of the peroxidase, o-phenylenediamine dihydrochloride (OPD tablets, Thermo Scientific). This resulted in a yellow product, which was detected in a plate reader (TECAN Safire SFluor4) at 492 nm.

2.4. Pull-Down Assay

GST-ERF4-A (49.6 kDa), GST-ERF4-R (51.7 kDa), 6xHIS-ERF4-A (24.5 kDa) and 6xHIS-ERF4-R (26.6 kDa) fusion proteins were expressed as previously described. 500 µg total protein of the crude extracts were incubated at room temperature for 1 h with continuous shaking. HIS-select nickel magnetic agarose beads (Sigma-Aldrich, St. Louis, MO, USA) were used according to manufacturer's instructions to pull on the 6xHIS-tagged fusion proteins (wash buffer: 50 mM NaH₂PO₄, 300 mM NaCl, 10 mM imidazole, elution buffer: 50 mM sodium phosphate pH 8.0, 0.3 M NaCl, 300 mM imidazole). The eluted fraction was analyzed by SDS-PAGE using a monoclonal anti-Glutathione-S-Transferase (GST) antibody (Sigma-Aldrich) and semi-dry Western Blot.

2.5. In Vitro Protein Degradation Assay

Leaf 7–8 and 9–13 of 49-day-old *Arabidopsis* Col-0 plants were harvested separately. Recombinant 6xHIS-ERF4-A and 6xHIS-ERF4-R fusion proteins were produced in bacteria as described earlier. The protein isolation buffer was exchanged by using Amicon Ultra-4 Centrifugal Filter Devices (Merck Millipore, Burlington, MA, USA) with a solution containing 20 mM Tris (pH 8.0) and 100 mM NaCl. The cell-free in vitro degradation assay was modified from Reference [35]. The leaf material was ground in liquid nitrogen and the powder was suspended in a buffer containing 50 mM Tris (pH 7.5), 10 mM NaCl, 10 mM MgCl₂, 5 mM dithiothreitol and 2 mM ATP. After centrifugation (14,000 rpm, 10 min, 4 °C) 25 µg total protein of the bacterial crude lysate were added into the plant extracts and incubated at room temperature for 0, 15, 30, 60 and 120 min. Subsequently, SDS loading buffer was added and the samples were boiled at 95 °C to terminate the reaction and to denature the proteins. The proteins were detected by SDS-PAGE and immunoblot analysis with a penta-HIS-HRP conjugate antibody (Qiagen). *E. coli* extracts were used as negative control.

2.6. Protoplast Leaf Transfection

The transient GUS (β-glucuronidase) reporter gene assays and BiFC were performed in protoplasts, which were derived from cell suspension culture cells of *Arabidopsis thaliana* Col-0 and in leaf protoplasts of Col-0, *erf4* and *esp/esr* knock-out mutants. They were transfected with plasmid DNA purified with the Gene JET Plasmid Midiprep kit (Thermo Scientific) for GUS Assays or the Nucleo-Bond Xtra Midi kit (Macherey-Nagel, Düren, Germany) for BiFC. Protoplasts were transiently transformed with different concentrations of the respective plasmid DNA following the protocol published in Reference [36]. For details, see the protocol on <http://www.zmbp.uni-tuebingen.de/c-facilit/plant-transformation.html>.

2.7. GUS Reporter-Gene Assay in Protoplasts

For the GUS assays, 1.8 kbp upstream of the start codon of *CAT3* and 2.8 kbp upstream of the start codon of *WRKY53* were cloned into the GUS reporter plasmid pBGWFS7.0, respectively. The coding sequences of ERF4-A and ERF4-R [27] were cloned in the binary plant transformation vector pJAN33. *Arabidopsis* protoplasts were transformed as previously described with 3 µg effector constructs, 2.5 µg reporter plasmid and 0.1 µg of a *35S:Luciferase* plasmid (pBT8-35SLUCm3) for normalization purposes. The protoplasts were incubated over night at room temperature and the GUS assay was performed the next morning as described by Jefferson et al. [37].

2.8. BiFC and Flow Cytometry

For the BiFC assay, the coding sequence of *ERF4-R* and *ERF4-A* as well as *WRKY53* (as a negative control with ERF4 isoforms and as positive control with itself) were cloned into the BiFC-2in1-NN vector [38]. It fuses the N- and C-terminal part of eYFP to the N-termini of both interaction partners and it contains RFP (red fluorescent protein) as a transformation control. Protoplasts were transfected with 3 µg of the plasmid, covering the 8 possible combinations between the potential interaction

partners and the negative control. After incubation overnight, fluorescence was quantified by flow cytometry using a CytoFLEX (Beckman Coulter, Brea, CA, USA). Both the internal mRFP and any reconstituted eYFP were excited by the on board 488 nm laser. For eYFP, peak emission was captured in FL1 (525/40 nm) and for RFP in FL3 (610/20 nm). After compensation, the percentage of cells with eYFP signal was determined. The results were means from 7 experiments for the ERF4 homo- and heterodimers and 3 experiments for the combinations with WRKY53. Furthermore, the interactions were visualized with a Leica TCS SP8 microscope. eYFP was excited at 514 nm and the emission was recorded at 519–560 nm, whereas mRFP was excited at 561 nm and the emission was recorded at 566–637 nm.

2.9. Plant Material

Arabidopsis thaliana plants were grown in standard soil under long-day conditions (16 h day, 8 h night) at an ambient temperature of 20 °C with a moderate light intensity (80–100 $\mu\text{E}/\text{m}^2/\text{s}$). Individual leaves were labelled with differently colored threads according to their age. This allowed the identification of the leaf numbers within the first rosette even in very late stages of senescence [39]. Plants were always harvested at the same time in the morning in order to avoid circadian effects. The T-DNA insertion lines of *ERF4* (SALK_073394), *FPA* (SAIL720_B10, SALK_011615, SAIL_849_F10) and *ESP/ESR* (SALK_055029C) were obtained from the Nottingham Arabidopsis Stock Centre (NASC). Homozygous plants were verified by PCR using combinations of gene specific primers and the T-DNA left border primer (Lba1). Plants overexpressing the different isoforms of ERF4, as well as complementation lines were kindly provided by G. Simpson and K. Shirasu [27]. Different plant lines overexpressing ERF4-R isoform were obtained from and published by T. Koyama [17].

2.10. Semi-quantitative-PCR (sqRT-PCR) and qRT-PCR

Total RNA was extracted with the RNeasy plant mini kit (Qiagen) and the subsequent cDNA synthesis was done with RevertAid reverse transcriptase (Thermo Scientific) and oligo (dT) primer using 200 μg of RNA. qRT-PCR was performed using Kapa SYBR®Fast Bio-rad iCycler (Kapa Biosystems, Wilmington, MA, USA) master mix following the manufacturer's instructions in a final volume of 8 μL including 3.5 μL of 1:5 diluted cDNA. The expression of the genes analyzed was normalized to *ACTIN2* (*ACT2*) according to the method published by Pfaffl [40]. sqRT-PCR products were amplified in 10 μL PCR reactions containing 1 μL of cDNA for amplification of *ACT2*, 2 μL for *ERF4-R* and 3 μL for *ERF4-A*. Red Mastermix (2x) (Genaxxon bioscience, Ulm, Germany) was used with 0.5 μM primer P1, P2 or P3 (see Table S1). The exponential range of amplification was determined for each set of primers and accordingly different numbers of cycles were used (26 for *ACT2*, 27 for *ERF4-R* and 36 for *ERF4-A*) with different annealing temperatures (55 °C for *ACT2*, 62 °C for *ERF4-R* and 64 °C for *ERF4-R*; Figure S3A). PCR products were separated on a 1% agarose gel with subsequent ethidium bromide staining and band intensity was analyzed using ImageJ.

2.11. Senescence Phenotyping

To assess differences in the progression of senescence between the plant lines, we measured a variety of parameters, which indicate the state of senescence from 25 up to 70 days after sowing (DAS). All methods are described in detail by Bresson et al. [39]. Electrolyte leakage was measured using a conductivity meter (CM100-2, Reid and Associates). In order to measure the hydrogen peroxide (H_2O_2) level, 3,3'-diaminobenzidine (DAB) staining or the fluorescent dye H2DCFDA were used. The activity of photosystem II (PSII) was assessed by Fv/Fm values (using the Imaging-PAM chlorophyll fluorometer Maxi version; ver. 2-46i, Walz GmbH, Effeltrich, Germany) and the status of chlorophyll breakdown was measured by extraction of chlorophyll (Chl). Leaf No. 6 was used for native catalase zymograms, RNA was extracted from leaves No. 7 and 8 and the leaf color was assessed with the automated colorimetric assay (ACA) published in Bresson et al. [39]. Chl content in the ERF4 complementation lines was measured with an *atLEAF+* Chl meter in leaf No. 5, three times

per leaf and the values were averaged. All phenotyping experiments were done with a minimum of four biological replicates and experiments were performed at least three times independently.

2.12. Catalase Zymograms and Immunodetection

Plant protein was extracted out of frozen leaves by grinding material in 200 μ L extraction buffer (100 mM Tris, 20% glycerol (v/v), 30 mM DTT, pH 8). The samples were centrifuged for 15 min at 14,000 rpm and 4 °C. Total protein concentration of the supernatant was measured via Bradford assay (Bio-Rad) and 10 μ g total protein was loaded on native polyacrylamide (PAA) gels (6% PAA, 1 M Tris, pH 6.8; running buffer: 25 mM Tris, 250 mM Glycine, pH 8.3). After protein separation, the gels were rinsed twice with water, incubated for 2 min in a 0.01% H₂O₂ solution and rinsed again twice with water. The staining was performed in a solution containing 1% FeCl₃ and 1% K₃(Fe(CN)₆) (w/v) until catalase activity bands became visible (~3 min). The reaction was stopped by rinsing gels with water. For immunodetection the native PAA gel was blotted on a nitrocellulose membrane. After blotting, the membrane was washed twice with Tris-buffered saline (TBS) and blocked with 3% milk powder in TBS-Tween 20 (TBS-T). Polyclonal anti-rye-CAT antibodies in 1.5% milk powder were used, followed by secondary peroxidase-conjugated antibodies for visualization.

3. Results

3.1. Impact of *ERF-A* and *ERF-R* on Senescence

ERF4 is a transcription factor, which can undergo alternative polyadenylation resulting in the co-existence of two different isoforms, *ERF-A* and *ERF-R* [27]. We were interested to find out when both forms are produced during plant development and whether or not they have an impact on senescence. Therefore, we used an *erf4* mutant line, an *ERF4-A* and different *ERF4-R* overexpressing lines all in Col-0 background. The plants were grown side by side with Col-0 wildtype plants to compare senescence onset and progression. These phenotyping experiments were repeated three times with similar results. In order to investigate leaf senescence of the different plant lines, optical appearance was scored for several parameters during leaf development at the same rosette position from 25 to 70 days after sowing (DAS). Therefore, the true leaves (without the cotyledons) were labelled with different threads following a color code. Leaves of one rosette were sorted according to their age and corresponding leaves of the different lines were compared (Figure 1A). A statistical analysis of at least five plants was used to capture variability between individual plants of the same lines. A colorimetric analysis consisted in categorizing leaves into four groups depending on their leaf color: fully green, green/yellow, fully yellow, brown/dry (Figure 1B). Compared to Col-0 the 35S:*ERF4-R* line showed more signs of senescence, whereas the *erf4* line was less senescent at the same time point according to visual features (Figure 1A,B) indicating that the 35S:*ERF4-R* plants were accelerated and the *erf4* plants delayed in senescence. The 35S:*ERF4-A* plants behaved intermediately; at 41 DAS they were slightly accelerated whereas from 46 DAS onward, they appeared to be more and more delayed. The photosynthetic capacity was analyzed by chlorophyll fluorescence measurements of leaf No. 5 (Figure 1C). Consistent with the colorimetric analysis, the activity of photosystem II declined earlier in 35S:*ERF4-R* leaves compared to Col-0 leaves, whereas this became more obvious in *erf4* mutant or *ERF4-A* overexpressing leaves much later. Membrane integrity was monitored by measuring electrolyte leakage (EL) of leaf No. 3 (Figure 1D). 35S:*ERF4-R* line displayed higher membrane deterioration at 37 DAS compared to Col-0. In very late stages (53 DAS), Col-0 and 35S:*ERF4-R* plants did not show any more differences, whereas *erf4* and 35S:*ERF4-A* had higher membrane integrity compared to wild type. Intracellular ROS production was measured in leaf No. 9 by H₂DCF-DA fluorescence (Figure 1E) and diaminobenzidine (DAB)-staining (Figure 1F). A significantly lower increase of intracellular H₂O₂ was detected in *erf4* mutant plants with advancing senescence compared to wildtype plants. Again, the 35S:*ERF4-A* overexpressing plants were more similar to the mutant line, whereas the 35S:*ERF4-R*

line showed a faster increase in H_2O_2 content supporting the results of the colorimetric analysis (Figure 1A).

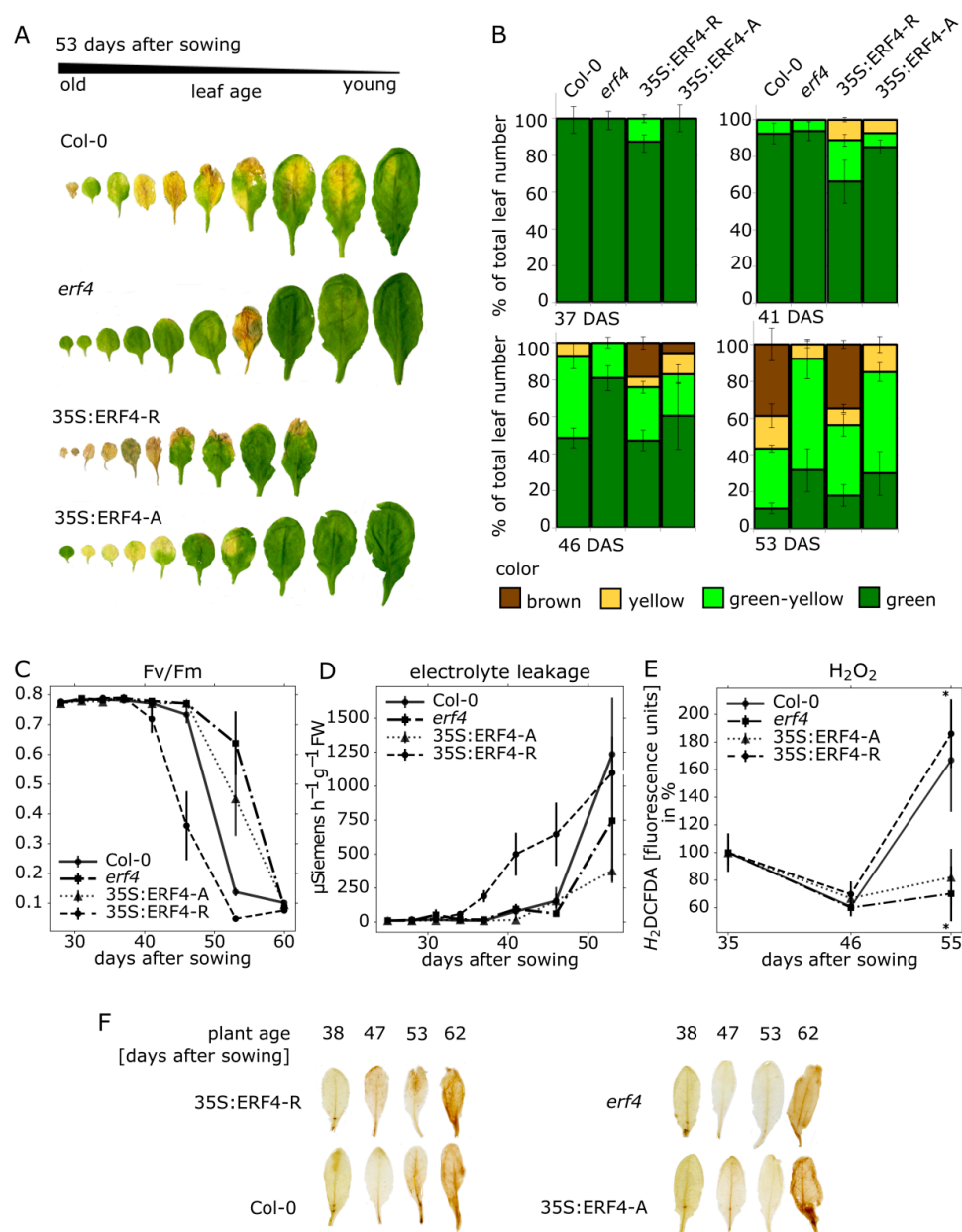


Figure 1. Senescence parameters analyzed in plant lines with altered *ERF4* expression. Col-0, 35S:ERF4-R, 35S:ERF4-A and *erf4* mutant plants were analyzed over development. (A) Representative pictures for rosette leaves No. 1–10, which were sorted according to their age 53 days after sowing (DAS). (B) Rosette leaves were categorized in four groups according to their color (fully green, green/yellow, fully yellow, brown/dry) and percentage of each category is depicted. (C) Fv/Fm values in leaf No. 5 were measured with the pulse amplitude modulation (PAM) method. (D) Electrolyte leakage (EL) over time was measured in single detached leaves No. 4 using a conductivity meter. Values are normalized to leaf fresh weight. (E) Intracellular H_2O_2 content per leaf was measured in leaf No. 9 using the fluorescent dye H₂DCFDA. Values are normalized to leaf weight. Data represent means of 5 (A–D) or 10 (E) biological replicates, error bars present \pm SE. (F) H_2O_2 content in leaf No. 9 is visualized by DAB (3,3-diaminobenzidine)-staining. One representative example is shown. Experiments were repeated three times with similar results.

For comparison of the different lines at the same time point, it is important that their general development is not significantly altered. None of the lines showed a severe impairment in development (Figure S1A–G). The *ERF4-R* overexpression lines showed a slightly delayed flowering and silique emergence (Figure S1E,F) and had more smaller, less dense leaves (Figure S1C,D,G) whereas *erf4* plants had a bigger leaf area and were heavier compared to wildtype plants (Figure S1D). These minor changes in overall development still allow comparison of the lines.

Gene expression of senescence-associated genes (SAGs) was analyzed by quantitative real-time PCR using leaf No. 7 (Figure S2). The lower transcript levels of the senescence-upregulated short chain alcohol dehydrogenase *SAG13* (At2g29350) suggest that the *erf4* and the 35S:*ERF4-A* line are both delayed in senescence-associated gene expression compared to Col-0. The *ERF4-R* overexpression line showed a faster increase of *SAG13* mRNA levels until 46 DAS, then transcript levels in Col-0 reached higher values pointing to a slightly accelerated senescence compared to Col-0. *SAG12* (At5g45890), a senescence-upregulated cysteine protease that is often used as marker gene in late senescence, showed a different pattern for the later stages of leaf senescence. Col-0 and the mutant line showed the highest expression level, whereas the overexpression of *ERF4-A* resulted in the lowest expression of *SAG12* at 53 DAS. Down-regulation of *RUBISCO* (*RBCS1*) was not much altered in all lines indicating that *ERF4* affects only part of the senescence reprogramming at different time points of senescence.

Taken together, the results of the phenotyping experiments reveal that the *erf4* plants show delayed senescence, 35S:*ERF4-A* plants are only slightly delayed in senescence and more similar to Col-0, 35S:*ERF4-R* plants show an accelerated senescence phenotype, more pronounced in earlier stages and then becoming progressively indistinguishable to Col-0 plants in later senescence stages.

3.2. *ERF4-A* mRNA is Less Abundant than *ERF4-R*, but the Protein is Less Prone to Degradation In Vitro

In order to get an idea about the abundance of the *ERF4* isoforms at different stages of leaf senescence, we analyzed the relative amount of the mRNA forms in Arabidopsis Col-0 plants from 31 to 46 DAS by conventional RT-PCR as described by Lyons et al. [27]. Three different mRNA molecules can be derived from *ERF4* transcription: *ERF4-R*, *ERF4-IR* and *ERF4-A* as illustrated in Figure 2A. *ERF4-R* is created by using the first polyadenylation site, *ERF4-IR* by using the second polyadenylation site without splicing of an intron, which now exists in the longer mRNA. Therefore, this form is called IR for intron retention. *ERF4-A* is also created by using the second polyadenylation site, however, in this form the intron is spliced out, which now leads to the loss of the repressing EAR domain. Therefore, this form is called A for activator. These three mRNA forms lead to two different protein variants whereby *ERF4-A* mRNA encodes the *ERF4-A* protein and *ERF4-R* and *ERF4-IR* mRNAs both lead to the *ERF4-R* protein. The nucleotide sequence of *ERF4-IR* entirely includes the sequence of *ERF4-R* and as well as of *ERF4-A*. This is the reason why no sequence specific primers can be designed to distinguish all three forms by quantitative RT-PCR. Therefore, a semi-quantitative RT-PCR approach was chosen using two different primer pairs: P1 and P3 differentiate the *ERF4-IR* form from the *ERF4-A* form by size and P1 and P2 amplify the *ERF4-R+IR*. For simplicity, we called the sum of *ERF4R+IR* only *ERF4-R* in the following as they encode the same protein. First, we determined the exponential range of amplification (Figure S3A). Thereafter, we used 36 cycles and 3 μ L cDNA for the *ERF4-A* and *ERF4-IR* amplification, 27 cycles and 2 μ L cDNA for *ERF4-R* and 27 cycles and 1 μ L of cDNA for *ACTIN2* as reference gene. These initial results indicated that the A-Form is much less abundant than the R-Form. The *ERF4-IR* mRNAs were even less abundant than the *ERF4-A* form and, since they code for the same protein as *ERF4-R*, were not analyzed separately. From these analyses, we determined that the *ERF4-A* and *ERF4-R* isoforms show an age-dependent expression, with a higher mRNA abundance in later stages of leaf senescence (Figure 2B). However, after bolting at 31 DAS, a decrease in the expression of *ERF4-A* can be observed, followed by a constant increase, indicating that both isoforms are not always produced at the same ratio over development (Figure 2C). Moreover, the expression of the different isoforms was also analyzed in the 35S:*ERF4-R* and 35S:*ERF4-A* as well as in the *erf4* mutant line. (Figure S3B). Both isoforms were clearly overexpressed and overexpression

of the *ERF4-R* led to a slight decrease of *ERF4-A* formation and *vice versa*. However, how this feedback loop on splicing and polyadenylation is achieved, has to be further investigated.

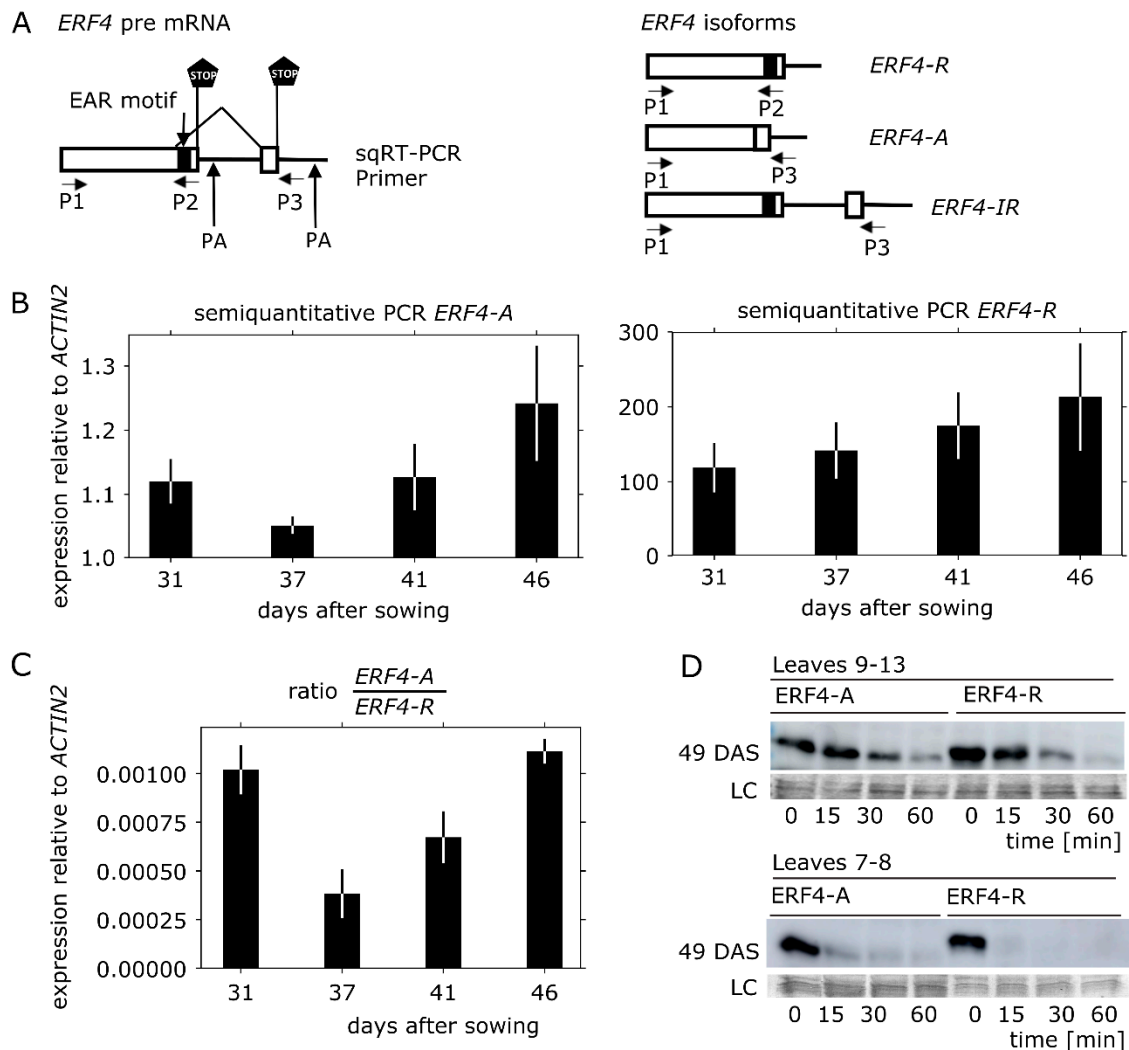


Figure 2. *ERF4* isoform expression and protein stability. (A) Schematic illustration of *ERF4* pre-mRNA with two different polyadenylation sites and primer binding sites for primer 1 (P1), primer 2 (P2) and primer 3 (P3), which were used for semi-quantitative reverse transcriptase PCR (sqRT-PCR) as described in [27]. Boxes denote exons, lines denote introns and untranslated regions, PA indicates alternative polyadenylation sites, black box indicates the repressing ERF-associated amphiphilic repression (EAR) motif. cDNA of the *ERF4* isoforms is shown on the right side. (B) Results of the sqRT-PCR using RNA isolated from Col-0 plants at different developmental stages indicated in days after sowing (DAS). Graph shows expression of *ERF4-A* (36 cycles, 3 μ L cDNA) and *ERF4-R* (27 cycles, 2 μ L cDNA), which was quantified using ImageJ and is presented relative to expression of *ACTIN2*. Error bars indicate \pm SE, $n = 3$. (C) Ratio of *ERF4-A* to *ERF4-R* mRNA at different developmental stages (D) Cell-free protein degradation assay. 6xHIS-tagged *ERF4-R* (26.6 kDa) and *ERF4-A* (24.5 kDa) proteins were incubated in protein extract of young (No. 9–13) and middle old leaves (No. 7 and 8) for 0–60 min. Five plants were pooled for protein extraction and were harvested 49 days after sowing (DAS). Amido black staining of the upper part of the polyvinylidene difluoride (PVDF) membrane is shown as loading control (LC).

To investigate whether the lower abundance of *ERF4-A* is counterbalanced by a higher protein stability, we subjected recombinant proteins of both isoforms to *in vitro* proteolysis by plant extracts. Therefore, epitope-tagged versions of the proteins were expressed in *E. coli* and 25 μ g of the protein

crude lysates containing the recombinant proteins were incubated for 0, 15, 30 and 60 min with Arabidopsis leaf extracts, which were derived from selected rosette leaves (9–13 or 7–8) at 49 DAS. The ERF protein amount, which remained after incubation, was assessed by immunodetection. Both ERF4 isoforms were rapidly degraded by the plant extracts (Figure 2D), whereas ERF4 protein amounts were not reduced under the same conditions by bacterial cell lysates (Figure S3C), suggesting that ERF4 isoforms are degraded by plant-specific proteins and/or the plants' proteasome. Both isoforms were more stable in extracts of younger leaves (No. 9–13) than in extracts of older leaves (No. 7–8); ERF4-A was in general more stable than ERF4-R. This suggests that both ERF4 isoforms are present throughout the whole process of leaf senescence, lower expression in younger leaves is counterbalanced by higher protein stability in this tissue, and, in addition, lower *ERF4-A* mRNA amounts are compensated by a higher protein stability of ERF4-A compared to ERF4-R.

3.3. Senescence Analyses of *erf4* Complementation Lines

To further analyze the impact of each isoform on senescence, we characterized complementation lines, which express the *ERF4-R* or *ERF4-A* coding sequence under the control of the native *ERF4* promoter in the *erf4* background (cERF4-R and cERF4-A). These lines were obtained from Lyons et al. [27]. After verification of the isoforms' expression by semi-quantitative PCR (Figure S4), the plants were grown along with Col-0 and the *erf4* plants under long-day conditions and low light intensities (30 $\mu\text{E}/\text{m}^2/\text{s}$) to slow down development and increase the resolution of senescence. As before, leaves were sorted according to their age and one example (55 DAS) is presented in Figure 3B. As the plants were grown under low light conditions, Col-0 leaves were less senescent at 55 DAS compared to Figure 1A,B at 53 DAS. The differences between the complementation lines were very subtle. In order to quantify leaf color more precisely than by eye, we used an automated colorimetric assay (ACA) to classify the color values pixel-wise (Figure 3A, [39]). According to the ACA, both lines were able to complement the mutation of *ERF4* almost completely with a tendency of cERF4-A to complement slightly better (Figure 3A,B).

DAB-staining indicated that H_2O_2 levels in *erf4* plants are lower compared to Col-0 levels as the plants age. Both, *ERF4-A* and *ERF4-R*, complemented the *erf4* mutant, with *ERF4-A* again slightly more effective than the *ERF4-R* form, as staining of cERF4-A leaves appear to be more similar to wildtype than to cERF4-R leaves (Figure 3C). Fv/Fm levels of cERF4-A resembled those of wildtype plants and decreased earlier than cERF4-R and the mutant line; however, from 55 DAS onwards both complementation lines complemented equally well (Figure 3D). With regard to EL in leaf No. 4, the cERF4-A line also shows the tendency of complementing *ERF4* loss slightly better than cERF4-R (Figure 3E). In summary, both isoforms can complement the loss of *ERF4* in *erf4* plants almost to wildtype level with a tendency of the *ERF4-A* for a slightly better complementation. This is very surprising as Lyons et al. [27] have already shown that both forms can act antagonistically on gene expression, at least on *PDF1.2*.

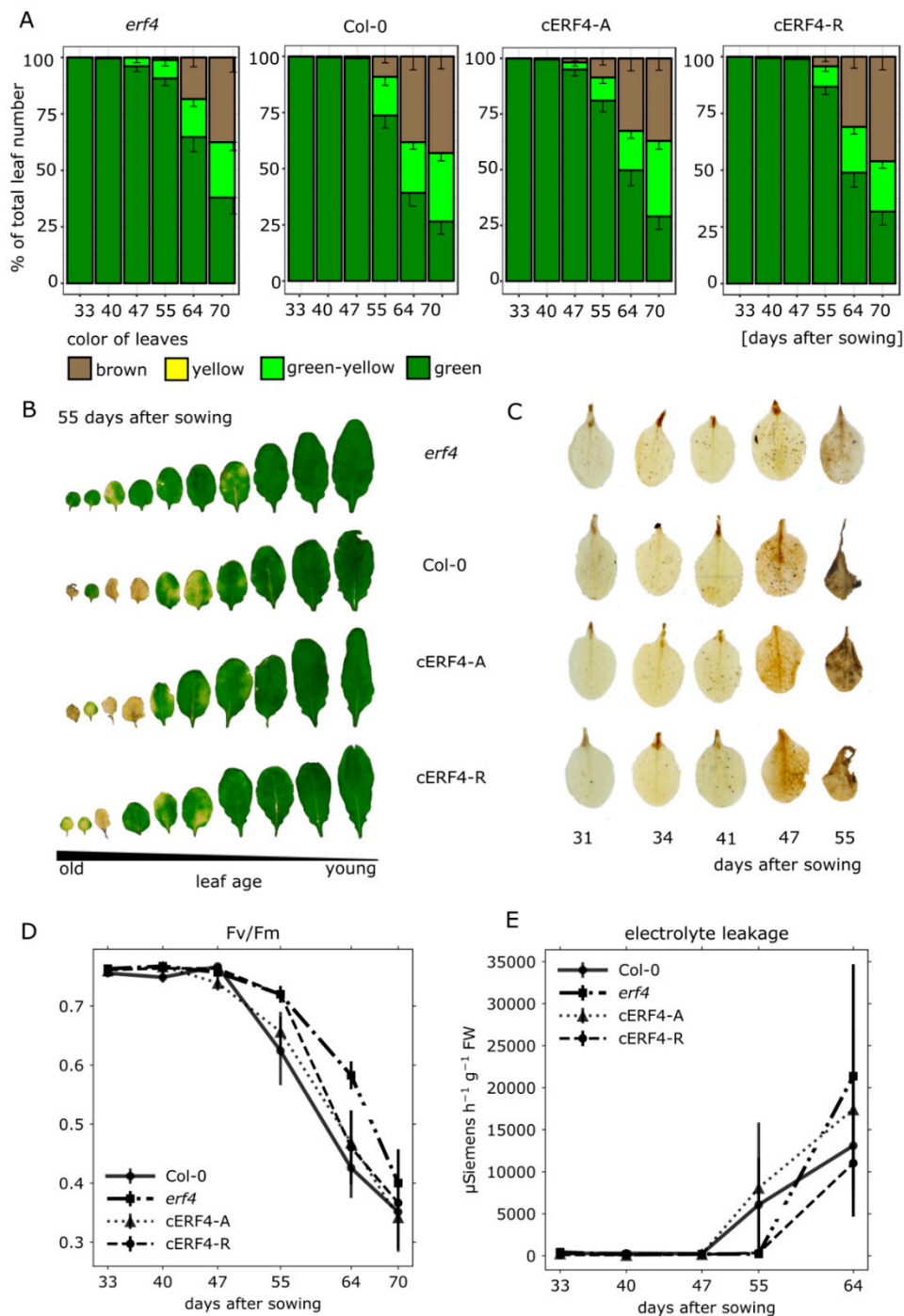


Figure 3. Complementation of ERF4 loss of function by ERF4-A or ERF4-R. Senescence phenotype and parameters were analyzed in Col-0, *erf4* mutants, and *erf4* mutant plants complemented with either *ERF4*-promoter:*ERF4-A* (cERF4-A) or *ERF4*-promoter:*ERF4-R* constructs (cERF4-R). (A) Automated colorimetric assay, in which rosette leaves are categorized according to color in four groups (green, green-yellow, yellow, brown). (B) Representative pictures of rosette leaves No. 1–10, which were sorted according to leaf age 55 DAS. (C) One representative picture of five biological replicates for DAB-staining in leaf No. 4 at 31–55 DAS. These plants have been raised under normal light intensities ($80 \mu\text{E}/\text{m}^2/\text{s}$). (D) Fv/Fm values in rosette leaves were measured with pulse amplitude modulation (PAM). (E) Electrolyte Leakage (EL) was measured with a conductivity meter in detached leaves No. 4 of another experimental series. Values are normalized to fresh weight. Data A, D and E represent means of at least four biological replicates, error bars indicate $\pm\text{SE}$.

3.4. Impact of ERF4 on the Senescence Regulator WRKY53

As shown by Koyama and coworkers [17], WRKY genes are significantly upregulated in *ERF4-R* overexpressing lines and *WRKY53* senescence-associated induction is eliminated in the *erf4/erf8* double mutant. The authors explained the effect by the action of ESP/ESR, which is a negative regulator of *WRKY53* expression and activity [18]. By ChIP, *ESP/ESR* was shown to be a direct target of ERF4 acting as repressor on *ESP/ESR* expression [17]. In order to investigate whether there is also a direct effect of both ERF4 isoforms on the expression of *WRKY53*, we transiently co-transformed a 2.8 kbp *WRKY53*-promoter:*GUS* construct with 35S:*ERF4-R* and 35S:*ERF4-A* effector constructs in Arabidopsis Col-0 or *esp/esr* protoplasts. In the presence of ESP/ESR, *WRKY53* expression was increased approx. 5-fold by *ERF4-R* overexpression (Figure 4), which is in the same range as in the microarray experiment of Koyama et al. [17]. However, in the absence of ESP/ESR in *esp/esr* protoplasts, *WRKY53* expression was induced approx. 2-fold by *ERF4-R* overexpression, indicating that *WRKY53* expression is also influenced in an ESP/ESR-independent pathway (Figure 4). Overexpression of ERF4-A showed a weak but positive effect (approx. 1.5-fold) on this promoter, which was almost completely missing in the *esr/esp* protoplasts (Figure 4) indicating that ERF4-A has only a weak effect but uses exclusively the ESP/ESR pathway.

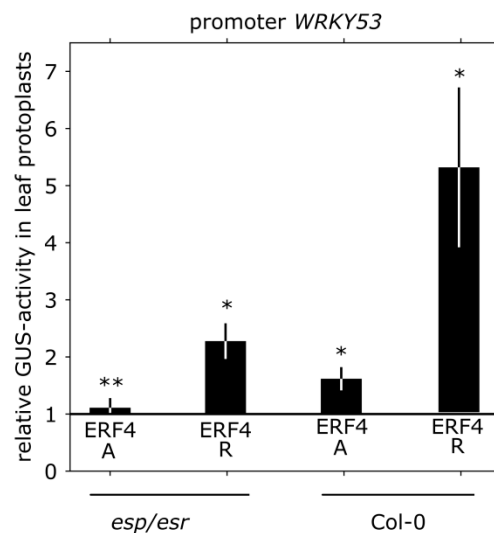


Figure 4. Impact of ERF4 on *WRKY53* expression. Transient expression assays were performed in Arabidopsis protoplasts with a 2.8 kbp fragment of the *WRKY53* promoter that drives expression of *GUS* in Col-0 and *esp/esr* mutant leaf protoplasts. Values represent fold-change of *GUS*-activity relative to the empty vector after normalization to luciferase activity from a minimum of four experiments. Error bars indicate \pm SE. Statistical differences were determined by one sample t-test (* $p \leq 0.05$, ** $p \leq 0.005$, *** $p \leq 0.0005$).

3.5. Isolation and Characterization of CATALASE3 (CAT3) as Direct Target Gene of ERF4

In a yeast-one-hybrid (Y1H) screen, which was performed to find potential regulatory proteins that interact with the *CAT3* promoter, different *CAT3* promoter fragments were cloned in front of reporter genes (*His* and *Ade*, *LacZ*) and brought into yeast cells together with a cDNA library obtained from 7-week-old Arabidopsis leaves. cDNA insertions were sequenced and identified from yeast cells growing on selection media. Among others, partial sequences of *ERF4* were identified in two independent clones to bind to a 150-bp fragment (−332 to −182) of the *CAT3* promoter (Figure 5A). Therefore, the full-length coding sequence of *ERF4-R*, which is the predominantly expressed isoform, was cloned into the pGADT7 vector and transformed into the reporter yeast strain Y187 [pHIS1-*CAT3*] and growth on selection media could be confirmed. Therefore, the full-length ERF4-R protein binds to a *cis*-element in the *CAT3* promoter. The DNA-binding of ERF4 to the *CAT3* promoter was further

analyzed *in vitro* by DPI-ELISA. For DPI-ELISA, the coding sequence of both *ERF4-R* and *ERF4-A* isoforms were cloned in pETG10A with N-terminal hexa-histidine-tag (6xHIS-tag) and expressed in bacteria. A 55-bp biotinylated DNA fragment of the *CAT3* promoter sequence, which was identified in the yeast-one-hybrid screen and contains the DRE motif CAGCC, an already known binding motif for ERF4 [41], was used (Figure 5A). Whereas the crude lysate of the *Escherichia coli* (*E. coli*) strain expressing the empty vector did not show any binding activity, both ERF4 isoforms were able to bind to this fragment (Figure 5B).

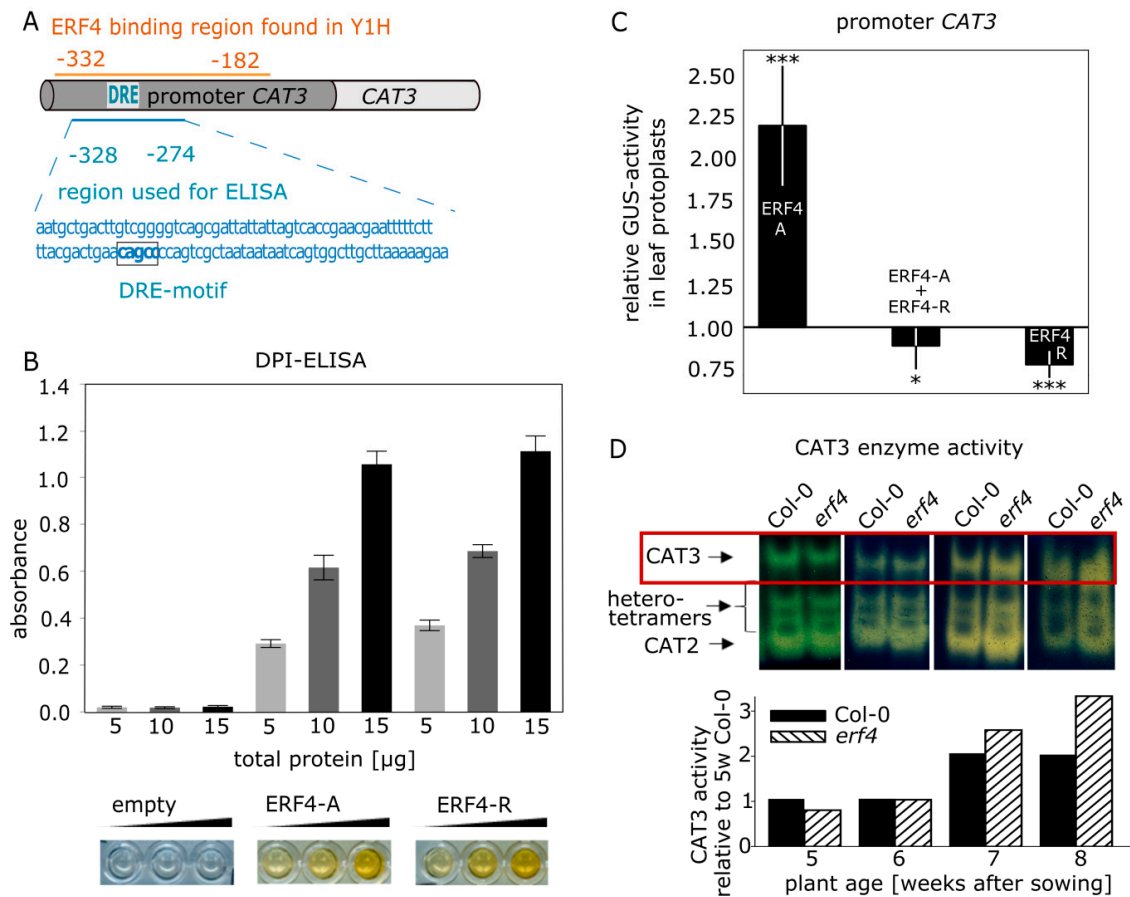


Figure 5. ERF4 binds to the *CATALASE3* promoter and can act as activator and repressor. (A) Schematic representation of the *CAT3* promoter fragments used for Y1H screen and for DPI-ELISA. (B) DPI-ELISA using bacterial crude extracts of *E. coli* BL21 Rosetta cells expressing 6xHis-ERF4-A, 6xHis-ERF4-R or the empty vector and a 55-bp biotinylated DNA fragment of the *CAT3* promoter, which contains the DRE motif CAGCC. Representative wells of the micro titer plate are shown below the graph. Yellow color indicates interaction. Error bars indicate \pm SE, $n = 4-5$. (C) Transient expression assays were performed using the 1.8 kbp fragment of the *CAT3* promoter upstream of the start codon in Arabidopsis Col-0 and *erf4* leaf protoplasts. Values represent fold-change of GUS-activity relative to the empty vector after normalization to luciferase activity to compensate for differences in transformation efficiency. Data are means of seven experiments ($n = 7$). Statistical differences were analyzed by one sample t-test (* $p \leq 0.05$, ** $p \leq 0.005$, *** $p \leq 0.0005$). (D) Enzyme activity of catalase isoforms of Col-0 and *erf4* mutant plants is visualized on a zymogram. Protein crude extract (10 μ g) of leaf No. 6 of 5- to 8-week-old plants were separated on 7.5% native gels and stained for catalase activity. Proteins were extracted of a pool of at least 10 leaves. Intensities of the *CAT3* bands were quantified using ImageJ.

To analyze the effect of ERF4 isoforms on the expression of *CAT3* *in vivo*, transient co-transformations of a 1.8 kbp *CAT3*-promoter:*GUS* construct along with 35S:*ERF4-R* or 35S:*ERF4-A* overexpression constructs in Arabidopsis Col-0 or *erf4* protoplasts were analyzed for GUS protein

expression (Figure 5C). Protein formation of ERF4-R and ERF4-A was identified in the transformed protoplasts by immunodetection (Figure S6). Reporter gene expression was repressed by the overexpression of *ERF4-R* as expected for a direct target gene of a protein containing an EAR motif, whereas overexpression of *ERF4-A* resulted in an increased reporter gene activity (Figure 5C). This clearly suggests that the isoforms have an antagonistic function in the regulation of *CAT3*. Simultaneous co-transformation of both isoforms led to reporter gene repression (Figure 5C) suggesting that the repressor isoform is dominant over the activator form.

CAT3 protein amount and activity increases during development and progression of senescence in wildtype plants (Figure S5A,B; [7,42]). When the activity of the catalase isoforms was analyzed by zymograms in Col-0 and *erf4* mutant plants during plant development, a peculiar activity pattern could be observed for *CAT3*. As band intensities on catalase zymograms are proportional to enzyme activity in a wide range [7], *CAT3* activity was quantified using ImageJ. In 5-week-old plants, *CAT3* activity was lower in *erf4* leaves compared to leaves of Col-0 plants, which is more obvious in the growth series shown in Figure S5, most likely due to slightly different velocities in development of different growth series. In 6-week-old plants, *CAT3* activity was equal in *erf4* plants compared to wildtype and in 7- and 8-week-old plants *CAT3* activity is higher than in Col-0 plants (Figure 5D; Figure S5B). This suggests that the loss of ERF4 has an age-dependent influence on *CAT3* activity: at early stages the activator ERF4-A appears to have a higher impact whereas at later stages of development the repressor ERF-R has a dominant effect.

3.6. ERF4 Isoforms Form Homo- and Heterodimers, but Homodimers are Less Favored

The existence of the two different isoforms raised the question, whether or not they form homo- and/or heterodimers. Therefore, we first analyzed the formation of different dimers in vitro by a pull-down of recombinant proteins via Ni-agarose-beads. *E. coli* BL21 Rosetta cells were transformed with constructs coding for N-terminal GST-tagged and N-terminal 6xHIS-tagged fusion proteins (Figure 6A). GST-ERF4-A and GST-ERF4-R could be successfully pulled down with both HIS-ERF4-A and HIS-ERF4-R proteins. These results demonstrate that in vitro both the formation of homo- and heterodimers is possible.

To confirm the dimerization in planta, bimolecular fluorescence complementation (BiFC) combined with flow cytometry was performed. Arabidopsis Col-0 protoplasts were transformed with constructs coding for the sequences of *ERF4-A* and *ERF4-R*, which were N-terminally fused to the sequences coding for the N- and C-terminal part of eYFP, respectively. As positive control *WRKY53* constructs were included, since *WRKY53* proteins are already shown to form homodimers [23]. Flow cytometry results show that homodimers of both ERF4 isoforms could be formed with the same probability as *WRKY53* homodimers (Figure 6B,C and Figure S7A). In contrast to the pull-down experiments, heterodimers between both ERF4 isoforms and with *WRKY53* are—if at all—formed with a much lower probability. They are not significantly different from the background signals of the mRFP control. Under the confocal laser-scanning microscope, the YFP signal of the BiFC is predominantly localized in the nucleus (Figure S7B).

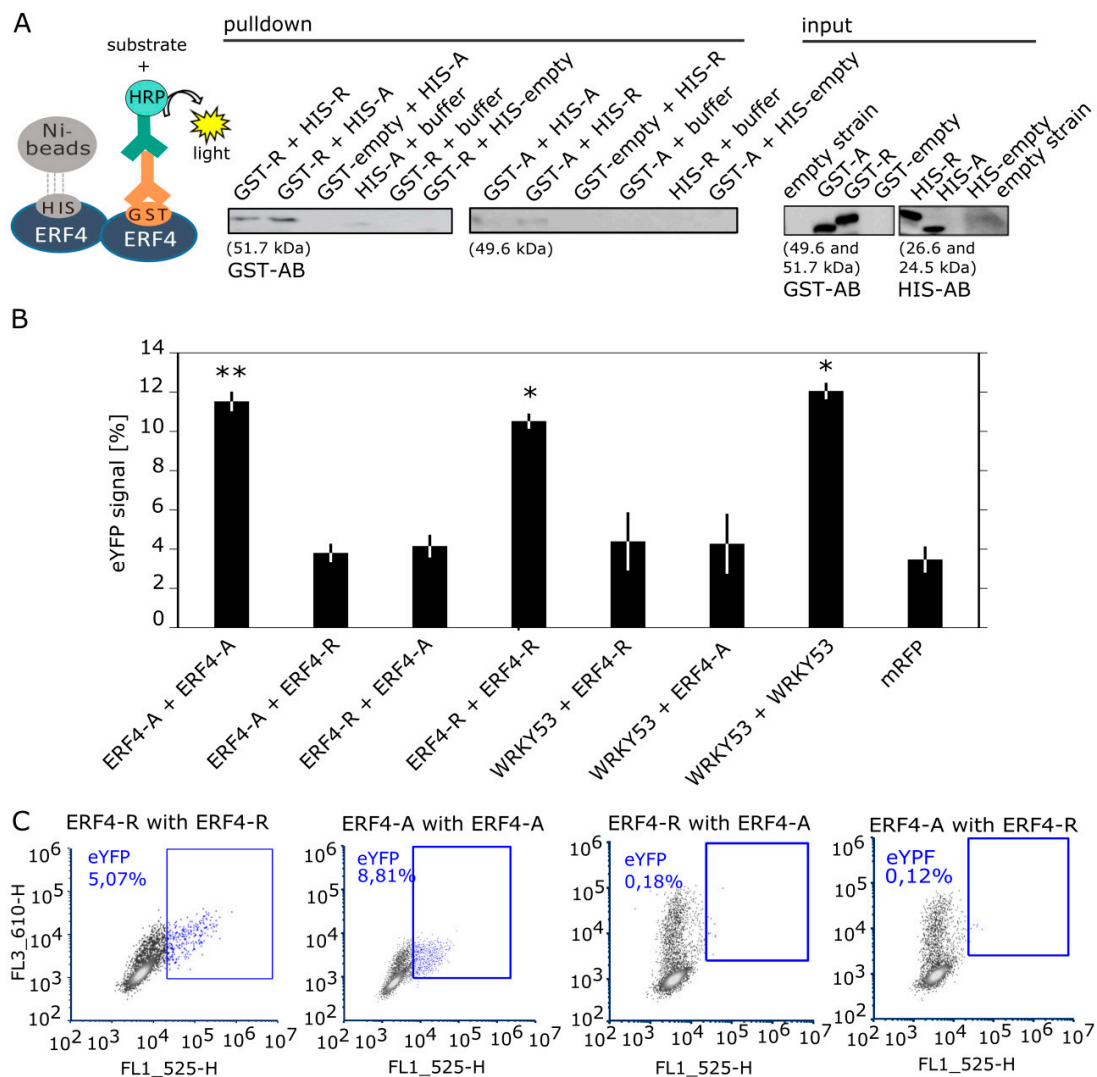


Figure 6. Protein–protein interaction of ERF4-A and ERF4-R. (A) Pull-down assay was performed using total protein extracts from *E. coli* BL21 Rosetta cells. GST-tagged ERF4-R (51.7 kDa) and ERF4-A (49.6 kDa) was pulled down with HIS-tagged ERF4-R (26.6 kDa) and ERF4-A (24.5 kDa) proteins and immunodetected with anti-GST antibodies. The input protein (25 µg) was visualized with anti-GST and anti-HIS antibodies. The experiment shown was performed three times with similar results. (B) BiFC flow cytometry experiments were performed in Arabidopsis protoplasts co-expressing ERF4-R and ERF4-A fused with YFP-N and YFP-C, respectively. YFP-N fusion with WRKY53 and YFP-C fusions with both ERF4 isoforms were used as negative controls and YFP-N and YFP-C fusions with WRKY53 as positive control. RFP is expressed as transfection control. Bars represent percentage of cells with eYFP signal (mean values (±SE), $n = 7$ for combinations with ERF4 isoforms, $n = 3$ for combinations with WRKY53). Data was subjected to quantile normalization and determination of statistical differences was carried out using Wilcoxon rank sum test (* $p \leq 0.05$, ** $p \leq 0.005$). (C) Representative graphs of the flow cytometry results for ERF4 homodimers and heterodimers. Blue dots represent eYFP signals of interaction. Blue squares mark the cells showing eYFP signal.

3.7. FPA Inhibits ERF4-A Formation and Appears to be Involved in Senescence Regulation

Lyons and coworkers observed that the RNA-binding protein FPA inhibits the formation of the ERF4-A form by promoting the polyadenylation in favor of the ERF4-R form [27]. We could show by qRT-PCR that FPA exhibited a senescence-specific expression pattern with rising expression levels in older plants (Figure 7A) that coincide with a decrease in ERF4A/ERF4R ratio (Figure 7B). In *erf4*

plants, the increase of FPA expression is delayed most likely due to the delayed senescence of *erf4*. Furthermore, sqRT-PCR confirmed that *ERF4-A* accumulates to much higher expression levels in *fpa* mutant plants (Figure 7C) as observed previously by Lyons et al. [27]. Therefore, we wanted to analyze whether FPA also has an influence on leaf senescence and therefore characterized two *fpa* T-DNA insertion lines (SAIL 849-F10 and SAIL 720-B10) in that regard. Each T-DNA insertion was confirmed by PCR. As FPA also controls flowering by repressing *FLOWERING LOCUS C* expression, the mutant plants have a strong delay in bolting and flowering. The shoot apical meristem (SAM) developed 30 and 40 leaves before the plant started bolting, as compared to Col-0, which had around 13 leaves (Figure 7D). Therefore, senescence phenotyping is very difficult as ideally plants of the same developmental stage should be compared. Nevertheless, with regard to the first 13 leaves, *fpa* mutants displayed accelerated senescence (Figure 7E) possibly indicating that FPA is not only involved in regulation of flowering time but also in senescence.

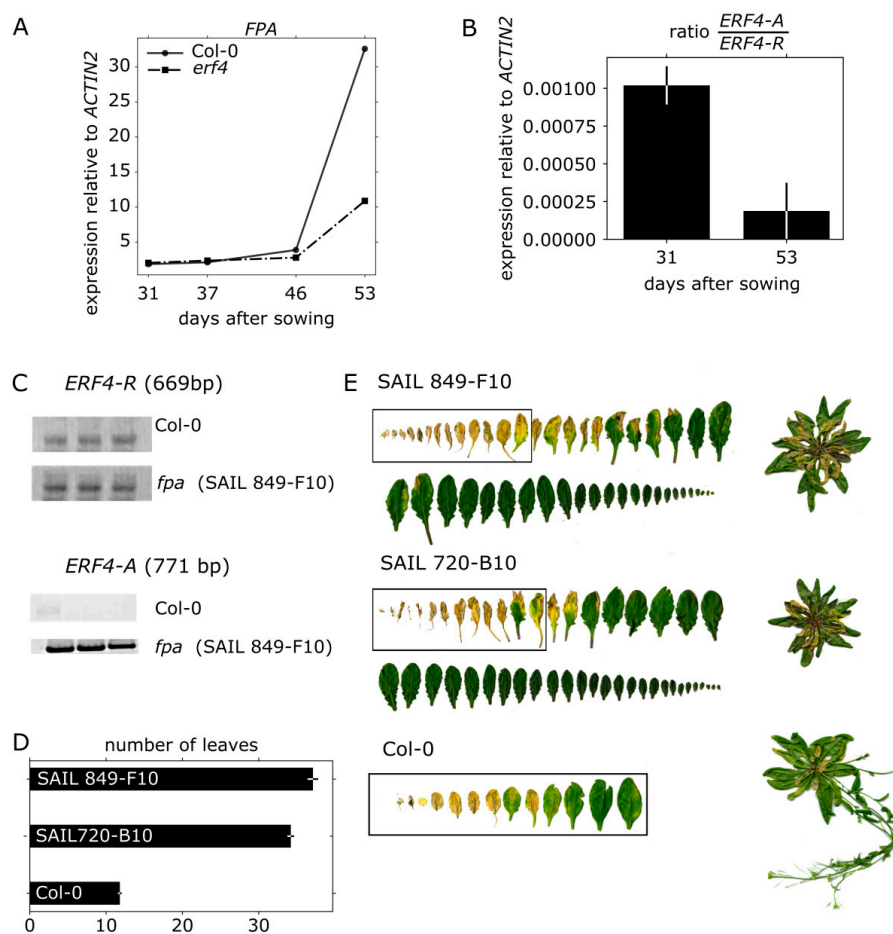


Figure 7. Characterization of *fpa* plants. (A) qRT-PCR data shows expression level of FPA in Col-0 and *erf4* plants relative to *ACTIN2*. Leaves No. 7 of 5 biological replicates were pooled. Data are means of two technical replicates. (B) Ratio between *ERF4-A* and *ERF4-R* mRNAs at early (31 DAS) and late stages of development (51 DAS) (C) Semi-quantitative-PCR (sqRT-PCR) with RNA isolated from a pool of 10 plants was performed. Images show representative bands on a 1% agarose gel for *ERF4-R* (27 cycles, 2 μ L cDNA, 669 bp) and *ERF4-A* (36 cycles, 3 μ L cDNA, 771 bp) in Col-0 and *fpa* (SAIL 849-F10) plants of three technical replicates. (D) Number of rosette leaves 6 weeks (42 DAS) after sowing of *fpa* and Col-0 plants. Error bars indicate \pm SE, $n = 10$. (E) Representative pictures of rosette leaves sorted according to their age 7.5 weeks (51 DAS) after sowing of two *fpa* lines (SAIL 849-F10 and SAIL 720-B10) and Col-0.

4. Discussion

Leaf senescence goes along with massive changes in gene expression [12] and transcription factors play a key role in the differential expression of genes. Class II ERFs are transcription factors involved in many different processes and signaling pathways. They participate in the responses to pathogen, ethylene, SA, JA, auxin, salt and ABA [43–48]. Moreover, they are involved in cell death and senescence processes. For example, NbCD1, a *Nicotiana benthamiana* class II ERF, has been characterized to positively regulate cell death [49] and the AP2/ERF factor MACD1 as well as ERF102 were also reported to be involved in phytotoxin-triggered programmed cell death in *Nicotiana umbratica* [50]. Furthermore, *NtERF3* and other ERFs containing the EAR motif of tobacco or rice were able to induce hypersensitive response (HR) when overexpressed in plants [51]. Koyama and coworkers [17] identified a regulatory cascade involving Arabidopsis ERF4 and ERF8 to promote leaf senescence. Even though the growth regulator ethylene is part of its name, responsiveness to this phytohormone is not a collective feature of all ERFs. Moreover, ERFs can have dual functions, as for example ERF-VII proteins act as positive regulators of the hypoxic response and as repressors of oxidative-stress related genes, depending on the developmental stage of the *A. thaliana* plants [52]. In this study, we expand the context and/or age-dependent function of ERFs to ERF4 of Arabidopsis and describe the role of two ERF4 isoforms derived from alternative polyadenylation in senescence. Phenotyping experiments show that both isoforms have a different and opposing impact on senescence: whereas 35S:ERF4-R plants show an accelerated phenotype, 35S:ERF4-A plants are slightly delayed in leaf senescence (Figure 1A–F). Complementation of the ERF4 loss in *erf4* mutant plants indicated that both isoforms were able to complement the delayed senescence of *erf4* with a tendency of ERF4-A to restore the wildtype phenotype slightly better (Figure 3A–E). This indicates that ERF4-A and ERF4-R both contribute to the senescence regulatory effect of ERF4 having partially overlapping functions and that alternative polyadenylation is part of the regulatory network of senescence. Nevertheless, it was unexpected that both isoforms were able to complement the mutant phenotype since both isoforms exhibit opposing effects on the expression of the direct target gene *CAT3* (Figure 5C) and *PDF1.2* [27]. However, *WRKY53* expression was affected in the same direction by both isoforms, either directly or indirectly. Microarray analyses of the *ERF4-R* overexpressing line revealed that not only *WRKY53* but also many other WRKY transcription factors are downstream targets of ERF4 [17] and many of those are involved in senescence regulation. Moreover, WRKYs act in a transcriptional network influencing the expression of each other so that the outcome on senescence can hardly be predicted [21,23]. On the other hand, single knock-out mutants of transcription factors involved in senescence regulation often do not show any obvious phenotype even though they are responsible for changes in the transcriptome. These changes in gene expression are contributing to the senescence process as a whole but do not necessarily relate to a visible phenotype. Therefore, complementing only one of the two isoforms might be sufficient to restore the phenotype even though the absence of the other still leads to changes in senescence-associated genes (SAG) expression, which could explain that both isoforms were able to complement the mutant phenotype. Therefore, a general transcriptome analysis of the complementation lines will be subject of further investigations and will give insight in differential changes to identify specific target genes of either isoform. Both complementation lines performed slightly different in complementing the mutant: ERF4-A appears to be more important at earlier stages of senescence and more involved in regulating intracellular H₂O₂ concentration (Figure 3C) whereas ERF4-R appears to promote membrane integrity (Figure 3E). Therefore, it can be assumed that different and specific target genes and pathways are targeted by the different isoforms. The simultaneous presence of the two opposing isoforms render *in planta* function of ERF4 very complex. The total amount of the *ERF4* mRNA increases with age and both isoforms can be detected in leaves throughout development from 31–46 DAS. However, the ratio between the mRNAs of the two isoforms changes over development. The *ERF4-A* form is always less abundant than the *ERF4-R* form, but at 31 DAS the A:R ratio is highest (Figure 2C). To counterbalance the low abundance of the *ERF4-A* mRNA, the resulting ERF4-A protein is more stable than the ERF4-R protein (Figure 2D).

The formation of the *ERF4-A* form was shown to be dependent on *FPA*, a RNA-binding protein, which inhibits the alternative polyadenylation [27]. Expression of *FPA* is dependent on plant age and increases with senescence (Figure 7A). Consistent with this increase, the ratio between *ERF4-A* and *ERF4-R* is lower at a later time point (Figure 7B). This increase in *FPA* expression is less pronounced in *erf4* mutant plants (Figure 7A) due to either delayed senescence or a feedback regulation of *ERF4* on *FPA*. As *FPA* also controls flowering by repressing *FLOWERING LOCUS C* expression, the mutants have a strong delay in bolting and flowering. Therefore, it is difficult to compare senescence with Col-0 plants, as, in general, plants of the same developmental stage should be compared. Whereas Col-0 plants developed only 13 leaves and had already flowers and siliques, *fpa* mutants continued to produce more than 30 leaves without bolting and flowering. However, if the first 13 leaves of plants with the same age are compared, *fpa* mutants might be accelerated in senescence in these leaves. As *fpa* plants have higher amounts of *ERF4-A* (Figure 7C), the phenotype should resemble the 35S:*ERF4-A* overexpressing line. However, this line shows only a slightly accelerated senescence at 41 DAS, and at later time points it appears to be slightly delayed, indicating that this needs further investigations and that *FPA* is most likely involved in the regulation of polyadenylation of more target genes. Remarkably, *FPA* is involved in the regulation of two processes, which show overlapping gene expression patterns with senescence, namely flowering and pathogen response. This suggests that alternative polyadenylation is another mean for the cross-talk between these three processes.

We identified *ERF4* as a DNA-binding protein of the *CAT3* promoter in an Y1H screen (Figure 5A). Some members of the ERF family have been shown to bind in vitro to an AGCCGCC motif (GCC-box) [53], while other ERFs have also been reported to bind DRE elements [41], or even novel DNA elements [54,55]. We confirmed the in vitro binding of both protein isoforms *ERF4-R* and *ERF4-A* to the *CAT3* promoter to a fragment containing the DRE motif with DPI-ELISA (Figure 5B). Reporter gene assays revealed that *ERF4-R* containing the EAR motif always had a repressing effect on reporter gene expression controlled by the *CAT3* promoter, whereas *ERF4-A* lacking the EAR motif activated *CAT3* driven reporter gene expression in leaf protoplasts (Figure 5C). The *ERF4* gene also contains a conserved motif with high number of acidic residues, which might function as activating domain in the absence of the EAR motif (Figure S8). Our results are consistent with that of Lyons and coworkers [27] who could also show the transcriptional activation of *ERF4-A* on a GAL4-GCC promoter and the *PDF1.2* expression. Co-transformation of both effectors led to a repression (Figure 5C). Therefore, *ERF4-A* can activate *CAT3* expression but, when both isoforms compete with each other, it appears to be less efficient.

CAT3 is an interesting target gene for a senescence-regulating transcription factor, as catalases control H_2O_2 levels, which have been shown to act as signaling molecules in senescence. In planta, *CAT3* activity increased with senescence in Col-0 plants (Figure 5D, Figure S5B). In contrast, a complex activity pattern became obvious in the *erf4* mutant. In younger plants, activity is lower compared to wildtype indicating the loss of a *CAT3* activating factor, whereas in older plants *CAT3* activity is higher compared to Col-0 plants pointing at the loss of a repressing factor. This suggests that the *ERF4-A* isoform has its highest impact at an early time point of senescence, whereas *ERF4-R* is more important at later stages. This is consistent with the inhibition of *ERF4-A* formation by *FPA* in later stages (Figure 7A–C). All three catalases in Arabidopsis display a senescence-associated activity pattern, in which *CAT2* is downregulated during early senescence, *CAT3* is upregulated during progression of senescence and *CAT1* is upregulated during late senescence. A fine-tuned regulatory loop between *CAT2*, *CAT3*, and ASCORBATE PEROXIDASE1 activities leads to an early peaking of H_2O_2 in senescence, which is used as a signal to induce senescence-associated gene expression [7,56]. Moreover, activity of many transcription factors is directly controlled by redox conditions [57]. Therefore, *ERF4* could affect senescence progression also via its impact on the signaling molecule H_2O_2 through activation or repression of *CAT3*. *CAT3* expression is in general induced by high levels of H_2O_2 ; however, during progression of senescence, this responsivity is specifically blocked while other stress responses are still working [58]. *ERF4-R* might be involved in the disruption of this

substrate induction to guarantee an increase in ROS during senescence, which is important to induce *SAG* expression and in later stages also for membrane deterioration and macromolecule breakdown.

Figure 8 illustrates our hypothesis of how *ERF4* isoforms influence the progression of leaf senescence. *ERF4* transcription rate increases with leaf age but due to increasing *FPA* levels in later stages of development the ratio between *ERF4-A* and *ERF4-R* forms is changed by alternative polyadenylation. In early stages, *ERF4-A* is enriched since *FPA* expression is low. At this time point *ERF4-A* positively influences the expression of *CAT3* and thereby keeps H_2O_2 levels low. With onset and progression of senescence, *FPA* levels increase and *ERF4-A* production is minimized. *ERF4-R* now negatively regulates *CAT3* expression leading to an increase in H_2O_2 production. This increased intracellular H_2O_2 levels now induce the expression of the senescence regulator *WRKY53* and many other senescence-associated transcription factors and *SAGs*.

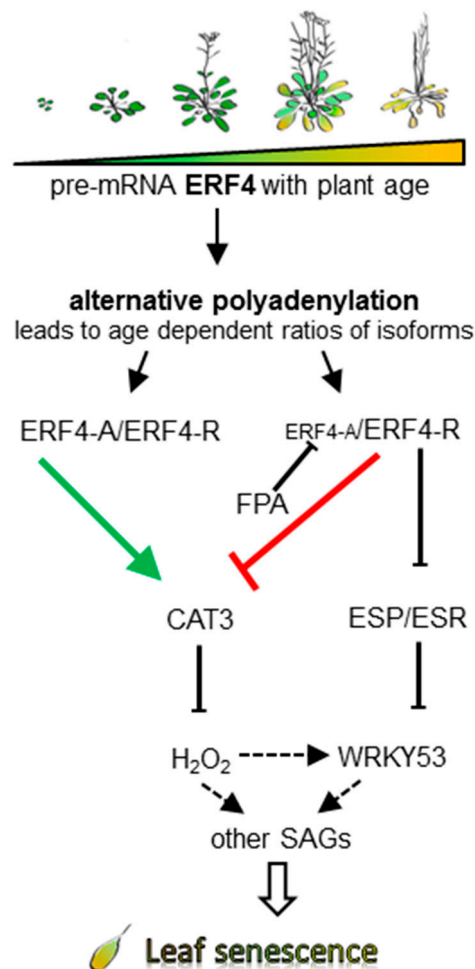


Figure 8. Model of the impact of the *ERF4* isoforms in early and late senescence. Alternative polyadenylation, influenced by the RNA-binding protein *FPA*, leads to different ratios between the two isoforms in early and late senescence. *FPA*, which increases with age, leads to a reduced amount of *ERF4-A* in older plants, and consequently reduces the activation potential of *ERF4-A* on *CAT3*. Increasing H_2O_2 levels trigger expression of *WRKY53* and other senescence-associated genes (*SAGs*) and thereby leaf senescence. *ERF4-R* acts as a negative regulator of *CAT3* and *ESP/ESR* and thereby indirectly as a positive regulator of *WRKY53* expression and activity.

Moreover, *ERF4-R* directly and negatively regulated the expression of *ESP/ESR*, which in turn is a negative regulator of *WRKY53* expression and activity. However, *WRKY53* appears to be upregulated by *ERF4* also in an *ESP/ESR*-independent pathway (Figure 4), but it is still unknown, whether this is

an indirect or direct regulation. The latter appears to be likely, since our *in silico* analyses identified at least four ethylene responsive *cis*-elements and a DRE element in the *WRKY53* 1000 bp upstream promoter region. Taken together, our findings reveal that ERF4-A and ERF4-R both contribute to the senescence regulatory effect of ERF4 and that alternative polyadenylation adds a further layer of complexity to the regulatory network of senescence.

Supplementary Materials: The following are available online at <http://www.mdpi.com/2073-4425/10/2/91/s1>. Figure S1: Measurement of different parameters over the development of Col-0, 35S:ERF4-R, 35S:ERF4-A and *erf4* mutant plant lines. Figure S2: Relative expression level of senescence-related genes. Figure S3: Isoform specific semi-quantitative RT-PCR. Figure S4: Isoform specific semi-quantitative RT-PCR of the complementation lines. Figure S5: CATALASE protein amounts and enzyme activity in 5- to 8- week-old Col-0 and *erf4* mutant plants. Figure S6: ERF4-A and ERF4-R protein expression in Arabidopsis protoplasts. Figure S7: Protein–Protein interactions in transiently transformed protoplasts. Figure S8: Protein alignment of the first 122 amino acids (AA) of *A. thaliana* and *N. tabacum* ERF4. Table S1: Primer sequences.

Author Contributions: Conceptualization, U.Z. and L.R.; Methodology, L.R., J.D. and K.W.B.; Validation, L.R., S.K.-H., J.D. and K.W.B.; Formal Analysis, L.R.; Investigation, L.R., S.K.-H., J.D. and K.W.B.; Writing - Original Draft Preparation, L.R.; Writing - Review & Editing, J.D.; K.W.B. and U.Z.; Visualization, L.R. and U.Z.; Supervision, U.Z. and J.D.; Project Administration, U.Z.; Funding Acquisition, U.Z.

Funding: This research was supported by the Deutsche Forschungsgemeinschaft (CRC 101, B06).

Acknowledgments: We greatly acknowledge Verena Kochan and Petra Müller (ZMBP, University of Tübingen) for providing the initial Y1H data on *CAT3* promoter fragments and data shown in Figure S5. We thank Gesine Seibold, Julian Fratte, Caterina Brancato and Manuela Freund for their technical support. We also thank Tobias Jachowski for programming the automated leaf segmentation tool for the ACA software. We are grateful to Koyama and coworkers as well as Lyons and coworkers for kindly providing seeds for the ERF4 overexpressing and complementation lines and J. Feierabend for providing the anti-rye-CAT antibody. Moreover, we thank Gero Hermsdorf and Steve Simmert for their advice and help in formatting plots in Python. Finally, we thank the Nottingham Arabidopsis Stock Center (NASC) for providing seeds SALK_073394, SAIL720_B10, SALK_011615, SAIL_849_F10, and SALK_055029C.

Conflicts of Interest: The authors declare no conflicts of interest.

References

1. Gan, S.; Amasino, R.M. Inhibition of leaf senescence by autoregulated production of cytokinin. *Science* **1995**, *270*, 1986–1988. [[CrossRef](#)] [[PubMed](#)]
2. Lim, P.O.; Kim, H.J.; Nam, H.G. Leaf Senescence. *Annu. Rev. Plant Biol.* **2007**, *58*, 115–136. [[CrossRef](#)] [[PubMed](#)]
3. Kim, J.; Kim, J.H.; Lyu, J.I.; Woo, H.R.; Lim, P.O. New insights into the regulation of leaf senescence in Arabidopsis. *J. Exp. Bot.* **2018**, *69*, 787–799. [[CrossRef](#)] [[PubMed](#)]
4. Buchanan-Wollaston, V.; Earl, S.; Harrison, E.; Mathas, E.; Navabpour, S.; Page, T.; Pink, D. The molecular analysis of leaf senescence—A genomics approach. *Plant Biotechnol. J.* **2003**, *1*, 3–22. [[CrossRef](#)]
5. Schildhauer, J.; Wiedemuth, K.; Humbeck, K. Supply of nitrogen can reverse senescence processes and affect expression of genes coding for plastidic glutamine synthetase and lysine-ketoglutarate reductase/saccharopine dehydrogenase. *Plant Biol.* **2008**, *10* (Suppl. 1), 76–84. [[CrossRef](#)]
6. Møller, I.M.; Sweetlove, L.J. ROS signalling—Specificity is required. *Trends Plant Sci.* **2010**, *15*, 370–374. [[CrossRef](#)]
7. Zimmermann, P.; Heinlein, C.; Orendi, G.; Zentgraf, U. Senescence-specific regulation of catalases in *Arabidopsis thaliana* (L.) Heynh. *Plant Cell Environ.* **2006**, *29*, 1049–1060. [[CrossRef](#)]
8. Zimmermann, P.; Zentgraf, U. The correlation between oxidative stress and senescence during plant development. *Cell. Mol. Biol. Lett.* **2005**, *10*, 515–534.
9. Lin, J.F.; Wu, S.H. Molecular events in senescing Arabidopsis leaves. *Plant J.* **2004**, *39*, 612–628. [[CrossRef](#)]
10. Balazadeh, S.; Riaño-Pachón, D.M.; Mueller-Roeber, B. Transcription factors regulating leaf senescence in *Arabidopsis thaliana*. *Plant Biol.* **2008**, *10* (Suppl. 1), 63–75. [[CrossRef](#)]
11. Buchanan-Wollaston, V.; Page, T.; Harrison, E.; Breeze, E.; Lim, P.O.; Nam, H.G.; Lin, J.F.; Wu, S.H.; Swidzinski, J.; Ishizaki, K.; et al. Comparative transcriptome analysis reveals significant differences in gene expression and signalling pathways between developmental and dark/starvation-induced senescence in Arabidopsis. *Plant J.* **2005**, *42*, 567–585. [[CrossRef](#)] [[PubMed](#)]

12. Breeze, E.; Harrison, E.; McHattie, S.; Hughes, L.; Hickman, R.; Hill, C.; Kiddle, S.; Kim, Y.S.; Penfold, C.A.; Jenkins, D.; et al. High-resolution temporal profiling of transcripts during Arabidopsis leaf senescence reveals a distinct chronology of processes and regulation. *Plant Cell* **2011**, *23*, 873–894. [[CrossRef](#)]
13. Riechmann, J.L.; Heard, J.; Martin, G.; Reuber, L.; Jiang, C.; Keddie, J.; Adam, L.; Pineda, O.; Ratcliffe, O.J.; Samaha, R.R.; et al. Arabidopsis transcription factors: Genome-wide comparative analysis among Eukaryotes. *Science* **2000**, *290*, 2105–2110. [[CrossRef](#)] [[PubMed](#)]
14. Nakano, T.; Suzuki, K.; Fujimura, T.; Shinshi, H. Genome-wide analysis of the ERF gene family in Arabidopsis and rice. *Plant Physiol.* **2006**, *140*, 411–432. [[CrossRef](#)] [[PubMed](#)]
15. Licausi, F.; Ohme-Takagi, M.; Perata, P. APETALA2/ethylene responsive factor (AP2/ERF) transcription factors: Mediators of stress responses and developmental programs. *New Phytol.* **2013**, *199*, 639–649. [[CrossRef](#)] [[PubMed](#)]
16. Mizoi, J.; Shinozaki, K.; Yamaguchi-Shinozaki, K. AP2/ERF family transcription factors in plant abiotic stress responses. *Biochim. Biophys. Acta* **2012**, 86–96. [[CrossRef](#)] [[PubMed](#)]
17. Koyama, T.; Nii, H.; Mitsuda, N.; Ohta, M.; Kitajima, S.; Ohme-Takagi, M.; Sato, F. A regulatory cascade involving class II ETHYLENE RESPONSE FACTOR transcriptional repressors operates in the progression of leaf senescence. *Plant Physiol.* **2013**, *162*, 991–1005. [[CrossRef](#)]
18. Miao, Y.; Zentgraf, U. The antagonist function of Arabidopsis WRKY53 and ESR/ESP in leaf senescence is modulated by the jasmonic and salicylic acid equilibrium. *Plant Cell* **2007**, *19*, 819–830. [[CrossRef](#)] [[PubMed](#)]
19. Miao, Y.; Laun, T.; Zimmermann, P.; Zentgraf, U. Targets of the WRKY53 transcription factor and its role during leaf senescence in Arabidopsis. *Plant Mol. Biol.* **2004**, *55*, 853–867. [[CrossRef](#)]
20. Ay, N.; Irmeler, K.; Fischer, A.; Uhlemann, R.; Reuter, G.; Humbeck, K. Epigenetic programming via histone methylation at WRKY53 controls leaf senescence in *Arabidopsis thaliana*. *Plant J.* **2009**, *58*, 333–346. [[CrossRef](#)]
21. Zentgraf, U.; Laun, T.; Miao, Y. The complex regulation of WRKY53 during leaf senescence of *Arabidopsis thaliana*. *Eur. J. Cell Biol.* **2010**, *89*, 133–137. [[CrossRef](#)] [[PubMed](#)]
22. Xie, Y.; Huhn, K.; Brandt, R.; Potschin, M.; Bieker, S.; Straub, D.; Doll, J.; Drechsler, T.; Zentgraf, U.; Wenkel, S. REVOLUTA and WRKY53 connect early and late leaf development in Arabidopsis. *Development* **2014**, *141*, 4772–4783. [[CrossRef](#)] [[PubMed](#)]
23. Potschin, M.; Schlienger, S.; Bieker, S.; Zentgraf, U. Senescence networking: WRKY18 is an upstream regulator, a downstream target gene, and a protein interaction partner of WRKY53. *J. Plant Growth Reg.* **2014**, *33*, 106–118. [[CrossRef](#)]
24. Fujimoto, S.Y.; Ohta, M.; Usui, A.; Shinshi, H.; Ohme-Takagi, M. Arabidopsis ethylene-responsive element binding factors act as transcriptional activators or repressors of GCC box-mediated gene expression. *Plant Cell* **2000**, *12*, 393–404. [[CrossRef](#)] [[PubMed](#)]
25. Ohta, M.; Ohme-Takagi, M.; Shinshi, H. Three ethylene-responsive transcription factors in tobacco with distinct transactivation functions. *Plant J.* **2000**, *22*, 29–38. [[CrossRef](#)] [[PubMed](#)]
26. Ohta, M.; Matsui, K.; Hiratsu, K.; Shinshi, H.; Ohme-Takagi, M. Repression domains of class II ERF transcriptional repressors share an essential motif for active repression. *Plant Cell* **2001**, *13*, 1959–1968. [[CrossRef](#)] [[PubMed](#)]
27. Lyons, R.; Iwase, A.; Gänsewig, T.; Sherstnev, A.; Duc, C.; Barton, G.J.; Hanada, K.; Higuchi-Takeuchi, M.; Matsui, M.; Sugimoto, K.; et al. The RNA-binding protein FPA regulates flg22-triggered defense responses and transcription factor activity by alternative polyadenylation. *Sci. Rep.* **2013**, *3*, 2866. [[CrossRef](#)]
28. Barbazuk, W.B.; Fu, Y.; McGinnis, K.M. Genome-wide analyses of alternative splicing in plants: Opportunities and challenges. *Genome Res.* **2008**, *18*, 1381–1392. [[CrossRef](#)]
29. Li, Q.; Lin, Y.C.; Sun, Y.H.; Song, J.; Chen, H.; Zhang, X.H.; Sederoff, R.R.; Chiang, V.L. Splice variant of the SND1 transcription factor is a dominant negative of SND1 members and their regulation in *Populus trichocarpa*. *Proc. Natl. Acad. Sci. USA* **2012**, *109*, 14699–14704. [[CrossRef](#)]
30. Mastrangelo, A.M.; Marone, D.; Laidò, G.; De Leonardis, A.M.; De Vita, P. Alternative splicing: Enhancing ability to cope with stress via transcriptome plasticity. *Plant Sci.* **2012**, *185–186*, 40–49. [[CrossRef](#)]
31. Severing, E.I.; van Dijk, A.D.J.; Morabito, G.; Busscher-Lange, J.; Immink, R.G.H.; van Ham, R.C.H.J. Predicting the impact of alternative splicing on plant MADS domain protein function. *PLoS ONE* **2012**, *7*, e30524. [[CrossRef](#)] [[PubMed](#)]

32. Slotte, T.; Huang, H.R.; Holm, K.; Ceplitis, A.; St. Onge, K.; Chen, J.; Lagercrantz, U.; Lascoux, M. Splicing variation at a *FLOWERING LOCUS C* homeolog is associated with flowering time variation in the tetraploid *Capsella bursa-pastoris*. *Genetics* **2009**, *183*, 337–345. [[CrossRef](#)] [[PubMed](#)]
33. Foyer, C.H.; Noctor, G. Oxygen processing in photosynthesis: Regulation and signalling. *New Phytol.* **2000**, *146*, 359–388. [[CrossRef](#)]
34. Mhamdi, A.; Queval, G.; Chaouch, S.; Vanderauwera, S.; Van Breusegem, F.; Noctor, G. Catalase function in plants: A focus on *Arabidopsis* mutants as stress-mimic models. *J. Exp. Bot.* **2010**, *61*, 4197–4220. [[CrossRef](#)] [[PubMed](#)]
35. Osterlund, M.T.; Hardtke, C.S.; Wei, N.; Deng, X.W. Targeted destabilization of HY5 during light-regulated development of *Arabidopsis*. *Nature* **2000**, *405*, 462–466. [[CrossRef](#)] [[PubMed](#)]
36. Mehlhorn, D.G.; Wallmeroth, N.; Berendzen, K.W.; Grefen, C. 2in1 vectors improve in planta BiFC and FRET analysis. *Methods Mol. Biol.* **2018**, *691*, 139–158.
37. Jefferson, R.A.; Kavanagh, T.A.; Bevan, M.W. GUS fusions: Beta-glucuronidase as a sensitive and versatile gene fusion marker in higher plants. *Embo J.* **1987**, *6*, 3901–3907. [[CrossRef](#)]
38. Grefen, C.; Blatt, M.R. A 2in1 cloning system enables ratiometric bimolecular fluorescence complementation (rBiFC). *Biotechniques* **2012**, *53*, 311–314. [[CrossRef](#)]
39. Bresson, J.; Bieker, S.; Riester, L.; Doll, J.; Zentgraf, U. A guideline for leaf senescence analyses: From quantification to physiological and molecular investigations. *J. Exp. Bot.* **2018**, *69*, 769–786. [[CrossRef](#)]
40. Pfaffl, M.W. A new mathematical model for relative quantification in real-time RT-PCR. *Nucleic Acids Res.* **2001**, *29*, 45e. [[CrossRef](#)]
41. Yang, S.; Wang, S.; Liu, X.; Yu, Y.; Yue, L.; Wang, X.; Hao, D. Four divergent *Arabidopsis* ethylene-responsive element-binding factor domains bind to a target DNA motif with a universal CG step core recognition and different flanking bases preference. *FEBS J.* **2009**, *276*, 7177–7186. [[CrossRef](#)] [[PubMed](#)]
42. Oñate-Sánchez, L.; Anderson, J.P.; Young, J.; Singh, K.B. AtERF14, a Member of the ERF family of transcription factors, plays a nonredundant role in plant defense. *Plant Physiol.* **2006**, *143*, 400–409. [[CrossRef](#)] [[PubMed](#)]
43. Ma, R.; Xiao, Y.; Lv, Z.; Tan, H.; Chen, R.; Li, Q.; Chen, J.; Wang, Y.; Yin, J.; Zhang, L.; et al. AP2/ERF Transcription Factor, Ii049, positively regulates lignan biosynthesis in *Isatis indigotica* through activating salicylic acid signaling and lignan/lignin pathway genes. *Front. Plant Sci.* **2017**, *8*, 1361. [[CrossRef](#)] [[PubMed](#)]
44. Eysholdt-Derzso, E.; Sauter, M. Root bending is antagonistically affected by hypoxia and ERF-mediated transcription via auxin signaling. *Plant Physiol.* **2017**, *175*, 412–423. [[CrossRef](#)] [[PubMed](#)]
45. Catinot, J.; Huang, J.B.; Huang, P.Y.; Tseng, M.Y.; Chen, Y.L.; Gu, S.Y.; Lo, W.S.; Wang, L.C.; Chen, Y.R.; Zimmerli, L. ETHYLENE RESPONSE FACTOR 96 positively regulates *Arabidopsis* resistance to necrotrophic pathogens by direct binding to GCC elements of jasmonate—And ethylene-responsive defence genes. *Plant Cell Environ.* **2015**, *38*, 2721–2734. [[CrossRef](#)] [[PubMed](#)]
46. Wang, X.; Liu, S.; Tian, H.; Wang, S.; Chen, J.G. The Small Ethylene Response Factor ERF96 is involved in the regulation of the abscisic acid response in *Arabidopsis*. *Front. Plant Sci.* **2015**, *6*, 1064. [[CrossRef](#)] [[PubMed](#)]
47. Zhang, L.; Li, Z.; Quan, R.; Li, G.; Wang, R.; Huang, R. An AP2 Domain-Containing Gene, ESE1, targeted by the ethylene signaling component EIN3 is important for the salt response in *Arabidopsis*. *Plant Physiol.* **2011**, *157*, 854–865. [[CrossRef](#)] [[PubMed](#)]
48. Nasir, K.H.; Takahashi, Y.; Ito, A.; Saitoh, H.; Matsumura, H.; Kanzaki, H.; Shimizu, T.; Ito, M.; Fujisawa, S.; Sharma, P.C.; et al. High-throughput in planta expression screening identifies a class II ethylene-responsive element binding factor-like protein that regulates plant cell death and non-host resistance. *Plant J.* **2005**, *43*, 491–505. [[CrossRef](#)] [[PubMed](#)]
49. Mase, K.; Ishihama, N.; Mori, H.; Takahashi, H.; Kaminaka, H.; Kodama, M.; Yoshioka, H. Transcription factor MACD1 participates in phytotoxin-triggered programmed cell death. *Mol. Plant-Microbe Interact.* **2013**, *26*, 868–879. [[CrossRef](#)] [[PubMed](#)]
50. Ogata, T.; Kida, Y.; Arai, T.; Kishi, Y.; Manago, Y.; Murai, M.; Matsushita, Y. Overexpression of tobacco ethylene response factor NtERF3 gene and its homologues from tobacco and rice induces hypersensitive response-like cell death in tobacco. *J. Gen. Plant Pathol.* **2012**, *78*, 8–17. [[CrossRef](#)]
51. Giuntoli, B.; Shukla, V.; Maggiorelli, F.; Giorgi, F.M.; Lombardi, L.; Perata, P.; Licausi, F. Age-dependent regulation of ERF-VII transcription factor activity in *Arabidopsis thaliana*. *Plant Cell Environ.* **2017**, *40*, 2333–2346. [[CrossRef](#)] [[PubMed](#)]

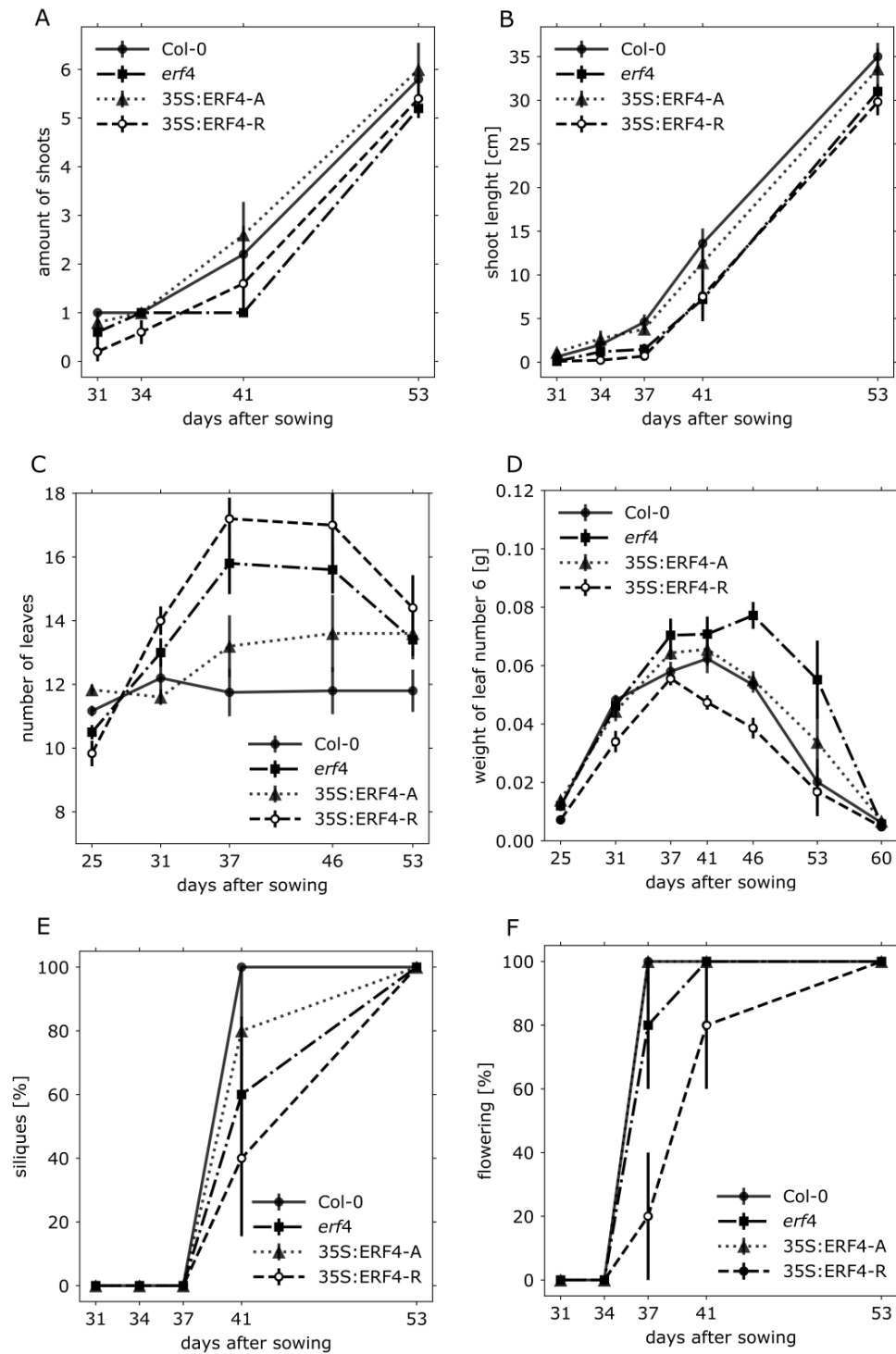
52. Hao, D.; Ohme-Takagi, M.; Sarai, A. Unique mode of GCC Box Recognition by the DNA-binding Domain of Ethylene-responsive Element-binding Factor (ERF domain) in plant. *J. Biol. Chem.* **1998**, *273*, 26857–26861. [[CrossRef](#)] [[PubMed](#)]
53. Welsch, R.; Maass, D.; Voegel, T.; Dellapenna, D.; Beyer, P. Transcription factor RAP2.2 and its interacting partner SINAT2: Stable elements in the carotenogenesis of *Arabidopsis* leaves. *Plant Physiol.* **2007**, *145*, 1073–1085. [[CrossRef](#)] [[PubMed](#)]
54. Shaikhali, J.; Heiber, I.; Seidel, T.; Ströher, E.; Hiltcher, H.; Birkmann, S.; Dietz, K.J.; Baier, M. The redox-sensitive transcription factor Rap2.4a controls nuclear expression of 2-Cys peroxiredoxin A and other chloroplast antioxidant enzymes. *BMC Plant Biol.* **2008**, *8*, 48. [[CrossRef](#)]
55. Bieker, S.; Riester, L.; Stahl, M.; Franzaring, J.; Zentgraf, U. Senescence-specific alteration of hydrogen peroxide levels in *Arabidopsis thaliana* and oilseed rape spring variety *Brassica napus* L. cv. Mozart. *J. Integr. Plant Biol.* **2012**, *54*, 540–554. [[CrossRef](#)] [[PubMed](#)]
56. He, H.; Van Breusegem, F.; Mhamdi, A. Redox-dependent control of nuclear transcription in plants. *J. Exp. Bot.* **2018**, *69*, 359–3372. [[CrossRef](#)] [[PubMed](#)]
57. Orendi, G.; Zimmermann, P.; Baar, C.; Zentgraf, U. Loss of stress-induced expression of catalase3 during leaf senescence in *Arabidopsis thaliana* is restricted to oxidative stress. *Plant Sci.* **2001**, *161*, 301–314. [[CrossRef](#)]
58. Hertwig, B.; Streb, P.; Feierabend, J. Light dependence of catalase synthesis and degradation in leaves and the influence of interfering stress conditions. *Plant Physiol.* **1992**, *100*, 1547–1553. [[CrossRef](#)]



© 2019 by the authors. Licensee MDPI, Basel, Switzerland. This article is an open access article distributed under the terms and conditions of the Creative Commons Attribution (CC BY) license (<http://creativecommons.org/licenses/by/4.0/>).

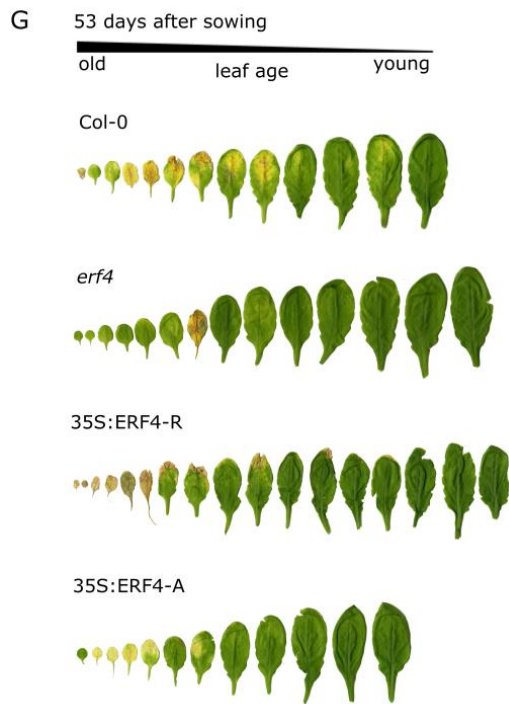
Supplemental Figures

Figure S1



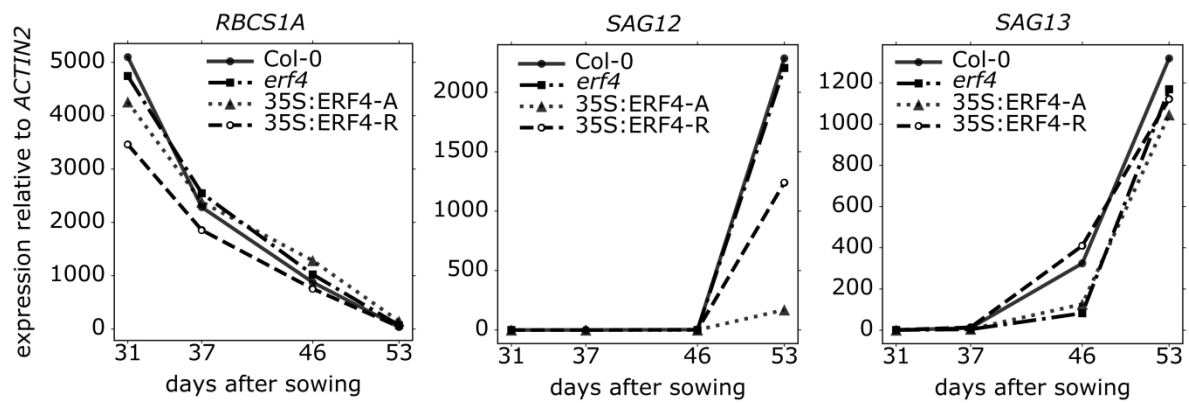
Continuation on next page

Continuation of Figure S1



Measurement of different parameters over the development of Col-0, 35S:ERF4-R, 35S:ERF4-A and erf4 mutant plant lines. (A) Shoot number and (B) shoot lengths (C) rosette leaf number and (D) fresh weight of leaf No. 6 were analyzed and percentage of plants with (E) siliques and (F) with flowers was determined at different time points. Bolting occurred between 28 and 31 DAS. Leaf number in (C) decreases at 53 days after sowing, because some leaves were already totally decayed and not counted any more. Data are means (\pm SE) of 5 biological replicates. Phenotyping experiments were performed in two different plant series with similar results. (G) Representative pictures of all rosette leaves, which were sorted according to their age, of different plant lines at 53 DAS.

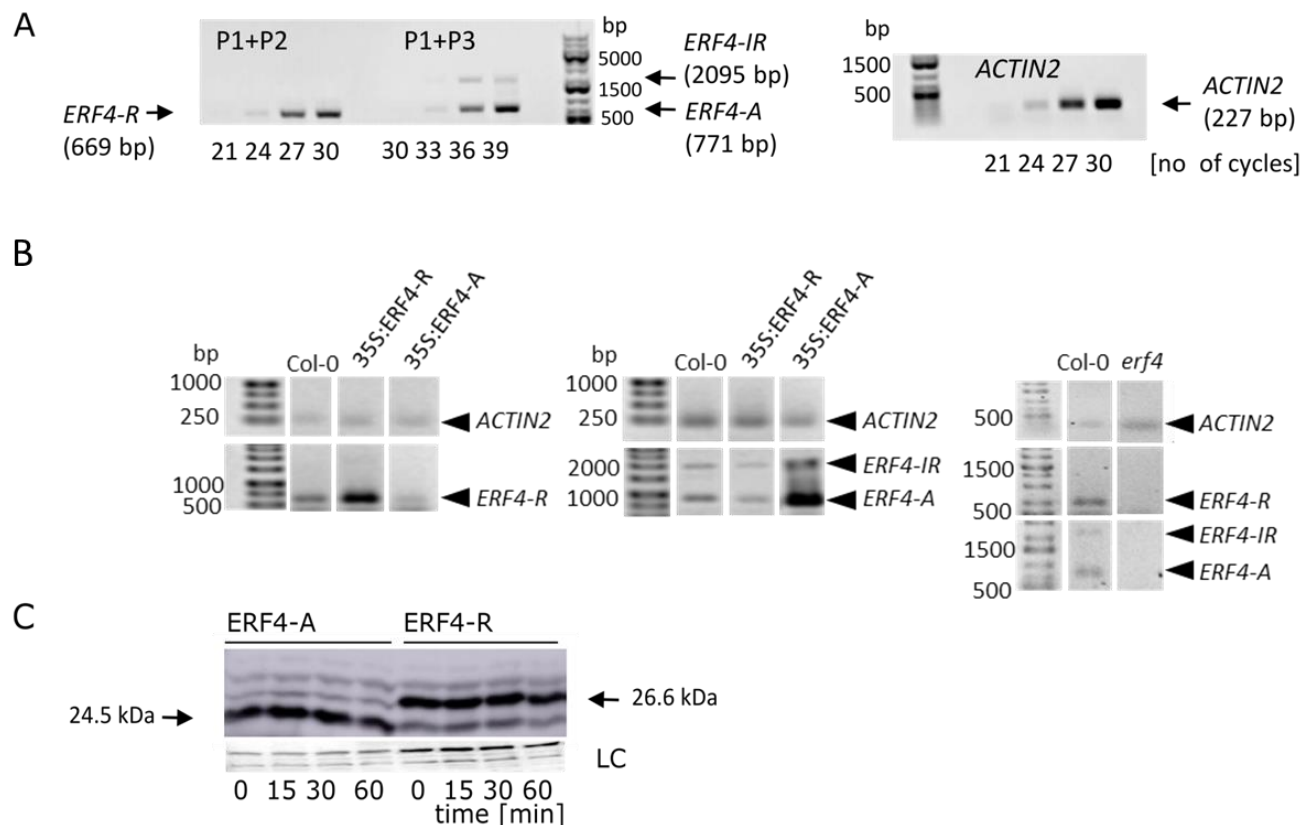
Figure S2



Relative expression level of senescence-related genes. qRT-PCR of senescence marker genes was performed in Col-0, *erf4*, 35S:ERF4-A and 35S:ERF4-R plants from 31-53 days after sowing for *RBCS1A*, *SAG13*, *SAG12*. Five leaves No. 7 were pooled for RNA isolation. Data are means of 2 technical replicates. Relative expression level was calculated and normalized to *ACTIN2* based on the method by Pfaffl *[40].

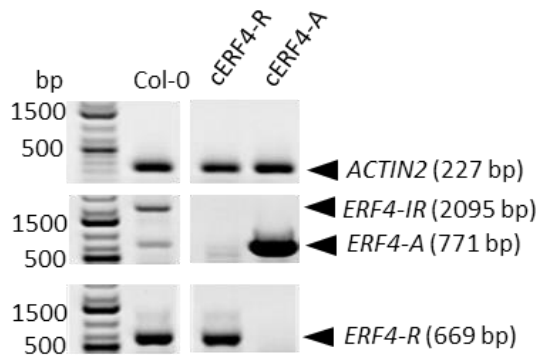
*[40] Pfaffl, M.W. A new mathematical model for relative quantification in real-time RT-PCR. *Nucleic Acids Res.* **2001**, 29, 45e.

Figure S3



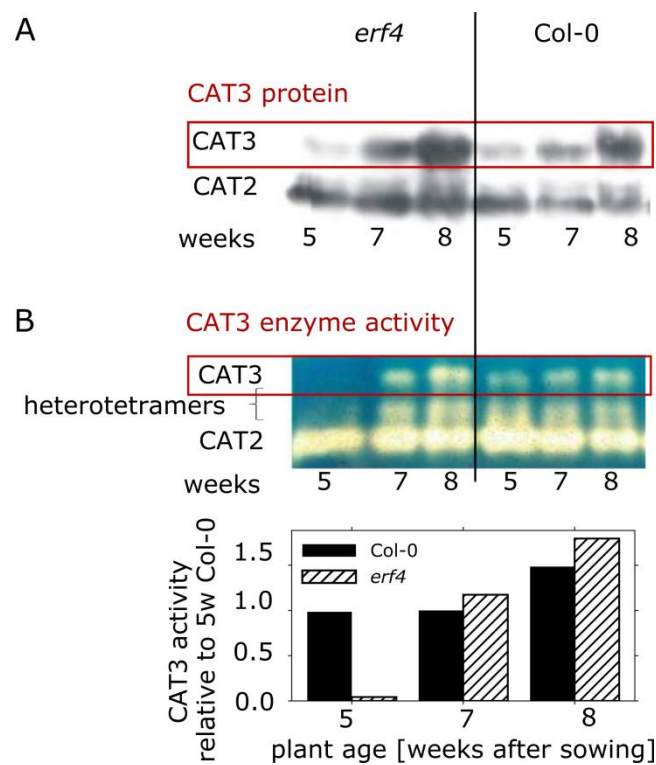
Isoform specific semi-quantitative RT-PCR. (A) Determination of the exponential range of amplification for *ERF4-A*, *ERF4-R* and *ACTIN2*. The genes were amplified using a pool of cDNAs, which originated from plants of different age. The PCR reaction is visualized on a 1% agarose gel. For optimal conditions for quantification, different amounts of cDNA were used for each isoform (*ERF4-A* 3 μ l, *ERF4-R* 2 μ l, *ACT2* 1 μ l). (B) Expression of the different *ERF4* isoforms in the 35S:*ERF4-R*, the 35S:*ERF4-A*, and the *erf4* mutant line compared to Col-0; one representative example of the semi-quantitative RT-PCR is shown, expression analyses were repeated at least three times with similar results. (C) In vitro plant protein stability in bacterial crude extracts was tested by using 25 μ g of bacterial crude protein extracts of *E. coli* BL21 Rosetta expressing recombinant HIS-tagged *ERF4-A* (24.5 kDa) and *ERF4-R* (26.6 kDa) proteins, respectively. Proteins were incubated for 0-60 min. In contrast to incubation with crude plant protein extracts (Figure 2D), no degradation was observed. Amido black staining of the upper region of the PVDF membranes is presented as loading control (LC).

Figure S4



Isoform specific semi-quantitative RT-PCR of the complementation lines. Representative agarose gel images of the semi-quantitative RT-PCR using RNA isolated from plants of different genotypes: Col-0, cERF4-A, cERF4-R. 36 cycles and 3 μ l cDNA were used for *ERF4-A/ERF4-IR* and 27 cycles and 2 μ l cDNA for *ERF4-R*. Experiments were repeated at least 3 times with similar results.

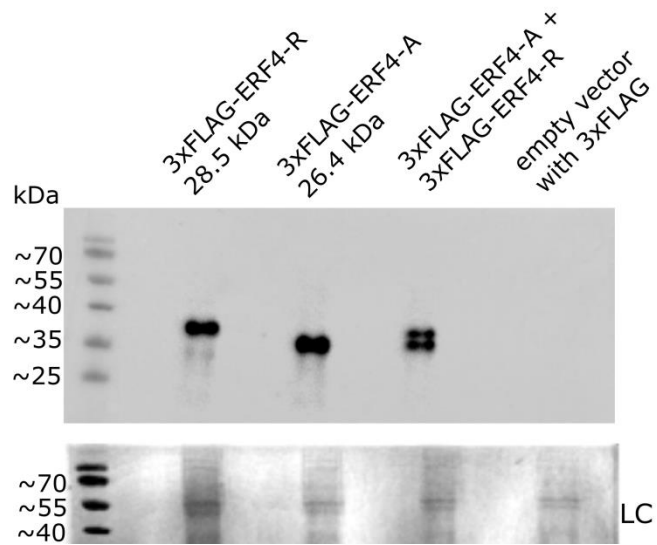
Figure S5



CATALASE protein amounts and enzyme activity in 5- to 8- week-old *Col-0* and *erf4* mutant plants. **(A)** Western Blot of 30 μ g of crude protein extracts separated on a 7.5% gel with subsequent immunodetection using polyclonal anti-rye-CAT antibodies, which were kindly provided by J. Feierabend*[58]. **(B)** Enzyme activity of catalase isoforms visualized in a native zymogram using 5 μ g of crude protein separated on a 7.5% native gel, Western Blotting and subsequent staining for catalase activity. Intensities of the CAT3 bands were quantified using *ImageJ*.

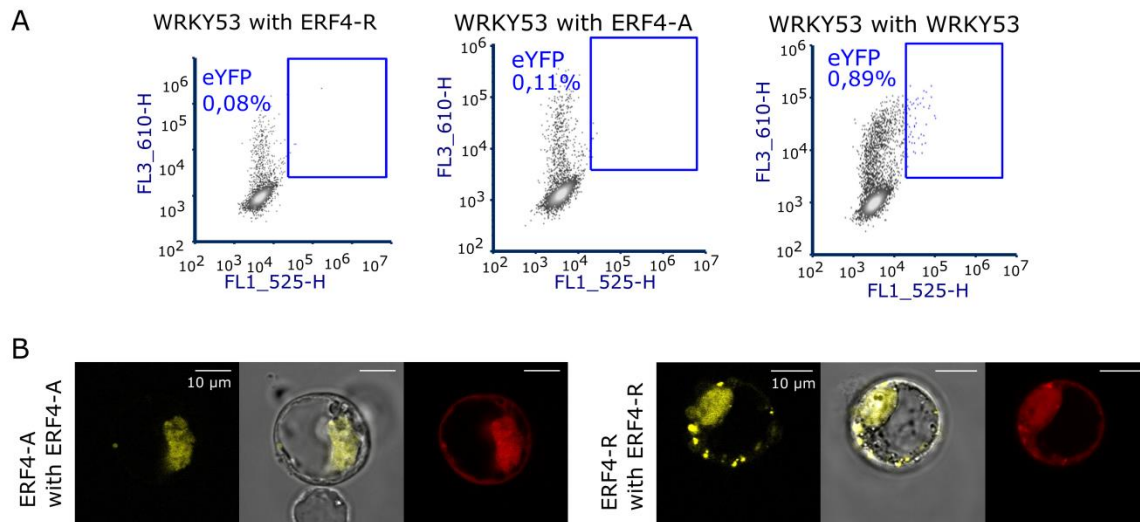
*[58] Hertwig, B.; Streb, P.; Feierabend, J. Light dependence of catalase synthesis and degradation in leaves and the influence of interfering stress conditions. *Plant Physiol.* **1992**, *100*, 1547-1553.

Figure S6



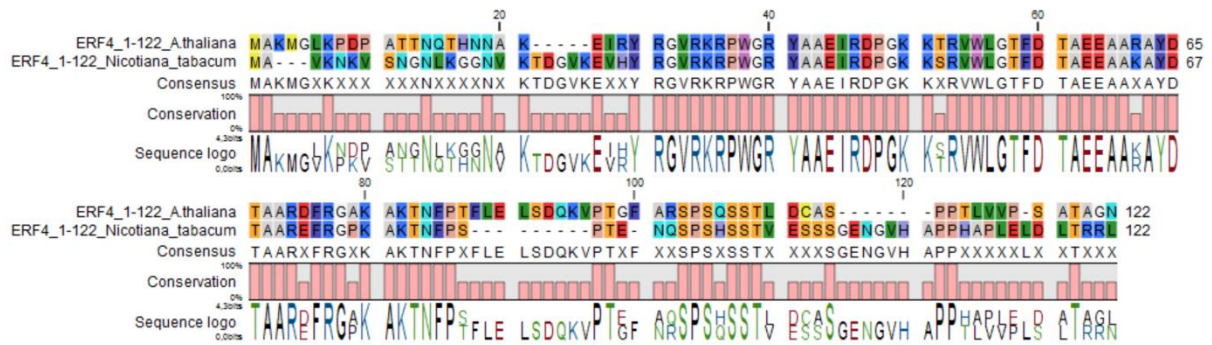
ERF4-A and *ERF4-R* protein expression in *Arabidopsis* protoplasts. Crude extracts of *Arabidopsis* protoplasts expressing 3xFLAG-tagged ERF4 isoforms and the empty vector with 3xFLAG were separated on a SDS gel. After Western blotting, proteins were immunodetected with monoclonal anti-FLAG primary antibodies (Sigma-Aldrich) and anti-mouse secondary antibodies (Sigma-Aldrich). As a loading control (LC), the proteins on the PVDF membrane were stained with amido black after immunodetection.

Figure S7



Protein-Protein interactions in transiently transformed protoplasts. (A) BiFC flow cytometry experiments were performed in Arabidopsis protoplasts co-expressing ERF4-R, ERF4-A and WRKY53 fused with YFP-N and YFP-C, respectively. Representative graphs of the flow cytometry results are shown. Blue dots represent eYFP signals of interaction. Blue squares mark the cells showing eYFP signal. (B) Confocal microscopy pictures of Arabidopsis protoplasts, transfected with the same BiFC constructs. eYFP indicates interaction; mRFP is a transfection control.

Figure S8



Protein alignment of the first 122 amino acids (AA) of *A. thaliana* and *N. tabacum* ERF4, 70 AA of the 122 AA (57.4%) are identical, AA at position No. 44-75 are highly conserved with 7 sour AA (indicated in red).

Table S1: Primer sequences

primer name	sequence	method	reference
ERF4R-qF	TTGCCTCCTCCATCGGAACAGG	qRT-PCR	Lyons et al., 2017
ERF4R-qR	CAAAAAGAAGAAGAAACGCATGCGC	qRT-PCR	Lyons et al., 2017
ERF4IR-qF	TTCCAGCAGACACGCAGCCG	qRT-PCR	Lyons et al., 2017
ERF4IR-qR	TGTCCGTA CTCTGTGAGTGGACCC	qRT-PCR	Lyons et al., 2017
ERF4A-qF	GGCTTGTGGTGCCCAAAGCG	qRT-PCR	Lyons et al., 2017
ERF4A-qR	TCACACCCTCTTATACGTCGTCGT	qRT-PCR	Lyons et al., 2017
CAT3-qF	AGGTACAGATCATGGGCACCAG	qRT-PCR	
CAT3-qR	AAGGATCGATCAGCCTGAGACC	qRT-PCR	
ACTIN2-f	ACCCGATGGGCAAGTCATCACG	qRT-PCR	
ACTIN2-r	TCCCACAAACGAGGGCTGGA	qRT-PCR	
SAG12-f	TCCTTACAAAGGCGAAGACGCTAC	qRT-PCR	
SAG12-r	ACCGGGACATCCTCATAACCTG	qRT-PCR	
SAG13-f	AGGGAGCATCGTGCTCATATCC	qRT-PCR	
SAG13-r	CCAGCTGATTCATGGCTCCTTTG	qRT-PCR	

WRKY53-f	ATCCCGGCAGTGTTCCAGAATC	qRT-PCR	
WRKY53-r	AGAACCTCCTCCATCGGCAAAC	qRT-PCR	
RBCS1A-f	ACCTTCCTGACCTTACCGATTCCG	qRT-PCR	
RBCS1A-r	GGTACACAAATCCGTGCTCCAAC	qRT-PCR	
CAB1-f	TGCACTACTCAACCTCAATGGC	qRT-PCR	
CAB1-r	AAAGCTTGACGGCCTTACCG	qRT-PCR	
FPA-f	CAACCACCAGCAGATAAGGC	qRT-PCR	
FPA-r	TGTTGTACCCTGACCATCCC	qRT-PCR	
ESP/ESR-f	GTGTGGGAAAAGTTGGGAGA	qRT-PCR	
ESP/ESR-r	CATGAGGAGGCCATTCTTTC	qRT-PCR	
ERF4-Start-f	ATGGCCAAGATGGGCTTGAAACCCGA	sqRT-PCR	Lyons et al., 2017
ERFA-STOP-r	CTACACGAGAATCACGAAAGGATAGTTATTGACT	sqRT-PCR	Lyons et al., 2017
ERF4R-STOP-r	TCAGGCCTGTTCCGATGGAGGAGG	sqRT-PCR	Lyons et al., 2017
Promoter-CAT3-f	AATGCTGACTTGTCGGGGTCAGCGATTATTATTAGTCACCGAACGAATTTTTC TT	EMSA, ELISA	
Promoter-CAT3-r	AAGAAAAATTCGTTTCGGTGACTAATAATAATCGCTGACCCCGACAAGTCAGC ATT	EMSA, ELISA	

PW53WBox1-f (mutated)	ATGGTTTGAAAATTTAAAAAAATTTTCA	EMSA	
PW53WBox1-r (mutated)	TGAAAATTTTTTTTAAATTTTCAAACCAT	EMSA	
ERF4-attB1-f	GGGGACAAGTTTGTACAAAAAAGCAGGCTTCATGGCCAAGATGGGCTTGAA	cloning	
ERF4A-attB2-r	GGGGACCACTTTGTACAAGAAAGCTGGGTTCATTGTTTTGTACCTTCGA	cloning	
ERF4R-attB2-r	GGGGACCACTTTGTACAAGAAAGCTGGGTTCAGGCCTGTTCCGATGGAG	cloning	
Promoter- CAT3-attB1-f	GGGGACAAGTTTGTACAAAAAAGCAGGCTGGGGTGAATCTAGATATCAG	cloning	
Promoter- CAT3-attB2-r	GGGGACCACTTTGTACAAGAAAGCTGGGTGGTGATGATAGAAGGTTGA	cloning	
pERF4-3kb-f	GGGGACAAGTTTGTACAAAAAAGCAGGCTTATCGCAACCAAACCTCTCTT	cloning	
pERF4-3kb-r	GGGGACCACTTTGTACAAGAAAGCTGGGTTCCTCGGATAGATAGATTAGA	cloning	
attR3-ERF4-f	GGGGACAACCTTTGTATAATAAAGTT GGAATGGCCAAGATGGGCTTGA	2in1 BiFC cloning	
attR1-ERF4-f	GGGGACAAGTTTGTACAAAAAAGCAGGCTTAATGGCCAAGATGGGCTTGA	2in1 BiFC cloning	
ERF4A-Stop- attR2	GGGGACCACTTTGTACAAGAAAGCTGGGTTCATTGTTTTGTACCTTCGAA	2in1 BiFC cloning	
ERF4R-Stop- attR2	GGGGACCACTTTGTACAAGAAAGCTGGGTTCAGGCCTGTTCCGAT	2in1 BiFC cloning	
ERF4R-Stop- attR4	GGGGACAACCTTTGTATAGAAAAGTTGGGTTCAGGCCTGTTCCGAT	2in1 BiFC cloning	
ERF4A-Stop- attR4	GGGGACAACCTTTGTATAGAAAAGTTGGGTTCATTGTTTTGTACCTTCGAA	2in1 BiFC cloning	
attR3-WRKY53	GGGGACAACCTTTGTATAATAAAGTTGGAATGATGGAAGGAAGAGATATGTTA	2in1 BiFC	

	AGTT	cloning	
attR1-WRKY53	GGGGACAAGTTTGTACAAAAAAGCAGGCTTAATGATGGAAGGAAGAGATATG TTAAGTT	2in1 BiFC cloning	
WRKY53-attR2	GGGGACCACTTTGTACAAGAAAGCTGGGTTTAATAATAAATCGACTCGTGTA AA	2in1 BiFC cloning	
WRKY53-attR4	GGGGACAACCTTTGTATAGAAAAGTTGGGTTTAATAATAAATCGACTCGTGTA AA	2in1 BiFC cloning	
Cat3-8 eco	ggaattccGAGCAATGCTGACTTGTCG	Cloning for Y1H	
		Cloning for Y1H	
Cat3-19-xba	ctctagagACATGTTTCGATCTTATCGCA		

Article

Nitrogen Supply Drives Senescence-Related Seed Storage Protein Expression in Rapeseed Leaves

Stefan Bieker ¹, Lena Riester ¹, Jasmin Doll ¹, Jürgen Franzaring ², Andreas Fangmeier ² and Ulrike Zentgraf ^{1,*}

¹ Centre of Molecular Biology of Plants, University of Tübingen, Auf der Morgenstelle 32, D-72076 Tübingen, Germany; stefan.bieker@zmbp.uni-tuebingen.de (S.B.); lena.riester@zmbp.uni-tuebingen.de (L.R.); jasmin.doll@zmbp.uni-tuebingen.de (J.D.)

² Institute of Landscape and Plant Ecology, University of Hohenheim, August-von-Hartmann-Str. 3, D-70599 Stuttgart, Germany; Juergen.Franzaring@uni-hohenheim.de (J.F.); andreas.fangmeier@uni-hohenheim.de (A.F.)

* Correspondence: ulrike.zentgraf@zmbp.uni-tuebingen.de

Received: 20 December 2018; Accepted: 17 January 2019; Published: 22 January 2019



Abstract: In general, yield and fruit quality strongly rely on efficient nutrient remobilization during plant development and senescence. Transcriptome changes associated with senescence in spring oilseed rape grown under optimal nitrogen supply or mild nitrogen deficiency revealed differences in senescence and nutrient mobilization in old lower canopy leaves and younger higher canopy leaves. Having a closer look at this transcriptome analyses, we identified the major classes of seed storage proteins (SSP) to be expressed in vegetative tissue, namely leaf and stem tissue. Expression of SSPs was not only dependent on the nitrogen supply but transcripts appeared to correlate with intracellular H₂O₂ contents, which functions as well-known signaling molecule in developmental senescence. The abundance of SSPs in leaf material transiently progressed from the oldest leaves to the youngest. Moreover, stems also exhibited short-term production of SSPs, which hints at an interim storage function. In order to decipher whether hydrogen peroxide also functions as a signaling molecule in nitrogen deficiency-induced senescence, we analyzed hydrogen peroxide contents after complete nitrogen depletion in oilseed rape and *Arabidopsis* plants. In both cases, hydrogen peroxide contents were lower in nitrogen deficient plants, indicating that at least parts of the developmental senescence program appear to be suppressed under nitrogen deficiency.

Keywords: senescence; nitrogen remobilization; nitrogen supply; oil seed rape; seed storage proteins; hydrogen peroxide

1. Introduction

Despite being a member of the glucosinolate producing Brassicaceae family, selection and breeding of oilseed rape (OSR, *Brassica napus* L.) has made it one of the most important oilseed crops after soybean and oil palm. In addition to high oil contents, its seeds contain high amounts of protein, constituting up to 20%–25% of seed dry weight [1]. Around 60% of this protein content are composed of seed storage proteins (SSPs), which in turn are mainly comprised of two protein families: 12S globulins (Cruciferins) and 2S albumins (Napins) [2,3]. Cruciferins and napins have distinct molecular characteristics and respond differentially to the changes in pH and temperature, therefore their functionalities are most likely contrasting rather than complementary [4]. SSPs are synthesized in the endoplasmatic reticulum and then stored in protein storage vacuoles. Seed storage reserves accumulate with progression of seed growth and development and in mature oilseed rape seeds, the endosperm and the cells of embryo are packed full of protein storage vacuoles and oil bodies.

The protein content in the seeds of the Brassica species is affected by the translocation of amino-N and loading of amino acids in the phloem sap of leaves, indicating that seed filling and seed quality strongly rely on remobilization of previously acquired nutrients from the leaves. Phloem unloading in the endosperm and embryo cells by specific transporters also plays an important role. In Arabidopsis, amino acid permease 1 and 2 (AAP1/2) and the cationic amino acid transporter 6 (AtCAT6) mediate AA uptake in the embryo and have an impact on SSP accumulation [5]. QTL mapping identified a total of 67 and 38 QTLs for seed oil and protein content and provided new insights into the complex genetic mechanism of oil and protein accumulation in the seeds of OSR [6]. During germination, the seed storage reserves deposited in the protein storage vacuoles and oil bodies in the endosperm and embryo tissue are degraded for energy supply and anabolic processes of seedling development. In-depth proteomic dissection contributed to a better understanding of the mobilization of seed storage reserves and regulatory mechanisms of the germination process in *B. napus* [7].

Before anthesis, sequential leaf senescence leads to the repartitioning of nutrients from older leaves to newly developing non-reproductive organs. The bottleneck of weak nitrogen (N) remobilization associated with senescence in vegetative stages appears not to be amino acid transport from leaf to phloem but rather an incomplete hydrolysis of foliar proteins [8]. After anthesis, monocarpic leaf senescence governs the nutrient reallocation to the now developing reproductive organs and therefore, has a critical impact on yield quality and quantity. For example in wheat, leaf-derived N remobilized by senescence processes accounts for up to 90% of the total grain N-content [9]. Consistent with the importance of senescence for the plants' reproductive success, highly controlled processes are put in place to govern it. A complex interplay between hormone action, genetic reprogramming as well as biotic and abiotic factors administer initiation, progression and termination of senescence and thus influences the outcome of nutrient recycling. In Arabidopsis, differential regulation of more than 6000 genes during onset and progression of leaf senescence emphasizes the importance of this developmental program [10]. In this analysis, autophagy, transport and response to reactive oxygen species (ROS) are the first processes activated in the chronology of leaf senescence [10]. ROS, especially H_2O_2 , are well known signaling molecules in senescence and we have demonstrated that developmental senescence in Arabidopsis as well as in OSR is associated with the down-regulation of central components of the anti-oxidative systems and thus associated with a transient increase in intracellular H_2O_2 contents [11,12]. If this H_2O_2 signal is suppressed in Arabidopsis, senescence is delayed [11].

Even though *B. napus*' performance regarding uptake of inorganic N is relatively high, N-remobilization during leaf senescence is believed to not be very efficient [13]. As a consequence of high demand and uptake during vegetative growth but rather low remobilization afterwards, surrounding ecosystems are often polluted by leaching of remaining soluble leaf-nitrogen (NO_3^-) into the water as well as by volatilization of N_2O and NH_3 into the atmosphere. In addition to the detrimental impacts on environment and water supply by oversaturation with nitrogenous compounds, production of inorganic nitrogen fertilizers is highly resource- and cost-intensive. Enormous progress has already been made by breeding plants with respective traits for high nutrient uptake and remobilization efficiencies, high photosynthetic rates, high sink capacities, variation of fatty acid contents etc. However, there seems to be a natural trade-off between high yield and high protein content [5,14,15]. Hence, besides new breeds, genetically modified crops seem to be one of the most viable and tangible options, not only to avoid a further increase of environmental pollution, but also to tackle upcoming bottlenecks in the global food supply.

Developmental senescence progresses sequentially from the lower to the upper leaves in which the sink leaves in young plants later turn into source leaves during pod ripening [16]. N-deficiency leads to earlier induction of senescence in older leaves, while senescence is delayed at higher leaf positions [17,18]. Transcriptome analyses of leaves in two canopy levels over development of plants grown under two N-fertilization regimes also revealed opposite effects of N-depletion on senescence in lower versus upper canopy leaves. Several transcriptional regulators and protein degradation genes

were identified to be differentially expressed in N-depleted lower leaf positions [19]. Morphology and performance analyses of exactly the same plants used in this study have been previously reported by Franzaring et al. [20] who analyzed the effect of today's and future CO₂ and its interaction with nitrogen supply. Even though the flowering window of OSR was largely extended due to elevated CO₂, plants were not able to produce more pods but strongly branched out and produced many side shoots pointing to a prevented apical switch-off by high CO₂ [20]. N-remobilization was more affected by the different N-supply than by the CO₂ enrichment. Under ambient CO₂ concentrations, the nitrogen use efficiency (NUE) of the seeds was reduced by 2%, 33% and 65% under low, optimal, and high N treatments, respectively [21]. Moreover, ¹⁵N-labeled fertilizer was supplied at three different time points to follow up nitrogen recovery over time and the distribution of the nutrient between source and sink organs. ¹⁵N-supplied at the beginning of plant development mainly accumulated in roots and shed senescent leaves while ¹⁵N-supplied at later stages ended up in late leaves, stem and reproductive tissue [21].

In order to understand the nitrogen remobilization processes in OSR under different nitrogen regimes more precisely, we analyzed the transcriptome data, which have been produced by Safavi-Rizi and co-workers [19] for genes involved in nitrogen remobilization and metabolism. Surprisingly, we realized that a remarkable amount of SSPs or proteins related to SSP expression were also expressed in leaf tissue, which we followed up in more detail to get some clues about their function in leaves. In a new growth experiment, we confirmed that the SSP genes *CRUCIFERIN* and *NAPIN* were expressed and that the corresponding proteins are produced in leaf tissue. *CRUCIFERIN* mRNA accumulated in leaf tissue at the onset of leaf senescence under high but not under low N-supply. In contrast, *NAPIN* expression was higher in leaves fertilized with low amounts of N but lower under high N-supply. SSP production progressed from the oldest to the youngest leaves and correlated with increasing hydrogen peroxide levels. SSPs were also detected in stem tissue and pod walls pointing to a possible function as an interim N-storage during N-remobilization. *In-silico* analysis of the corresponding promoter sequences identified motifs suggesting a (redox-) stress and nutritional supply dependent expression control. Moreover, when N was completely withdrawn, N-starvation induced premature senescence, but at the same time, a reduction of intracellular H₂O₂ contents in OSR as well as in *Arabidopsis* was observed. This indicates that N-starvation induced senescence is driven by different signals compared to developmental senescence and that at least the hydrogen peroxide-driven parts of the developmental senescence processes appear to be suppressed in N-starvation induced senescence.

2. Material and Methods

2.1. Plant Growth Conditions

Oilseed rape plants (*Brassica napus* cv Mozart):

Nitrogen starvation and developmental OSR series on soil: Plants were grown in greenhouses at 19–22 °C, with a 16 h photoperiod. All plants were sown on *Einheitserde classic-Topferde* (*Einheitserde* Werkverband e.V., Sinntal-Altengronau, Germany) in 6 × 6 cm pots. Later, plants for N-starvation experiments were put on a nutrient depleted soil (*Einheitserde Typ 0*). This was combined with repotting at around 4 weeks of plant age. Here, only control plants received fertilization with *Wuxal*[®] *Super* (Wilhelm Haug GmbH & Co KG, Ammerbuch-Pfäffingen, Germany) containing 99.2g N/L. Each pot was watered with 1 L of a 0.2% fertilizer solution once a week. After 4 days of habituation, harvests were conducted as indicated. Plants for developmental senescence assays were kept on *Einheitserde classic-Topferde*. Plants were sown in a weekly rhythm for 16 weeks in the green house. Leaf positions 5, 8, 12, the leaf residing directly below the first developing pods (terminal leaf/T-Leaf), the stem between T-leaf and first pod, and the siliques were sampled on the same day at the same time point.

Field-near conditions: Climate conditions were simulated in growth chambers at the University of Hohenheim, using the seasonal changes of day length and temperature of South-Western Germany as described in Franzaring, Weller, Schmid and Fangmeier [20]. N was supplied in three different regimes,

namely *low* (N_L), *optimal* (N_O) and *plus* (N_P), fertilized with 75, 150 and 225 kg ha⁻¹, respectively. Nutrient supply and atmospheric conditions were kept as described in Franzaring, Gensheimer, Weller, Schmid and Fangmeier [21]. Plants were ¹⁵N-labeled with double labeled ammonium nitrate with a ¹⁵N excess of 10% ($\delta^{15}\text{N}$ of 100‰) at DC 0 (first fertilization at 0 DAS, “old N”), at DC 30 (second fertilization at 72 DAS) or at DC 59 (third fertilization at 80 DAS, “new N”) as described in Franzaring, Gensheimer, Weller, Schmid and Fangmeier [21].

Nitrogen starvation on hydroponics: Plants were germinated at a 16 h photoperiod, 18–22 °C and 75% relative humidity (RH) on filter paper sandwiched between sponges and PVC-plates on both sides. After seven days, the seedlings were transferred to pots with 6 liters liquid medium in a greenhouse with also 16 h photoperiod and 75% RH. After 28 days pre-culture at 2 mM N, N-starved plants received low N liquid medium (0.1 mM N), full N plants continued receiving N-rich medium (4 mM N). For more detailed composition see Supplementary Materials Table S1 (published in Koeslin-Findeklee et al. [22])

Arabidopsis thaliana Col-0 plants: Plants were grown on a modified Araponics© system (Araponics SA, Liege, Belgium) including aeration of the liquid medium. Moreover, plants were grown on sterilized mineral-wool instead of the recommended agarose. Seeds were stratified for 4 days at 4 °C, and then moved into growth chambers. Temperature was kept at 21 °C, day length was 8 h. Liquid media were exchanged every second day. During the first week after germination, tap water was used as hydroponic medium. Afterwards, plants received 0.5 mM N during the second week and 1 mM N during the third week. With the beginning of the treatment (the fourth week onwards) 0 and 4 mM were supplied to N-starved and control plants, respectively (for more detailed media composition and schedule see Supplementary Materials Table S2).

2.2. H₂O₂ Measurements

Leaf discs (1 cm diameter, *B. napus*) or whole leaves (*A. thaliana*) were sampled from the same leaf positions and then incubated in MS-Medium (pH 5.7) with 9.5 μM 5(6)-Carboxy-Di-Hydro-Di-Chloro-Fluorescein-Di-Acetate (Carboxy-H₂DCFDA). After 45 min incubation, samples were rinsed twice with distilled water and frozen in liquid nitrogen. Homogenization was conducted on ice in 500 μL 40 mM Tris-HCl pH 7. After 30 min of centrifugation at 4 °C and 14,000 rpm, fluorescence of supernatant was determined (480 nm excitation, 525 nm emission, Berthold TriStar LB941, BERTHOLD TECHNOLOGIES, Bad Wildbad, Germany). H₂DCFDA solution was prepared freshly for each harvest and calibrated by chemical de-acetylation and oxidation following Cathcart et al. [23].

2.3. Generation of Anti-SSP Antisera

Antisera were generated against VVEFEDDA (NAPIN) and VVRPLLQR (CRUCIFERIN) peptides. Peptide synthesis and animal immunization were carried out by BioGenes (Berlin, Germany). Peptide sequences were chosen based on alignments of Arabidopsis and *B. napus* seed storage protein. Antisera were used directly without further purification.

2.4. Protein Extraction and Western-Blotting

Samples were homogenized on liquid nitrogen. Protein extraction buffer was added according to the sample amount (modified QB-Buffer; 100 mM KPO₄, 1 mM EDTA, 1% Triton-X100, 10% glycerol, 1 mM DTT, 150 mM NaCl), samples were then incubated for 20–30 min on ice. After subsequent centrifugation at 20.800 g and 4 °C for 20–60 min (depended on sample type: shoot material with many fibers as well as oily seed material were centrifuged longer) total protein content of the supernatant was determined. 15 μg total protein of the very same *B. napus* (cv. Mozart) seed sample as positive control and 25 μg of total protein of all other samples were then separated by SDS-DISC-PAGE (15% PAA separating, 3.5% PAA stacking gel). After transfer on PVDF-membranes by semi-dry blotting, membranes were washed twice with TBS-T, incubated for 1 h in 5% milk-powder TBS-T and after

another washing with TBS-T incubated in 1.5% milk-powder TBS-T with 1:500 diluted antisera for 1–2 h. Anti-rabbit-HRP antibody (CellSignaling, #7074) was used as secondary antibody in a 1:3,000 dilution in 1.5% milk-powder TBS-T. Blots were incubated another hour in this solution. After three times washing with TBS-T, detection was carried out with luminol detection kit (*Pierce ECL* or *BioRad Clarity*) in an *Amersham Imager 600* (GE Healthcare, Berlin, Germany).

For relative quantification, the gel analyzer plugin of *ImageJ* was used. Integrated band intensities were normalized to bands of the respective positive controls. As different antisera were used, NAPIN and CRUCIFERIN signals could not be directly compared and signal intensities were normalized to appropriate bands in whole seed extracts that served as positive controls.

2.5. RNA Extraction and qRT-PCR

Primer design for qRT-PCR was done via QuantPrime [24]. RNA extraction and cDNA synthesis were conducted with InviTrap Spin Universal RNA Mini Kit (Invitex Inc, San Francisco, CA, USA) and qScript cDNA SuperMix (Quanta Biosciences, Beverly, Massachusetts, USA) according to the manufacturer's protocols. qRT-PCR was performed with Perfect CTa SybrGreen Fast Mix (Quanta Biosciences, Beverly, MA, USA) in an iCycler IQ system (Biorad, München, Germany). Relative quantification to *ACTIN2* was calculated with $\Delta\Delta C_T$ -Method [25]. Primers used for *B. napus* *NAPIN2* (*Bna.2093*) were: 5'-TGG CAA GCT CTT AGG TGT TGA GC (FW) and 5'-CCG GCC CAT TTA GGA TTC CAA G (REV). For *CRUCIFERIN1* (*Bna.2089*): 5'-AGA CCA CTT TGA CGC ACA GCA G (FW) and 5'-AAG CCC TTA AGC ATC AGC CTT CC (REV).

2.6. Chlorophyll Measurements

Chlorophyll (Chl) contents were estimated via a *SPAD 502* (*KONICA MINOLTA*) photometer or the *atLEAF +* (*FT Green, LLC*) device. Measurements were conducted at least three times per leaf on varying positions to avoid positional effects.

2.7. Microarray Data Evaluation

The plant material of *Brassica napus* cv. Mozart, which was used for transcriptome analyses, the design of the *B. napus* custom microarray, the identification of *Arabidopsis thaliana* homologues of the *B. napus* unigenes, and the basic data analysis workflow are described in Safavi-Rizi et al. [19]. In this experiment, oilseed rape plants were grown under two different nitrogen regimes, optimal (N_O) and low (N_L) nitrogen. The lower canopy leaf No. 4 was harvested at 78, 85, 92, and 99 days after sowing (DAS) and the upper canopy leaf No. 8 at 92 and 106 DAS (Figure 1A). Physiological analysis with respect to carbon and N-dependent effects as well as detailed description of growth conditions were published in Franzaring, Weller, Schmid and Fangmeier [20] and Franzaring, Gensheimer, Weller, Schmid and Fangmeier [21]. Briefly, expression data analysis was conducted in R [26] with the *Linear Model for Microarray and RNA-Seq Data* (LIMMA) package [27] applying the standard time-course experiment workflow. Contrast matrixes were built within one treatment with a *p*-value cut-off 0.05 (Benjamini Hochberg correction) and log₂ fold-change cut-off of 1. *B. napus* genes were annotated by their most similar *A. thaliana* orthologue, identified by local BLAST+ (version 2.2.30 +, build Aug 28 2015 11:17:27, [28]) against the *TAIR-10-Database* [29]. Blast results with an e-value > 10⁻³ were excluded from further analysis. Finally, all transcripts associated with SSPs were extracted by matching *AGI* identifiers to a list of identifiers of SSP associated genes (for listings see Supplementary Materials Table S3).

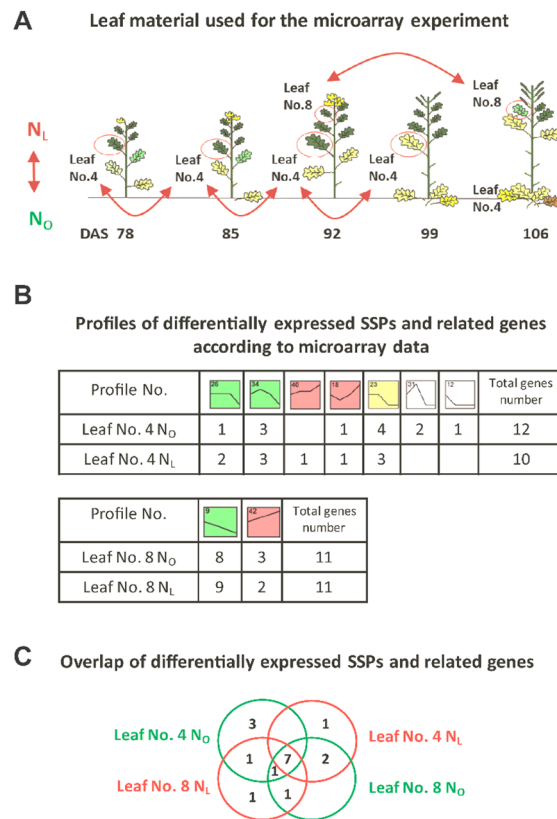


Figure 1. SSPs and related genes differentially expressed during development and/or N-supply assigned to 9 different expression profiles. (A) Illustration of the leaf material used in the microarray experiment (modified after Safavi-Rizi et al. [19]). Leaf No. 4 was analyzed at 4 different time points, leaf No.8 was analyzed at 2 different time points under N_L or N_O supply, respectively. (B) Number of SSPs and related genes, which were differentially expressed in leaf No. 4 and leaf No. 8 under N_L and under N_O conditions. Each box represents one of 50 pre-defined expression profiles [19]. The number of each model expression profile is shown in the top left corner of each box, all colored profiles contain a significant number of temporally and N-dependently regulated genes. Profiles with the same color are very similar and defined as one cluster in Safavi-Rizi et al. [19]. (C) Overlap of differentially expressed SSPs and related genes between leaf No. 4 and No. 8 and the growth conditions N_L and N_O.

2.8. Total N and $\delta^{15}\text{N}$ -Measurements

Seeds were ground in liquid nitrogen. Subsequently, the homogenized powder was lyophilized and total N-content was measured by a CN-element analyzer (Elementar Vario EL III, Elementar Analysensysteme GmbH, Langensfeld, Germany) via heat combustion at 1150 °C and thermal conductivity detection. The stable isotope ratio $^{15}\text{N}/^{14}\text{N}$ was measured as described in Franzaring, Gensheimer, Weller, Schmid and Fangmeier [20] using an isotope ratio mass spectrometer (Deltaplus XL, Thermo Finnigan, Bremen, Germany) connected by an open split device (ConFlow II, Thermo Finnigan, Bremen, Germany). The $^{14}\text{N}/^{15}\text{N}$ ratio was expressed relative to the isotopic signature of N₂ in the air as δ values (in ‰).

2.9. Catalase Zymograms

Leaf discs (1 cm diameter) were taken from approx. the same position within the respective leaf and frozen in liquid nitrogen. After homogenization on ice with extraction buffer (100 mM Tris, 20% glycerol (*v/v*), 30 mM DTT, pH 8.0) samples were centrifuged for 15 min at 4 °C and 14,000 rpm. Total protein concentration of the supernatant was determined and 15 μg protein were separated via native PAGE (7.5% polyacrylamide, 1.5 M Tris, pH 8.8; running buffer: 25 mM Tris, 250 mM Glycin, pH 8.3). After protein separation, gels were rinsed twice with distilled water, incubated for 2 min in 0.01%

hydrogen peroxide solution and then rinsed again twice with water. Incubation in staining solution (1% FeCl₃ and 1% K₃[Fe(CN)₆]) was carried out under constant agitation until bands became visible (4–6 min). To stop any staining reaction, the solution was removed and the gel was rinsed with water.

3. Results

3.1. Transcriptome Analysis of OSR during Induction of Senescence under Two Different N-Supplies

To investigate the process of senescence induction and N-remobilization in OSR in more detail, microarray data made available by Safavi-Rizi et al. [19] were screened for genes related to nitrogen metabolism and nitrogen storage differentially expressed under optimal (N_O) and low (N_L) nitrogen. Among the genes that we identified to be related to nitrogen metabolism, we found a substantial number of genes encoding SSPs or proteins related to them, which were initially described to be exclusively expressed in seed tissue. However, here we found a reasonable expression in leaf tissue. An AGI code list with SSP and SSP-associated transcripts was compiled (Supplementary Materials Table S3). Out of the 124 AGI identifiers, 17 *Bn* unigenes or gene clusters were differentially expressed in OSR according to development and/or N-supply. These could be assigned to 9 different expression profiles which have been defined by Safavi-Rizi and co-workers [19]; all colored profiles contain a significant number of temporally and N-dependently regulated genes [19]. Seven SSP and/or related genes were differentially expressed in leaf No. 4 and leaf No. 8 under both N-supplies, 15 under optimal N-supply (N_O) and 14 under low N-supply (N_L). A fairly high number of SSP related genes were differentially regulated in both leaves (11 out of 17), indicating that these transcripts appear to play a role during senescence progression at different canopies of the OSR plants (Figure 1B,C).

One important signaling molecule governing senescence regulation is hydrogen peroxide. Therefore, intracellular hydrogen peroxide contents of the same plant material were measured in leaf No.5 and already published in Bieker et al. [11]. Under optimal N-supply H₂O₂ reached its maximum levels at 12 weeks after sowing (85 DAS) and these high levels were maintained until week 13, while under low N the maximum was higher and was reached at week 13 (92 DAS). H₂O₂ declined at week 14 under both treatments. In order to get some hints whether H₂O₂ is involved in regulation of N-dependent senescence-associated gene expression and in the transcriptional regulation of the SSP-associated genes, we analyzed the correlation between H₂O₂ profiles and gene expression. Transcripts similar to *CRUCIFERIN3* (*CRU3*, At4G28520) and *MAIGO2* (*MAG2*, At3G47700) were induced in parallel to the H₂O₂ increase. *CRU3* belongs to the SSPs of the Cruciferin superfamily whereas the *MAG2* protein is involved in the ER exit of SSPs [30,31]. Interestingly, *SEED STORAGE ALBUMIN4* (*SESA4*, At4g27170) expression was reduced with rising H₂O₂ contents and induced when H₂O₂ levels declined again. This antagonistic behavior was also observed for *ECTOPIC EXPRESSION OF SSP1* (*ESSP1*, At2g19560) and several bifunctional-lipid transfer proteins (*BI-LTPs*). The same analysis was conducted for N_L data. Again, some SSPs were found to follow the H₂O₂ profile. However, instead of *CRUCIFERIN* transcripts, *NAPIN* (*SESA4*) peaked in its expression together with highest H₂O₂ levels, thus showing the exact adverse behavior compared to N_O. Moreover, under N_L conditions, *MAG2* was found to be repressed with increasing H₂O₂ contents and expression increased again with decreasing H₂O₂ levels. Disregarding H₂O₂ contents, overall up-regulated transcripts included transcripts similar to *BRAHMA* (*BRM*, At2gG46020) and SSP processing enzymes (homologues to At4g32940 e.g., *GAMMA-VPE*, γ -vacuolar processing enzyme). Interestingly, the *BRM* protein mediates SSP repression in vegetative tissues. Down-regulated transcripts contained multiple homologues to bifunctional-lipid transfer proteins (*BI-LTPs*), *VACUOLAR SORTING RECEPTOR HOMOLOG1* (*VSRI*, At3G52850) and *ESSP1*.

3.2. Verification of SSP Expression via qRT-PCR and Western-Blot

In order to confirm the expression patterns of the mayor seed storage proteins, the 12S globulins (Cruciferins) and 2S albumins (Napins) via qRT-PCR and to verify the production of the corresponding

proteins in leaves, another series of OSR plants was grown under constant greenhouse conditions. Again, an increase in SSP gene expression upon accumulation of H_2O_2 in *B. napus* leaves was observed. Moreover, timing of induction and repression of *CRUCIFERIN* coincided with the accumulation and decrease of intracellular H_2O_2 . However, in contrast to the microarray-experiment, in this experiment both, *CRUCIFERIN* and *NAPIN* were up-regulated which might be due to different growth conditions and uncontrolled N-supply. In addition, protein levels were analyzed via Western blot and subsequent immune detection of SSPs. Here, a progressive accumulation pattern emerged, starting with SSP production in the leaves at the lower canopy level when plants were still young. Later, expression continued with a build-up in upper canopy leaves when development progressed and SSPs usually start to accumulate in siliques and seeds. In addition, accumulation of SSPs was also observed in shoot tissue (Figure 2).

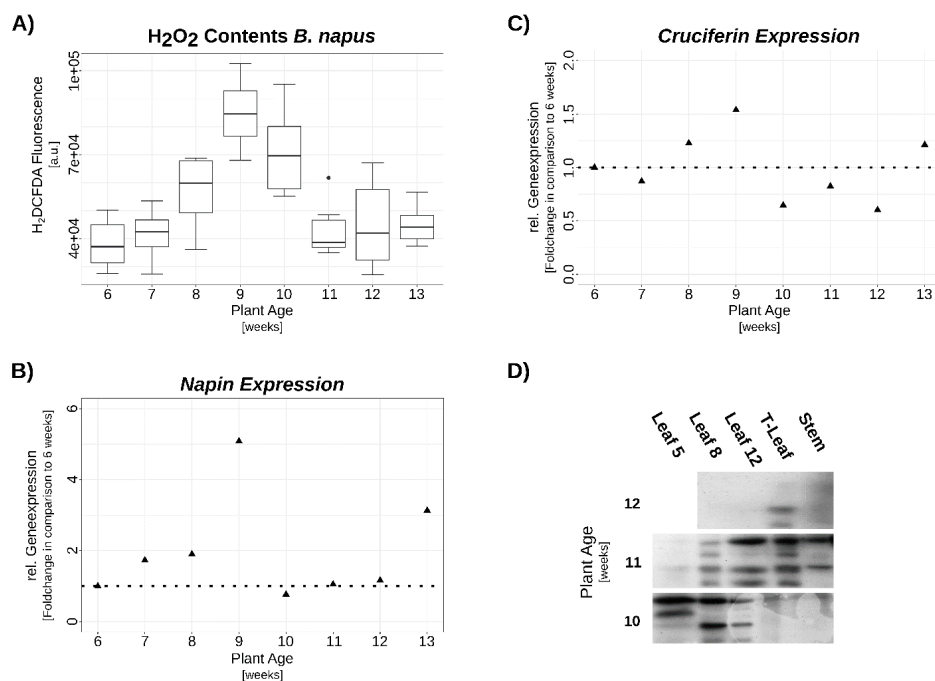


Figure 2. OSR developmental series. Exemplary plants grown in the green house under stable conditions are shown at the top, numbers indicate weeks after sowing. (A) H_2O_2 contents in leaf No. 8. (B) and (C) relative gene-expression of *NAPIN* and *CRUCIFERIN*, respectively, analyzed by qRT-PCR. Expression was normalized to *ACTIN2* and expressed relative to value at 6 weeks. (D) Western-blot of the corresponding plant material immune-detected with anti-*NAPIN* antiserum. Analyzed proteins are samples of 3–5 biological replicates pooled in equal amounts. Leaves are numbered according to their appearance; terminal leaf (T-leaf) is the leaf residing directly below the first developing pods. H_2O_2 data are medians ± 1.5 IQR of at least 3 biological and 2 technical replicates each. Gene expression data are means of 3 technical replicates from pools of at least 3 biological replicates.

To confirm the protein expression also under controlled N conditions as described in references [19,20], leaf positions 4, 8 and 12, the terminal leaf as well as shoot tissue and siliques were harvested of another growth series. Chlorophyll contents were measured via *atLeaf+*. Leaf No.4, the lowest leaf position analyzed, remained on the plant only until week 8 under N_0 conditions, whereas under N_I conditions this leaf was shed between week 11 and 12. Longer maintenance of photosynthetic capacities, especially of lower canopy leaves, enhanced assimilate supply to the pods as well as the roots [22]. The higher canopy leaves exhibited a slightly higher Chl-content under higher N-supply.

Under N_0 conditions, quantification of detected CRU proteins showed a similar pattern to the CRU transcripts in the microarray and the qRT-PCR experiments. A stepwise increase in CRU protein contents in the leaves was observed beginning at the lowest positions with peak levels between

weeks 8 and 10 (Figure 3A). Under N_L conditions CRU production was reduced approx. 10-fold and no comparable pattern became clear. For NAPIN, the detected amount of protein was much higher under N_L conditions than under N_O like in the microarray expression data. Accumulation patterns were similar, but expression was more pronounced in the lower leaf positions, analogous to the prolonged Chl retention observed there. However, a direct comparison between NAPIN and CRUCIFERIN contents is not possible as both proteins were detected with different antisera. Therefore, the signals were normalized to the respective signals of the controls. Nevertheless, both proteins could be detected not only in leaves but also in stems (Figure 3A,B,D). Moreover, total N-content in the seeds was approx. 25% higher under N_O than under N_L conditions (Supplementary Materials Figure S1). Gironde et al. [32] have already indicated an interim storage function for shoot tissue upon asynchronous senescence and seed filling. Our results support this possible function. Even under N-starvation conditions, where a reduction of H_2O_2 contents and barely detectable CRU synthesis was shown in leaves, still a minimal build-up of SSPs occurred in the shoot (Supplementary Materials Figure S2).

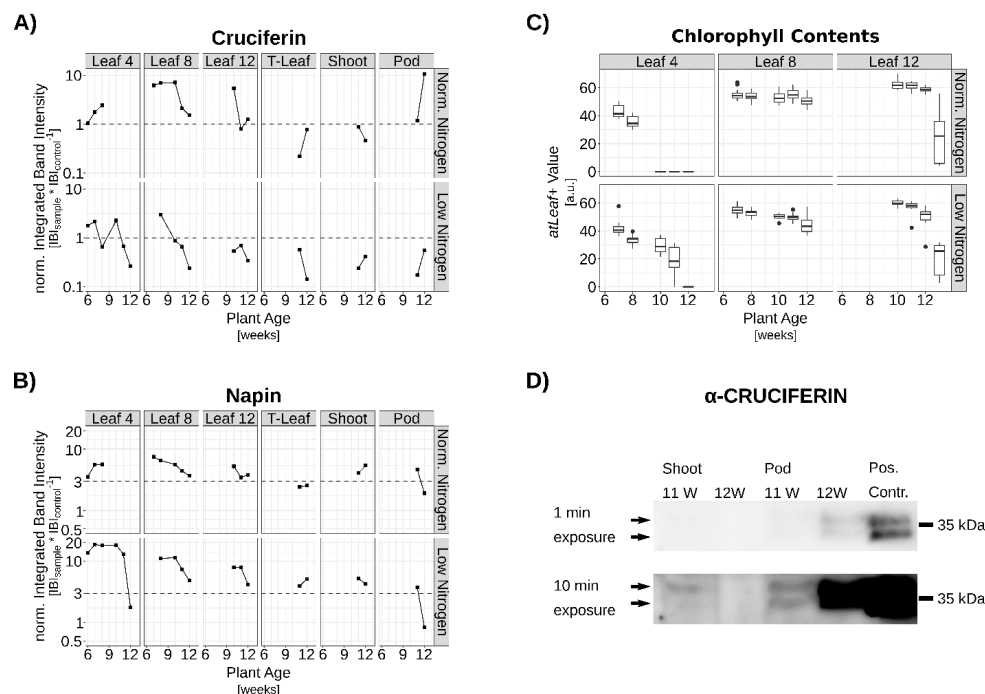


Figure 3. Seed storage protein (SSP) levels of OSR plants grown under normal and limiting nitrogen (N) supply. Quantification of (A) CRUCIFERIN and (B) NAPIN signals. Material analyzed are samples of 3–5 biological replicates pooled in equal amounts. (C) Corresponding chlorophyll contents (median $\pm 1.5 \times IQR$ of 3 biological replicates). Upper graphs normal N-supply, lower graphs N-limitation. (D) Exemplary signal of stem and pod material detected in a Western blot (marked by arrows, 25 μ g total protein). One min exposure (top) to show non-oversaturated positive control (15 μ g total protein) and 10 min exposure for the shoot and pod signals (bottom).

The idea of an interim N-storage is also supported by the follow-up of ^{15}N -labeled nitrogen over time in parallel to the expression profiling [21]. ^{15}N -labeled fertilizer was supplied at three different time points, directly after sowing (DC 0), 72 DAS (DC 30), and 80 DAS (DC 59). Nitrogen recovery and the distribution of the labeled N to different organs was measured by isotope ratio mass spectrometry [21]. Here, we present the $\delta^{15}N$ mean values for pooled green and senescent leaves as well as for the individual leaves No. 4, 5 and 8 at harvest 4 (92 DAS). Exactly the same leaf material was also used for expression profiling (No. 4 and 8; [19]) and hydrogen peroxide measurements (No. 5; [11]). At this time point, early supplied nitrogen (DC 0) appeared to be inefficiently remobilized and mainly rested in the older leaves (No. 4 and 5) while the highest proportion was shed in senescent leaves.

In contrast, nitrogen originating from the second and third N gift (DC 30 and DC 59) accumulated less in shed senescent leaves but more in the younger leaf No.8. This can be observed under both N-supplies in which the effect is most prominent under N_L and DC 30 labelling (Figure 4). This might indicate that N taken up at flowering time appears to be stored temporarily in the younger leaves most likely to be further remobilized to the developing seeds after anthesis. Possibly, also stems and pods contribute to this interim storage, as total N in stem and pods declined while total N in seeds increased (Supplementary Materials Figure S3).

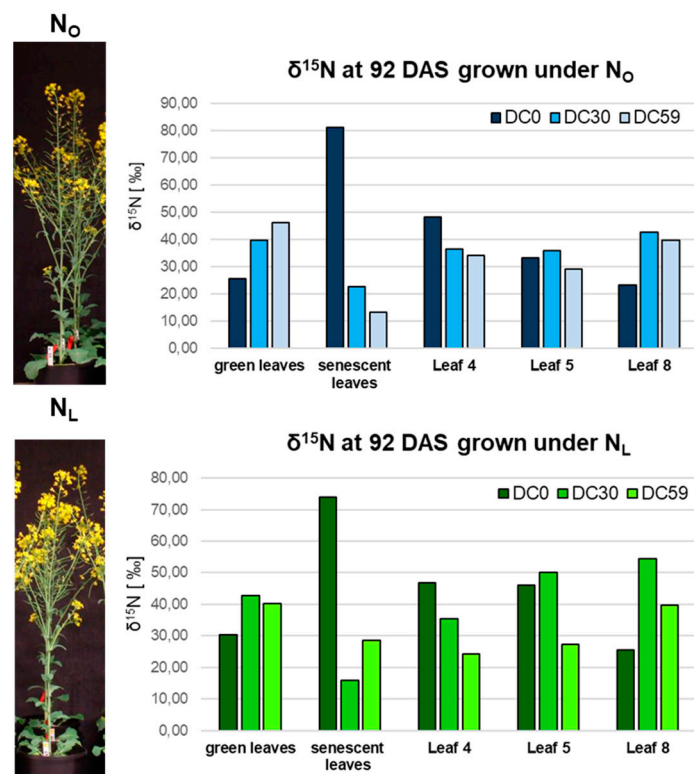


Figure 4. Nitrogen recovery and the distribution of the labeled N to different organs. $\delta^{15}\text{N}$ signatures at 92 DAS (days after sowing) in pooled green and senescent leaves as well as in leaves No. 4, No. 5 and No. 8 of plants grown under N_L (lower chart) and under N_O (upper chart) conditions are presented (DC0: fertilization at 0 DAS, “old N”, DC30: fertilization at 72 DAS, DC59: fertilization at 80 DAS, “new N”). The stable isotope ratio $^{15}\text{N}/^{14}\text{N}$ was related to the isotopic signature of N_2 in the air and is reported here as “delta” δ values in ‰. Exactly the same plant material was used for the microarray analyses of Safavi-Rizi et al. [19] and physiological analyses in Franzaring et al. [20,21].

Taken together, our results indicate that a transcriptional control of SSP expression via H_2O_2 but also via the plants’ N-status appears to be in place. Therefore, we wanted to identify possible regulatory elements (RE) in the promoter regions of the respective genes by in silico analyses. As *Brassica napus* was formed ~7500 years ago by hybridization between *B. rapa* and *B. oleracea*, followed by chromosome doubling, and most orthologous gene pairs in *B. rapa* and *B. oleracea* remain as homologous pairs in *B. napus* [33], we analyzed the promoter regions of both SSP gene copies, respectively. The NSITEM-PL program with RegSite PL Database of Plant Regulatory Elements (Release 14, May 03, 2014; default parameters were set) [34] tests for the presence of known REs in conjunction with positional conservation within the supplied sequence sets comprising 3kb upstream sequences of *B. oleracea* and *B. rapa* as well as of the *B. napus* *CRUCIFERIN* or *NAPIN* homologues. Remarkably, several binding sites for transcription factors involved in either ROS response or N-management or both were identified (Supplementary Materials Figure S4). For example, binding elements for TGACG-BINDING FACTOR2 (TGA2, a bZIP transcription factor involved in general

ROS-and pathogen-response, TEOSINTE BRANCHED1/CYCLOIDEA /PROLIFERATING CELL FACTOR20 (TCP20, involved in systemic N-status signaling and leaf-senescence) and ELONGATED HYPOCOTYL5 (HY5, a ROS-responsive bZIP transcription factor involved in N management) were found (for a complete listing see Supplementary Materials Tables S4 and S5).

3.3. Hydrogen Peroxide Signaling under Complete N-Starvation

To explore a possible interplay between the plants' nitrogen status and H_2O_2 as signaling molecule during the induction of leaf senescence and SSP expression, N-starvation experiments with OSR plants grown on hydroponics were conducted. As expected, N-starvation led to the induction of premature senescence indicated by the decrease in chlorophyll contents, especially in older leaves. However, no increase in intracellular H_2O_2 contents could be measured, as would have been expected for a senescence signaling molecule, but rather a slight reduction of H_2O_2 was determined (Figure 5). Nevertheless, a reduction of catalase activity was observed (Supplementary Materials Figure S5) as was already described during developmental senescence under full N-supply [11].

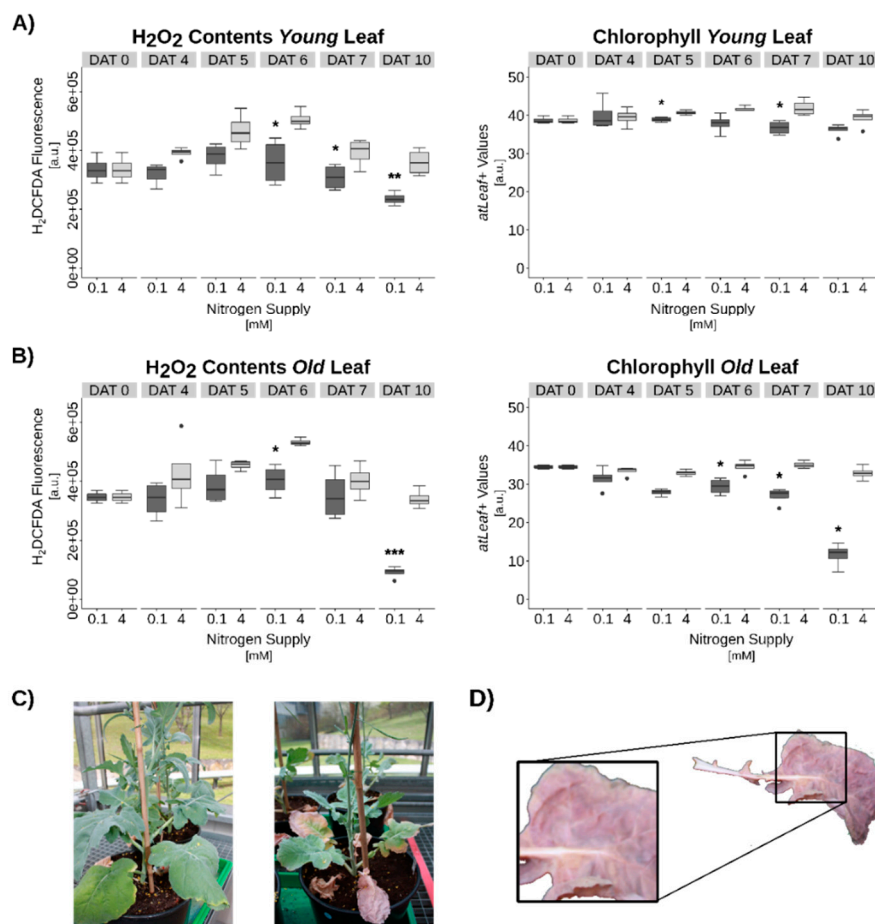


Figure 5. Nitrogen (N) starvation induced senescence in *Brassica napus*. (A) and (B) Hydrogen peroxide (H_2O_2) and chlorophyll contents in young leaves (A) and in old leaves (B). (C) Plant grown under full N-supply (left) and under N-starvation (right). (D) Exemplary anthocyanin accumulation pattern in N-starved plants. Statistics: Welch's t-test. Significance levels: $p < 0.001 = ***$; $p < 0.01 = **$; $p < 0.05 = *$. Data are medians \pm $1.5 \times$ IQR of at least 3 biological and 2 technical replicates each.

Arabidopsis plants subjected to N-starvation on hydroponic culture consistently exhibited similar effects. Shortly before anticipated senescence induction, hydroponic medium was switched from full nutrient supply to N-free medium. Now, an even more pronounced reduction of H_2O_2 contents was detected (Figure 6). However, in both cases, an extensive production of anthocyanins

became visible. In *Arabidopsis*, anthocyanin production was strongest at vasculature during the early phases of N-depletion (Figure 6D). In OSR, anthocyanin accumulation was also observed after N-depletion (Figure 5C,D) but for OSR the vasculature seemed to remain with very low anthocyanin production (Figure 5D). Obviously, OSR leaf vein and leaf laminae are tissues with different regulatory mechanisms during senescence. Besides other functions, anthocyanins were discussed to act as ROS scavenging molecules. Accordingly, reduction of intracellular H_2O_2 was observed in N-starved *Arabidopsis* as well as in OSR leaves (Figures 5A,B and 6A,B). For both species, Chl-contents remained constant in young leaves during the treatment, while older leaves showed a significant reduction in Chl-contents (Figures 5A,B and 6A,B). These findings tempted us to speculate that one possible role of anthocyanin production during N-starvation-induced senescence is the scavenging of the signaling molecule H_2O_2 and by that a suppression of at least part of the developmental senescence program. SSP accumulation under complete N-starvation conditions was barely detectable in leaf tissue (Supplementary Materials Figure S2).

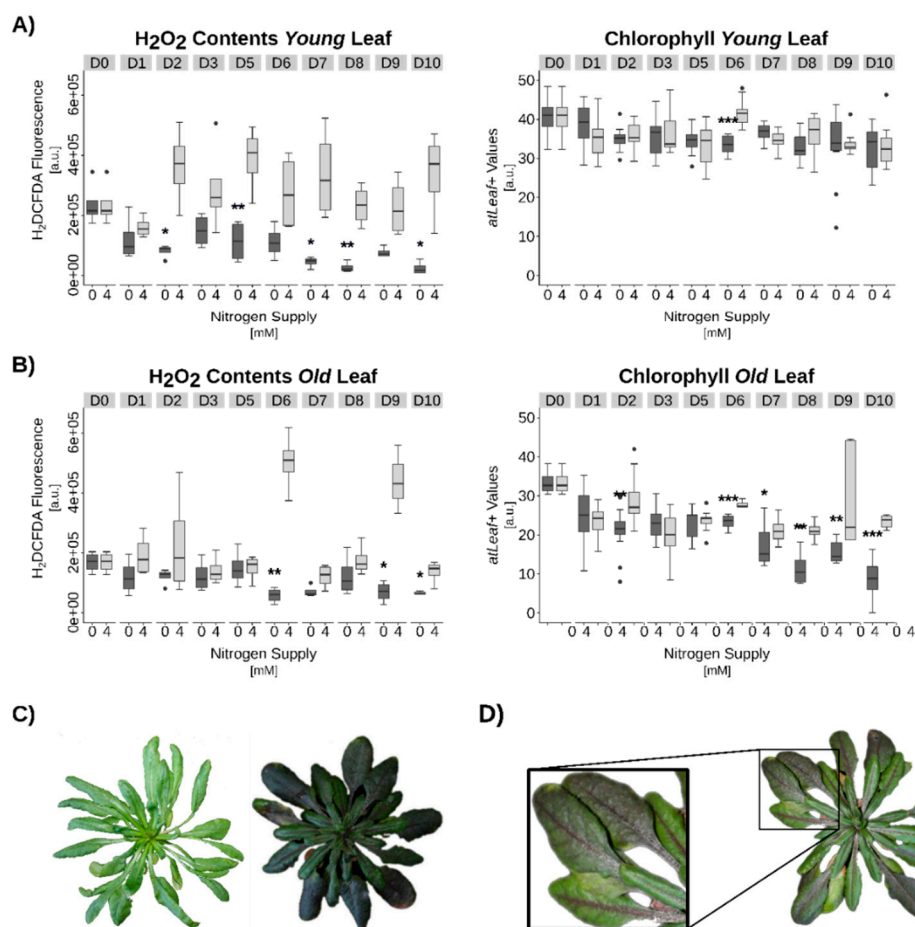


Figure 6. Nitrogen (N) starvation induced senescence in *Arabidopsis thaliana*. (A) Hydrogen peroxide (H_2O_2) and chlorophyll contents in young leaves, (B) in old leaves. (C) Left: plants grown under full N-supply, right under N-starvation. (D) Exemplary anthocyanin accumulation pattern in N-starved plants. Statistics: Welch's t-test. Significance levels: $p < 0.001 = ***$; $p < 0.01 = **$; $p < 0.05 = *$. Data are medians $\pm 1.5 \times IQR$ of at least 3 biological and 2 technical replicates each.

4. Discussions

Genome-wide expression analyses of OSR grown under two different N-regimes revealed that, according to the gene expression profiles, long-term and mild N-deficiency provokes accelerated senescence in lower canopy leaves but delayed senescence in upper canopy leaves [19]. The most important feature of senescence is the remobilization of nutrients out of the senescing tissue into

developing parts of the plants, especially to fruits and seeds. By ^{15}N -labelling at different time points in the same experiment, we could show that N taken up early during development was not efficiently remobilized and a high proportion of the labeled N was shed with senescent leaves. N taken up at flowering time appeared to be better remobilized and stored temporarily in the younger leaves. It was also most likely to be further translocated to the developing seeds after anthesis. This effect is most prominent under low N-supply (Figure 4) when N-remobilization is most likely to be more important. N-recovery in general and to the seeds was improved under low N, as 50.7% of the total N-gift was deposited in the seeds compared to 44.5% under N_0 conditions [21]. A genome-wide expression analyses via microarrays of exactly the same plant material offered the possibility to analyze the expression profiles of genes involved in N-remobilization and N-storage (Supplementary Materials Table S3). The most striking result for us in this analysis was that transcripts of seed storage protein genes or genes related to them, which were formerly thought to be restricted to seed tissue, were identified in leaves at different canopies like leaf No. 4 and No. 8 (Figure 1). Moreover, not only the transcripts but also the proteins were detected in leaf tissue (Figures 2 and 3). However, the accumulation of these storage proteins was not equally distributed across all leaves but a wave-like spreading of SSPs was observed starting in the oldest leaves when plants were still young and climbing up into younger leaves with the progression of development and declining again in later stages with a residual SSP content in the terminal leaf (Figure 2). SSP protein accumulation was also detected in shoots and pods (Figure 3). Considerable differences were observed between the two different N regimes: While *NAPINS* appeared to be more highly expressed under N_L conditions, more *CRUCIFERINS* were produced under higher N supply, creating the SSPs possible candidates for interim storage of N in leaves during N remobilization processes of senescence. As *CRUCIFERINS* and *NAPINS* have distinct molecular characteristics and functionalities [4], it makes sense that these two classes of SSPs are also expressed in contrary ways under different nitrogen regimes in leaves. SSP proteins also detected in stems and pods and total N-analyses in stems and pods additionally points to interim N-storage in these tissues as total N in stem and pods declined while total N in seeds increased (Supplementary Materials Figures S1 and S3). In maize *opaque-2* knock-out plants, storage protein synthesis significantly reduced the pool of free AAs in mature endosperm [35] and could thus enhance sink strength for further N-remobilization. A similar mechanism could possibly operate in leaf tissue as source strength of the disintegrating leaves might exceed sink strength of the newly developing organs [32]. Therefore, the pool of free AAs could be reduced by the built-up of storage proteins decreasing the source strength of the respective leaves. As such, a stepwise N remobilization from lower leaf canopies could take place, which coincides with the wave-like expression of the SSPs (Figure 2). How this is coordinated in oilseed rape plants is still an open question. However, accurate QTL mapping and potential candidates identified based on high-density linkage map and BSA analyses revealed that complex genetic mechanisms for oil and protein accumulation in the seeds of rapeseed are in place [6]. Further analyses of these candidate genes will allow for finding out whether they are also expressed in leaf tissue and contribute to storage reserves in seeds through an interim storage of N via SSPs in leaves. To function as an efficient interim storage, two main prerequisites need to be fulfilled, namely an efficient and compact storage and an easy access for remobilization [32], which both holds true for SSPs. SSPs are usually stored in higher complexes with multimeric conformation in protein storage vacuoles [5]. To achieve this conformation, extensive processing of pre-cursor proteins by VPEs (vacuolar processing enzymes) is necessary. Indeed, γ -VPE (AT4G32940) and other VPEs were differentially expressed in leaves under both N treatments (Table S3) indicating that SSP storage in a processed multimeric form is also possible in leaves. In the three plant growth series conducted under different conditions, *CRUCIFERIN* and *NAPIN* expression and accumulation correlated with intracellular hydrogen peroxide contents (Figure 2, [11]), which might be the link to the regulation of senescence processes, as hydrogen peroxide is a well-known signaling molecule in leaf senescence. Many transcriptional regulators and SAGs are up-regulated by increasing intracellular hydrogen peroxide concentrations. In silico analyses of 3 kbp upstream of the coding regions of *CRUCIFERIN*

and *NAPIN* genes also supported the existence of a direct link between SSP expression and oxidative status of the cells (Supplementary Materials Figure S4, Tables S4 and S5). Spatiotemporal occurrence and distribution of SSPs and the corresponding mRNAs were shown to be tightly regulated and were so far thought to be restricted to the developing seeds [36]. In consistence, most of the *cis* elements identified by *in silico* analyses of the SSP promoter regions (Supplementary Materials Figure S4, Tables S4 and S5) are characteristic for seed-specific expression in various species. Multiple abscisic acid (ABA) responsive elements were found in *CRUCIFERIN* as well as *NAPIN* upstream regions. ABA is known to be a key factor during seed maturation by suppressing premature germination and regulating a variety of processes during embryogenesis [37,38]. This also points to seed-specific expression. During SSP deposition, ABA contents steadily rise until they decrease again during desiccation. However, ABA is also a senescence-promoting hormone accumulating during developmental as well as N-starvation induced senescence [39,40]. For *CRUCIFERINs*, besides the known RY/G-Box and ABA responsive elements, a further motif for seed specific *GLUTELIN* expression known from *Oryza sativa* (OSMYB5 binding site) was found [41]. Additionally, an OPAQUE-2 binding site, a *cis* element identified in *Zea mays* regulating *ZEIN* expression [42], was found to be present in *CRUCIFERIN* upstream sequences.

Studies on SSPs in *A. thaliana* have shown the interplay of the bZIP transcription factors bZIP53, bZIP10 and ABI3 to be necessary for full promoter activation [43]. Simultaneous overexpression of all three factors led to most pronounced promoter activation. Although expression of one of these factors alone showed only marginal SSP promoter induction in transient assays, the authors have depicted the crucial role of bZIP53, since constitutive *bZIP53* overexpression *in planta* was able to induce seed-specific promoter activation in non-seed tissue [43]. Therefore, we screened the OSR microarray data for the expression of the corresponding transcription factors. None of these transcription factors (TFs) were expressed in leaves throughout development of the OSR plants and transient overexpression of *AtbZIP53* together with a *BnSSP:GUS* construct in Arabidopsis protoplasts did not change expression of the reporter gene (Data have been provided as non-published material). Accordingly, a different mechanism of leaf-specific expression has to be in place in OSR.

The overall SSP expression pattern suggests a correlation with the developmental senescence program coupled to ROS contents and N availability. In 2001, Desikan and colleagues already identified Arabidopsis seed storage proteins to be responsive to oxidative stress [44]. Here, expression of *NAPIN* and *CRUCIFERIN* coincided with the hydrogen peroxide peak in the microarray experiment and was also confirmed by qRT-PCR in a second growth experiment on soil (Figure 2). Moreover, this also concurs with our database-aided motif identification. *Cis* elements known for redox-responsiveness were found in the upstream sequences of both SSP-classes. Besides the direct ROS responsive elements of *HY5*, other motifs suggesting an indirect coupling to ROS were identified. The LS7 Box of the PATHOGENESIS RELATED GENE1 (PR-1) and the G-Box of the VEGETATIVE STORAGE PROTEIN-A gene (*VSP-A*) of soybean, which are both involved in pathogen responses and ROS bursts, were identified [45–47]. Furthermore, we found a TGA2 binding site. TGA2 is involved in salicylic acid and late jasmonic acid signaling pathways, and is an interaction partner of NON-EXPRESSION OF PR-GENES1 (NPR1), which acts as a central transcription activator of many defense-related genes. NPR1 is redox sensitive and cytoplasmic H₂O₂ prevents the translocation of NPR1 to the nucleus [48]. Earlier publications have reported that SSPs can be massively oxidized, especially by carbonylation [49,50]. Besides an easier access to SSP monomers after multimer destabilization upon carbonylation, a ROS scavenging function has been proposed [51]. Recently, Nguyen et al. [52] have shown anti-oxidative functions for *CRUCIFERINs* in Arabidopsis seeds. Seeds generated from Arabidopsis triple *cruciferin* KO lines (*crua/crub/cruc*) displayed a much higher sensitivity to artificial ageing as well as considerably higher protein carbonylation.

More evidence for N-status dependent transcription of SSPs is given by the presence of a TCP20 binding site in *NAPIN* upstream regions. TCP20 participates in systemic N-status signaling as well as in leaf senescence [53,54]. This dependency on the plant N-status is also reflected in our analyses of the microarray expression data. When plants were grown under N_I conditions, the expression of

NAPIN was induced whereas under N_0 conditions, *CRUCIFERIN* was predominantly expressed. Thus, the type of SSP which is expressed in leaf tissue under different N availability might be selected by its capability to store N as the amount of N per protein molecule is more than 3-fold higher for *CRUCIFERIN* than for *NAPIN*. *CRUCIFERIN* (488 amino acids) is much larger than *NAPIN* (159 amino acids) and thus requires more input but also has more N storage capacity (698 N atoms vs. 228 N atoms, respectively). A similar mechanism for nutrient availability-dependent SSP expression was shown already for sulfur. Low sulfur supply increased the ratio between S-rich *CRUCIFERIN* and S-poor *NAPIN* significantly and reduced total fatty-acid contents [1]. Accordingly, SSP accumulation under complete N-starvation conditions was barely detectable in leaf tissue, as an interim storage is not necessary under these conditions. Remarkably, also no H_2O_2 accumulation was observed (Figure 5, Supplementary Materials Figure S2). However, how differential expression of *CRUCIFERIN* under N_0 and *NAPIN* under N_L is achieved and which role hydrogen peroxide exactly plays, still needs to be further investigated. Besides *TCP20*, *HY5* is also not solely involved in ROS responses but also in N management by regulating expression of *NITRITE-REDUCTASE-1* (*NIR1*) and *AMMONIUM-TRANSPORTER-1;2* (*AMT1;2*) in dependence of N-supply [55]. Moreover, *HY5* can interact with *PHYTOCHROME B* (*PHYB*) during prolonged red-light exposure and induce *EDS1* (*ENHANCED DISEASE SUSCEPTIBILITY-1*), which then promotes ROS production [56]. This interaction hints at a possible link to *PHYTOCHROME-INTERACTING FACTOR7* (*PIF7*). *PIF7* binding elements are present in *NAPIN* upstream sequences and could be targeted by *PHYB*-recruited *PIF7* as part of a *HY5-PHYB* response.

Another indirect mechanism might be emanating from a NAC (NAM/ATAF1/2/CUC2) recognition site (NACRS) in *NAPIN* upstream regions, which is known to be bound by ANAC019, 055 and 072 [57]. Thus, another link to the senescence program in general is given. These factors take part in the regulation of major chlorophyll catabolic genes and ANAC019 has been identified as an activator of senescence in *Arabidopsis* [58,59]. More recently, a *Brassica napus* NAC factor, *NAC87*, which also binds the NACRS, has been characterized to regulate both, ROS generation and leaf senescence regulatory genes [60]. An additional indirect N-dependent regulation might be exerted by *GNC* (*GATA*, Nitrate-inducible, Carbon metabolism-involved), which controls expression of ANAC019 [61].

Complete N-starvation appeared to elicit premature senescence and most likely a stress-induced N-remobilization program. A general indicator for several stress responses is the induction of the phenylpropanoid pathway, which in turn leads to lignification, anthocyanin production and build-up of other repellents and protective secondary metabolites. Several studies in different plant species have shown the induction of the phenylpropanoid pathway or an increase in anthocyanin production provoked by N-limitation [62–64]. In our experiments, anthocyanins were present in high amounts, so that they were visible with the naked eye and most likely were able to reduce ROS contents. This might explain why despite an induction of premature senescence and reduction of catalase activity no increase of H_2O_2 was measured (Figures 5 and 6, Supplementary Materials Figure S5). In contrast, H_2O_2 levels were even reduced. The hypothesis that anthocyanins scavenge substantial amounts of H_2O_2 and thus simply mask the increment in ROS contents will be further investigated by experiments with anthocyanin synthesis mutants *transparent testa* (*tt*) in *Arabidopsis*. Remarkably, *tt* mutants grown under limiting nitrogen supply did not show a difference in senescence measured by chlorophyll loss and *SAG12* expression [65]. Moreover, non-enzymatic scavengers like ascorbate and tocopherol are elevated during senescence under low nitrogen in OSR in the leaf laminae as well as in the leaf veins [66]. However, *nla* (*nitrogen limitation adaptation*) mutant *Arabidopsis* plants grown under low N could not accumulate anthocyanins and instead produced a severe N-limitation-induced early senescence phenotype, perhaps due to the fact that the senescence-inducing H_2O_2 signal was not quenched by anthocyanins [63]. Therefore, anthocyanin production under N-starvation might also serve the repression of at least the H_2O_2 -controlled part of the senescence program. While reduction of catalase activity hints at a promotion of the standard developmental senescence program (Supplementary Materials Figure S4), the apparent decrease in H_2O_2 contents contradicts

this assumption (Figure 6). In accordance with these observations, comparative expression analyses have shown strong differences between stress-induced and developmental senescence programs in early stages, which then converged in later stages [67]. Taken together, a complex interplay between intracellular hydrogen peroxide contents and nitrogen availability appears to govern the senescence program and N-remobilization efficiency.

Supplementary Materials: The following are available online at <http://www.mdpi.com/2073-4425/10/2/72/s1>. Supplementary Figure S1: Total N-content in seeds under N_O and N_L conditions; Supplementary Figure S2: Quantification of immune-detection of CRU proteins from N-starved plants; Supplementary Figure S3: Total N-content in the shoots, pods and seeds over development; Supplementary Figure S4: Catalase zymogram of N-starved Arabidopsis plants; Supplementary Figure S5: Schematic drawing of promoter regions of OSR NAPIN and OSR CRUCIFERIN; Supplementary Table S1: Hydroponic media N-starvation *A. thaliana*; Supplementary Table S2: Hydroponic media N-starvation *B. napus*; Table S3: Cis elements identified in upstream regions of OSR CRUCIFERIN; Supplementary Table S4: AGI codes and description of SSP associated transcripts in *A. thaliana*; Supplementary Table S5: Cis elements identified in upstream regions of OSR NAPIN Supplementary.

Author Contributions: Conceptualization, U.Z. and S.B.; Methodology, S.B., J.D., J.F. and L.R.; Validation, S.B., L.R., J.D. and J.F.; Formal Analysis, S.B.; J.F.; Investigation, L.R., J.F., J.D. and S.B.; Writing—Original Draft Preparation, S.B.; Writing—Review & Editing, J.D.; A.F., J.F. and U.Z.; Visualization, S.B. and U.Z.; Supervision, U.Z.; Project Administration, S.B. and U.Z.; Funding Acquisition, A.F. and U.Z.

Funding: This research was supported by the Deutsche Forschungsgemeinschaft (FOR948 (ZE 313/8-1, ZE 313/8-2), ZE 313/9-1, CRC 1101 (B06)).

Acknowledgments: We thank Daniel Werner Jeschke and Gabriele Eggers-Schumacher (ZMBP, University of Tuebingen, Germany) for their excellent technical assistance. We are grateful to Fabian Koeslin-Findeklee and Walter Horst (University of Hannover, Germany) for providing leaf material of OSR grown in hydroponics. We thank Reinhard Kunze (Free University of Berlin, Germany) for providing the transcriptome data and for critical discussion on the manuscript.

Conflicts of Interest: The authors declare no conflict of interest.

References

- Brunel-Muguet, S.; D’Hooghe, P.; Bataille, M.P.; Larre, C.; Kim, T.H.; Trouverie, J.; Avicé, J.C.; Etienne, P.; Durr, C. Heat stress during seed filling interferes with sulfur restriction on grain composition and seed germination in oilseed rape (*Brassica napus* L.). *Front. Plant Sci.* **2015**, *6*, 213. [CrossRef] [PubMed]
- Monsalve, R.I.; Lopez-Otin, C.; Villalba, M.; Rodriguez, R. A new distinct group of 2 S albumins from rapeseed. Amino acid sequence of two low molecular weight napins. *FEBS Lett.* **1991**, *295*, 207–210. [CrossRef]
- Schwenke, K.D.; Raab, B.; Linow, K.J.; Pahtz, W.; Uhlig, J. Isolation of the 12 S globulin from rapeseed (*Brassica napus* L.) and characterization as a “neutral” protein. On seed proteins. Part 13. *Die Nahrung* **1981**, *25*, 271–280. [CrossRef] [PubMed]
- Perera, S.P.; McIntosh, T.C.; Wanasundara, J.P. Structural properties of cruciferin and napin of *Brassica napus* (Canola) show distinct responses to changes in pH and temperature. *Plants* **2016**, *5*, 36. [CrossRef] [PubMed]
- Gacek, K.; Bartkowiak-Broda, I.; Batley, J. Genetic and Molecular Regulation of Seed Storage Proteins (SSPs) to Improve Protein Nutritional Value of Oilseed Rape (*Brassica napus* L.) Seeds. *Front. Plant Sci.* **2018**, *9*, 890. [CrossRef] [PubMed]
- Chao, H.; Wang, H.; Wang, X.; Guo, L.; Gu, J.; Zhao, W.; Li, B.; Chen, D.; Raboanatahiry, N.; Li, M. Genetic dissection of seed oil and protein content and identification of networks associated with oil content in *Brassica napus*. *Sci. Rep.* **2017**, *7*, 46295. [CrossRef]
- Gu, J.; Chao, H.; Gan, L.; Guo, L.; Zhang, K.; Li, Y.; Wang, H.; Raboanatahiry, N.; Li, M. Proteomic Dissection of Seed Germination and Seedling Establishment in *Brassica napus*. *Front. Plant Sci.* **2016**, *7*, 1482. [CrossRef]
- Tilsner, J.; Kassner, N.; Struck, C.; Lohaus, G. Amino acid contents and transport in oilseed rape (*Brassica napus* L.) under different nitrogen conditions. *Planta* **2005**, *221*, 328–338. [CrossRef]
- Kichey, T.; Hirel, B.; Heumez, E.; Dubois, F.; Le Gouis, J. In winter wheat (*Triticum aestivum* L.), post-anthesis nitrogen uptake and remobilisation to the grain correlates with agronomic traits and nitrogen physiological markers. *Field Crop. Res.* **2007**, *102*, 22–32. [CrossRef]

10. Breeze, E.; Harrison, E.; McHattie, S.; Hughes, L.; Hickman, R.; Hill, C.; Kiddle, S.; Kim, Y.S.; Penfold, C.A.; Jenkins, D.; et al. High-resolution temporal profiling of transcripts during Arabidopsis leaf senescence reveals a distinct chronology of processes and regulation. *Plant Cell* **2011**, *23*, 873–894. [[CrossRef](#)]
11. Bieker, S.; Riester, L.; Stahl, M.; Franzaring, J.; Zentgraf, U. Senescence-specific alteration of hydrogen peroxide levels in Arabidopsis thaliana and oilseed rape spring variety *Brassica napus* L. cv. Mozart. *J. Integr. Plant Biol.* **2012**, *54*, 540–554. [[CrossRef](#)] [[PubMed](#)]
12. Zimmermann, P.; Heinlein, C.; Orendi, G.; Zentgraf, U. Senescence-specific regulation of catalases in *Arabidopsis thaliana* (L.) Heynh. *Plant Cell Environ.* **2006**, *29*, 1049–1060. [[CrossRef](#)] [[PubMed](#)]
13. Rossato, L.; Lainé, P.; Ourry, A. Nitrogen storage and remobilization in *Brassica napus* L. during the growth cycle: Nitrogen fluxes within the plant and changes in soluble protein patterns. *J. Exp. Bot.* **2001**, *52*, 1655–1663. [[CrossRef](#)] [[PubMed](#)]
14. Oury, F.-X.; Godin, C. Yield and grain protein concentration in bread wheat: How to use the negative relationship between the two characters to identify favourable genotypes? *Euphytica* **2007**, *157*, 45–57. [[CrossRef](#)]
15. Bogard, M.; Jourdan, M.; Allard, V.; Martre, P.; Perretant, M.R.; Ravel, C.; Heumez, E.; Orford, S.; Snape, J.; Griffiths, S.; et al. Anthesis date mainly explained correlations between post-anthesis leaf senescence, grain yield, and grain protein concentration in a winter wheat population segregating for flowering time QTLs. *J. Exp. Bot.* **2011**, *62*, 3621–3636. [[CrossRef](#)] [[PubMed](#)]
16. Avice, J.C.; Etienne, P. Leaf senescence and nitrogen remobilization efficiency in oilseed rape (*Brassica napus* L.). *J. Exp. Bot.* **2014**, *65*, 3813–3824. [[CrossRef](#)]
17. Desclos, M.; Dubousset, L.; Etienne, P.; Le Caherec, F.; Satoh, H.; Bonnefoy, J.; Ourry, A.; Avice, J.C. A proteomic profiling approach to reveal a novel role of *Brassica napus* drought 22 kD/water-soluble chlorophyll-binding protein in young leaves during nitrogen remobilization induced by stressful conditions. *Plant Physiol.* **2008**, *147*, 1830–1844. [[CrossRef](#)]
18. Etienne, P.; Desclos, M.; Le Gou, L.; Gombert, J.; Bonnefoy, J.; Maurel, K.; Le Dily, F.; Ourry, A.; Avice, J.-C. N-protein mobilisation associated with the leaf senescence process in oilseed rape is concomitant with the disappearance of trypsin inhibitor activity. *Funct. Plant Biol.* **2007**, *34*, 895–906. [[CrossRef](#)]
19. Safavi-Rizi, V.; Franzaring, J.; Fangmeier, A.; Kunze, R. Divergent N Deficiency-Dependent Senescence and Transcriptome Response in Developmentally Old and Young *Brassica napus* Leaves. *Front. Plant Sci.* **2018**, *9*, 48. [[CrossRef](#)]
20. Franzaring, J.; Weller, S.; Schmid, I.; Fangmeier, A. Growth, senescence and water use efficiency of spring oilseed rape (*Brassica napus* L. cv. Mozart) grown in a factorial combination of nitrogen supply and elevated CO₂. *Environ. Exp. Bot.* **2011**, *72*, 284–296. [[CrossRef](#)]
21. Franzaring, J.; Gensheimer, G.; Weller, S.; Schmid, I.; Fangmeier, A. Allocation and remobilisation of nitrogen in spring oilseed rape (*Brassica napus* L. cv. Mozart) as affected by N supply and elevated CO₂. *Environ. Exp. Bot.* **2012**, *83*, 12–22. [[CrossRef](#)]
22. Koeslin-Findeklee, F.; Meyer, A.; Girke, A.; Beckmann, K.; Horst, W.J. The superior nitrogen efficiency of winter oilseed rape (*Brassica napus* L.) hybrids is not related to delayed nitrogen starvation-induced leaf senescence. *Plant Soil* **2014**, *384*, 347–362. [[CrossRef](#)]
23. Cathcart, R.; Schwiers, E.; Ames, B.N. Detection of picomole levels of hydroperoxides using a fluorescent dichlorofluorescein assay. *Anal. Biochem.* **1983**, *134*, 111–116. [[CrossRef](#)]
24. Arvidsson, S.; Kwasniewski, M.; Riano-Pachon, D.M.; Mueller-Roeber, B. QuantPrime—a flexible tool for reliable high-throughput primer design for quantitative PCR. *BMC Bioinf.* **2008**, *9*, 465. [[CrossRef](#)] [[PubMed](#)]
25. Pfaffl, M.W. A new mathematical model for relative quantification in real-time RT-PCR. *Nucl. Acids Res.* **2001**, *29*, e45. [[CrossRef](#)] [[PubMed](#)]
26. R Development Core Team. *R: A Language and Environment for Statistical Computing*; R Foundation for Statistical Computing: Vienna, Austria, 2017.
27. Ritchie, M.E.; Phipson, B.; Wu, D.; Hu, Y.; Law, C.W.; Shi, W.; Smyth, G.K. Limma powers differential expression analyses for RNA-sequencing and microarray studies. *Nucl. Acids Res.* **2015**, *43*, e47. [[CrossRef](#)] [[PubMed](#)]
28. Camacho, C.; Coulouris, G.; Avagyan, V.; Ma, N.; Papadopoulos, J.; Bealer, K.; Madden, T.L. BLAST+: Architecture and applications. *BMC Bioinf.* **2009**, *10*, 421. [[CrossRef](#)] [[PubMed](#)]

29. Lamesch, P.; Berardini, T.Z.; Li, D.; Swarbreck, D.; Wilks, C.; Sasidharan, R.; Muller, R.; Dreher, K.; Alexander, D.L.; Garcia-Hernandez, M.; et al. The Arabidopsis Information Resource (TAIR): Improved gene annotation and new tools. *Nucl. Acids Res.* **2012**, *40*, D1202–D1210. [[CrossRef](#)]
30. Li, L.; Shimada, T.; Takahashi, H.; Ueda, H.; Fukao, Y.; Kondo, M.; Nishimura, M.; Hara-Nishimura, I. MAIGO2 is involved in exit of seed storage proteins from the endoplasmic reticulum in *Arabidopsis thaliana*. *Plant Cell* **2006**, *18*, 3535–3547. [[CrossRef](#)]
31. Li, L.; Shimada, T.; Takahashi, H.; Koumoto, Y.; Shirakawa, M.; Takagi, J.; Zhao, X.; Tu, B.; Jin, H.; et al. MAG2 and three MAG2-INTERACTING PROTEINs form an ER-localized complex to facilitate storage protein transport in *Arabidopsis thaliana*. *Plant J.* **2013**, *76*, 781–791. [[CrossRef](#)]
32. Gironde, A.; Etienne, P.; Trouverie, J.; Bouchereau, A.; Le Caherec, F.; Lepout, L.; Orsel, M.; Niogret, M.F.; Nesi, N.; Carole, D.; et al. The contrasting N management of two oilseed rape genotypes reveals the mechanisms of proteolysis associated with leaf N remobilization and the respective contributions of leaves and stems to N storage and remobilization during seed filling. *BMC Plant Biol.* **2015**, *15*, 59. [[CrossRef](#)] [[PubMed](#)]
33. Chalhoub, B.; Denoeud, F.; Liu, S.; Parkin, I.A.; Tang, H.; Wang, X.; et al. Plant genetics. Early allopolyploid evolution in the post-Neolithic *Brassica napus* oilseed genome. *Science* **2014**, *345*, 950–953. [[CrossRef](#)] [[PubMed](#)]
34. Solovyev, V.V.; Shahmuradov, I.A.; Salamov, A.A. Identification of promoter regions and regulatory sites. *Methods Mol. Biol.* **2010**, *674*, 57. [[PubMed](#)]
35. Wang, X.; Larkins, B.A. Genetic analysis of amino acid accumulation in opaque-2 maize endosperm. *Plant Physiol.* **2001**, *125*, 1766–1777. [[CrossRef](#)]
36. Fernandez, D.E.; Turner, F.R.; Crouch, M.L. In situ localization of storage protein mRNAs in developing meristems of *Brassica napus* embryos. *Development* **1991**, *111*, 299–313. [[PubMed](#)]
37. Finkelstein, R.R.; Tenbarger, K.M.; Shumway, J.E.; Crouch, M.L. Role of ABA in Maturation of Rapeseed Embryos. *Plant Physiol.* **1985**, *78*, 630–636. [[CrossRef](#)]
38. Rajjou, L.; Duval, M.; Gallardo, K.; Catusse, J.; Bally, J.; Job, C.; Job, D. Seed germination and vigor. *Ann. Rev. Plant Biol.* **2012**, *63*, 507–533. [[CrossRef](#)]
39. Lim, P.O.; Kim, H.J.; Nam, H.G. Leaf senescence. *Ann. Rev. Plant Biol.* **2007**, *58*, 115–136. [[CrossRef](#)]
40. Koeslin-Findeklee, F.; Becker, M.A.; van der Graaff, E.; Roitsch, T.; Horst, W.J. Differences between winter oilseed rape (*Brassica napus* L.) cultivars in nitrogen starvation-induced leaf senescence are governed by leaf-inherent rather than root-derived signals. *J. Exp. Bot.* **2015**, *66*, 3669–3681. [[CrossRef](#)]
41. Suzuki, A.; Wu, C.Y.; Washida, H.; Takaiwa, F. Rice MYB protein OSMYB5 specifically binds to the AACA motif conserved among promoters of genes for storage protein glutelin. *Plant Cell Physiol.* **1998**, *39*, 555–559. [[CrossRef](#)] [[PubMed](#)]
42. Schmidt, R.J.; Burr, F.A.; Aukerman, M.J.; Burr, B. Maize regulatory gene opaque-2 encodes a protein with a “leucine-zipper” motif that binds to zein DNA. *Proc. Natl. Acad. Sci. USA* **1990**, *87*, 46–50. [[CrossRef](#)] [[PubMed](#)]
43. Alonso, R.; Onate-Sanchez, L.; Weltmeier, F.; Ehlert, A.; Diaz, I.; Dietrich, K.; Vicente-Carbajosa, J.; Droge-Laser, W. A pivotal role of the basic leucine zipper transcription factor bZIP53 in the regulation of *Arabidopsis* seed maturation gene expression based on heterodimerization and protein complex formation. *Plant Cell* **2009**, *21*, 1747–1761. [[CrossRef](#)] [[PubMed](#)]
44. Desikan, R.; S, A.H.-M.; Hancock, J.T.; Neill, S.J. Regulation of the Arabidopsis transcriptome by oxidative stress. *Plant Physiol.* **2001**, *127*, 159–172. [[CrossRef](#)] [[PubMed](#)]
45. Berger, S.; Bell, E.; Sadka, A.; Mullet, J.E. *Arabidopsis thaliana* Atvsp is homologous to soybean VspA and VspB, genes encoding vegetative storage protein acid phosphatases, and is regulated similarly by methyl jasmonate, wounding, sugars, light and phosphate. *Plant Mol. Biol.* **1995**, *27*, 933–942. [[CrossRef](#)] [[PubMed](#)]
46. Liu, Y.; Ahn, J.E.; Datta, S.; Salzman, R.A.; Moon, J.; Huyghues-Despointes, B.; Pittendrigh, B.; Murdock, L.L.; Koiwa, H.; Zhu-Salzman, K. *Arabidopsis* vegetative storage protein is an anti-insect acid phosphatase. *Plant Physiol.* **2005**, *139*, 1545–1556. [[CrossRef](#)] [[PubMed](#)]
47. Chen, D.; Xu, G.; Tang, W.; Jing, Y.; Ji, Q.; Fei, Z.; Lin, R. Antagonistic basic helix-loop-helix/bZIP transcription factors form transcriptional modules that integrate light and reactive oxygen species signaling in *Arabidopsis*. *Plant Cell* **2013**, *25*, 1657–1673. [[CrossRef](#)] [[PubMed](#)]

48. Peleg-Grossman, S.; Melamed-Book, N.; Cohen, G.; Levine, A. Cytoplasmic H₂O₂ prevents translocation of NPR1 to the nucleus and inhibits the induction of PR genes in Arabidopsis. *Plant Signal Behav.* **2010**, *5*, 1401–1406. [[CrossRef](#)]
49. Job, C.; Rajjou, L.; Lovigny, Y.; Belghazi, M.; Job, D. Patterns of protein oxidation in *Arabidopsis* seeds and during germination. *Plant Physiol.* **2005**, *138*, 790–802. [[CrossRef](#)]
50. Barba-Espin, G.; Diaz-Vivancos, P.; Job, D.; Belghazi, M.; Job, C.; Hernandez, J.A. Understanding the role of H₂O₂ during pea seed germination: A combined proteomic and hormone profiling approach. *Plant Cell Environ.* **2011**, *34*, 1907–1919. [[CrossRef](#)]
51. El-Maarouf-Bouteau, H.; Meimoun, P.; Job, C.; Job, D.; Bailly, C. Role of protein and mRNA oxidation in seed dormancy and germination. *Front. Plant Sci.* **2013**, *4*, 77. [[CrossRef](#)]
52. Nguyen, T.P.; Cueff, G.; Hegedus, D.D.; Rajjou, L.; Bentsink, L. A role for seed storage proteins in *Arabidopsis* seed longevity. *J. Exp. Bot.* **2015**, *66*, 6399–6413. [[CrossRef](#)] [[PubMed](#)]
53. Guan, P.; Wang, R.; Nacry, P.; Breton, G.; Kay, S.A.; Pruneda-Paz, J.L.; Davani, A.; Crawford, N.M. Nitrate foraging by Arabidopsis roots is mediated by the transcription factor TCP20 through the systemic signaling pathway. *Proc. Natl. Acad. Sci. USA* **2014**, *111*, 15267–15272. [[CrossRef](#)] [[PubMed](#)]
54. Danisman, S.; van Dijk, A.D.; Bimbo, A.; van der Wal, F.; Hennig, L.; de Folter, S.; Angenent, G.C.; Immink, R.G. Analysis of functional redundancies within the Arabidopsis TCP transcription factor family. *J. Exp. Bot.* **2013**, *64*, 5673–5685. [[CrossRef](#)]
55. Huang, L.; Zhang, H.; Zhang, H.; Deng, X.W.; Wei, N. HY5 regulates nitrite reductase 1 (NIR1) and ammonium transporter1;2 (AMT1;2) in Arabidopsis seedlings. *Plant Sci.* **2015**, *238*, 330–339. [[CrossRef](#)] [[PubMed](#)]
56. Chai, T.; Zhou, J.; Liu, J.; Xing, D. LSD1 and HY5 antagonistically regulate red light induced-programmed cell death in *Arabidopsis*. *Front. Plant Sci.* **2015**, *6*, 292. [[CrossRef](#)] [[PubMed](#)]
57. Tran, L.S.; Nakashima, K.; Sakuma, Y.; Simpson, S.D.; Fujita, Y.; Maruyama, K.; Fujita, M.; Seki, M.; Shinozaki, K.; Yamaguchi-Shinozaki, K. Isolation and functional analysis of *Arabidopsis* stress-inducible NAC transcription factors that bind to a drought-responsive cis-element in the early responsive to dehydration stress 1 promoter. *Plant Cell* **2004**, *16*, 2481–2498. [[CrossRef](#)] [[PubMed](#)]
58. Zhu, X.; Chen, J.; Xie, Z.; Gao, J.; Ren, G.; Gao, S.; Zhou, X.; Kuai, B. Jasmonic acid promotes degreening via MYC2/3/4- and ANAC019/055/072-mediated regulation of major chlorophyll catabolic genes. *Plant J.* **2015**, *84*, 597–610. [[CrossRef](#)]
59. Hickman, R.; Hill, C.; Penfold, C.A.; Breeze, E.; Bowden, L.; Moore, J.D.; Zhang, P.; Jackson, A.; Cooke, E.; Bewicke-Copley, F.; et al. A local regulatory network around three NAC transcription factors in stress responses and senescence in Arabidopsis leaves. *Plant J.* **2013**, *75*, 26–39. [[CrossRef](#)]
60. Yan, J.; Tong, T.; Li, X.; Chen, Q.; Dai, M.; Niu, F.; et al. A Novel NAC-Type Transcription Factor, NAC87, from Oilseed Rape Modulates Reactive Oxygen Species Accumulation and Cell Death. *Plant Cell Physiol.* **2018**, *59*, 290–303. [[CrossRef](#)]
61. Bi, Y.M.; Zhang, Y.; Signorelli, T.; Zhao, R.; Zhu, T.; Rothstein, S. Genetic analysis of Arabidopsis GATA transcription factor gene family reveals a nitrate-inducible member important for chlorophyll synthesis and glucose sensitivity. *Plant J.* **2005**, *44*, 680–692. [[CrossRef](#)]
62. Fritz, C.; Palacios-Rojas, N.; Feil, R.; Stitt, M. Regulation of secondary metabolism by the carbon-nitrogen status in tobacco: Nitrate inhibits large sectors of phenylpropanoid metabolism. *Plant J.* **2006**, *46*, 533–548. [[CrossRef](#)] [[PubMed](#)]
63. Peng, M.; Hudson, D.; Schofield, A.; Tsao, R.; Yang, R.; Gu, H.; Bi, Y.M.; Rothstein, S.J. Adaptation of Arabidopsis to nitrogen limitation involves induction of anthocyanin synthesis which is controlled by the NLA gene. *J. Exp. Bot.* **2008**, *59*, 2933–2944. [[CrossRef](#)] [[PubMed](#)]
64. Soubeyrand, E.; Basteau, C.; Hilbert, G.; van Leeuwen, C.; Delrot, S.; Gomes, E. Nitrogen supply affects anthocyanin biosynthetic and regulatory genes in grapevine cv. Cabernet-Sauvignon berries. *Phytochemistry* **2014**, *103*, 38–49. [[CrossRef](#)]
65. Misyura, M.; Colasanti, J.; Rothstein, S.J. Physiological and genetic analysis of Arabidopsis thaliana anthocyanin biosynthesis mutants under chronic adverse environmental conditions. *J. Exp. Bot.* **2013**, *64*, 229–240. [[CrossRef](#)] [[PubMed](#)]

66. Clément, G.; Moison, M.; Soulay, F.; Reisdorf-Cren, M.; Masclaux-Daubresse, C. Metabolomics of laminae and midvein during leaf senescence and source-sink metabolite management in *Brassica napus* L. leaves. *J. Exp. Bot.* **2018**, *69*, 891–903. [[CrossRef](#)] [[PubMed](#)]
67. Guo, Y.; Gan, S.S. Convergence and divergence in gene expression profiles induced by leaf senescence and 27 senescence-promoting hormonal, pathological and environmental stress treatments. *Plant Cell Environ.* **2012**, *35*, 644–655. [[CrossRef](#)]



© 2019 by the authors. Licensee MDPI, Basel, Switzerland. This article is an open access article distributed under the terms and conditions of the Creative Commons Attribution (CC BY) license (<http://creativecommons.org/licenses/by/4.0/>).

Seed Storage Protein Expression in Vegetative Tissue is driven by Nitrogen Supply during Senescence in Oil Seed Rape Plants

Stefan Bieker¹, Lena Riester¹, Jasmin Doll¹, Jürgen Franzaring², Andreas Fangmeier², Ulrike Zentgraf^{1*}

¹Centre of Molecular Biology of Plants, University of Tübingen, Auf der Morgenstelle 32, D-72076 Tübingen, Germany

² Institute of Landscape and Plant Ecology, University of Hohenheim, August-von-Hartmann-Str. 3, D-70599 Stuttgart, Germany

Correspondence:

*Ulrike Zentgraf

ulrike.zentgraf@zmbp.uni-tuebingen.de

Supporting Figures

Supplementary Figure S1

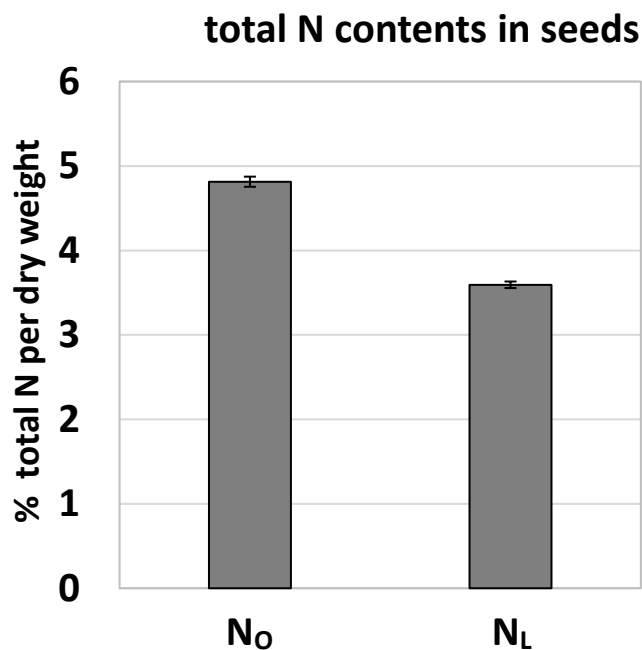
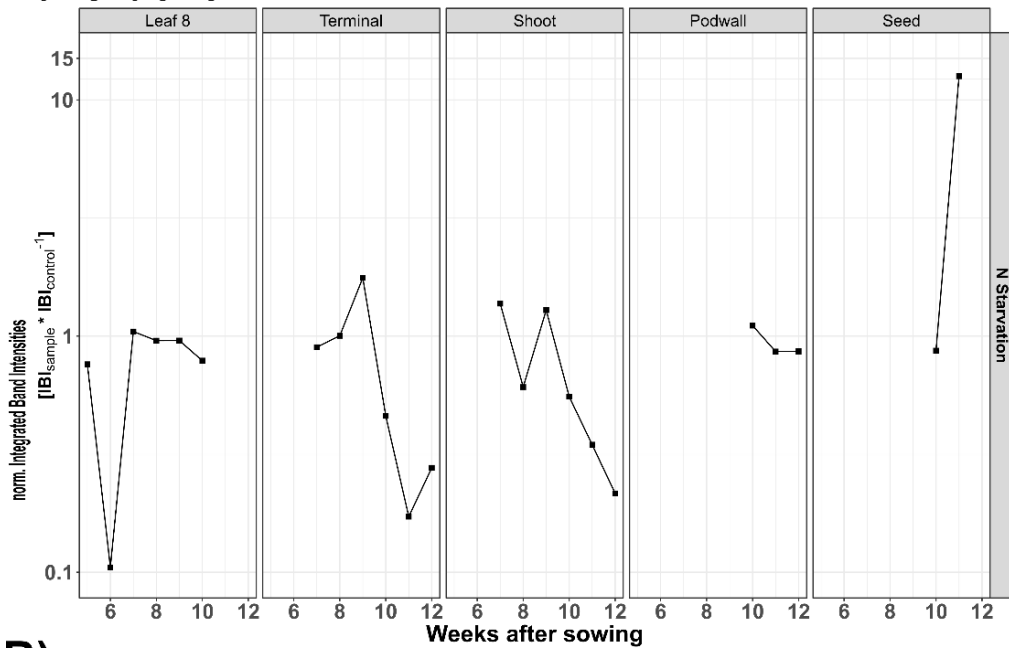


Figure S1. *Total N content in seeds.*

Total N content was measured by a CN-element analyser in % of the dry weight of the seeds collected from plants grown under N_L and N_O conditions. Error bars represent *SD* of two biological replicates.

Supplementary Figure S2

A) Cruciferin



B) Chlorophyll

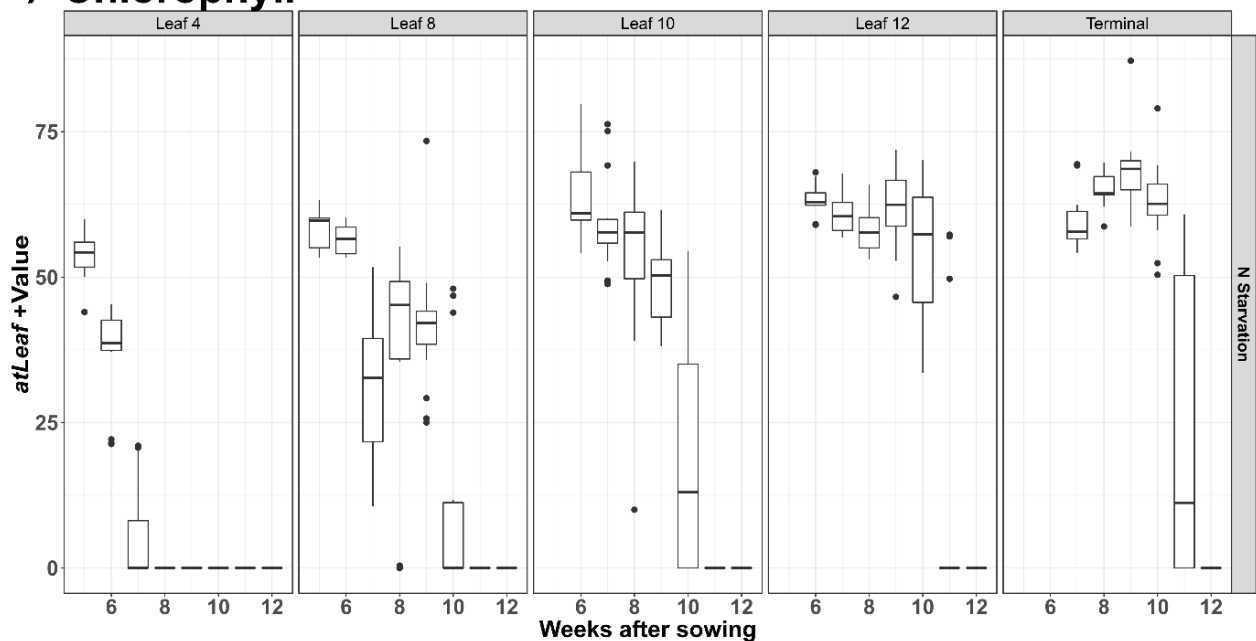


Figure S2. Prolonged N-Starvation in *B. napus*.

A) Quantification of immune-detection of CRU proteins in material from OSR (cv. Mozart) plants grown under N-starvation conditions. Accumulation of protein is barely detectable in leaf No. 8, the terminal leaf and the shoot show minimal build-ups. Seed extracts display highest accumulation of CRU proteins. **B)** Corresponding chlorophyll contents of different leaf positions of N-starved plants. Between week 5 and 7 values decreased at all analysed leaf positions. In the following weeks, leaf No. 4 is shed, all other positions exhibit an interruption of the decline or even an increase in chlorophyll content followed by a final rapid decrease before shedding. Chlorophyll contents are shown as median +/- 1.5xIQR of 3 biological replicates.

Supplementary Figure S3

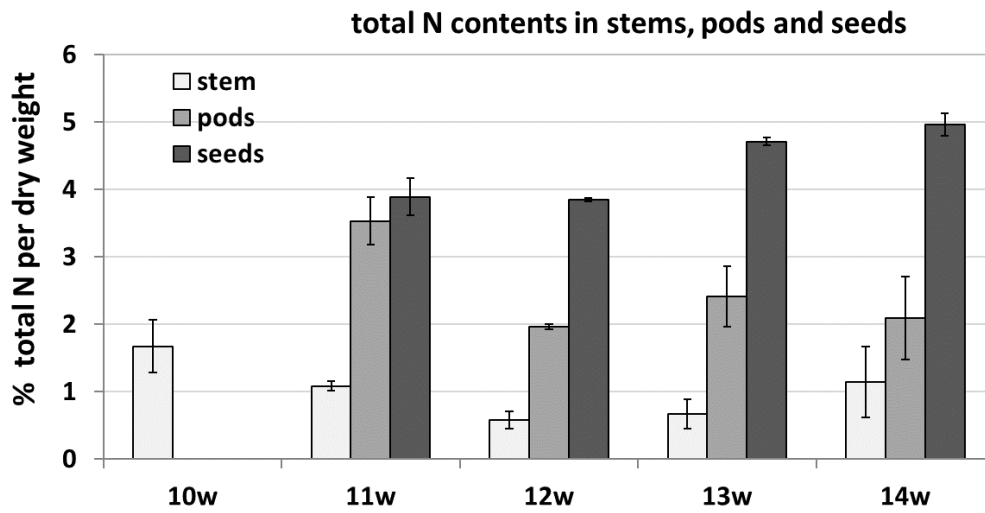


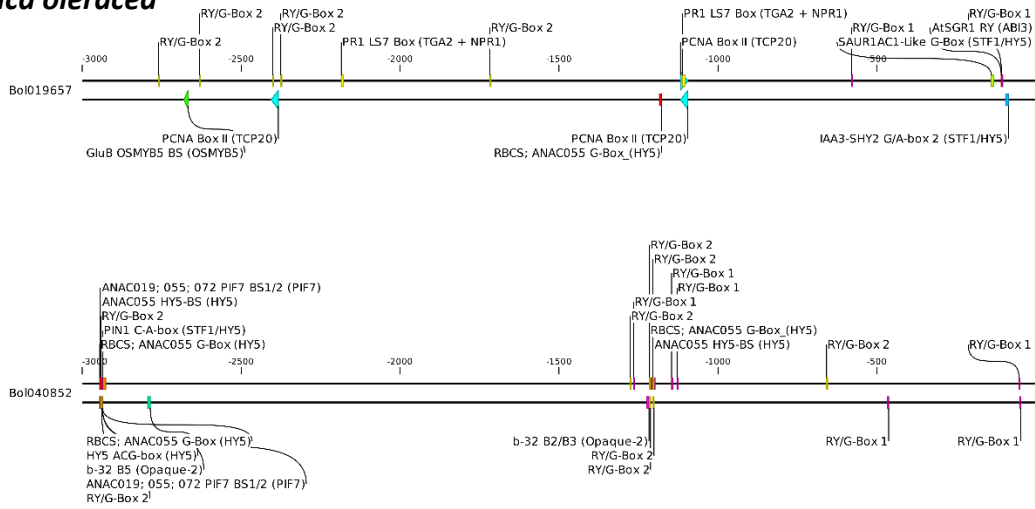
Figure S3. *Total N contents of stems pods and seeds.*

Total N content was measured by a CN-element analyzer in % of the dry weight of the respective tissue, stem, pods and seeds over development from week 10 to week 14. Error bars represent *SD* of two biological replicates.

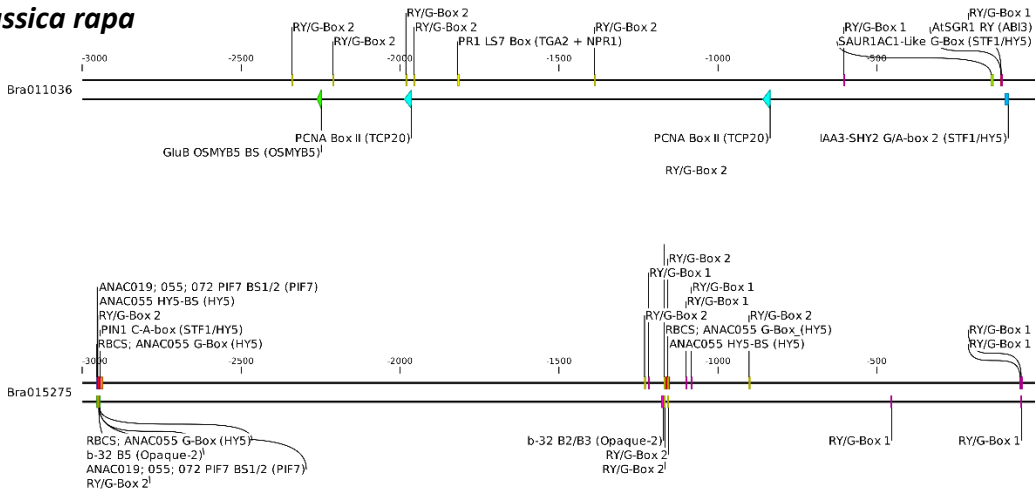
Supplementary Figure S4

Cruciferin

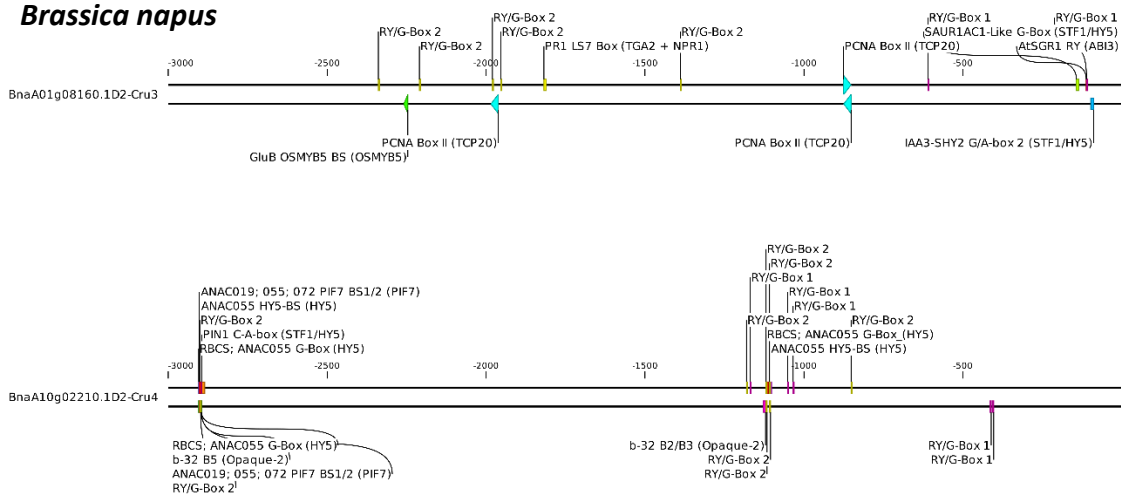
Brassica oleracea



Brassica rapa



Brassica napus



Napin

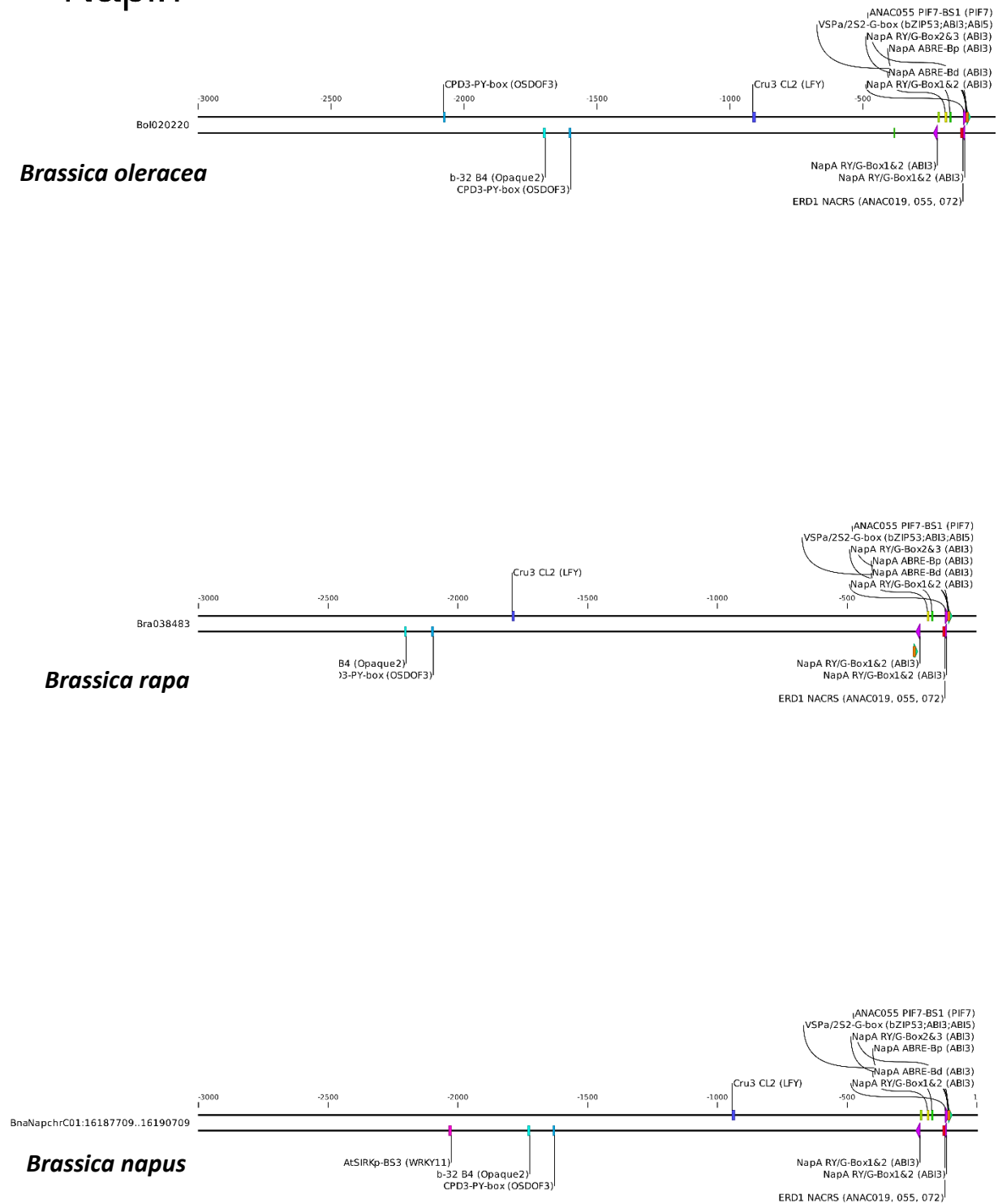


Figure S4. Seed storage protein (SSP) promotor structure and identified binding elements. Oilseed rape (*Brassica napus* L.) was formed ~7500 years ago by hybridization between *B. rapa* and *B. oleracea*, followed by chromosome doubling. Therefore, 3kb upstream of *B. rapa* (top) and *B. oleracea* (middle) as well as *B. napus* (bottom) *NAPIN* and *CRUCIFERIN* genomic sequences were analysed for *cis* elements. Depictions generated with CLC Main Workbench.

Supplementary Figure S5

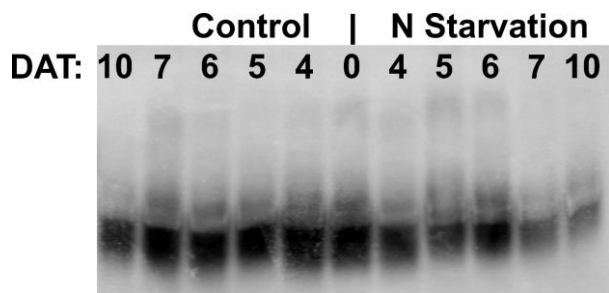


Figure S5: *Catalase (CAT) zymogram of nitrogen (N) starved OSR plants (cv. NPZ1).* CAT activity declines in N-starved plants from 5 DAT on (right), whereas control plants exhibit only minor variations in CAT activity over time (left). Media for N-starvation see Table S2. DAT: days after treatment. Image of CAT zymogram was transformed to grayscale and inverted.

1 ***Arabidopsis thaliana* WRKY25 transcription factor mediates**
2 **oxidative stress tolerance and regulates senescence in a redox-**
3 **dependent manner**

4 **Jasmin Doll[#], Maren Muth[#], Lena Riester, Kenneth Wayne Berendzen, Justine Bresson, Ulrike**
5 **Zentgraf***

6 Center for Plant Molecular Biology (ZMBP), University of Tuebingen, Auf der Morgenstelle 32,
7 72076 Tuebingen, Germany

8 **#Shared first author**

9 *** Correspondence:**
10 Corresponding Author
11 email@uni.edu

12 **Keywords: Arabidopsis, transcription factor network, WRKY factors, oxidative stress**
13 **tolerance, redox-dependent DNA-binding, leaf senescence**

14 **Abstract**

15 Senescence is the last developmental step in plant life and is accompanied by a massive change in gene
16 expression implying a strong participation of transcriptional regulators. In the past decade, the
17 WRKY53 transcription factor was disclosed to be a central node of a complex regulatory network of
18 leaf senescence and to underlie a tight multi-layer control of expression, activity and protein stability.
19 Here, we identify WRKY25 as a redox-sensitive up-stream regulatory factor of *WRKY53* expression.
20 Under non-oxidizing conditions, WRKY25 binds to a specific W-box in the *WRKY53* promoter and
21 acts as a positive regulator of *WRKY53* expression in a transient expression system using Arabidopsis
22 protoplasts, whereas oxidizing conditions dampened the action of WRKY25. However, overexpression
23 of *WRKY25* did not accelerate senescence but increased lifespan of Arabidopsis plants, whereas the
24 knock-out of the gene resulted in the opposite phenotype, indicating a more complex regulatory
25 function of WRKY25 within the WRKY subnetwork of senescence regulation. In addition,
26 overexpression of WRKY25 mediated higher tolerance to oxidative stress and the intracellular H₂O₂
27 level is lower in *WRKY25* overexpressing plants and higher in *wrky25* mutants compared to wild-type
28 plants suggesting that WRKY25 is also involved in controlling intracellular redox conditions.
29 Consistently, *WRKY25* overexpressers had higher and *wrky* mutants lower H₂O₂ scavenging capacity.
30 Like already shown for WRKY53, MEKK1 positively influenced the action of WRKY25. Taken
31 together, WRKY53, WRKY25, MEKK1 and H₂O₂ interplay with each other in a complex network. As
32 H₂O₂ signaling molecule participates in many stress responses, WRKY25 acts most likely as
33 integrators of environmental signals into senescence regulation.

34

35 **1 Introduction**

WRKY25, a redox-dependent senescence regulator

36 Senescence is the last step during plant development and is genetically programmed to maximize the
37 remobilization of nutrients out of the senescing tissue into developing parts of the plants before organs
38 finally die. Before anthesis, sequential leaf senescence leads to the reallocation of mineral, nitrogen
39 and carbon sources from older leaves to newly developing non-reproductive organs. After anthesis,
40 monocarpic leaf senescence is launched and governs the nutrient repartitioning to the now developing
41 reproductive organs and, therefore, has a critical impact on yield quality and quantity. Induction and
42 progression of leaf senescence is mainly achieved by switching-on genes involved in degradation and
43 mobilization of macromolecules and turning-off genes related to photosynthesis. A temporal transcript
44 profiling, using microarrays with high-resolution covering 22 time points of a defined leaf of
45 *Arabidopsis thaliana* during onset and progression of leaf senescence, revealed a distinct chronology
46 of events (Breeze et al., 2011). Remarkably, the first processes to be activated are autophagy and
47 transport followed by reactions to reactive oxygen species (ROS) and subsequently to salicylic acid
48 (SA) and jasmonic acid (JA). This clearly indicates that ROS, SA and JA are important early signals
49 in leaf senescence. In consistence, intracellular hydrogen peroxide contents increase during bolting and
50 flowering of *Arabidopsis* plants when monocarpic senescence is induced (Zimmermann et al., 2006)
51 while decreasing hydrogen peroxide levels lead to a delay of the onset of leaf senescence (Bieker et
52 al., 2012).

53 These massive changes in the transcriptome suggest a central role for transcriptional regulators. The
54 two transcription factor families of WRKY and NAC factors, which largely expanded in the plant
55 kingdom, are overrepresented in the senescence transcriptome of *Arabidopsis* (Guo et al., 2004) and
56 appear to be ideal candidates for regulatory functions. Several members of both families play important
57 roles in senescence, not only in *Arabidopsis* but also in other plant species (Balazadeh et al., 2010,
58 2011; Besseau et al., 2012; Breeze et al., 2011; Miao et al., 2004; Uauy et al., 2006; Ülker et al., 2007;
59 Wu et al., 2012; Yang et al., 2011, Gregerson et al., 2013).

60 The WRKY transcription factor family of *Arabidopsis thaliana* consists of 75 members, subdivided
61 into three different groups according to their protein motifs and domains (Eulgem et al., 2000; Rushton
62 et al., 2010). Many WRKY factors are activated after pathogen attack but also in response to abiotic
63 stress (for review see Birkenbihl et al., 2017; Jiang et al., 2017). Moreover, members of all three groups
64 are involved in senescence regulation and many of these react to ROS, SA and JA signals indicating a
65 cross-talk between stress responses and senescence. Besides this cross-talk to stress responses, the
66 WRKY53 upstream regulator REVOLUTA mediates a redox-related communication between early leaf
67 patterning and senescence as REVOLUTA is involved in both processes (Xie et al., 2014, Kim et al.,
68 2017).

69 Interestingly, almost all members of the WRKY family contain one or more W-boxes (the consensus
70 binding motif TTGACC/T of all WRKY factors) in their promoters, pointing to a WRKY
71 transcriptional network (Dong et al., 2003; Llorca et al., 2014). However, besides regulating
72 transcription of each other, WRKY factors are also able to form heterodimers, leading to a change in
73 DNA-binding specificity (Xu et al., 2006). In addition, many other proteins interact physically with
74 WRKY proteins influencing their activity and stability (for review see Chi et al., 2013). One central
75 node in the WRKY network regulating early senescence is WRKY53. WRKY53 underlies a tight
76 regulation governed by multi-layer mechanisms to control expression, activity and protein stability.
77 When leaf senescence is induced, the WRKY53 gene locus is activated by the histone modifications
78 H3K4me2 and H3K4me3 (Ay et al., 2009; Brusslan et al., 2012), whereas DNA methylation remains
79 unchanged and overall very low (Zentgraf et al., 2010). At least 12, most likely even more, proteins
80 are able to bind to the promoter of WRKY53 (GATA4, AD-Protein, WRKY53 itself, several other
81 WRKYs, MEKK1, REVOLUTA, WHIRLY1) and influence the expression of WRKY53 (Miao et al.,
82 2004, 2007, 2008; Potschin et al., 2014; Xie et al., 2014; Ren et al., 2017, unpublished results).
83 Moreover, the WRKY53 protein also directly interacts with a histone deacetylase 9 (HDA9) to recruit
84 POWERDRESS and HDA9 to W-box containing promoter regions to remove H3 acetylation marks

WRKY25, a redox-dependent senescence regulator

85 and thereby suppress the expression of key negative senescence regulators (Chen et al., 2016). This
86 clearly suggests that WRKY53 itself is also involved in changing epigenetic marks of senescence
87 regulators in a feedback loop. Phosphorylation by the MAP kinase kinase kinase MEKK1 or the
88 interaction with the epithiospecifier ESP/ESR directly influence the DNA-binding activity of
89 WRKY53 (Miao et al., 2007; Miao and Zentgraf, 2007). On top of that, the E3 ubiquitin ligase UPL5
90 tightly controls the protein amount of WRKY53 (Miao et al., 2010). The complexity of the WRKY
91 network is illustrated by the fact that one and the same WRKY factor, namely WRKY18, acts as
92 upstream regulator, downstream target and protein interaction partner of WRKY53 (Potschin et al.,
93 2014).

94 In order to unravel the molecular mechanisms of the senescence regulating WRKY network in more
95 detail, we screened the W-boxes of the *WRKY53* promoter for DNA-protein interactions with other leaf
96 senescence-associated WRKY proteins and tested their impact on *WRKY53* expression using a
97 transient expression system in Arabidopsis protoplasts. While WRKY18 was the strongest negative
98 regulator of *WRKY53* expression (Potschin et al., 2014), WRKY25 had the strongest positive effect.
99 Therefore, we wanted to analyze the interplay between WRKY53 and WRKY25 in more detail. DNA-
100 binding as well as transcriptional activation potential of WRKY25 is dependent on the redox
101 conditions. Intracellular hydrogen peroxide concentrations are altered in plants with altered *WRKY25*
102 expression and the *WRKY25* overexpressing plants are more tolerant against oxidative stress. Like
103 WRKY18, WRKY53 and WRKY25 are also able to form homo- and heterodimers. WRKY25 appears
104 to foster the activation of the H₂O₂-mediated expression of the transcription factors *WRKY18* but
105 dampened the H₂O₂-response of *WRKY53*, *ZAT12*, and *NAC92* in mature leaves. However,
106 contradicting its positive effect on *WRKY53* expression and the senescence phenotype of the *WRKY53*
107 overexpressing plants, *WRKY25* overexpressing plants exhibited a delayed senescence phenotype,
108 whereas *wrky25* mutant plants showed slightly accelerated senescence. This clearly points to a more
109 complex regulatory network. Moreover, the influence of MEKK1 as modulator of WRKY53 activity
110 on the action of WRKY25 was tested.

111

112 2 Results

113 Transcriptional reprogramming is a central feature of senescence onset and progression and the WRKY
114 transcription factor family is one of the very important groups of transcription factors involved in this
115 process. The WRKY transcription factors built up a subnetwork in the complex senescence regulatory
116 network as almost all members of the WRKY family contain W-boxes in their promoter regions. Even
117 though all WRKYs bind to these consensus sequences, there appears to be a selectivity of specific
118 factors for specific boxes most likely due to the surrounding sequences (Rushton et al., 2010; Brand et
119 al., 2013; Potschin et al., 2014). Moreover, heterodimer formation can lead to changes in binding
120 preferences (Xu et al., 2006). As WRKY53 is one of the important nodes of convergence between
121 stress responses and senescence and is involved in several different mechanisms of senescence
122 regulation, we analyzed which senescence-associated WRKY factors bind to the W-boxes of the
123 *WRKY53* promoter (Potschin et al., 2014). Out of the 15 WRKYs analyzed by an ELISA-based DNA-
124 protein interaction assay, WRKY18 had a very strong binding affinity to all W-boxes of the *WRKY53*
125 promoter but a very low selectivity. Moreover, WRKY18 was characterized to be a negative regulator
126 of *WRKY53* expression (Potschin et al., 2014). Besides WRKY18, WRKY25 was one of the strongest
127 interaction partners of the *WRKY53* promoter but in this case turned out to be a positive regulator of
128 *WRKY53* expression. Therefore, we now analyzed the interplay between WRKY53 and WRKY25 in
129 more detail.

130

131 **2.1 WRKY25 binds directly to the promoter of *WRKY53* in a redox-sensitive manner**

132 In contrast to WRKY18, which strongly binds to all W-boxes in the *WRKY53* promoter, WRKY25 also
133 had a strong binding activity but selectively bound to W-box1, to a much lesser extent to W-box2 and
134 3, the TGAC cluster and an artificial 3x W-box (Fig. 1A, B). Binding was completely abolished when
135 W-box1 was mutated or an unrelated G-box motive was coupled to the ELISA plates. All binding
136 reactions increased with protein concentrations and no binding could be detected with crude extracts
137 of *E. coli* cells expressing no recombinant protein. Both proteins were present approximately to the
138 same extent in *E. coli* crude extracts (Fig. S1). As many WRKY factors signal back to their own
139 promoters in positive or negative feedback loops, we also tested whether WRKY25 can bind to the W-
140 boxes in its own promoter. Here, WRKY25 was able to bind to W-box1 and 4, whereas W-box2 and 3
141 exhibited lower binding affinities. *Vice versa*, WRKY53 also bound preferentially to W-box 1 of the
142 *WRKY25* promoter but to W-box2 of its own promoter, as already shown before (Fig. 1C, Potschin et
143 al., 2014). This indicates that according to DNA-binding, there is a cross-regulation between both genes
144 and both genes are regulated by feedback mechanisms.

145 We already know for a long time that *WRKY53* expression can be induced by H₂O₂ treatment (Miao et
146 al., 2004; Xie et al., 2014). As the WRKY25 protein contains two potentially redox-sensitive zinc-
147 finger DNA-binding domains, it is an excellent candidate for direct redox regulation (Arrigo, 1999).
148 Therefore, we wanted to test whether the WRKY25 DNA-binding reaction is sensitive to reducing or
149 oxidizing agents and analyzed the ability of WRKY25 to bind to W-box1 of the *WRKY53* promoter
150 and W-box1 of the *WRKY25* promoter under different redox conditions. Whereas reducing conditions
151 (DTT addition) clearly and significantly increased DNA-binding ability to both W-boxes, oxidizing
152 conditions (H₂O₂ addition) significantly reduced the binding activity in comparison to standard binding
153 conditions (Fig. 2). In order to test whether this redox-dependent binding can be driven back and forth
154 when redox conditions change, we added increasing amounts of H₂O₂ to the DTT pre-treated binding
155 reactions and *vice versa*. Both redox-related changes in DNA-binding activity of WRKY25 were
156 reversible indicating that WRKY25 can directly adapt its DNA-binding activity to the redox status of
157 the cell. However, not all WRKYs show this redox-sensitivity, e.g. WRKY18 appears to be insensitive,
158 whereas WRKY53 DNA-binding seems to be diminished under oxidizing and reducing conditions, but
159 this reduction was not statistically significant (Fig. S2).

161 **2.2 WRKY25 acts as positive regulator of *WRKY53* expression under non-oxidizing conditions**

162 To investigate, how WRKY25 affects the expression of *WRKY53* and *vice versa*, we performed a
163 transient co-transformation of *WRKY53* or *WRKY25* promoter:*GUS* constructs with 35S:*WRKY25* and
164 35S:*WRKY53* effector constructs, respectively, using an Arabidopsis protoplast system (Fig. 3A). Here,
165 the WRKY25 effector significantly up-regulated promoter *WRKY53*-driven *GUS* expression. In
166 contrast, it down-regulated *GUS* expression driven by its own promoter pointing to a negative feedback
167 regulation. The WRKY53 effector slightly activated reporter gene expression driven by its own
168 promoter as already described before (Potschin et al., 2014). Surprisingly, WRKY53 had only low
169 effects (1.4-fold) on reporter gene expression driven by the promoter of *WRKY25* (Fig. 3A), even
170 though WRKY53 is able to bind strongly to the W-boxes of this promoter (Fig. 1C) indicating that
171 strong binding does not necessarily mean that gene expression is highly affected. If both effector
172 constructs were co-expressed, additive effects were detected leaving the question open whether or not
173 heterodimers are formed.

174 As DNA-binding of WRKY25 was redox-sensitive, we wanted to find out, whether also target gene
175 expression is affected by the redox conditions. Since we wanted to change the redox conditions within
176 a physiological range, we did not treat protoplasts directly with high amounts of H₂O₂. Instead, we
177 developed a transient expression system using Arabidopsis protoplast in the presence of 3-Amino-
178 Triazol (3'-AT), which inhibits catalase function, and would therefore provoke physiological changes
179

WRKY25, a redox-dependent senescence regulator

180 in intracellular H₂O₂ levels. Inhibition of catalase activity was almost complete and lead to increasing
181 concentrations of H₂O₂ in the cells, but had no effect on the GUS activity measurement (Fig. S3). Using
182 this assay, WRKY25 effector proteins were significantly less efficient under oxidizing conditions, most
183 likely due to lower DNA-binding affinity. WRKY53 effector proteins appeared also to be less efficient,
184 but the effect was only significant for the WRKY25 promoter, not for its own. The effects were still
185 significant when a combination of both effectors constructs was used (Fig. 3B).

186

2.3 MEKK1 increases the effect of WRKY25 proteins on P_{WRKY53} driven gene expression

187 As expression of *WRKY53* is enhanced by a direct binding of MEKK1 to the promoter region of
188 *WRKY53* and a protein-protein interaction between WRKY53 and MEKK1 leads to phosphorylation
189 of WRKY53 (Miao et al., 2007), we tested whether WRKY25 activity can also be enhanced by adding
190 a 35S:*MEKK1* construct as additional effector in a protoplast co-transformation assay. Indeed, the
191 presence of the MEKK1 protein significantly increased *WRKY53* promoter-driven reporter gene
192 expression by WRKY25 to approximately the same extent as MEKK1 presence exhibits on WRKY53
193 activity itself (Fig. 3C). Thus, MEKK1 interplay with WRKY factors is not restricted to WRKY53, but
194 appears to be a more general phenomenon. First evidence for a direct protein-protein interaction
195 between several WRKY factors and MEKK1 was obtained in a Yeast-Split-Ubiquitin system, in which
196 many, but not all tested WRKYs could interact with MEKK1 (data not shown). WRKY18, which acted
197 as a repressor on promoter *WRKY53*-driven reporter gene expression (Potschin et al., 2014), even
198 changed its activity in the presence of MEKK1 from a repressor to an activator (Fig. S4A). Moreover,
199 we tested the role of MEKK1 in senescence regulation. As *MEKK1* knockout plants die before they
200 develop the first true leaves, we used an estradiol-inducible amiRNA_{*MEKK1*} line to knockdown MEKK1
201 by treatment with 3 μM β-estradiol or mock every 7 days starting on day 25 after germination. In this
202 system, knockdown of MEKK1 can be controlled by GFP expression, which is under the control of the
203 same amiRNA (Li et al., 2013). Here we could show that conditional knockdown of *MEKK1* in plants
204 exhibit an accelerated senescence phenotype (Fig. S4B-D). Taken together, MEKK1 appears to act as
205 negative regulator of senescence at least in part by modulating the activity of different WRKY factors.
206 However, whether the interaction with WRKY25 or WRKY18 is direct as it is for WRKY53, or is
207 mediated by the classical MAPK pathway, still has to be elucidated.

208

2.4 WRKY25 is involved in senescence regulation

210 To evaluate the participation of WRKY25 in senescence regulation, we analyzed plants with altered
211 *WRKY25* expression levels. A T-DNA insertion in the last of five exons of *WRKY25* (SAIL_529_B11)
212 was confirmed by PCR and expression of *WRKY25* was analyzed by qRT-PCR (Fig. S5). Moreover,
213 for overexpression of *WRKY25*, we first tried to transform plants using a 35S:*WRKY25* construct.
214 However, qRT-PCR revealed that *WRKY25* was not overexpressed; in contrast, the endogenous gene
215 expression was severely silenced so that we used this line as knockdown line (35S:*WRKY25si*) to
216 confirm the results of the *wrky25* mutant plants. In a second attempt, we used the *UBIQUITIN10*
217 promoter for more moderate overexpression and we created two independent plant lines overexpressing
218 *WRKY25* to different extents with different transgene expression levels (Fig. S5). In addition, double-
219 knock-out mutants were created by crossing the single mutant lines *wrky25* (SAIL_529_B11) and
220 *wrky53* (SALK_034157; Miao et al., 2004) with each other. F2 progenies were screened for
221 homozygous double-knock-out plants. In order to compare leaves of the same position within the
222 rosette for senescence symptoms, leaves were color-coded during development (Bresson et al., 2018).
223 Altered *WRKY25* expression had almost no effect on general development of the plants (Fig. S6). Bolts
224 appeared at approx. week 5 in all lines. Leaf size increased in the overexpression lines whereas leaves
225 of the *wrky25* mutant, the *wrky25/wrky53* double-knock-out plants and the *WRKY25* silenced line were
226 slightly smaller. To evaluate senescence in detail, we sorted the rosette leaves of all lines by the color
227 code according to their age to compare the respective leaves with each other. A typical example of 8-
228

229 week old plants is shown in Fig. 4A. However, as there are always differences between individual
230 plants of one line, a statistical analysis of at least 6 plants was done by grouping the leaves into four
231 categories by an automated colorimetric assay (ACA; Bresson et al., 2018) according to their leaf color
232 (green; green/yellow; fully yellow and brow/dry) from week 5 to 8 (Fig. 4B). The photosynthetic status
233 of the plants was analyzed using a Pulse-Amplitude-Modulation (PAM) method (Fig. 4C). Amongst
234 the chlorophyll fluorescence imaging parameters, the Fv/Fm ratio is reflecting the maximal quantum
235 yield of PSII photochemistry. Moreover, the expression of the senescence marker genes *CABI* being
236 downregulated, *ANAC092*, and *SAG12* being upregulated were analyzed by qRT-PCR (Fig. 4D). In
237 comparison to Col-0 wildtype plants, *WRKY25* overexpressing plants showed significantly delayed
238 visible senescence symptoms, which was in consistence with a delay in the decrease of the Fv/Fm ratio
239 measured in leaf No. 5 and leaf No. 10 (Fig. 4C, Fig. S7). Furthermore, a higher expression of *CABI*
240 in 7-week-old plants as well as a lower expression of *ANAC092* and *SAG12* in 6-week-old plants of
241 *WRKY25* overexpressing line compared to wildtype confirmed a delayed senescence phenotype. In
242 contrast, senescence and loss of photosynthetic activity was accelerated in the *wrky25* mutant plants
243 and the 35S:*WRKY25si* line (Fig. 4A-C). Higher up-regulation of *ANAC092* and *SAG12* expression in
244 6-week-old plants and lower *CABI* expression in 7-week-old plants in *wrky25* mutant line clearly
245 indicate an accelerated senescence phenotype (Fig. 4D). Remarkably, the expression of *WRKY53* was
246 lower in the *WRKY25* overexpressing as well as in the *wrky25* mutant lines in comparison to WT (Fig.
247 5), suggesting a more complex regulation of *WRKY53* expression during development. Moreover, the
248 expression of two tested *WRKY* genes (*WRKY18* and *WRKY40*) was antagonistic in *WRKY25*
249 overexpressing and mutant plants, but only at week 5; at later stages also these two *WRKY* genes were
250 down-regulated in both lines. This clearly indicates that no simple regulatory circuits are in place
251 between these *WRKY* proteins and genes. *WRKY25* as well as *WRKY53* and *WRKY18* appear to be
252 part of a *WRKY* subnetwork, which is embedded in the overall complex senescence regulatory
253 network. Interfering on the expression of one *WRKY* gene can lead to an imbalance in the subnetwork,
254 which might explain that mutant and overexpressing plants showed the same effects on the expression
255 of specific *WRKY*s. Taken together, *WRKY25* appears to be part of the *WRKY* subnetwork and a
256 redox-sensitive negative regulator of senescence.

257

258 **2.5 WRKY25 mediates tolerance against oxidative stress**

259 As *WRKY25* action appears to be redox-sensitive, we wanted to analyze whether *WRKY25* is also
260 involved in the response to oxidative stress or plays a role in the signaling of H₂O₂ *in planta*. Therefore,
261 we germinated seeds of WT, *wrky25* mutant, 35S:*WRKY25si*, the *WRKY25* overexpressing lines as
262 well as the double mutant *wrky25/wrky53* on plates containing 10 mM H₂O₂ (Fig. 6A). After 7 to 10
263 days, the percentages of green seedlings per total seedling numbers were counted. The experiment was
264 repeated six times and the outcome of these series were summarized in a heat map showing the
265 tolerance against H₂O₂ (Fig. 6B). The germination rate on the control plates without H₂O₂ was almost
266 100% for all plant lines used. The 35S:*WRKY25si* and the *WRKY25* overexpressing lines (UBI:*W25-1*
267 and UBI:*W25-2*) germinated much better on H₂O₂ plates in comparison to WT. In contrast, the *wrky25*
268 as well as the *wrky25/wrky53* mutant seeds germinated significantly worse compared to WT.
269 Therefore, *WRKY25* seems to mediate a higher tolerance against H₂O₂.

270 In order to test whether this tolerance is due to higher antioxidative capacities in these lines, we
271 measured intracellular H₂O₂ contents of leaf No. 8 in 8-week-old plants of these lines (Fig. 6C). Less
272 intracellular H₂O₂ was measured in the overexpressing lines, while more H₂O₂ appears to be present
273 in the mutants and the silenced line in comparison to WT (Fig. 6C). Moreover, the H₂O₂ scavenging
274 capacity of leaf discs of the different lines was tested by incubating these discs for 2 h in H₂O₂ solution
275 and measure the remaining H₂O₂ using peroxide strips (Fig. 6D). As expected, the antioxidative
276 capacity of the *WRKY25* overexpressing lines was slightly higher, whereas scavenging in the mutant
277 and silencing lines was lower. Taken together, *WRKY25* does not only mediate a higher tolerance

WRKY25, a redox-dependent senescence regulator

278 against oxidative stress but is also involved in the regulation of intracellular H₂O₂ levels, at least in
279 later developmental stages. This might also contribute to the negative effect of WRKY25 on
280 senescence since H₂O₂ acts as signaling molecule to induce senescence and, most likely, also
281 participates in membrane deterioration and lipid peroxidation processes in later stages (Chia et al.,
282 1981). The conclusions on the role of WRKY25 in senescence-related redox signal transduction is
283 further supported by a dark-induced senescence experiment including *wrky25*, *catalase2* (*cat2*) and
284 *wrky25/cat2* double-knock-out plants (Fig S8). As expected, *cat2* and *wrky25* had lower H₂O₂
285 scavenging capacity than wildtype plants resulting in a higher H₂O₂ content in the mutant lines (Fig
286 S8B,C). Remarkably, *wrky25/cat2* double mutants showed an additive effect indicating that higher
287 H₂O₂ content in *wrky25* mutant plants is not due to lower catalase activity. This was also visualized by
288 the CAT-activity staining of a native PAGE, in which CAT2 activity of wildtype and *wrky25* mutant
289 plants appear to be very similar (Fig. S8A). Moreover, dark-induced senescence was more pronounced
290 in *wrky25* or *cat2* mutant compared to wildtype leaves and was enhanced in the *wrky25/cat2* double-
291 mutant, correlating with their intracellular H₂O₂ contents (Fig. S8D)

292

293 **2.6 WRKY25 enhances WRKY53 response to oxidizing conditions**

294 Because *WRKY53* is strongly up-regulated after treatment with H₂O₂ in Arabidopsis (Miao et al., 2004;
295 Xie et al. 2014) and WRKY25 DNA-binding is redox-sensitive (Fig. 2A) and its positive effect on
296 *WRKY53* expression is diminished under oxidizing conditions (Fig. 3B), we wanted to find out,
297 whether WRKY25 is required for the induction of *WRKY53* expression after H₂O₂ treatment.
298 Therefore, leaves of *wrky25* and *wrky53* single as well as double mutants and WT plants were detached
299 and incubated in 10 mM H₂O₂. The expression of *WRKY53* and several other H₂O₂-responsive genes
300 (*WRKY25*, *ANAC092*, *WRKY18* and *ZAT12*) was determined after 0 min, 30 min, 1 h and 3 h using
301 qRT-PCR (Fig. 7). All tested genes were responsive to H₂O₂ in wildtype. *WRKY53* expression
302 increased most prominently in 7-week-old plants after 1 h of H₂O₂ treatment. This response is clearly
303 dampened in *wrky25* mutant leaves. In contrast, the *WRKY25* mRNA level highly increased in leaves
304 of young 5-week old wildtype plants 1 h after H₂O₂ treatment and responsiveness becomes lower with
305 age. Again, this response is diminished in *wrky53* mutant leaves in all tested developmental stages
306 indicating that WRKY25 is involved in H₂O₂ response of *WRKY53* and *vice versa*. *ANAC092*
307 responded most prominent also in 7-week-old leaves, similar to *WRKY53*. This response is also
308 suppressed in the *wrky25* and in the *wrky53* leaves, and even more in the double mutant suggesting
309 that both factors are involved in the H₂O₂ responsiveness of *ANAC092*. The same held true for *ZAT12*
310 expression, here a higher basal expression could be observed in 7-week-old leaves of *wrky53* so that
311 the H₂O₂ treatment did not lead to a further induction. In contrast, induction of *WRKY18* expression by
312 H₂O₂ was much more pronounced in 5-week-old *wrky25*, *wrky53* and the double mutant compared to
313 wildtype leaves, whereas the response was attenuated in older stages in all mutant lines. This supports
314 the idea of a variable function of *WRKY53* and *WRKY25* on the *WRKY18* promoter: in early
315 developmental stages, they act as repressors, in later stages as activators. Taken together, *WRKY25* as
316 well as *WRKY53* are involved in H₂O₂ induction of variable genes including each other and, depending
317 on the developmental stage of the plants; they can have opposing effects on the same gene promoters,
318 again indicating a very complex regulatory interaction.

319

320 **2.7 Protein-protein interaction between WRKY25 and WRKY53.**

321 Many different proteins are able to interact with WRKY proteins like e.g. VQ proteins, MAPKs or 14-
322 3-3 proteins (for review see Chi et al., 2013). WRKY proteins also interact with each other, but they
323 appear to have clear preferences. Besseau et al. (2012) could show that *WRKY53* is able to interact
324 with *WRKY30*, but not with *WRKY54*, *WRKY70* and not with itself in the Yeast-Two-Hybrid system.
325 However, we could show in a previous study using FRET-fluorescence life time imaging that
326 *WRKY53* can form homodimers as well as heterodimers with *WRKY18* (Potschin et al., 2014).

327 Heterodimer formation can alter DNA-binding selectivity as shown by Xu et al. (2006) for WRKY18,
328 WRKY40 and WRKY60 heterodimers versus homodimers indicating another level of complexity in
329 the WRKY subnetwork. Here, we analyzed whether WRKY25 can also interact with WRKY53. To
330 get a first hint whether the interaction is possible, we also used the GAL4-based Yeast-Two-Hybrid
331 system. WRKY25 was able to interact with WRKY53 and with itself forming hetero- and homodimers
332 (Fig. S9). However, the combination WRKY25 as bait construct and the empty prey construct as
333 negative control also resulted in yeast growth in approx. 30 % of our assays indicating that the
334 interaction results in yeast using WRKY25 as bait might be artefacts. Therefore, we concentrated on
335 *in vivo* analyses by **Bimolecular Fluorescence Complementation (BiFC)** in transiently transformed
336 Arabidopsis protoplasts (Fig. 8). We looked at the transformed protoplast under the confocal laser-
337 scanning microscope and analyzed YFP fluorescence for protein-protein interaction and RFP
338 fluorescence for transformation control. YFP signals could be detected in all combinations, WRKY25-
339 WRKY25, WRKY53-WRKY53, WRKY25-WRKY53, in the nucleus as well as in the cytoplasm (Fig.
340 8A). Moreover, we analyzed the population of fluorescent cells with a CytoFLEX cytometer (*Beckman*
341 *Coulter*) and calculated its corresponding BiFC YFP fluorescence index (Fig. 8 B,C). Overall, these
342 results clearly suggest that WRKY25 is able to form homodimers as well as heterodimers with
343 WRKY53 *in vivo*.

344 **3 Discussion**

345 ROS, especially hydrogen peroxide, act as signaling molecules during senescence and/or stress
346 responses. However, how this signal is perceived and transmitted into senescence onset and
347 progression or stress response activation is still far from being understood. One of the central features
348 of senescence is a massive change in the transcriptome, in which photosynthesis related genes are shut
349 down and genes related to degradation and remobilization processes are turned on. Therefore,
350 transcription factors would be ideal candidates to take up ROS signals directly. Indeed, for some
351 transcription factors of different families such as class I TCP factors (Viola et al., 2013), HSF8 (Giesgut
352 et al., 2015) or the bZIP factor GBF1 (Shaikhali et al., 2012), a redox-sensitive action has already been
353 disclosed. Moreover, the plant specific protein GIP1 enhances DNA-binding activity of GBF3 and
354 reduces DNA-binding activity of other members of the G-group bZIP factors in Arabidopsis, namely
355 bZIP16, bZIP68, and GBF1, under non-reducing conditions through direct physical interaction.
356 Whereas reduced GIP1 predominantly exists in a monomeric form and is involved in formation of
357 DNA-protein complexes of G-group bZIPs, oxidized GIP1 is released from these complexes and
358 instead performs chaperone function (Shaikhali, 2015). Due to space limitation, not all examples can
359 be mentioned here, but taken together, redox conditions can influence gene expression through the
360 action of transcription factors in several ways: changing either DNA-binding activity or activation
361 potential or intracellular localization or interaction with specific partners or proteolytic degradation or
362 a combination of those. He et al., (2018) just recently reviewed this topic very nicely. Here, we could
363 show that WRKY25 DNA-binding activity is redox-sensitive, and that these redox-sensitive changes
364 in activity are reversible as a function of the redox conditions (Fig. 2). Not all WRKY factors show
365 these features, as e.g. WRKY18 DNA-binding activity appears not to be redox-sensitive at all and
366 WRKY53 DNA-binding activity was only very slightly influenced by changes in the redox
367 environment (Fig. S2). In contrast to WRKY18, which strongly binds to all W-boxes of the *WRKY53*
368 promoter (Potschin et al., 2014), WRKY25 binds selectively to a specific W-box in the promoter of
369 *WRKY53* and can positively influence its expression (Fig. 1, 3). Under oxidizing conditions, activation
370 of *WRKY53* expression by WRKY25 is dampened (Fig. 3). Even though binding and transactivation is
371 lower under oxidizing conditions, WRKY25 is still involved in the response of the *WRKY53* promoter
372 to oxidizing conditions *in planta*, as H₂O₂ response of *WRKY53* was much lower in the *wrky25* mutants
373 compared to WT plants, especially in later stages (Fig. 7). At the first glance, this appears to be a

WRKY25, a redox-dependent senescence regulator

374 contradiction, but as WRKY25 is also involved in down-regulation of H₂O₂ contents, negatively
375 regulates its own expression and is restricted in its action by the formation of heterodimers with its
376 target factor WRKY53, three negative feedback loops are at work. This indicates that WRKY25
377 function might be to prevent an overshooting of the reaction to H₂O₂. In addition, not only *WRKY53*
378 response to oxidative stress appears to be attenuated by WRKY25 but also *ZAT12* and *ANAC092*
379 response. In contrast, *WRKY18* reaction appears to be enhanced, but only in young plants (Fig. 7). As
380 already mentioned before, *WRKY25* expression is induced by H₂O₂, whereas WRKY25 at the same
381 time reduces intracellular H₂O₂ contents, especially in later stages of senescence, as lower or higher
382 H₂O₂ levels were measured in *WRKY25* overexpressing plants and *wrky25* mutant or knockdown lines,
383 respectively (Fig. 6, 7). High H₂O₂ contents in later stages of senescence are most likely involved in
384 membrane deterioration and lipid peroxidation processes as part of the senescence degradation
385 processes (Chia et al., 1981). This is in line with the senescence acceleration or delay of the *WRKY25*
386 overexpressing plants and *wrky25* mutant or knockdown lines, respectively (Fig. 4, Fig. S9).

387 A simple gene for gene relationship between *WRKY25* and *WRKY53* would suggest opposite
388 phenotypes. As *WRKY53* has been characterized as positive regulator of leaf senescence (Miao et al.,
389 2004), overexpression of *WRKY25* should lead to increased *WRKY53* levels and to the same senescence
390 phenotype as *WRKY53* overexpression. *Vice versa*, knockdown or mutation of *WRKY25* should exhibit
391 the same phenotype as knockdown or mutation of *WRKY53*. However, the senescence phenotype of
392 *WRKY25* overexpressing plants and *wrky25* mutant or knockdown lines was found to be exactly
393 opposite to the expected phenotype of a positive *WRKY53* regulator. This can be explained by the fact
394 that WRKY25 and WRKY53 are not acting in a simple signal transduction pathway but in a complex
395 regulatory network between many members of the WRKY transcription factor family showing
396 multilayer feedback regulations. In the same line of evidence, WRKY18 was characterized to be a
397 negative up-stream regulator as well as a down-stream target and a protein interaction partner of
398 WRKY53 (Potschin et al., 2014). Here, we could show that WRKY25 is also a redox sensitive up-
399 stream regulator and down-stream target gene of WRKY53 (Fig. 3, 7) as well as a protein interaction
400 partner of WRKY53 (Fig. 8). Moreover, WRKY25 appears to be involved in the H₂O₂ response of
401 WRKY18 and WRKY53 expression but in opposite directions and at different times (Fig. 7). In
402 addition, MEKK1 action brings in a further layer of complexity. Co-expression of MEKK1 led to a
403 reversal of WRKY18 action on *WRKY53* expression, since a 35S:*MEKK1* construct as co-effector to
404 35S:*WRKY18* reversed the repressor function of WRKY18 on the *WRKY53* promoter to an activator
405 (Fig. S4A). In contrast, the activator function of WRKY25 on the expression of the *WRKY53* promoter
406 is enhanced approx. 2-fold by the addition of 35S:*MEKK1* as co-effector construct (Fig. 3). Whether
407 this is due to a direct phosphorylation of WRKY25 by MEKK1, taking the same short cut as already
408 shown for WRKY53 (Miao et al., 2007), or through classical MAPK signal transduction will be subject
409 of further investigations. Noteworthy, WRKY25 and WRKY33 interact with many VQ proteins
410 (Cheng et al., 2012), one of which is MKS1 (MAP KINASE SUBSTRATE 1), a substrate of MPK4
411 (Andreasson et al., 2005). For WRKY33 it was shown that it exists in nuclear complexes with MPK4
412 and MKS1. Upon activation of MPK4 via MEKK1 and MKK1/2 signaling, MKS1 is phosphorylated
413 by MPK4 and WRKY33 is released from MPK4 interaction and activates its downstream genes such
414 as *PAD3* encoding an enzyme required for antimicrobial camalexin production (Qiu et al., 2008).
415 Moreover, WRKY25 negatively regulates SA-mediated defense responses against *Pseudomonas*
416 *syringae* (Zheng et al., 2007) and MPK4 is a repressor of SA-dependent defense responses (Petersen
417 et al., 2000). Furthermore, MEKK1 kinase activity and protein stability is regulated by H₂O₂ in a
418 proteasome-dependent manner and *mekk1* heterozygous mutants were compromised in ROS-induced
419 MPK4 activation. Like WRKY25, MEKK1 regulates accumulation of intracellular H₂O₂ and alters
420 expression of genes related to ROS signaling and homeostasis such as *ZAT12* (Nakagami et al., 2006).
421 Like *WRKY25* and *WRKY53*, *MEKK1* expression is up-regulated by H₂O₂ treatment and mRNA levels
422 start to increase with onset of senescence in parallel to *WRKY53* (Miao et al., 2007). Therefore, the

423 influence of MEKK1 on the transactivation activity of WRKY25 provides another link to redox
424 signaling. Moreover, we could show by conditional knockdown of *MEKK1* in plants that MEKK1 is
425 part of the complex senescence regulation (Fig. S4).

426 Expression of *WRKY25* is not only induced by oxidative stress but also during heat or salt stress.
427 Moreover, *WRKY25* overexpressing plants were not only more tolerant to oxidative stress (Fig. 6) but
428 also to salt stress (Jiang and Deyholos, 2009) as well as to high temperatures (Li et al., 2011). During
429 heat stress, *WRKY25*, *WRKY26*, and *WRKY33* were positively cross-regulated, which confirms the
430 complexity of the WRKY network (Li et al., 2011). Remarkably, ROS levels increase during salt and
431 heat stress pointing to the possibility that *WRKY25* induction under salt and heat stress is mediated by
432 oxidizing conditions. Many WRKY factors including *WRKY25* and *WRKY53* are up-regulated more
433 than 5-fold in various plant lines with altered intracellular levels of specific ROS (Gadjev et al., 2006).
434 In the same line of evidence, expression of *WRKY18*, *WRKY25* and *WRKY53* was also increased in
435 *cat1,2,3* triple mutant plants (Su et al., 2018). Moreover, not only *WRKY25* gene expression and its
436 DNA-binding activity are altered by higher ROS levels but *WRKY25* is also involved in the regulation
437 of the intracellular H₂O₂ content, especially in later stages of development (Fig. 6) creating a feedback
438 loop.

439 A further level of complexity is installed by epigenetic control of the WRKY gene expression. JMJ27,
440 a jumonji-family demethylases, removes repressive H3K9me2 and H3K9me1 marks and thereby
441 activates transcription. ChIP analysis revealed that the chromatin at the *WRKY25* promoter was hyper-
442 methylated in *jmj27* mutants indicating that JMJ27 regulates *WRKY25* expression at least in part by
443 directly controlling methylation levels of H3K9 histones (Dutta et al., 2017). *WRKY53* expression is
444 also regulated by epigenetic changes in histone methylation (Ay et al., 2009). Moreover, the *WRKY53*
445 protein was detected in a complex with histone deacetylase 9 (HDA9) and POWERDRESS to recruit
446 this complex to W-box containing promoter regions of key negative senescence regulators to remove
447 H3 acetylation marks (Chen et al., 2016). Therefore, *WRKY53* expression is regulated by epigenetic
448 changes on its own promoter but the *WRKY53* protein is also involved in changing epigenetic marks
449 on other promoters.

450 We have summarized our data in a model, which describes a small subnetwork between *WRKY18*,
451 *WRKY25* and *WRKY53* and the role of H₂O₂ in this subnetwork (Fig. 9). Several feedback loops are
452 installed to control an overshooting of the system and to supply a high plasticity, which is needed to
453 constantly integrate all kinds of incoming intracellular and environmental signals. The complex
454 interactions within this subnetwork of just three WRKY factors illustrates the high complexity of the
455 whole WRKY network, which is not only regulated by H₂O₂ as signaling molecule but also highly
456 controlled by salicylic and jasmonic acid. Moreover, the WRKY network is just a subsection of the
457 higher order regulatory network of leaf senescence. Nevertheless, understanding the regulation of
458 single components or subnetworks will in the long run help to decipher the different mechanisms acting
459 in the whole network and contribute to modeling approaches.

460

461 4 Materials and Methods

462 4.1. Protein expression and extraction for DPI-ELISA

463 For protein expression of *WRKY25* and *WRKY53* in the *E. coli* strain BL21-SI, the coding sequences
464 of *WRKY25* (1182 bp) and *WRKY53* (975 bp) were cloned into the vector pETG-10A to be coupled
465 with an N-terminal fused 6xHis-tag. The *E. coli* cells were grown in 10 ml selective medium overnight.
466 100 ml LB-medium were inoculated with 3 ml of this pre-culture and, after shaking for 1.5 h at 37°C,
467 a final concentration of 1 mM IPTG was added for induction of protein expression. After 1 h of shaking
468 at 18°C, cells were harvested (2500 g, 20 min, 4°C) and suspended in protein extraction buffer (4 mM

WRKY25, a redox-dependent senescence regulator

469 Hepes pH 7.5, 100 mM KCl, 8% (v/v) glycerol, 1x complete proteinase inhibitor (*Roche*) without
470 EDTA). Proteins were extracted by sonication to keep native conditions. The protein concentrations of
471 the crude extracts were detected by Bradford assays (*Bio-Rad*).

472

473 4.2. DPI-ELISA

474 The ELISA-based DNA-protein interaction assay was performed as described by Potschin et al. (2014).
475 In brief, the 5' biotinylated double-stranded oligonucleotides were added to streptavidin-coated ELISA
476 plates (*Thermo Scientific*). After blocking the plate with blocking solution (*Roche*), crude extracts were
477 diluted with protein dilution buffer (4 mM Hepes pH 7.5, 100 mM KCl, 8% (v/v) glycerol) and
478 increasing protein concentrations (5, 10, 25 µg) were added to the DNA bound to the plates. The plates
479 were incubated 1 h with mild shaking so that the biotinylated DNA-protein complexes were formed.
480 Subsequently, wells were washed at least twice (*Qiagen wash buffer*) and incubated for another hour
481 with Anti His-HRP conjugate antibodies (*Qiagen*) diluted 1:1500. After washing several times,
482 positive interactions were detected by a peroxidase reaction with ortho-phenylenediamine (OPD-
483 tablets, *Thermo Scientific*). The yellow color was measured using a plate-reader (*TECAN*, Safire
484 XFluor4). For Redox-DPI-ELISAs, 25 µg of the protein crude extracts were used. Reduction or
485 oxidation of the protein extracts was performed by adding either DTT or H₂O₂ (final concentration 5
486 mM). In order to show reversibility of the redox effects, a fraction of the DTT-reduced proteins was
487 oxidized again by addition of increasing amounts of H₂O₂ (final concentration 5, 10 and 20 mM).
488 Similarly, the oxidized proteins were reduced again by adding increasing amounts of DTT. After these
489 redox-treatments, a DPI ELISA was performed as described above. To conserve the redox-state of the
490 proteins bound to the biotinylated DNA, the same DTT or H₂O₂ concentrations were added to the
491 washing buffer and the antibody solution. The antibody reaction was not altered by these treatments.

492

493 4.3. Protoplast transformation

494 Protoplasts derived from a cell culture of *Arabidopsis thaliana* var. Columbia 0 were transiently
495 transformed with different concentrations of the respective plasmid DNA following the protocol
496 published in Mehlhorn et al. (2018). For details, see the protocol on [http://www.zmbp.uni-
497 tuebingen.de/c-facilit/plant-transformation.html](http://www.zmbp.uni-tuebingen.de/c-facilit/plant-transformation.html). Protoplasts were used for GUS reporter assays and
498 BiFCs.

499

500 4.4. GUS reporter assay

501 *Arabidopsis* protoplasts were transformed using 5 µg of effector and 5 µg of reporter plasmid DNA.
502 As an internal transformation control, a luciferase construct (pBT8-35SLUCm3) was co-transfected.
503 After incubation overnight in the dark, GUS activity assays were performed with the protoplast as
504 described by Jefferson et al. (1987). To correct for transformation efficiency, GUS activity was
505 normalized to luciferase fluorescence. As effector constructs, the coding sequences of *WRKY25* (1182
506 bp), *WRKY53* (975 bp) and *MEKK1* (1827 bp) cloned into the vector pJAN33 were used. As reporter
507 construct, a 3000-bp-fragment upstream of the *WRKY25* start codon and a 2759-bp-sequence upstream
508 of the start codon of *WRKY53* was cloned into the binary vector pBGWFS7.0. The 3'-AT (3-Amino-
509 1,2,4-triazole) GUS assays were performed as described above except that 10 mM 3'-AT or the same
510 volume of water was added before overnight incubation.

511

512 4.5. Plant material and cultivation

513 All experiments were performed with *Arabidopsis thaliana* Ecotype Columbia 0 (Col-0). Plants were
514 grown on standard soil under long day conditions (16 h of light) with only moderate light intensity (60-
515 100 µmol s⁻¹ m⁻²) in a climatic chamber at 20°C (day) and 18°C (night). Bolts and flowers developed
516 within approx. 4-5 weeks. Individual leaf positions within the rosettes were coded with different
517 colored threads, so that individual leaves could be analyzed according to their age even at very late

WRKY25, a redox-dependent senescence regulator

518 stages of development (Hinderhofer and Zentgraf, 2001; Bresson et al., 2018). Plant material was
519 harvested always at the same time to avoid circadian effects. The Nottingham Arabidopsis Stock Centre
520 (NASC) kindly provided the T-DNA insertion line of *WRKY25* (SAIL_529_B11), of *WRKY53*
521 (SALK_034157), and *CAT2* (SALK_057998). Using PCR, homozygous plants were characterized
522 with different combinations of gene specific and T-DNA left border primers. Double-knock-out
523 mutants (*wrky25/wrky53*) were generated by crossing *wrky25* and *wrky53* mutants. F2 progenies were
524 selected for homozygous double-knock-out plants by PCR. Dr. Changle Ma, Shangdong Normal
525 University, China (Su et al., 2018), kindly provided seeds of the homozygous *wrky25/cat2* double-
526 knock-out plants. The *WRKY25* overexpressing plants were transformed by floral dip of Col-0 wildtype
527 plants into *Agrobacterium tumefaciens* cultures in two different attempts. First, a 35S:*WRKY25*
528 construct was transformed leading to plants in which the transgene induced gene silencing (plant line
529 35S:*W25si*; pB7RWG2) and, therefore, was used as a *knockdown* line. Second, a *UBQ10:WRKY25*
530 construct was transformed (plant line UBI:*W25-1* and UBI:*W25-2*; pUBN-GFP-Dest) and
531 overexpression was confirmed by qRT-PCR. For the germination experiments, seeds of different plant
532 lines were sterilized by sodium hypochlorite and plated on ½ MS-plates (1 L: 2.15 g MS micro and
533 macro elements (Duchefa), 15 g sucrose, pH 5.7-5.8, 8 g agar).

534

535 4.6. Senescence phenotyping

536 For the evaluation of leaf senescence phenotypes, rosette leaves were aligned according to the age of
537 the leaves with the help of a color code and a variety of parameters indicating the state of senescence
538 were measured (Bresson et al., 2018). Leaves of six plants per timepoint were analyzed. At position 5
539 and 10, Fv/Fm values were determined using the Imaging-Pulse-Amplitude-Modulation (PAM)
540 method, indicating the activity of the photosystem II (PSII) (Chlorophyll fluorometer Maxi version;
541 ver. 2-46i, Walz GmbH, Effeltrich, Germany). Leaves were photographed according to their age and
542 by an automated colorimetric assay (ACA) pixelwise grouped into four categories: green leaves
543 (green), leaves starting to get yellow (green-yellow), completely yellow leaves (yellow) and brown
544 and/or dead leaves (brown/dead). (ACA; Bresson et al., 2018; <http://www.zmbp.uni-tuebingen.de/gen-genetics/research-groups/zentgraf/resources.html>)

545 In addition, RNA was extracted from leaves No. 6 and 7 and qRT-PCR analyses were performed for
546 the senescence-associated marker genes *ANAC092* (At5g39610) encoding a NAC-domain transcription
547 factor, *CABI* (At1g29930) encoding a subunit of light-harvesting complex II, *SAG12* (At5g45890)
548 encoding a cysteine protease and different WRKY genes (*WRKY53* (At4g23810), *WRKY18*
549 (At4g31800), *WRKY40* (At1g80840)). Expression was normalized to *ACTIN2* (At3g18780).

550

551 552 4.7. Quantitative RT-PCR

553 Total RNA was extracted with the RNeasy Plant Mini Kit (*Qiagen*). Subsequent cDNA synthesis was
554 performed with RevertAid Reverse Transcriptase (*Thermo Scientific*). For the qRT-PCR, KAPA
555 SYBR® Fast Biorad iCycler (*KAPA Biosystems*) master mix was used following the manufacturer's
556 protocol. Expression of analyzed genes was normalized to *ACTIN2*. Relative quantification to *ACTIN2*
557 was calculated with the $\Delta\Delta$ CT-method according to Pfaffl (2001). Primers and Atg numbers are
558 indicated in Table S1.

559

560 4.8. H₂O₂ measurement and treatments

561 For oxidative stress treatment during germination, 10 mM H₂O₂ was added to the 1/2 MS agar (1 L:
562 2.15 g MS micro and macro elements (*Duchefa*), 15 g sucrose, pH 5.7-5.8, 8 g agar) and seeds were
563 spread on plates with and without H₂O₂. After 3 days in darkness, the plates were incubated in light in
564 the climate chambers and the number of green seedlings was counted after 7-10 days. This experiment
565 was repeated 6 times, plates were photographed, green seedlings counted and summarized according
566 to their tolerance against H₂O₂ in a heat map.

WRKY25, a redox-dependent senescence regulator

567 For intracellular H₂O₂ measurement, carboxy-H₂DCFDA (2',7'-Dichlorodihydrofluorescein-diacetat)
568 was chosen, which is able to passively diffuse across cellular membranes as non-polar dye. After
569 deacetylation by an intracellular esterase, the molecule gets polar and is trapped inside the cells. The
570 deacetylated carboxy-H₂DCFDA can then be oxidized by H₂O₂ and converted to the highly fluorescent
571 di-chlorofluorescein (DCF). Therefore, only intracellular H₂O₂ is measured. Leaves of position 8 of 4-
572 to 8-week-old plants were harvested and incubated for exactly 45 min in carboxy-H₂DCFDA working-
573 solution (200 µg in 40 mL MS-Medium pH 5.7–5.8). Subsequently, the leaves were rinsed with water
574 and frozen in liquid nitrogen. After homogenization in 500 µL 40 mM Tris pH 7.0, the samples were
575 centrifuged at 4°C for 15 min. Fluorescence of the supernatant was measured in a *Berthold* TriStar
576 LB941 plate reader (480 nm excitation, 525 nm emission).

577 For testing the response to H₂O₂ treatment, leaves of position 8 of 5, 6 and 7-week-old plants were
578 incubated for 0, 30 min, 1 h and 3 h in 10 mM H₂O₂ including 0.1% Tween. After incubation time,
579 leaves were washed in water and immediately frozen in liquid nitrogen. Gene expression was
580 determined by qRT-PCR.

581 The decomposition of H₂O₂ was examined using commercially available peroxide strips (Dosatest
582 peroxide test strips 100, VWR Chemicals). Therefore, leaf discs were excised of leaves of position 5
583 of 6- and 7-week-old plants and were incubated into a 30mg/l H₂O₂ solution. Strips were submerged
584 for 1 sec into the solution immediately after placing the leaf disc into the solution (timepoint 0 min)
585 and again after 2 h. The amount of peroxide can be read out by the given control color scale. The
586 weaker the blue color the less peroxide is present in the solution.

587

588 **4.9. Bimolecular Fluorescence Complementation (BiFC), cytometry and confocal microscopy**

589 Ratiometric BiFC assays were conducted to study the homo- and heteromeric interaction of WRKY25
590 and WRKY53. Therefore, a single vector was used that holds an internal red fluorescent (RFP) marker
591 gene for expression control and both candidate genes cloned simultaneously to N- or C-terminal parts
592 of the yellow fluorescent protein (YFP), respectively, allowing expression of fusion proteins under the
593 control of a 35S promoter (pBiFCt-2in-NN; Grefen and Blatt, 2012). For protoplast transfection, 2 µg
594 of the plasmid DNA was used to express the fusion proteins. YFP fluorescence is restored if the
595 proteins interact with each other bringing the YFP-N and YFP-C parts together. Interactions were
596 visualized 1 day after transfection by confocal microscopy (Leica SP8) by excitation at 488 nm and
597 measuring fluorescence emitted at 594 nm.) Fluorescence was quantified by flow cytometry using a
598 CytoFLEX (*Beckman Coulter*). Both the internal mRFP1 and any reconstituted YFP were excited by
599 the on board 488nm laser. Peak emission was captured for YFP in FL1 (525/40 nm) and for RFP in
600 FL3 (610/20 nm). After compensation, the Fluorescence Index (FI) was calculated based on the mean
601 fluorescence intensity multiplied by the fraction of fluorescent cells (Li et al., 2010). The results were
602 calculated from 6 independent experiments and normalized using quantile normalization.

603 **5 Conflict of Interest**

604 The authors declare that the research was conducted in the absence of any commercial or financial
605 relationships that could be construed as a potential conflict of interest.

606 **6 Author Contributions**

607 Conceptualization was done by U.Z., M.M. and J.D.; Methodology was developed by M.M., K.B. and
608 J.D.; Experiments very performed by J.D., M.M., L.R., K.B., and J.B.; Data and Formal analysis was
609 done by J.D., J.B., L.R. and K.B., The original draft was written by U.Z.; Reviewing and Editing was
610 done by J.D., L.R., K.B., M.M, J.B., and U.Z; Funding Acquisition: U.Z.; Supervision: U.Z.

611 **7 Funding**

612 This work was financially supported by the Deutsche Forschungsgemeinschaft (DFG), Collaborative
613 Research Centre 1101 (SFB1101, TP B06). The Alexander v. Humboldt Foundation supported JB.

614 **8 Acknowledgments**

615 We are grateful for the excellent technical assistance of Gesine Seibold. We thank the NASC for
616 supplying seeds of the *WRKY25* (SAIL_529_B11) and *WRKY53* (SALK_034157) T-DNA insertion
617 lines and Dr. Ma, Shandong Normal University, China for seeds of the homozygous *wrky25/cat2*
618 double mutant. We also thank Christopher Grefen, ZMBP for providing different the cloning vectors
619 pUBN-GFP-Dest and pBiFCt-2in1-NN.
620
621

622 **9 References**

- 623 **Andreasson, E., Jenkins, T., Brodersen, P., Thorgrimsen, S., Petersen, N.H., Zhu, S., Qiu, J.L.,**
624 **Micheelsen, P., Rocher, A., Petersen, M. et al.** (2005). The MAP kinase substrate MKS1 is a
625 regulator of plant defense responses. *EMBO J.* **24**: 2579-2589.
- 626 **Arrigo, A.P.** (1999). Gene expression and the thiol redox state. *Free Radical Biol. & Med.* **27**: 936–
627 944.
- 628 **Ay, N., Irmeler, K., Fischer, A., Uhlemann, R., Reuter, G., and Humbeck, K.** (2009). Epigenetic
629 programming via histone methylation at *WRKY53* controls leaf senescence in *Arabidopsis*
630 *thaliana*. *Plant J.* **58**: 333-346.
- 631 **Balazadeh, S., Kwasniewski, M., Caldana, C., Mehrnia, M., Zanon, M.I., Xue, G.P., and**
632 **Mueller-Roeber, B.** (2011). ORS1, an H₂O₂-responsive NAC transcription factor, controls
633 senescence in *Arabidopsis thaliana*. *Mol. Plant* **4**: 346-360.
- 634 **Balazadeh, S., Siddiqui, H., Allu, A.D., Matallana-Ramirez, L.P., Caldana, C., Mehrnia, M.,**
635 **Zanon, M.I., Köhler, B., and Mueller-Roeber, B.** (2010). A gene regulatory network controlled
636 by the NAC transcription factor ANAC092/AtNAC2/ORE1 during salt-promoted senescence.
637 *Plant J.* **62**: 250-264.
- 638 **Besseau, S., Li, J., and Palva, E.T.** (2012). WRKY54 and WRKY70 co-operate as negative
639 regulators of leaf senescence in *Arabidopsis thaliana*. *J. Exp. Bot.* **63**: 2667-2679.
- 640 **Bieker, S., Riester, L., Stahl, M., Franzaring, J., and Zentgraf, U.** (2012). Senescence-specific
641 alteration of hydrogen peroxide levels in *Arabidopsis thaliana* and oilseed rape spring variety
642 *Brassica napus* L. cv. Mozart. *J. Integr. Plant Biol.* **54**: 540-554.
- 643 **Birkenbihl, R.P., Liu, S., and Somssich, I.E.** (2017). Transcriptional events defining plant immune
644 responses. *Curr. Opin. Plant Biol.* **38**: 1-9.
- 645 **Brand, L.H., Fischer, N.M., Harter, K., Kohlbacher, O., and Wanke, D.** (2013). Elucidating the
646 evolutionary conserved DNA-binding specificities of WRKY transcription factors by molecular
647 dynamics and in vitro binding assays. *Nucleic Acids Res* **41**: 9764–9778.
- 648 **Breeze, E., Harrison, E., McHattie, S., Hughes, L., Hickman, R., Hill, C., Kiddle, S., Kim, Y.S.,**
649 **Penfold, C.A., Jenkins, D., et al.** (2011). High-resolution temporal profiling of transcripts during
650 *Arabidopsis* leaf senescence reveals a distinct chronology of processes and regulation. *Plant Cell*
651 **23** :873-894.
- 652 **Bresson, J., Bieker, S., Riester, L., Doll, J., and Zentgraf, U.** (2018). A guideline for leaf
653 senescence analyses: from quantification to physiological and molecular investigations. *J. Exp.*
654 *Bot.* **69**: 769-786.

WRKY25, a redox-dependent senescence regulator

- 655 **Brusslan, J.A., Rus Alvarez-Canterbury, A.M., Nair, N.U., Rice, J.C., Hitchler, M.J., and**
656 **Pellegrini, M.** (2012). Genome-wide evaluation of histone methylation changes associated with
657 leaf senescence in *Arabidopsis*. *PLoS ONE* **7**: e33151.
- 658 **Chen, X., Lu, L., Mayer, K.S., Scalf, M., Qian, S., Lomax, A., Smith, L.M., and Zhong, X.**
659 (2016). POWERDRESS interacts with HISTONE DEACETYLASE 9 to promote aging in
660 *Arabidopsis*. *ELife* **5**: e17214.
- 661 **Cheng, Y., Zhou, Y., Yang, Y., Chi, Y.J., Zhou, J., Chen, J.Y., Wang, F., Fan, B., Shi, K., Zhou,**
662 **Y.H., et al.** (2012). Structural and functional analysis of VQ motif-containing proteins in
663 *Arabidopsis* as interacting proteins of WRKY transcription factors. *Plant Physiol.* **159**: 810-825.
- 664 **Chi, Y., Yang, Y., Zhou, Y., Zhou, J., Fan, B., Yu, J.Q., and Chen, Z.** (2013). Protein-Protein
665 Interactions in the Regulation of WRKY Transcription Factors. *Mol. Plant* **6**: 287-300.
- 666 **Dong, J., Chen, C., and Chen, Z.** (2003). Expression profiles of the *Arabidopsis* WRKY gene
667 superfamily during plant defense response. *Plant Mol. Biol.* **51**: 21-37.
- 668 **Dutta, A., Choudhary, P., Caruana, J., Raina, R.** (2017). JM27, an *Arabidopsis* H3K9 histone
669 demethylase, modulates defense against *Pseudomonas syringae* and flowering time. *Plant J.* **91**:
670 1015-1028.
- 671 **Eulgem, T., Rushton, P.J., Robatzek, S., and Somssich, I.E.** (2000). The WRKY superfamily of
672 plant transcription factors. *Trends Plant Sci.* **5**: 199-206.
- 673 **Gadjev, I., Vanderauwera, S., Gechev, T.S., Laloi, C., Minkov, I.N., Shulaev, V., Apel, K., Inzé,**
674 **D., Mittler, R., and Van Breusegem, F.** (2006) Transcriptomic footprints disclose specificity of
675 reactive oxygen species signaling in *Arabidopsis*. *Plant Physiol.* **141**: 436-445.
- 676 **Giesguth, M., Sahn, A., Simon, S., and Dietz, K.J.** (2015). Redox-dependent translocation of the
677 heat shock transcription factor AtHSFA8 from the cytosol to the nucleus in *Arabidopsis thaliana*.
678 *FEBS Lett.* **589**: 718-725.
- 679 **Grefen, C., and Blatt, M.R.** (2012). A 2in1 cloning system enables ratiometric bimolecular
680 fluorescence complementation (rBiFC). *Biotechniques* **53**: 311-314.
- 681 **Gregersen, P.L., Culetic, A., Boschian, L., and Krupinska, K.** (2013). Plant senescence and crop
682 productivity. *Plant Mol. Biol.* **82**: 603-622.
- 683 **Guo, Y., Cai, Z., and Gan, S.** (2004). Transcriptome of *Arabidopsis* leaf senescence. *Plant Cell &*
684 *Environ.* **27**: 521-549.
- 685 **He, H., Van Breusegem, F., and Mhamdi, A.** (2018) Redox-dependent control of nuclear
686 transcription in plants. *J Exp. Bot.* **69**:3359-3372.
- 687 **Hinderhofer, K., and Zentgraf, U.** (2001). Identification of a transcription factor specifically
688 expressed at the onset of leaf senescence. *Planta* **213**: 469-473.
- 689 **Jefferson, R.A., Kavanagh, T.A., and Bevan, M.W.** (1987) GUS fusions: β -glucuronidase as a
690 sensitive and versatile gene fusion marker in higher plants. *EMBO J.* **6**:3901-3907
- 691 **Jiang, J., Ma, S., Ye, N., Jiang, M., Cao, J., and Zhang, J.** (2017). WRKY transcription factors in
692 plant responses to stresses. *J. Integr. Plant Biol.* **59**: 86-101.
- 693 **Jiang, Y., and Deyholos, M.K.** (2009). Functional characterization of *Arabidopsis* NaCl-inducible
694 WRKY25 and WRKY33 transcription factors in abiotic stresses. *Plant Mol. Biol.* **69**: 91-105.
- 695 **Kim, J., Kim, J.H., Lyu, J.I., Woo, H.R., and Lim, P.O.** (2017). New insights into the regulation
696 of leaf senescence in *Arabidopsis*. *J. Exp. Bot.* **69**: 787-799.
- 697 **Li, J.F., Chung, H.S., Niu, Y., Bush, J., McCormack, M., and Sheen J.** (2013). Comprehensive
698 protein-based artificial microRNA screens for effective gene silencing in plants. *Plant Cell* **2**:
699 1507-1522.
- 700 **Li, M., Doll, J., Weckermann, K., Oecking, C., Berendzen, K.W., and Schöffl, F.** (2010).
701 Detection of in vivo interactions between *Arabidopsis* class A-HSFs, using a novel BiFC
702 fragment, and identification of novel class B-HSF interacting proteins. *Eur. J. Cell Biol.* **89**: 126-
703 132.

WRKY25, a redox-dependent senescence regulator

- 704 **Li, S., Fu, Q., Chen, L., Huang, W., and Yu, D.** (2011). *Arabidopsis thaliana* WRKY25,
705 WRKY26, and WRKY33 coordinate induction of plant thermotolerance. *Planta* **233**: 1237-1252.
- 706 **Llorca, M.C., Potschin, M., and Zentgraf, U.** (2014). bZIPs and WRKYs: two large transcription
707 factor families executing two different functional strategies. *Front. Plant Sci.* **5**: 169.
- 708 **Mehlhorn, D.G., Wallmeroth N., Berendzen, K.W., and Grefen, C.** (2018). 2in1 vectors improve
709 *in planta* BiFC and FRET analyses. In: Hawes, C., Kriechbaumer, V. (eds) *The Plant Endoplasmic*
710 *Reticulum. Methods in Molecular Biology*, Vol 1691. Humana Press, New York, NY.
- 711 **Miao, Y., and Zentgraf, U.** (2007). The antagonist function of *Arabidopsis* WRKY53 and ESR/ESP
712 in leaf senescence is modulated by the jasmonic and salicylic acid equilibrium. *Plant Cell* **19**: 819-
713 830.
- 714 **Miao, Y., and Zentgraf, U.** (2010). A HECT E3 ubiquitin ligase negatively regulates *Arabidopsis*
715 leaf senescence through degradation of the transcription factor WRKY53. *Plant J.* **63**: 179-188.
- 716 **Miao, Y., Laun, T., Zimmermann, P., and Zentgraf, U.** (2004). Targets of the WRKY53
717 transcription factor and its role during leaf senescence in *Arabidopsis*. *Plant Mol. Biol.* **55**: 853-
718 867.
- 719 **Miao, Y., Laun, T.M., Smykowski, A., and Zentgraf, U.** (2007). *Arabidopsis* MEKK1 can take a
720 short cut: it can directly interact with senescence-related WRKY53 transcription factor on the
721 protein level and can bind to its promoter. *Plant Mol. Biol.* **65**: 63-76.
- 722 **Miao, Y., Smykowski, A., and Zentgraf, U.** (2008). A novel upstream regulator of WRKY53
723 transcription during leaf senescence in *Arabidopsis thaliana*. *Plant Biol.* **10** Suppl. 1: 110-120.
- 724 **Nakagami, H., Soukupová, H., Schikora, A., Zárský, V., and Hirt, H.** (2006). A Mitogen-
725 activated protein kinase kinase kinase mediates reactive oxygen species homeostasis in
726 *Arabidopsis*. *J. Biol. Chem.* **281**: 38697-38704.
- 727 **Petersen, M., Brodersen, P., Naested, H., Andreasson, E., Lindhart, U., Johansen, B., Nielsen,
728 H.B., Lacy, M., Austin, M.J., Parker, J.E., et al.** (2000). *Arabidopsis* map kinase 4 negatively
729 regulates systemic acquired resistance. *Cell* **103**:1111–1120.
- 730 **Pfaffl, M.W.** (2001). A new mathematical model for relative quantification in real-time RT-PCR.
731 *Nucl. Acids Res.* **29**: e45.
- 732 **Potschin, M., Schlienger, S., Bieker, S., and Zentgraf, U.** (2014). Senescence Networking:
733 WRKY18 is an upstream regulator, a downstream target gene, and a protein interaction partner of
734 WRKY53. *J. Plant Growth Reg.* **33**:106-118.
- 735 **Qiu, J.L., Fiil, B.K., Petersen, K., Nielsen, H.B., Botanga, C.J., Thorgrimsen, S., Palma, K.,
736 Suarez-Rodriguez, M.C., Sandbech-Clausen, S., Lichota, J., et al.** (2008). *Arabidopsis* MAP
737 kinase 4 regulates gene expression through transcription factor release in the nucleus. *EMBO J.*
738 **27**: 2214-2221.
- 739 **Ren, Y., Li, Y., Jiang, Y., Wu, B., and Miao, Y.** (2017). Phosphorylation of WHIRLY1 by CIPK14
740 Shifts Its Localization and Dual Functions in *Arabidopsis*. *Mol. Plant* **10**:749-763.
- 741 **Rushton, P.J., Somssich, I.E., Ringler, P., and Shen Q.J.** (2010). WRKY transcription factors.
742 *Trends Plant Sci.* **15**: 247-258.
- 743 **Shaikhali, J.** (2015). GIP1 protein is a novel cofactor that regulates DNA-binding affinity of redox-
744 regulated members of bZIP transcription factors involved in the early stages of *Arabidopsis*
745 development. *Protoplasma* **252**: 867-883.
- 746 **Shaikhali, J., Norén, L., de Dios Barajas-López, J., Srivastava, V., König, J., Sauer, U.H.,
747 Wingsle, G., Dietz, K.J., and Strand, Å.** (2012). Redox-mediated mechanisms regulate DNA
748 binding activity of the G-group of basic region leucine zipper (bZIP) transcription factors in
749 *Arabidopsis*. *J. Biol. Chem.* **287**: 27510-25.
- 750 **Su, T., Wang, P., Li, H., Zhao, Y., Lu, Y., Dai, P., Ren, T., Wang, X., Li, X., Shao, Q., Zhao, D.,
751 Zhao, Y., Ma, C.** (2018). The *Arabidopsis* catalase triple mutant reveals important roles of

WRKY25, a redox-dependent senescence regulator

- 752 catalases and peroxisome-derived signaling in plant development. *J. Integr. Plant Biol.* **60**: 591-
753 607.
- 754 **Uauy, C., Distelfeld, A., Fahima, T., Blechl, A., and Dubcovsky, J.** (2006). A NAC Gene
755 regulating senescence improves grain protein, zinc, and iron content in wheat. *Science* **314**:1298-
756 1301.
- 757 **Ülker, B., Shahid Mukhtar, M., and Somssich, I.E.** (2007). The WRKY70 transcription factor of
758 *Arabidopsis* influences both the plant senescence and defense signaling pathways. *Planta* **226**:125-
759 137.
- 760 **Viola, I.L., Güttlein, L.N., and Gonzalez, D.H.** (2013). Redox modulation of plant developmental
761 regulators from the class I TCP transcription factor family. *Plant Physiol.* **162**:1434-1447.
- 762 **Wu, A., Allu, A.D., Garapati, P., Siddiqui, H., Dortay, H., Zanol, M.I., Asensi-Fabado, M.A.,
763 Munné-Bosch, S., Antonio, C., Tohge, T., et al.** (2012). JUNGBRUNNEN1, a reactive oxygen
764 species-responsive NAC transcription factor, regulates longevity in *Arabidopsis*. *Plant Cell*
765 **24**:482-506.
- 766 **Xie, Y., Huhn, K., Brandt, R., Potschin, M., Bieker, S., Straub, D., Doll J., Drechsler, T.,
767 Zentgraf, U., and Wenkel, S.** (2014). REVOLUTA and WRKY53 connect early and late leaf
768 development in *Arabidopsis*. *Development* **141**:4772-4783.
- 769 **Xu, X., Chen, C., Fan, B., and Chen, Z.** (2006). Physical and functional interactions between
770 pathogen-induced *Arabidopsis* WRKY18, WRKY40, and WRKY60 transcription factors. *Plant*
771 *Cell* **18**:1310-26.
- 772 **Yang, S.D., Seo, P.J., Yoon, H.K., and Park, C.M.** (2011). The *Arabidopsis* NAC transcription
773 factor VNI2 integrates abscisic acid signals into leaf senescence via the COR/RD genes. *Plant Cell*
774 **23**:2155-2168.
- 775 **Zentgraf, U., Laun, T., and Miao, Y.** (2010). The complex regulation of WRKY53 during leaf
776 senescence of *Arabidopsis thaliana*. *Eur. J. Cell Biol.* **89**:133-137.
- 777 **Zheng, Z., Mosher, S.L., Fan, B., Klessig, D.F., and Chen, Z.** (2007). Functional analysis of
778 *Arabidopsis* WRKY25 transcription factor in plant defense against *Pseudomonas syringae*. *BMC*
779 *Plant Biol.* **7**:2.
- 780 **Zimmermann, P., Heinlein, C., Orendi, G. and Zentgraf, U.** (2006). Senescence specific
781 regulation of catalases in *Arabidopsis thaliana* (L.) Heynh. *Plant, Cell & Environ.* **29**:1049-1060.

782

783 **10 Supplementary Material**

784 **10.1 Figures:**

785 **S1:** WRKY protein expression in *E. coli*

786 **S2:** Redox-DPI-ELISA with WRKY18 and WRKY53 protein

787 **S3:** 3'-AT treatment of protoplasts provokes an oxidative cell status

788 **S4:** Role of MEKK1 in WRKY18 driven *WRKY53* expression and senescence

789 **S5:** *WRKY25* expression analysis for lines with altered *WRKY25* expression

790 **S6:** Comparison of plant development

791 **S7:** Chlorophyll fluorescence imaging

792 **S8:** Dark-induced senescence and antioxidative capacity of *wrky25*, *cat2* and *wrky25/cat2*

793 **S9:** Yeast-Two-Hybrid interaction assay

794

795

796 **10.2 Tables:**

797 **S1:** Oligonucleotides for qRT-PCR

798

799 **10.3 Methods related to supplemental Figures:**

800 **SM1:** Dark-induced senescence phenotyping

801 **SM2:** Cell-free GUS reaction

802 **SM3:** H₂O₂ content in Arabidopsis protoplasts

803 **SM4:** Catalase zymograms

804 **SM5:** Yeast-Two-Hybrid Interaction Assay

805

806 **11 Figure Legends**

807 **Figure 1: WRKY25 is able to bind directly to the WRKY53 promoter.**

808 (A) Schematic drawing of positions and sequences of the W-boxes in the *WRKY53* and *WRKY25*
809 promoters used for DPI-ELISAs; perfect W-box motifs are highlighted in red; the TGAC core
810 sequence is indicated in bold and underlined; the direction of the motif is indicated by the arrows. An
811 artificial sequence containing three perfect W-boxes was used as a positive control (Art. W-box), a
812 G-box of the *CATALASE2* promoter was used as a negative control. (B) DPI-ELISA with different
813 amounts of crude extracts of *E. coli* BL21 cells expressing WRKY25 proteins and different
814 biotinylated DNA fragments. (C) DPI-ELISA with different amounts of crude extracts of *E. coli*
815 BL21 cells expressing WRKY53 proteins and different biotinylated DNA fragments. Absorbance
816 values are indicated relative to values of 25 µg WRKY25 or WRKY53 to W-box2 P_{W53}, respectively,
817 (mean values ±SD, n=3-4). Kruskal-Wallis-test was performed for statistically significant differences
818 of all values compared to 25 µg BL21 control (**P* ≤ 0.05, ***P* ≤ 0.01, ****P* ≤ 0.001).

819

820 **Figure 2: WRKY25 binding to the WRKY53 promoter is redox-dependent.**

821 Redox-DPI-ELISA with 25 µg of crude extracts of *E. coli* BL21 cells expressing WRKY25 proteins
822 and the 5'biotinylated annealed oligonucleotides W-box1 P_{W53} and W-box1 P_{W25}. Protein extracts
823 were reduced or oxidized by addition of either DTT or H₂O₂ to examine a redox-dependent binding
824 of WRKY25. A fraction of the DTT-reduced proteins was re-oxidized by addition of increasing H₂O₂
825 concentrations to prove the reversibility of the redox effect. The same procedure was applied to the
826 H₂O₂-oxidized proteins using increasing amounts of DTT. Absorbance values are indicated relative
827 to control without treatment (mean values ±SD, n = 4). Kruskal-Wallis-test was performed for
828 statistically significant differences of all values compared to control (**P* ≤ 0.05, ***P* ≤ 0.01).

829

830 **Figure 3: WRKY25 positively regulates WRKY53 under non-oxidizing conditions.**

831 (A) Arabidopsis protoplasts were transiently transformed with 5 µg of effector-, 5 µg of reporter-
832 plasmid DNA and 0.1 µg of a luciferase construct for normalization. A 2.8-kbp-fragment of the
833 *WRKY53* promoter and a 3.0-kbp-sequence of the *WRKY25* promoter fused to the *GUS* gene were
834 used as reporter constructs. 35S:*WRKY25* and 35S:*WRKY53* constructs were used as effector
835 plasmids. GUS activity was measured on the next day. The values are presented relative to the empty
836 vector control (mean values ±SD, n = 6). One sample t-test was performed, (**P* ≤ 0.05, ***P* ≤ 0.01,
837 ****P* ≤ 0.001) (B) GUS assays were performed with protoplasts, which were simultaneously
838 incubated overnight with 10 mM 3'-AT to inhibit catalase activities leading to higher H₂O₂ level. The
839 values are presented relative to the untreated control transformations (mean values ±SD, n = 3-7).
840 One sample t-test was performed, (**P* ≤ 0.05, ***P* ≤ 0.01). (C) Co-transformation assays with
841 35S:*MEKK1* were performed. The values are presented relative to transformation without MEKK1
842 (mean values ±SD, n = 4-5). Kruskal-Wallis-test was performed, (**P* ≤ 0.05, ***P* ≤ 0.01).

843

844 **Figure 4: Senescence phenotypes of WRKY25 transgenic and mutant lines.**

WRKY25, a redox-dependent senescence regulator

845 (A) Col-0 wildtype (WT), *wrky25* mutant (*wrky25*), *WRKY25* overexpressing (*UBI:W25-1* and
846 *UBI:W25-2*), *WRKY25* silenced (*35S:W25si*) and *wrky25-wrky53* double-knock-out (*w25/w53*) plants
847 were analyzed over development. A photograph of rosette leaves of 8-week-old plants sorted
848 according to their age is shown. (B) Quantitative evaluation of leaf senescence by categorizing
849 individual leaves of at least six plants into four groups according to their color: green, green leaves
850 starting to get yellow (green-yellow), completely yellow leaves (yellow) and dead and/or brown
851 leaves (brown/dry). The percentage of each group with respect to total leaf numbers are presented
852 (mean values \pm SE, n=6). (C) Fv/Fm values were measured with PAM for leaves of position 5 of 7-
853 week-old plants (mean values \pm SE, n=6). One sample t-test was performed for statistical differences
854 of all values compared to Col-0 ($*P \leq 0.05$) (D) Expression of the senescence associated marker
855 genes *ANAC092*, *CABI*, *SAG12* were analyzed by qRT-PCR and normalized to the expression of the
856 *ACTIN2* gene. *SAG12* in 6-week and *ANAC092* and *CABI* in 7-week-old plants. Shown are *wrky25*
857 and *UBI:W25-1* plants normalized to Col-0 (mean values \pm SE, n=3). Kruskal-Wallis-test was
858 performed for statistically significant differences ($*P \leq 0.05$, $**P \leq 0.01$).

859

860 **Figure 5: WRKY genes expression analyses.**

861 Expression of different WRKY genes (*WRKY53*, *WRKY18*, *WRKY40*) were analyzed in Col-0 (WT),
862 *wrky25* mutant and *WRKY25* overexpression line (*UBI:WRKY25-1*) by qRT-PCR and normalized to
863 the expression of the *ACTIN2* gene. Three pools were analyzed; one pool consists of leaf No. 6 and 7
864 of two different plants. In week 7, only two pools of the *35S:W25si* plant line and of the *wrky25* line
865 were analyzed but here with six technical replicates. Expression values were normalized to Col-0 and
866 Col-0 was set to 1 (mean values, n=3, \pm SE). Kruskal-Wallis-test was performed for statistically
867 significant differences of all value compared to Col-0 ($*P \leq 0.05$, $**P \leq 0.01$, $***P \leq 0.001$).

868

869 **Figure 6: WRKY25 mediates H₂O₂ tolerance.**

870 (A-B) Col-0 (WT), *wrky25* mutant, *WRKY25* overexpressing (*UBI:W25-1*; *UBI:W25-2*) and
871 *WRKY25* silenced (*35S:W25si*) as well as the double-knock-out plants (*w25/w53*) were sown on ½
872 MS plates with and without 10 mM H₂O₂. A minimum of 30 seeds were put onto the plates and the
873 experiment repeated 6 times (n=6) (A) shows a representative sector of the plates with and without
874 H₂O₂ in media. (B) summarizes the 6 independent experiments in a heat map. Dark green means the
875 most tolerant against H₂O₂, dark red the most sensitive towards H₂O₂. (C) H₂O₂ content was
876 measured over plant development using H₂DCFDA fluorescence; leaves No. 8 of 8-week-old plants
877 are shown. Fluorescence is indicated in arbitrary units (a.u.), normalized to leaf weight and expressed
878 relative to WT (\pm SE, n=4). One Sample t-test was performed for statistical differences of all values
879 compared to WT ($*P \leq 0.1$) (D) Leaf discs of leaf No. 5 of 6-week-old plants were incubated in a 30
880 mg/l H₂O₂ solution. As control H₂O₂ solution without leaf discs was measured. At timepoint 0 min
881 and 2 h the decomposition of H₂O₂ was determined using commercially available peroxide sticks,
882 color scale for H₂O₂ content is provided on the right.

883

884 **Figure 7: Influence of oxidizing conditions on gene expression.**

885 Leaves of position 10 were harvested of Col-0 (WT), *wrky25* (orange) and *wrky53* (blue) single and
886 double (purple) mutant plants. Leaves of 5, 6 and 7 week-old-plants were incubated in 10 mM H₂O₂
887 for 0-3 hours. Expression of *WRKY18*, *WRKY25*, *WRKY53*, *ZAT12* and *ANAC092* was determined by
888 qRT-PCR. Expression values normalized to *ACTIN2* expression are presented (mean values \pm SD,
889 n=2, one biological replicate consists already of a pool of 3 plants for each timepoint). Kruskal-
890 Wallis-test was performed for statistically significant differences of all values at each timepoint
891 compared to Col-0 ($*P \leq 0.05$, $**P \leq 0.01$, $***P \leq 0.001$).

892

893 **Figure 8: Protein-protein interaction of WRKY25 and WRKY53.**

WRKY25, a redox-dependent senescence regulator

894 Protoplasts co-transformed with BiFC constructs were used to visualize interaction. YFP-N and YFP-
895 C fusions with the respective WRKYs were transformed into Arabidopsis protoplasts and
896 fluorescence was quantified using a cytometer (CytoFLEX; *Beckman Coulter*). (A) Confocal
897 microscopy images. Combinations of the YFP-N and YFP-C constructs are indicated on the left. YFP
898 fluorescence (left) was overlaid with the bright field images (middle). Additionally, mRFP was used
899 as an internal control (right) to detect transformed cells. Scale bar = 10 μm . (B) Flow cytometry
900 analyses. Fluorescence Indices were calculated by multiplying the mean fluorescence by the fraction
901 of fluorescent cells and finalized with quantile normalization (mean values +SD, n = 6).). Kruskal-
902 Wallis-test was performed for statistical differences of all values compared to RFP control (* $P \leq$
903 0.05, ** $P \leq 0.01$). (C) Representative graphs of the flow cytometry results. Blue dots represent eYFP
904 signals of interaction. Blue squares mark the cells showing eYFP signal.

905

906 **Figure 9: Model of H₂O₂ and the WRKY18-53-25 subnetwork**

907 A model summarizing the impact of H₂O₂ and WRKY25 on senescence is presented. Solid lines
908 show direct interactions whereas dotted lines show interaction, which may be direct or indirect. Black
909 arrows describe the effects on gene expression, red arrows effects on protein activity, and the grey
910 line effects on the intracellular hydrogen peroxide level. The expression of all three WRKY genes of
911 the small WRKY53-25-18 subnetwork are controlled by hydrogen peroxide contents and hydrogen
912 peroxide has a direct negative effect on the binding activity of WRKY25 to DNA. All three genes are
913 under feedback control of their own gene products. In addition, MEKK1 increases the activity of all
914 three WRKY factors. Moreover, WRKY25 can form heterodimers with WRKY53 and the
915 heterodimer has a lower transactivation activity compared to the WRKY25 homodimer. This
916 interplay determines in the end whether leaf senescence is accelerated or delayed.

917

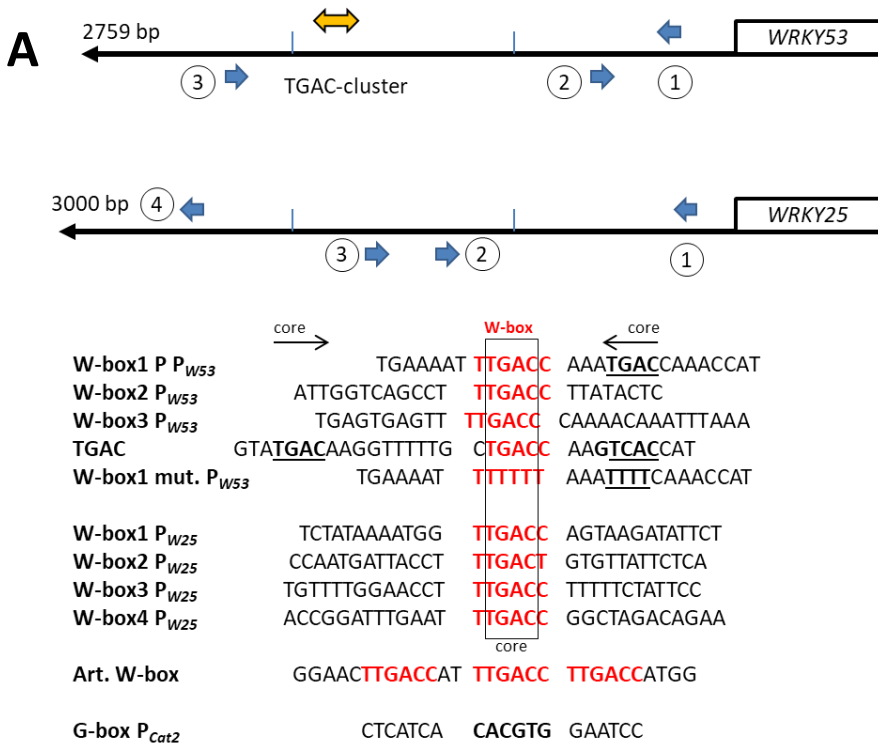
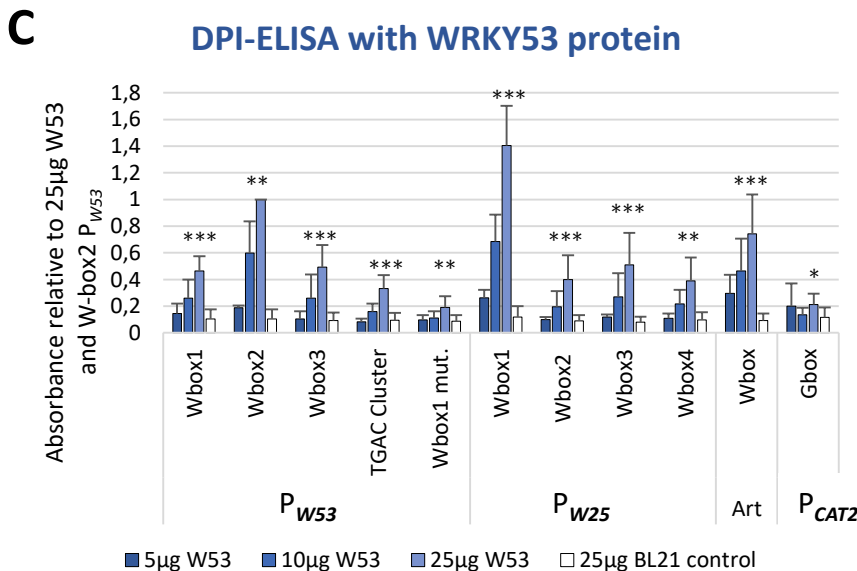
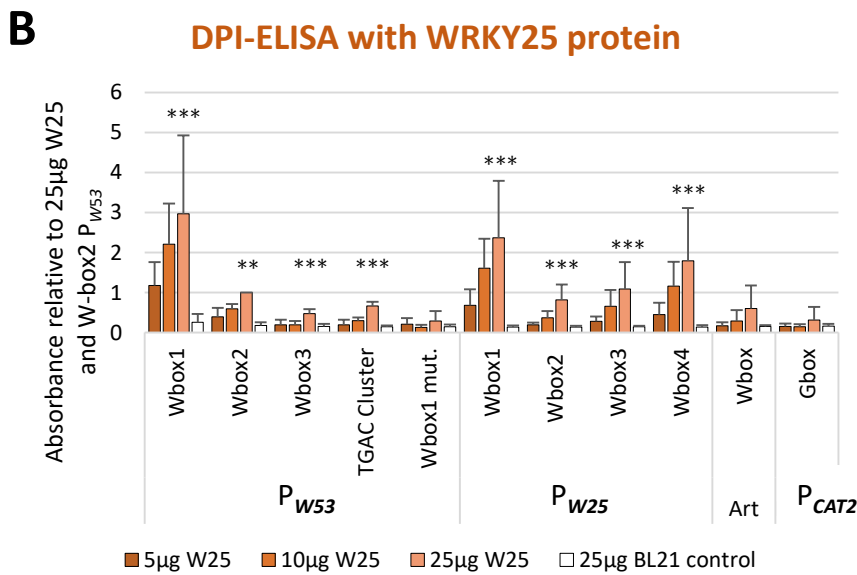


Figure 1: WRKY25 is able to bind directly to the WRKY53 promoter.

(A) Schematic drawing of positions and sequences of the W-boxes in the WRKY53 and WRKY25 promoters used for DPI-ELISAs; perfect W-box motifs are highlighted in red; the TGAC core sequence is indicated in bold and underlined; the direction of the motif is indicated by the arrows. An artificial sequence containing three perfect W-boxes was used as a positive control (Art. W-box), a G-box of the CATALASE2 promoter was used as a negative control. (B) DPI-ELISA with different amounts of crude extracts of *E. coli* BL21 cells expressing WRKY25 proteins and different biotinylated DNA fragments. (C) DPI-ELISA with different amounts of crude extracts of *E. coli* BL21 cells expressing WRKY53 proteins and different biotinylated DNA fragments. Absorbance values are indicated relative to values of 25 μ g WRKY25 or WRKY53 to W-box2 P_{W53}, respectively, (mean values \pm SD, n=3-4). Kruskal-Wallis test was performed for statistically significant differences of all values compared to 25 μ g BL21 control (* $P \leq 0.05$, ** $P \leq 0.01$, *** $P \leq 0.001$).



Redox-DPI-ELISA with WRKY25 protein

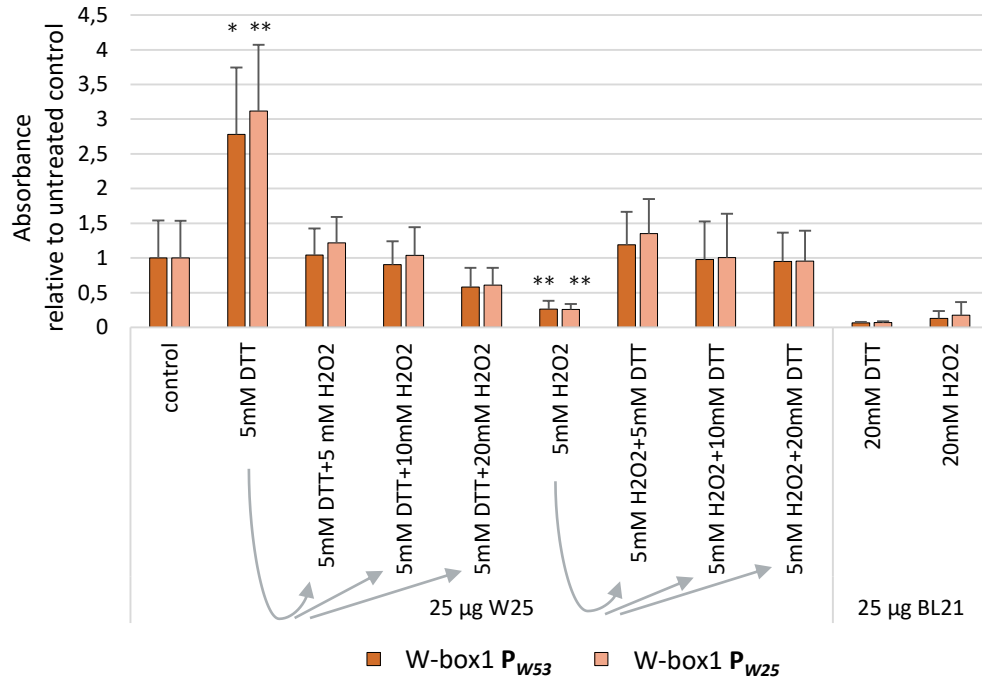
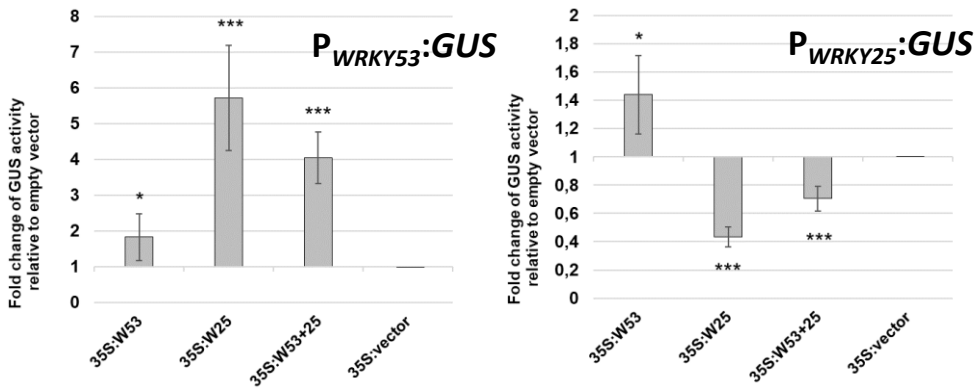


Figure 2: WRKY25 binding to the WRKY53 promoter is redox dependent.

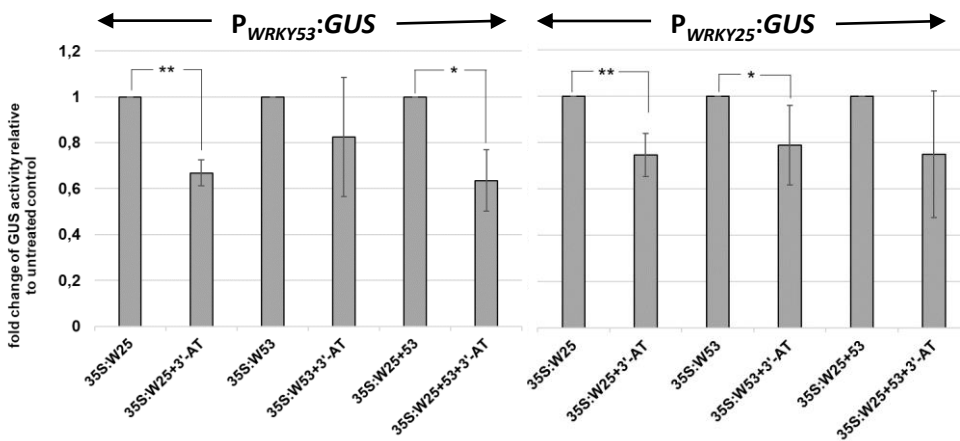
Redox-DPI-ELISA with 25 μ g of crude extracts of *E. coli* BL21 cells expressing WRKY25 proteins and the 5'biotinylated annealed oligonucleotides W-box1 P_{W53} and W-box1 P_{W25}. Protein extracts were reduced or oxidized by addition of either DTT or H₂O₂ to examine a redox-dependent binding of WRKY25. A fraction of the DTT-reduced proteins was re-oxidized by addition of increasing H₂O₂ concentrations to prove the reversibility of the redox effect. The same procedure was applied to the H₂O₂-oxidized proteins using increasing amounts of DTT. Absorbance values are indicated relative to control without treatment (mean values \pm SD, n = 4). Kruskal-Wallis-test was performed for statistically significant differences of all values compared to control (* $P \leq 0.05$, ** $P \leq 0.01$).

A

Arabidopsis protoplasts transformed with promoter:*GUS* and different effector constructs

**B**

Arabidopsis protoplasts transformed with promoter:*GUS* and different effectors constructs under normal and oxidizing conditions

**C**

Arabidopsis protoplasts transformed with $P_{WRKY53}:GUS$ and different effector constructs with and without *MEKK1*

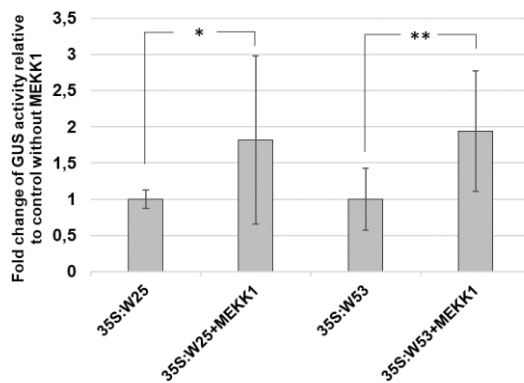


Figure 3: WRKY25 positively regulates WRKY53 under non-oxidizing conditions.

(A) Arabidopsis protoplasts were transiently transformed with 5 μ g of effector-, 5 μ g of reporter-plasmid DNA and 0.1 μ g of a luciferase construct for normalization. A 2.8-kbp-fragment of the *WRKY53* promoter and a 3.0-kbp-sequence of the *WRKY25* promoter fused to the *GUS* gene were used as reporter constructs. 35S:*WRKY25* and 35S:*WRKY53* constructs were used as effector plasmids. GUS activity was measured on the next day. The values are presented relative to the empty vector control (mean values \pm SD, n = 6). One sample t-test was performed, (* $P \leq 0.05$, ** $P \leq 0.01$, *** $P \leq 0.001$) (B) GUS assays were performed with protoplasts, which were simultaneously incubated overnight with 10 mM 3'-AT to inhibit catalase activities leading to higher H_2O_2 level. The values are presented relative to the untreated control transformations (mean values \pm SD, n = 3-7). One sample t-test was performed, (* $P \leq 0.05$, ** $P \leq 0.01$). (C) Co-transformation assays with 35S:*MEKK1* were performed. The values are presented relative to transformation without *MEKK1* (mean values \pm SD, n = 4-5). Kruskal-Wallis-test was performed, (* $P \leq 0.05$, ** $P \leq 0.01$).

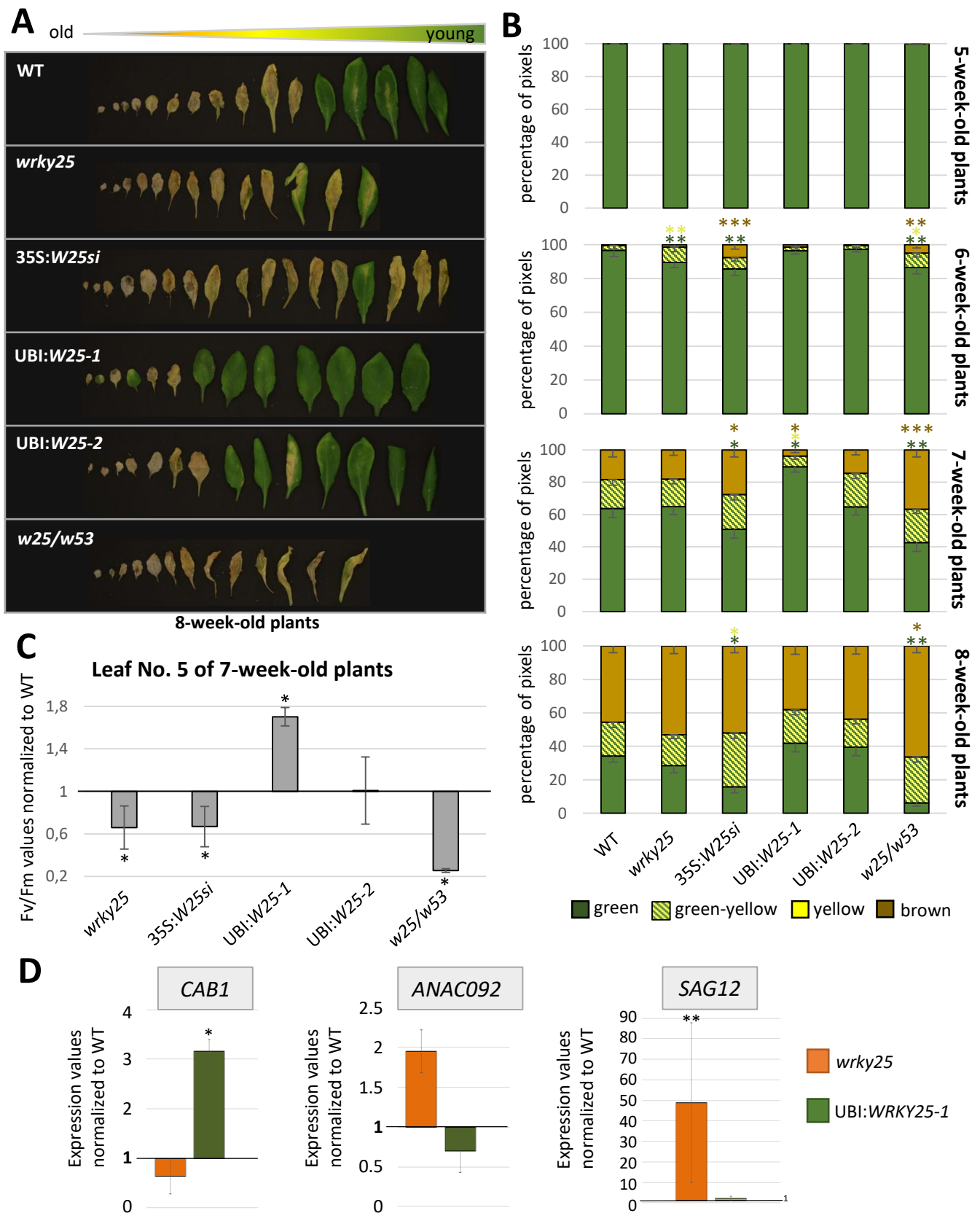


Figure 4: Senescence phenotypes of WRKY25 transgenic and mutant lines.

(A) Col-0 wildtype (WT), *wrky25* mutant (*wrky25*), *WRKY25* overexpressing (UBI:W25-1 and UBI:W25-2), *WRKY25* silenced (35S:W25si) and *wrky25-wrky53* double-knock-out (*w25/w53*) plants were analyzed over development. A photograph of rosette leaves of 8-week-old plants sorted according to their age is shown. (B) Quantitative evaluation of leaf senescence by categorizing individual leaves of at least six plants into four groups according to their color: green, green leaves starting to get yellow (green-yellow), completely yellow leaves (yellow) and dead and/or brown leaves (brown/dry). The percentage of each group with respect to total leaf numbers are presented (mean values \pm SE, $n=6$). (C) Fv/Fm values were measured with PAM for leaves of position 5 of 7-week-old plants (mean values \pm SE, $n=6$). One sample t-test was performed for statistical differences of all values compared to Col-0 ($*P \leq 0.05$) (D) Expression of the senescence associated marker genes *ANAC092*, *CAB1*, *SAG12* were analyzed by qRT-PCR and normalized to the expression of the *ACTIN2* gene. *SAG12* in 6-week and *ANAC092* and *CAB1* in 7-week-old plants. Shown are *wrky25* and UBI:W25-1 plants normalized to Col-0 (mean values \pm SE, $n=3$). Kruskal-Wallis-test was performed for statistically significant differences ($*P \leq 0.05$, $**P \leq 0.01$, $***P \leq 0.001$).

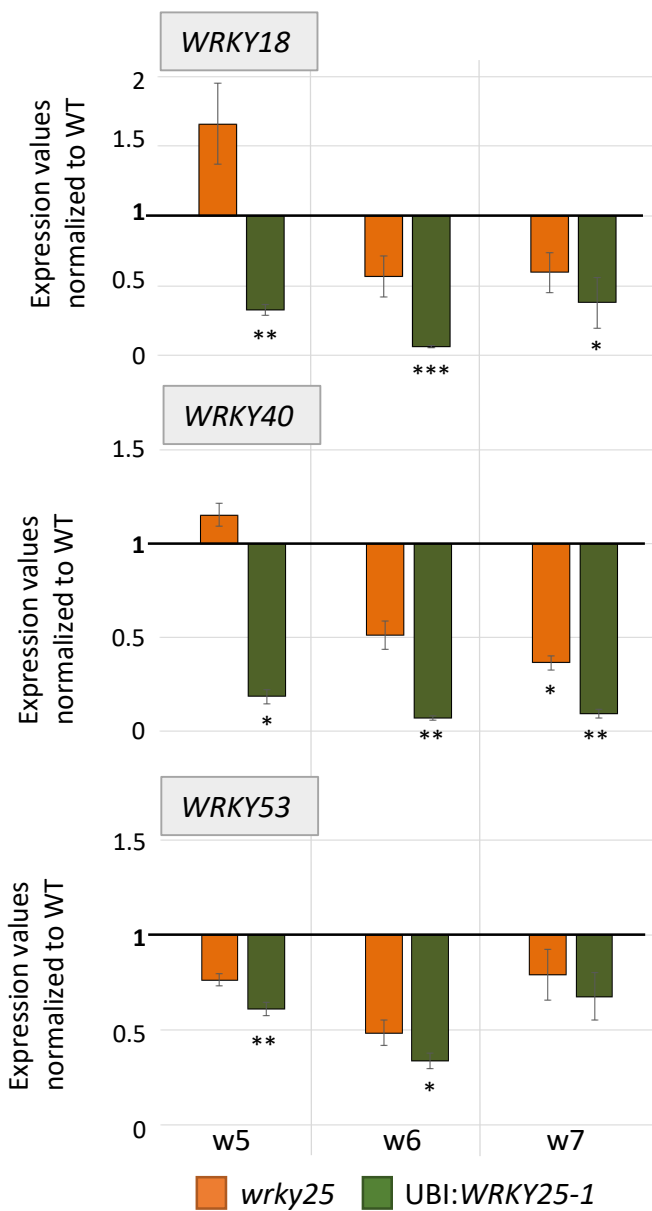


Figure 5: WRKY genes expression analyses.

Expression of different WRKY genes (*WRKY53*, *WRKY18*, *WRKY40*) were analyzed in Col-0 (WT), *wrky25* mutant and *WRKY25* overexpression line (*UBI:WRKY25-1*) by qRT-PCR and normalized to the expression of the *ACTIN2* gene. Three pools were analyzed; one pool consists of leaf No. 6 and 7 of two different plants. In week 7, only two pools of the *35S:W25si* plant line and of the *wrky25* line were analyzed but here with six technical replicates. Expression values were normalized to Col-0 and Col-0 was set to 1 (mean values, n=3, ±SE). Kruskal-Wallis-test was performed for statistically significant differences of all value compared to Col-0 (* $P \leq 0.05$, ** $P \leq 0.01$, *** $P \leq 0.001$).

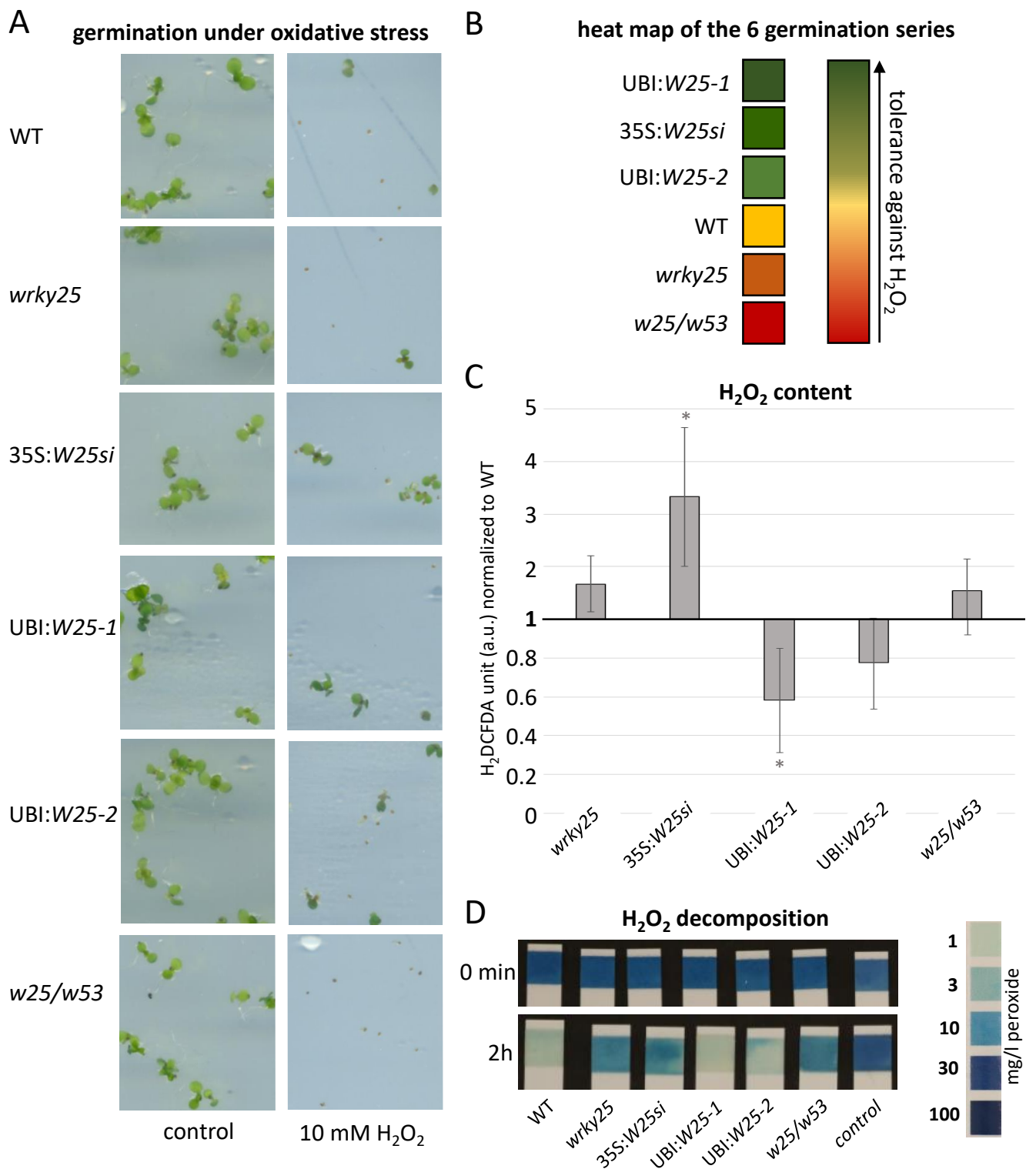


Figure 6: WRKY25 mediates H_2O_2 tolerance.

(A-B) Col-0 (WT), *wrky25* mutant, *WRKY25* overexpressing (*UBI:W25-1*; *UBI:W25-2*) and *WRKY25* silenced (*35S:W25si*) as well as the double-knock-out plants (*w25/w53*) were sown on $\frac{1}{2}$ MS plates with and without 10 mM H_2O_2 . A minimum of 30 seeds were put onto the plates and the experiment repeated 6 times ($n=6$) (A) shows a representative sector of the plates with and without H_2O_2 in media. (B) summarizes the 6 independent experiments in a heat map. Dark green means the most tolerant against H_2O_2 , dark red the most sensitive towards H_2O_2 . (C) H_2O_2 content was measured over plant development using H_2DCFDA fluorescence; leaves No. 8 of 8-week-old plants are shown. Fluorescence is indicated in arbitrary units (a.u.), normalized to leaf weight and expressed relative to WT ($\pm SE$, $n=4$). One Sample t-test was performed for statistical differences of all values compared to WT ($*P \leq 0.1$) (D) Leaf discs of leaf No. 5 of 6-week-old plants were incubated in a 30 mg/l H_2O_2 solution. As control H_2O_2 solution without leaf discs was measured. At timepoint 0 min and 2 h the decomposition of H_2O_2 was determined using commercially available peroxide sticks, color scale for H_2O_2 content is provided on the right.

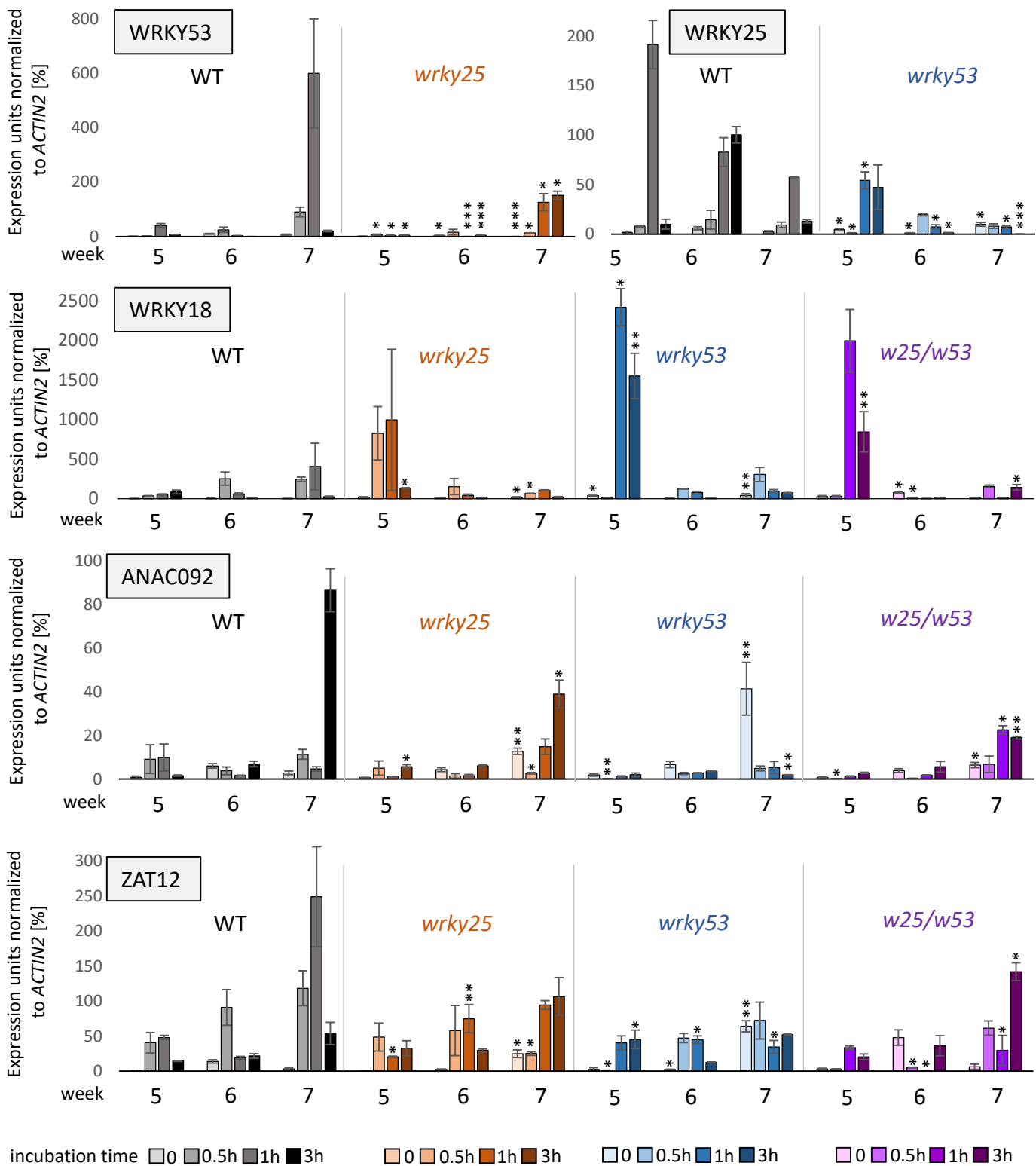


Figure 7: Influence of oxidizing conditions on gene expression.

Leaves of position 10 were harvested of Col-0 (WT), *wrky25* (orange) and *wrky53* (blue) single and double (purple) mutant plants. Leaves of 5, 6 and 7 week-old-plants were incubated in 10 mM H₂O₂ for 0-3 hours. Expression of *WRKY18*, *WRKY25*, *WRKY53*, *ZAT12* and *ANAC092* was determined by qRT-PCR. Expression values normalized to *ACTIN2* expression are presented (mean values ±SD, n=2, one biological replicate consists already of a pool of 3 plants for each timepoint). Kruskal-Wallis-test was performed for statistically significant differences of all values at each timepoint compared to Col-0 (*P ≤ 0.05, **P ≤ 0.01, ***P ≤ 0.001).

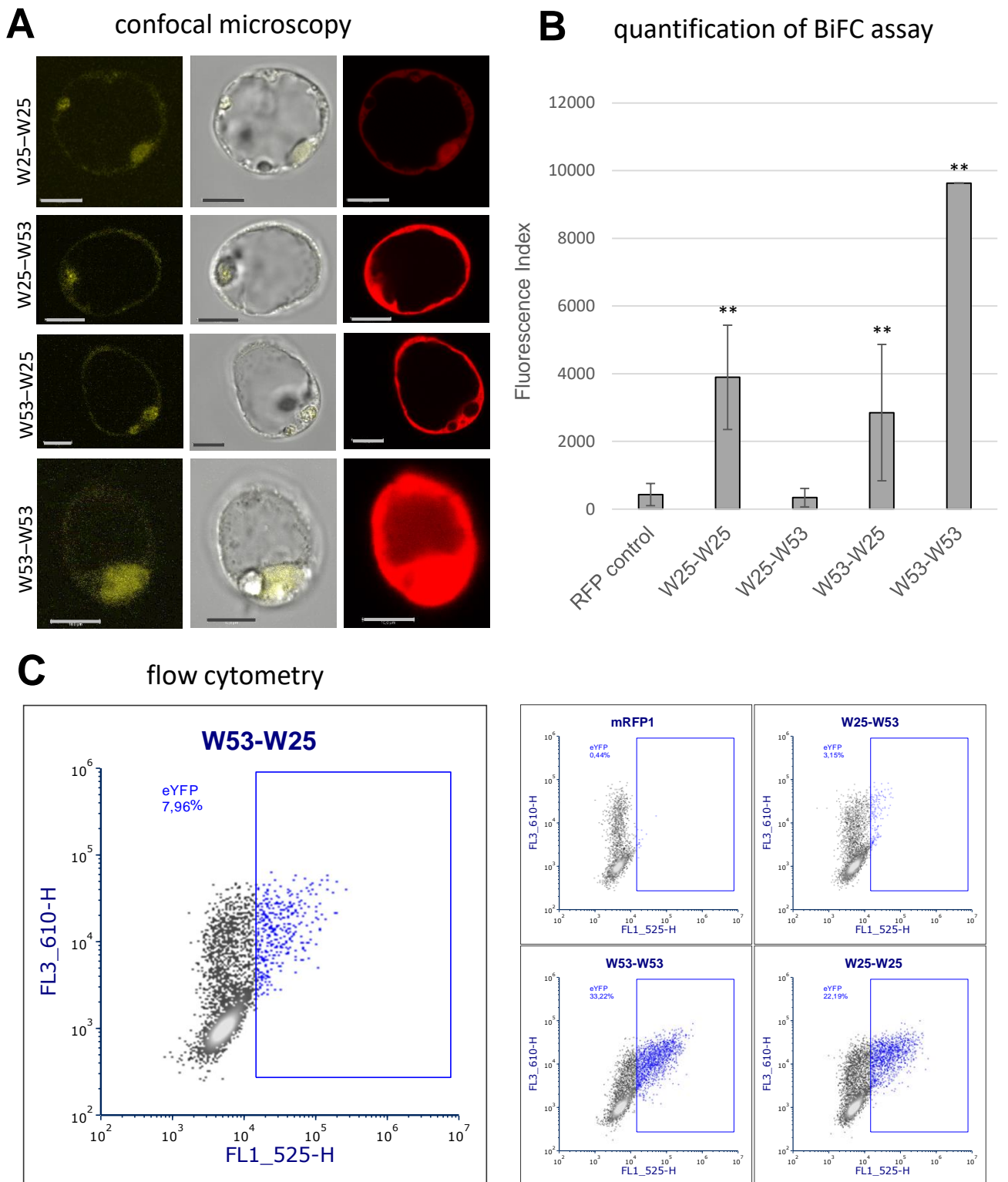


Figure 8: Protein-protein interaction of WRKY25 and WRKY53.

Protoplasts co-transformed with BiFC constructs were used to visualize interaction. YFP-N and YFP-C fusions with the respective WRKYs were transformed into Arabidopsis protoplasts and fluorescence was quantified using a cytometer (CytoFLEX; Beckman Coulter). (A) Confocal microscopy images. Combinations of the YFP-N and YFP-C constructs are indicated on the left. YFP fluorescence (left) was overlaid with the bright field images (middle). Additionally, mRFP was used as an internal control (right) to detect transformed cells. Scale bar = 10 μ m. (B) Flow cytometry analyses. Fluorescence Indices were calculated by multiplying the mean fluorescence by the fraction of fluorescent cells and finalized with quantile normalization (mean values +SD, n = 6). Kruskal-Wallis-test was performed for statistical differences of all values compared to RFP control (* $P \leq 0.05$, ** $P \leq 0.01$). (C) Representative graphs of the flow cytometry results. Blue dots represent eYFP signals of interaction. Blue squares mark the cells showing eYFP signal.

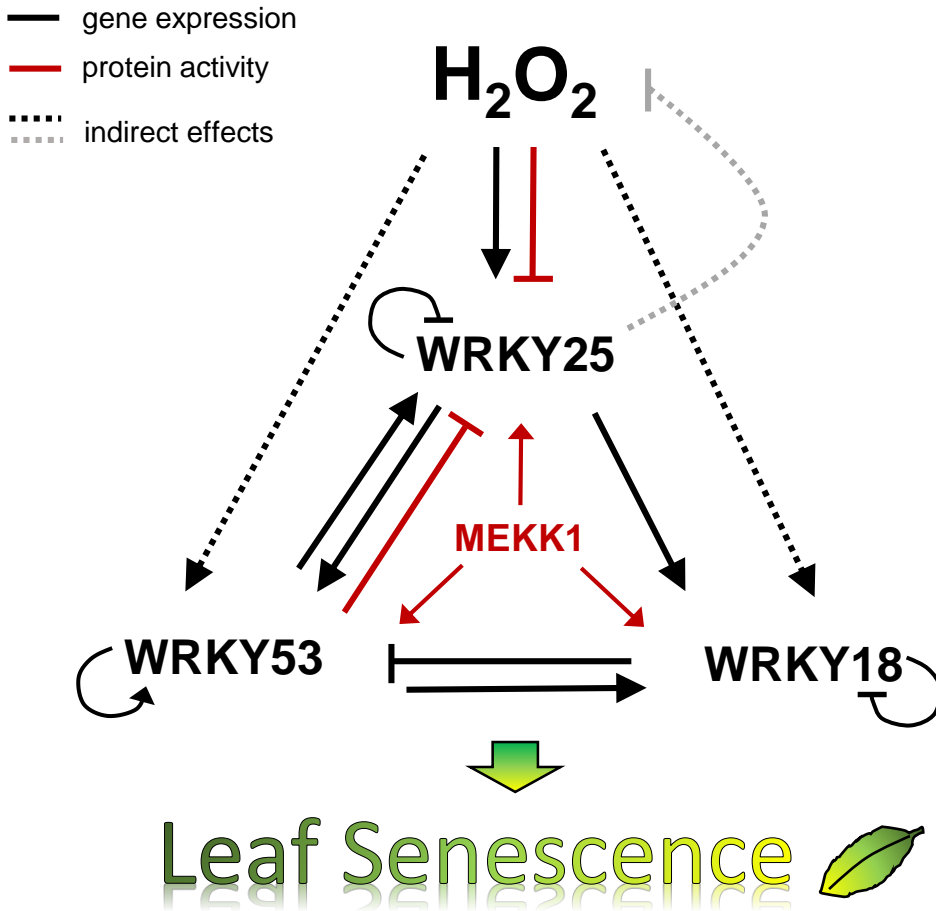


Figure 9: Model of H₂O₂ and the WRKY53-25-18 subnetwork

A model summarizing the impact of H₂O₂ and WRKY25 on senescence is presented. Solid lines show direct interactions whereas dotted lines show interaction, which may be direct or indirect. Black arrows describe the effects on gene expression, red arrows effects on protein activity, and the grey line effects on the intracellular hydrogen peroxide level. The expression of all three WRKY genes of the small WRKY53-25-18 subnetwork are controlled by hydrogen peroxide contents and hydrogen peroxide has a direct negative effect on the binding activity of WRKY25 to DNA. All three genes are under feedback control of their own gene products. In addition, MEKK1 increases the activity of all three WRKY factors. Moreover, WRKY25 can form heterodimers with WRKY53 and the heterodimer has a lower transactivation activity compared to the WRKY25 homodimer. This interplay determines in the end whether leaf senescence is accelerated or delayed.

***Arabidopsis thaliana* WRKY25 transcription factor mediates oxidative stress tolerance and regulates senescence in a redox-dependent manner.**

Jasmin Doll, Maren Muth, Lena Riester, Kenneth Berendzen, Justine Bresson, Ulrike Zentgraf

Center for Plant Molecular Biology (ZMBP), University of Tuebingen, Auf der Morgenstelle 32, 72076 Tuebingen, Germany

Supplementary Material

Figures:

S1: WRKY protein expression in *E. coli*

S2: Redox-DPI-ELISA with WRKY18 and WRKY53 protein

S3: 3'-AT treatment of protoplasts provokes an oxidative cell status

S4: Role of MEKK1 in WRKY18 driven *WRKY53* expression and senescence

S5: *WRKY25* expression analysis for lines with altered *WRKY25* expression

S6: Comparison of plant development

S7: Chlorophyll fluorescence imaging

S8: Dark-induced senescence and antioxidative capacity of *wrky25*, *cat2* and *wrky25/cat2*

S9: Yeast-Two-Hybrid interaction assay

Tables:

S1: Oligonucleotides for qRT-PCR

Methods related to supplemental Figures:

SM1: Dark-induced senescence phenotyping

SM2: Cell-free GUS reaction

SM3: H₂O₂ content in *Arabidopsis* protoplasts

SM4: Catalase zymograms

SM5: Yeast-Two-Hybrid Interaction Assay

**Expression of 6xHis tagged
WRKY proteins in *E. coli***

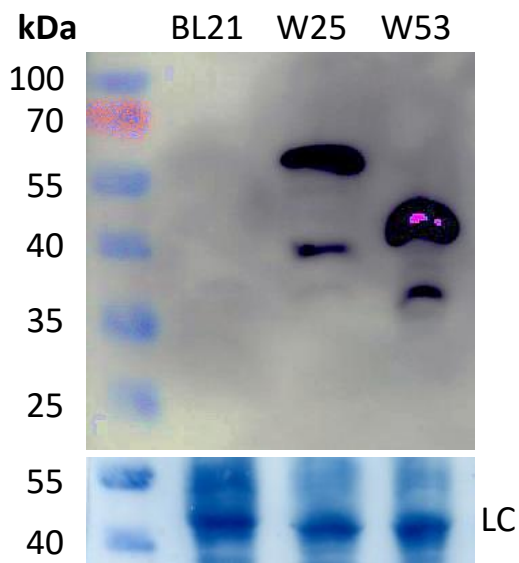


Figure S1: WRKY protein expression in *E. coli*.

Crude extracts of empty *E. coli* BL21 cells and BL21 cells expressing 6xHis-tagged WRKY25 or WRKY53 were prepared under native conditions and 25 μ g of the raw lysates were loaded on the SDS PAGE. After blotting, the PVDF membrane was detected using Penta-His-HRP conjugate kit (*Qiagen*, 1:1500). After antibody detection, the PVDF membrane was stained with amido black as loading control (LC).

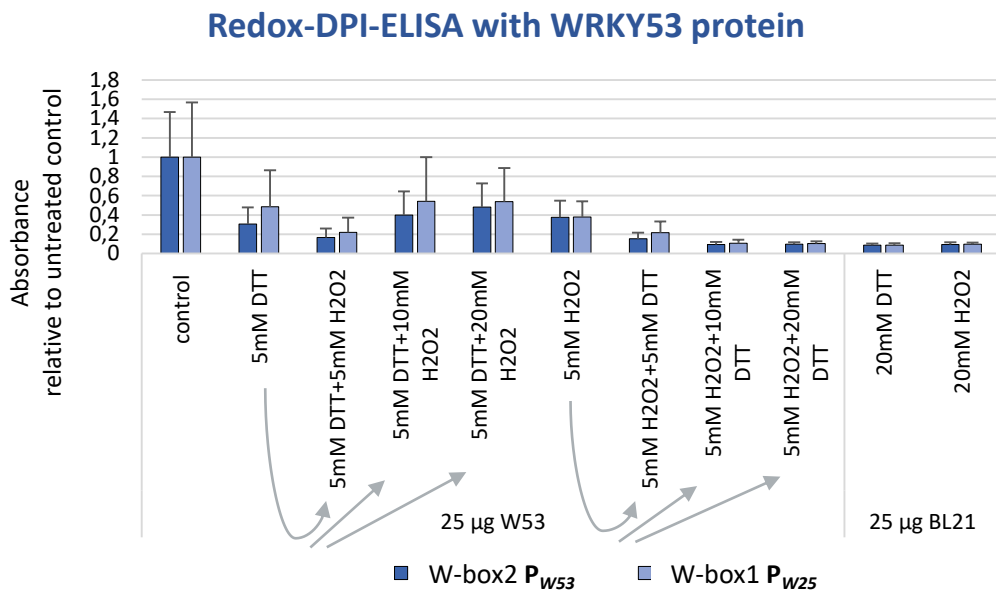
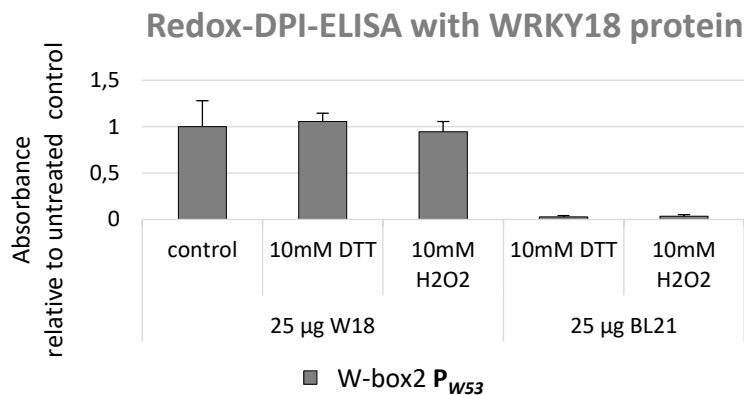
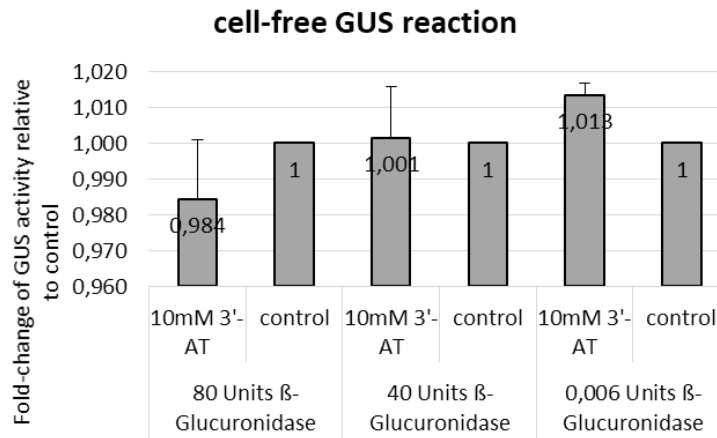
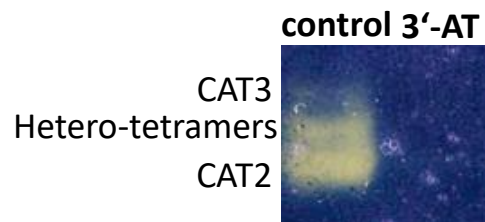
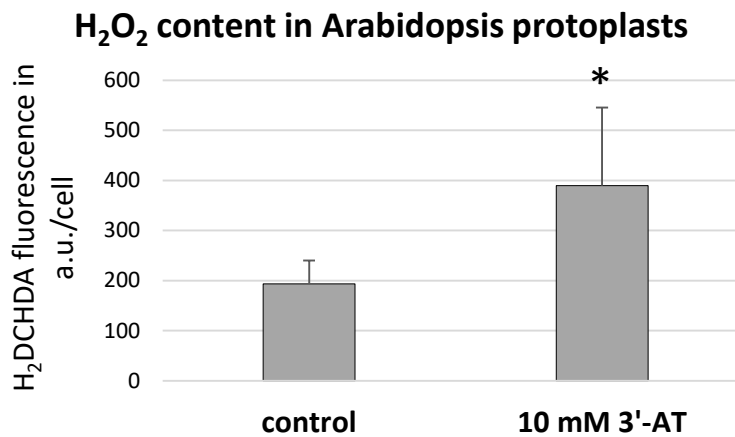
A**B**

Figure S2: Redox-DPI-ELISA with WRKY18 and WRKY53 protein.

A. Redox-DPI-ELISA with 25 µg of crude extracts of *E. coli* BL21 cells expressing WRKY53 proteins and the 5'biotinylated annealed oligonucleotides W-box2 P_{W53} and W-box1 P_{W25}. Absorbance values are indicated relative to control without treatment (mean values + SD, n = 3).

B. Redox-DPI-ELISA with 25 µg of crude extracts of *E. coli* BL21 cells expressing WRKY18 proteins and the 5'biotinylated annealed oligonucleotide W-box2 of the promoter of *WRKY53*. Protein extracts were reduced or oxidized by addition of either DTT or H₂O₂ to examine a redox-dependent binding. Absorbance values are indicated relative to control without treatment (mean values ±SD, n = 2). Kruskal-Wallis-test was performed for statistically significant differences (**P* ≤ 0.05). No significant differences were detected.

A**B****catalase activity in Arabidopsis protoplasts****C****Figure S3: 3'-AT treatment of protoplasts provokes an oxidative cell status**

(A) To prove that the 3'-AT treatment of the protoplasts has no influence on the GUS reaction itself, 10 mM 3'-AT or only buffer (control) was added to different concentrations of lyophilized β-Glucuronidase (*Sigma-Aldrich*) and a normal GUS assay was performed. The values are presented relative to control (mean values ±SD, n = 3). (B) To show that the 3'-AT treatment of the protoplasts lowers the cellular catalase activity, 10 mM 3'-AT or water was added to isolated protoplasts overnight and catalase zymograms were performed. One example of a zymogram is presented (n = 3). (C) H₂O₂ content in Arabidopsis protoplasts was measured by using H₂DCFDA fluorescence; protoplasts were treated with 10 mM 3'-AT or water (control). The values are indicated relative to cell number (mean values ±SD, n = 5), Kruskal-Wallis-test was performed for statistical differences (*P ≤ 0.1).

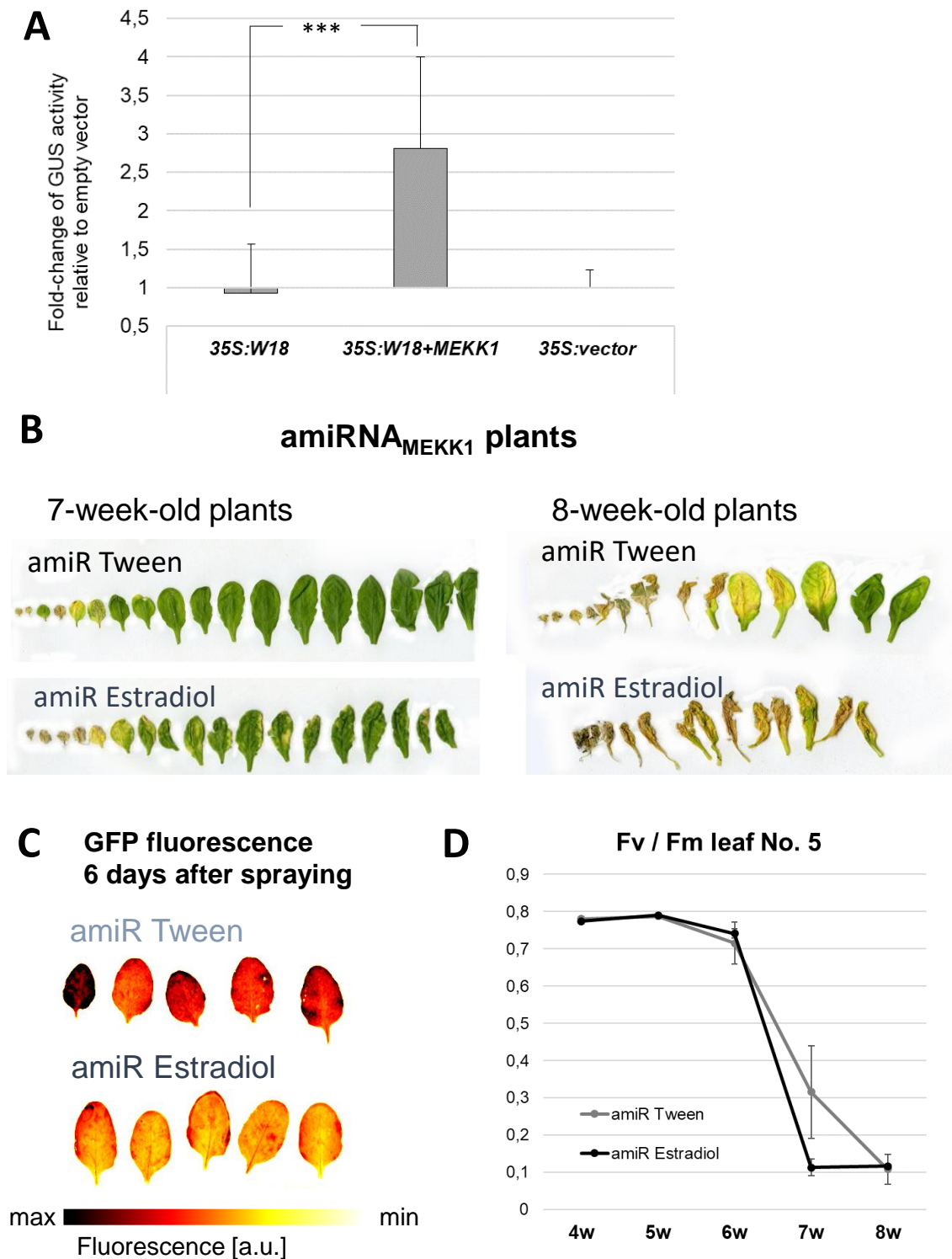


Figure S4: Role of MEKK1 in WRKY18 driven WRKY53 expression and senescence.

(A) GUS-Assays were performed in *Arabidopsis* protoplasts using the *WRKY53* promoter and 35S:*WRKY18* and 35S:*MEKK1* as effector constructs. The empty vector was used as reference (mean values \pm SE, n=4). (B) Rosette leaves of a β -estradiol inducible amiRNA-*MEKK1* line were arranged according to their age and representative pictures that show the senescence phenotype are presented. Plants were sprayed with 3 μ M β -estradiol; Tween-20 was used as a mock treatment. (C) The amiRNA-*MEKK1* plants also contain a 35S:*GFP* fused to the target sequence of the amiRNA-*MEKK1*. Therefore, β -estradiol induction of the amiRNA was assessed via the GFP fluorescence visualized with a Typhoon FLA 9500 laser scanner (*GE Healthcare*) 6 days after spraying (Li et al., 2013) (D) Fv/Fm values in leaf No. 5 were measured with the pulse amplitude modulation (PAM) method (mean values \pm SE, n=5). Kruskal-Wallis-test was performed for statistical differences (* $P \leq 0.05$, ** $P \leq 0.01$, *** $P \leq 0.001$).

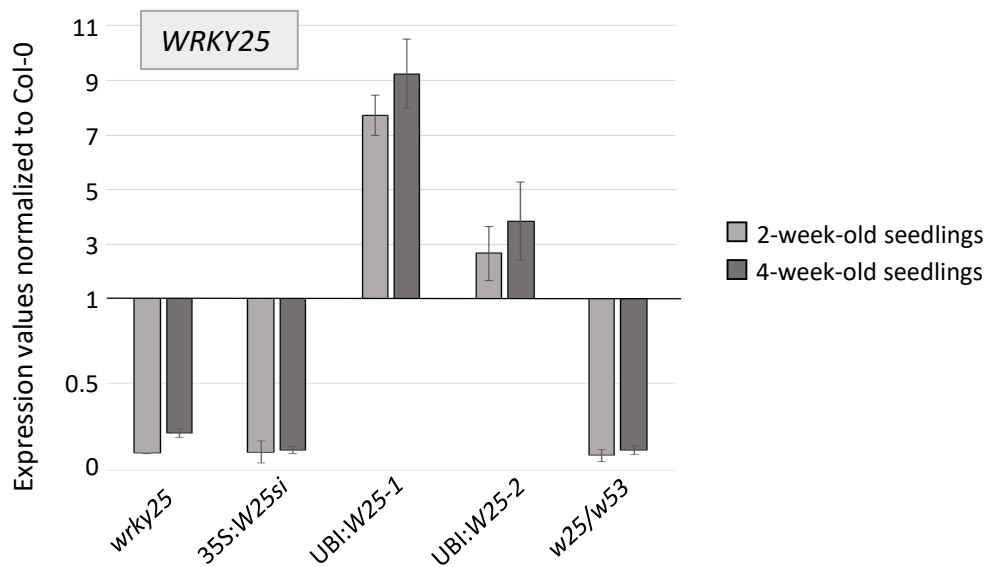


Figure S5: Gene expression analysis for lines with altered *WRKY25* expression.

Expression of *WRKY25* was analyzed in different *WRKY25* transgenic lines by qRT-PCR and normalized to the expression of the *ACTIN2* gene. Leaf material of at least 15 two-week-old seedlings or 4-week-old plants were harvested and pooled. The mean of values for Col-0 was set to 1 and values of the mutants were normalized to Col-0 (means of two technical replicates, \pm SE).

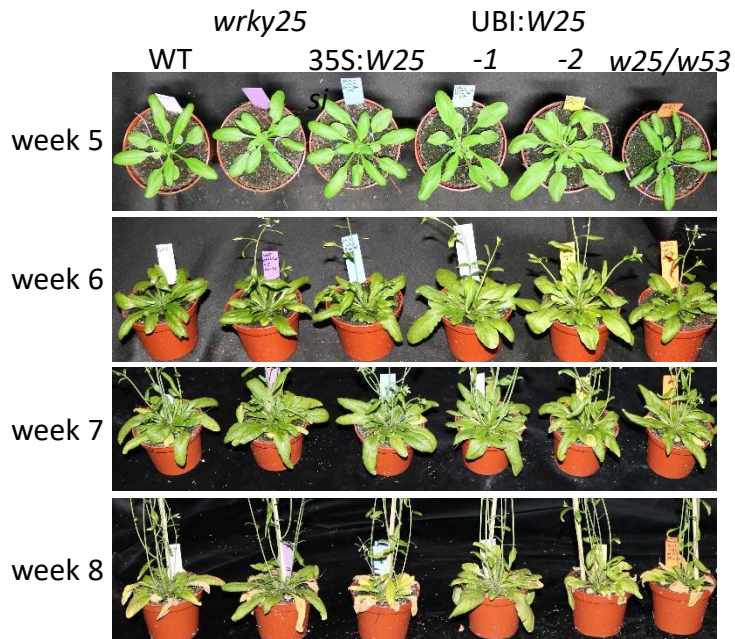


Figure S6: Comparison of plant development.

Representative example of Col-0 (WT), *wrky25* mutant (*wrky25*), *WRKY25* overexpressing (UBI:W25-1 and UBI:W25-2), *WRKY25* silenced (35S:W25si) and *wrky25-wrky53* double-knock-out-mutant (*w25/w53*) plants from week 5 to 8.

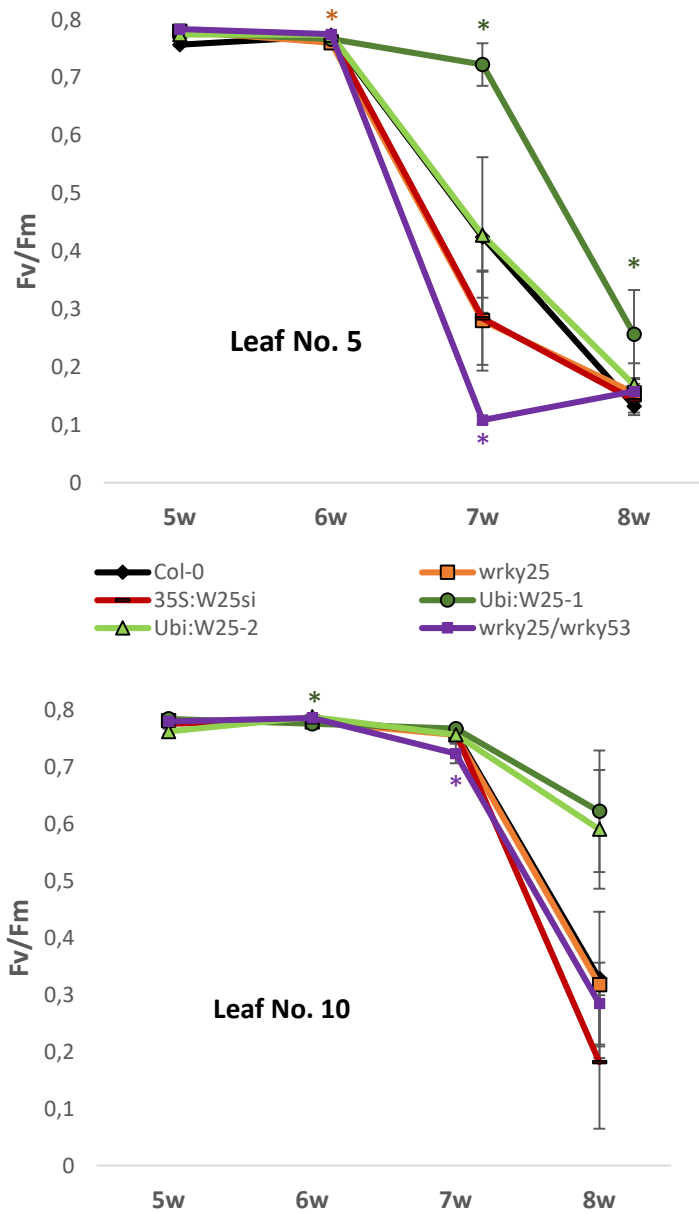


Figure S7: Chlorophyll fluorescence imaging.

Col-0 (WT), *wrky25* mutant (*wrky25*), *WRKY25* overexpressing (UBI:W25-1 and UBI:W25-2), *WRKY25* silenced (35S:W25si) and *wrky25-wrky53* double-knock-out (*w25/w53*) plants were analyzed over development. Fv/Fm values were measured with PAM for leaves No. 5 and 10 for 5- to 8-week-old plants (mean values \pm SE, n=6). Kruskal-Wallis-test was performed for statistical differences of all values compared to Col-0 (* $P \leq 0.05$).

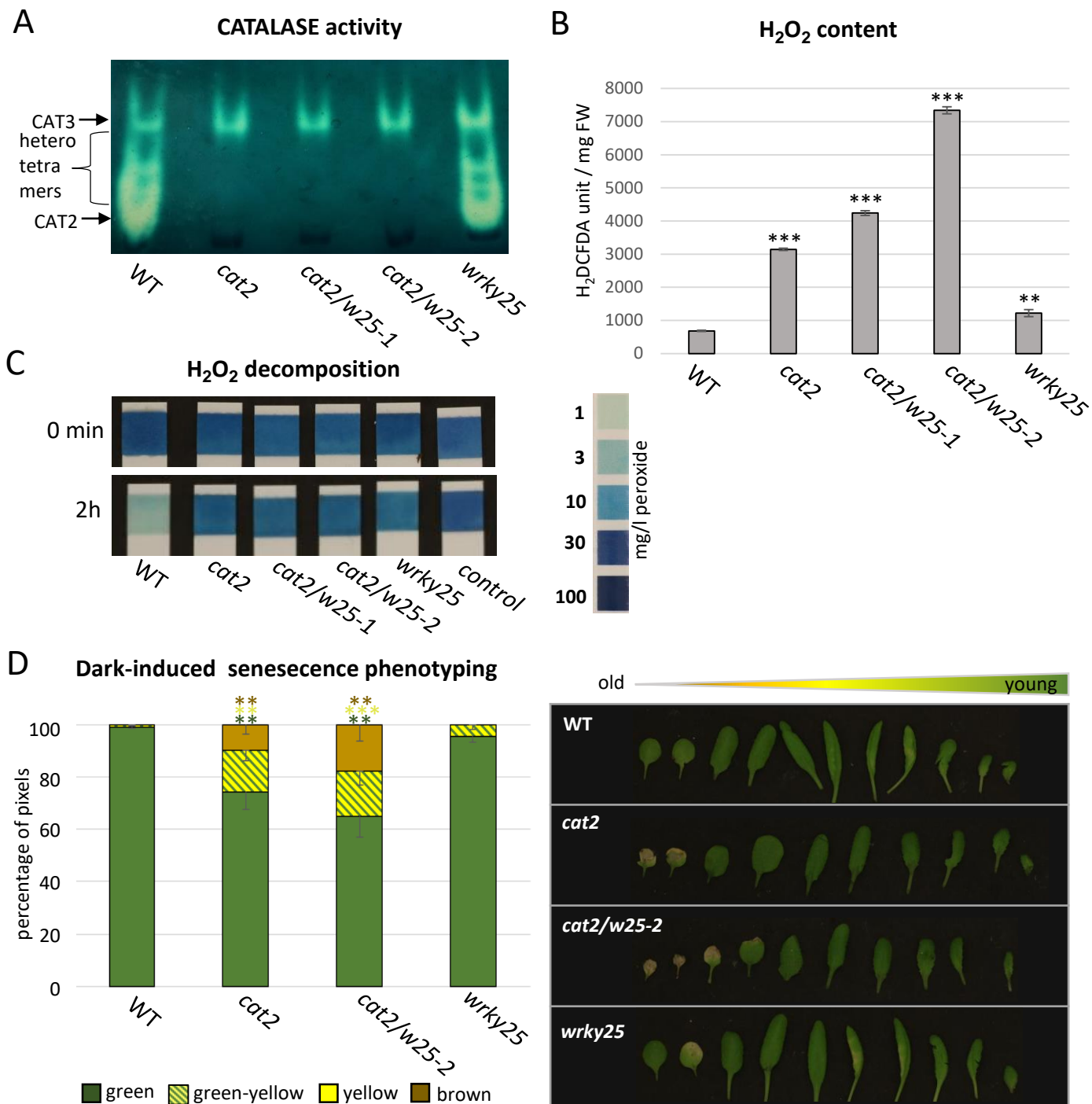


Figure S8: WRKY25 is involved in H₂O₂ clearance

(A) Protein crude extract was isolated from leaves of 7-week-old plants of Col-0 (WT), *wrky25* mutant (*wrky25*), *catalase2* mutant (*cat2*) and double-knock-out-mutant (*cat2/w25*) plants. Proteins were separated on a 7.5 % native gel and stained for catalase activity. Enzyme activity of CAT2 and CAT3 as well as the hetero-tetramers are visualized on a zymogram. (B) Intracellular H₂O₂ content was measured in leaves No. 8 of 6-week-old plants using the fluorescent dye H₂DCFDA. Values are normalized to mg freshweight (FW) (n=3, ±SE). (C) Decomposition of H₂O₂ was measured using commercially available peroxide strips. Two leaf discs of 7-week-old plants were incubated in 1 mM H₂O₂. As control H₂O₂ solution without leaf discs was measured. The peroxide content was measured immediately (0 min) and after 2 hours incubation (2h). (D) For dark-induced senescence, 4.5-week-old-plants were transferred into darkness for 7 days. A picture of the rosette leaves sorted according their age is shown. An automated colorimetric assay (ACA) categorizes the leaves into four groups according to their color (green, green/yellow, yellow, brown) and percentage of each category is depicted (mean values ±SE, n=3). Kruskal-Wallis-test was performed for statistically significant differences of all value compared to Col-0 (**P* ≤ 0.05, ***P* ≤ 0.01, ****P* ≤ 0.001).

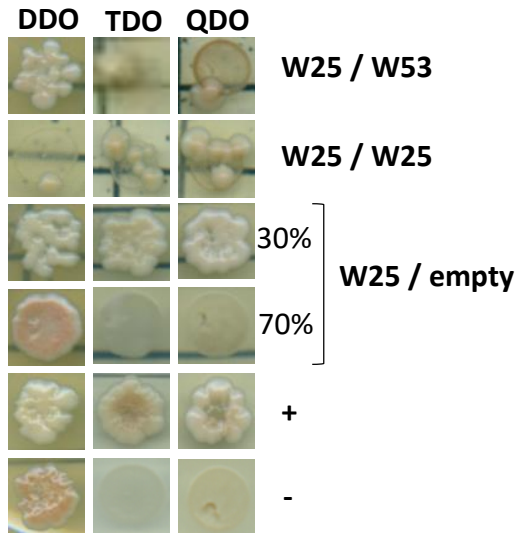


Figure S9: Yeast-Two-Hybrid interaction assay.

Yeast-Two-Hybrid assays were performed using Clontech's Matchmaker® Gold Y2H System. After mating of the yeast strain Y2H Gold containing bait vectors with the yeast strain Y187 containing prey vectors, diploid cells were checked on DDO media for co-transformation of both vectors and interaction was identified on selection media TDO and QDO (bait/prey). Positive (+) and negative (-) system controls were performed. W25 as bait construct and the empty prey construct also resulted in yeast growth in approx. 30 % of our assays indicating that the interaction results in yeast using W25 as bait might be artefacts.

Table S1: Oligonucleotides for qRT-PCR.

Gene	Atg number	Forward primer 5'-3'	Reverse primer 5'-3'
WRKY25	Atg30250	GGTTGTGGAGTGAAGAAGCA	TCGTGATTGTGTCTTCCTTCA
WRKY53	At4g23810	ATCCCGGCAGTGTTCCAGAATC	AGAACCTCCTCCATCGGCAAAC
WRKY18	At4g31800	TGGACGGTTCTTCGTTTCTCGAC	TCGTAACCTCACTTGCGCTCTCG
WRKY40	At1G80840	AAGCTTCTGACACTACCCTCGTTG	TTGACAGAACAGCTTGGAGCAC
ANAC092	At5g39610	CTTACCATGGAAGGCTAAGATGGG	TTCCAATAACCGGCTTCTGTCG
CAB1	At1g29930	TGCACTACTCAACCTCAATGGC	AAAGCTTGACGGCCTTACCG
SAG12	At5g45890	GCTTTGCCGGTTTCTGTTG	GTTTCCCTTTCTTTATTTGTGTTG
ZAT12	At5g59820	TTGGTTACACGCGCTTTGTTGC	ACAAGCCACTCTCTTCCCCTG
ACTIN2	At3g18780	ACCCGATGGGCAAGTCATCAC	TCCCACAAACGAGGGCTGGA

SUPPLEMENTAL METHODS

SM1: Dark-induced senescence phenotyping

For dark-induced senescence phenotyping, plants grew 4.5 weeks under long-day conditions, color-coded according to their age, and were then transferred into darkness for 7 days. The color of the leaves were categorized by an automated colorimetric assay (ACA, Bresson et al., 2018). All mutants have Columbia-0 (Col-0) background and Col-0 was used as control. T-DNA insertion lines in *CAT2* (SALK_057998) were obtained from the Nottingham Arabidopsis Stock Centre (NASC). Seeds of the homozygous double-knock-out line *wrky25/cat2* were kindly provided by Dr. Changle Ma, Shandong Normal University, China (Su et al., 2018).

SM2: Cell-free GUS activity measurements

To prove that the 3'-AT treatment of the protoplasts has no influence on the GUS reaction itself, different concentrations of β -Glucuronidase (*Sigma-Aldrich*) or the same volume of protein extraction buffer (control) was added. These 'protein solutions' were used for the normal GUS assay procedure.

SM3: H₂O₂ content in Arabidopsis protoplasts

To confirm that the 3'-AT treatment of the protoplasts results indeed in a higher H₂O₂ level, 10 mM 3'-AT or the same volume of water was added to isolated protoplasts. After overnight incubation, H₂DCFDA stock-solution (2',7'-dichlorodihydrofluorescein diacetate, 400 μ g in 400 μ L DMSO, then add 400 μ L H₂O) was added with a dilution factor of 1:100. Protoplasts were then incubated for exactly 45 min in H₂DCFDA. After centrifugation in Fall Buffer (0.5 M mannitol, 15 mM MgCl₂, 0.1% MES, pH 5.8) and washing twice with 40 mM Tris pH 7.0, a fraction was taken for counting protoplasts and then they were grinded in 500 μ L 40 mM Tris pH 7.0. The samples were centrifuged at 4°C for 15 min and the fluorescence (480 nm excitation, 525 nm emission) of the supernatant was measured in a Berthold TriStar LB941 plate reader.

SM4: Catalase zymograms

To show that the 3'-AT treatment of the protoplasts lowers catalase activity, 10 mM 3'-AT or the same volume of water was added to isolated protoplasts. After overnight incubation and centrifugation in Fall Buffer (0.5 M mannitol, 15 mM MgCl₂, 0.1% MES, pH 5.8), protein extraction buffer was added (100 mM Tris, 20% Glycerol (v/v), 30 mM DTT, pH 8), the samples were ground with pestle and mortar, and then centrifuged for 15 min at 14 000 rpm and 4°C. Total protein concentration of the supernatant was determined via Bradford assay (*Bio-Rad*), and 10 μ g total protein was loaded on native PAA gels (7.5% PAA, 1.5 M Tris, pH 8.8; running buffer: 25 mM Tris, 250 mM Glycin, pH 8.3). After protein separation (1h, 120V), the gels were rinsed twice with water, incubated for 2 min in a 0.01% H₂O₂ solution, again rinsed twice with water and stained in a solution containing 1% FeCl₃ and 1% K₃(Fe(CN)₆); (w/v) until activity bands became visible (~ 4 min). The staining reaction was

stopped by removing the staining solution and rinsing gels in water. The same procedure was applied to analyze the catalase activity of leaf material. Here, one leaf of Col-0, *wrky25*, *cat2*, *wrky25/cat2* plants was harvested, respectively, and ground in 200 μ l protein extraction buffer.

SM5: Yeast-Two-Hybrid (YTH) Interaction Assay

Full-length coding sequences of Arabidopsis *WRKY25* and *WRKY53*, respectively were cloned into bait vector fused to the GAL4 DNA-binding domain (pGBKT7), and prey vector fused to the GAL4 activation domain, pGAD424. The bait vector was transformed into yeast Y2HGold and prey vectors into Y187 according to Matchmaker® Gold Yeast Two Hybrid System Manual (*Clontech*). The YTH assay was performed according to manufacturer's instructions. Homologous and heterologous WRKY interactions were identified on selection media (TDO, QDO).

REVIEW

A guideline for leaf senescence analyses: from quantification to physiological and molecular investigations

Justine Bresson^{1,†,*}, Stefan Bieker^{1,†}, Lena Riester^{1,†}, Jasmin Doll^{1,†} and Ulrike Zentgraf¹

¹ ZMBP, General Genetics, University of Tübingen, Auf der Morgenstelle 32, 72076 Tübingen, Germany

* Correspondence: j.bresson34@gmail.com

† These authors contributed equally to this work.

Received 31 March 2017; Editorial decision 22 June 2017; Accepted 23 June 2017

Editor: Christine Foyer, Leeds University, UK

Abstract

Leaf senescence is not a chaotic breakdown but a dynamic process following a precise timetable. It enables plants to economize with their resources and control their own viability and integrity. The onset as well as the progression of leaf senescence are co-ordinated by a complex genetic network that continuously integrates developmental and environmental signals such as biotic and abiotic stresses. Therefore, studying senescence requires an integrative and multi-scale analysis of the dynamic changes occurring in plant physiology and metabolism. In addition to providing an automated and standardized method to quantify leaf senescence at the macroscopic scale, we also propose an analytic framework to investigate senescence at physiological, biochemical, and molecular levels throughout the plant life cycle. We have developed protocols and suggested methods for studying different key processes involved in senescence, including photosynthetic capacities, membrane degradation, redox status, and genetic regulation. All methods presented in this review were conducted on *Arabidopsis thaliana* Columbia-0 and results are compared with senescence-related mutants. This guideline includes experimental design, protocols, recommendations, and the automated tools for leaf senescence analyses that could also be applied to other species.

Keywords: *Arabidopsis thaliana*, automated colourimetric assay, genetic regulation, ion leakage, leaf senescence, lipid peroxidation, photosynthetic capacities, redox regulation.

Introduction

Senescence in annual plants is described as the essential last developmental stage aimed at recycling and reallocation of valuable resources to actively growing organs. When plants are confronted with drastic stresses, senescence can also be an exit strategy to ensure the most optimal survival chances for its offspring. However, senescence is not a chaotic breakdown but a highly complex and dynamic process,

following a precise timetable driven by genetic, developmental, and environmental factors (Jansson and Thomas, 2008). Senescence can thus be affected in different ways: in the onset and/or in the intensity and the rate of progression. As senescence is a relatively long process, it can be conceptually divided into three phases: initiation, reorganization, and termination.

Abbreviations: ACA, Automated colourimetric assay; carboxy-H₂DCFDA 5(6), carboxy-dichloro-fluorescein diacetate; Chl, chlorophyll; ChlF, chlorophyll fluorescence; DAB, 3,3'-diaminobenzidine; DCF, dichlorofluorescein; EL, electrolyte leakage; F₀, minimal fluorescence emission of a dark-adapted plant; F_m, maximum fluorescence emission after a short pulse of a saturating light; F_v, variable fluorescence, the difference between F₀ and F_m; F_v/F_m, maximum quantum efficiency of PSII photochemistry (photosynthetic efficiency); H₂O₂, hydrogen peroxide; HSV, hue saturation value; MDA, malondialdehyde; PAM, pulse amplitude modulation; PS, photosystem; ROS, reactive oxygen species; SAG, senescence-associated gene; SDG, senescence down-regulated gene; TBARS, thiobarbituric acid-reactive-substances; TF, transcription factor.

The onset of senescence is the consequence of a constant integration between intrinsic and environmental signals at cellular, tissue, and organ levels. Generally, plants grow continuously until they reach a maximum size, after which senescence can occur (Thomas, 2013). Without exogenous stress input, leaf senescence mainly depends on two endogenous parameters: leaf age and developmental stage at the whole-plant level (Zentgraf *et al.*, 2004). In *Arabidopsis thaliana*, the initiation of senescence usually coincides with the transition to flowering and is concomitant with cessation of vegetative meristem activity (Thomas, 2013). However, senescence can be triggered and modulated by a wide variety of abiotic and biotic stresses such as drought, shade, and pathogen infection (Lim *et al.*, 2007). The timing of leaf senescence initiation is crucial: if it is too late, it would allow only partial and incomplete remobilization of nutrients, whereas if initiated too early, it would reduce carbon assimilation and nitrogen uptake (Malagoli *et al.*, 2004; Masclaux-Daubresse *et al.*, 2010). The initiation of senescence is driven by multiple and co-ordinated signals through hormones, sugars, reactive oxygen species (ROS), and calcium (Lim *et al.*, 2007). At the molecular level, many different transcription factors (TF) are successively activated, forming a clear schedule of events taking place in the course of senescence. Almost 6500 differentially regulated genes have been identified via reverse-genetic approaches and large-scale transcriptome profiling in *A. thaliana* senescence, grouped into 48 clusters according to their differential expression patterns, thus indicating the complexity of the regulatory network (Breeze *et al.*, 2011).

Senescence progresses until fruit development and maturation is finished and ends with the complete disintegration of leaf tissues (Hensel *et al.*, 1993). During the reorganization phase, the cells are subjected to an intensive restructuring, notable by the breakdown of macromolecules, e.g. chlorophyll (Chl), and the remobilization of salvaged nutrients. Breakdown of proteins involves many plastidial and nuclear proteases and regulators of their activities, but also dynamic protein trafficking to bring about the conversion of larger macromolecular structures into transportable and useful breakdown products (Diaz-Mendoza *et al.*, 2016). Moreover, chaperones can also play important roles during the reorganization phase, as for example in protein carbonylation leading to irreversible oxidation, and thereby to a loss of function of the modified proteins (Johansson *et al.*, 2004). However, the extensive degradation of macromolecules can lead to the accumulation of toxic intermediates and by-products, which have to be dealt with by the senescing cells. In particular, anti-oxidative enzymes, such as peroxidases and catalases, play a crucial role in detoxifying highly reactive compounds generated during degradation processes (Buchanan-Wollaston *et al.*, 2003; Zimmermann *et al.*, 2006). Anthocyanin, a natural antioxidant, which has also been reported to protect against oxidative stress-induced damage, increases during senescence (He and Giusti, 2010). Detoxification is essential as the nucleus as well as the mitochondria have to remain functional in order to maintain transcriptional control and to provide sufficient energy throughout the whole process. During the termination phase, the vacuoles are disrupted and

collapse, thus releasing nucleases and proteases into the cytoplasm, which is then contracted and acidified. This leads to the gradual degradation of the cytoplasm, fragmentation of the nuclear DNA and the organelles, and the deterioration of the membranes (Kuriyama and Fukuda, 2002; Ondzighi *et al.*, 2008). Cell death is thus initiated, progressively leading to an irreversible loss of cell integrity (Zimmermann and Zentgraf, 2005).

As senescence occurs in a progressive manner, its quantification throughout the plant life cycle needs reproducible and standardized methods in order to allow comparisons between genotypes and experiments. In addition, studying senescence requires an integrative multi-scale analysis of the dynamic changes occurring in different key processes. However, senescence phenotyping is still diverse, leading to low comparability of plant lines and experiments. Single time-point comparisons often clearly reveal that senescence is somehow disturbed, but they do not precisely indicate in which sense: the time-point of onset, the velocity of progression, or specific processes could be altered. Due to the lack of a general agreement on how senescence phenotyping should be conducted, we suggest a guideline that attempts to standardize leaf senescence analyses. In this review, we first propose an experimental design concerning environmental conditions, growth, and plant sampling for measuring key senescence-related markers. We describe a complete set of methods to assess senescence at physiological, biochemical, and molecular levels. In addition, we provide a novel automated quantification of leaf senescence based on macroscopic colourimetric assays. These complementary analyses will allow an overview of the whole process to be gained, and thus provide an ability to decide whether the initiation, reorganization, and termination phases are differently affected. We conducted the senescence analyses using the widely used *A. thaliana* Columbia-0 (Col-0) genotype as an example, and as a proof of concept we compared the results of our current and previous experiments in senescence-related mutants. All methods and computing tools are described in detail and all protocols, including ImageJ and R scripts, are provided to serve as recommendations for measurements and data analyses.

General considerations for experimental design

Environmental growth conditions such as photoperiod, light intensity, ambient temperature, and nutrient availability are key factors when analysing plant growth. Therefore, choosing the growth conditions is of utmost importance in the experimental design of senescence phenotyping. Amongst these conditions, light plays a crucial role in plant development and leaf morphogenesis, but also in senescence initiation and progression (Biswal and Biswal, 1984; Vasseur *et al.*, 2011). In *Arabidopsis*, light can promote or retard senescence in a photoperiodic and dose-dependent manner (Nooden *et al.*, 1996). Here, we grew our plants in standard soil (9:1 soil and sand; see Supplementary Table S1 at *JXB* online) in long days (16 h day; 8 h night), low light ($\sim 70\text{--}80 \mu\text{E m}^{-2} \text{s}^{-1}$

at plant height), and an ambient temperature of 21 °C. Long days accelerate development (i.e. flowering time), while low light can lead to an extended period of senescence (Nooden *et al.*, 1996). This allows detailed analyses of all three different phases of senescence. A further advantage of plants grown under long days is a lower leaf number and thus less overlapping of the leaf blades within the rosette, compared with plants grown at photoperiods of 12 h or 8 h. This greatly facilitates the analysis of plant growth and quantification of senescence, especially at the whole-rosette level. In addition, to improve later image acquisition, the soil was covered with black sand to enhance the contrast between plant and soil and to reduce background noise.

The timing of sampling and measurements is also a crucial point. We have established a precise design for sampling and

measurements that allows analyses of both growth and senescence (Fig. 1). Growth and development were non-invasively examined in all plants (80 in total) through measurements of rosette area and leaf number until the bolting stage (determined by macroscopic examination of flower buds). Stem and total silique dry mass were assessed every week from flowering time (first flower open) until first yellowish siliques stage (Fig. 1). In parallel, leaf senescence was analysed weekly for five consecutive weeks, including the specific developmental hallmarks. Depending on the experiment, sampling can be done according to days/weeks after sowing or germination. However, plant development should be considered when comparing different plant lines with significant differences in their growth (e.g. different bolting times). In this case, sampling could be done at different defined developmental stages

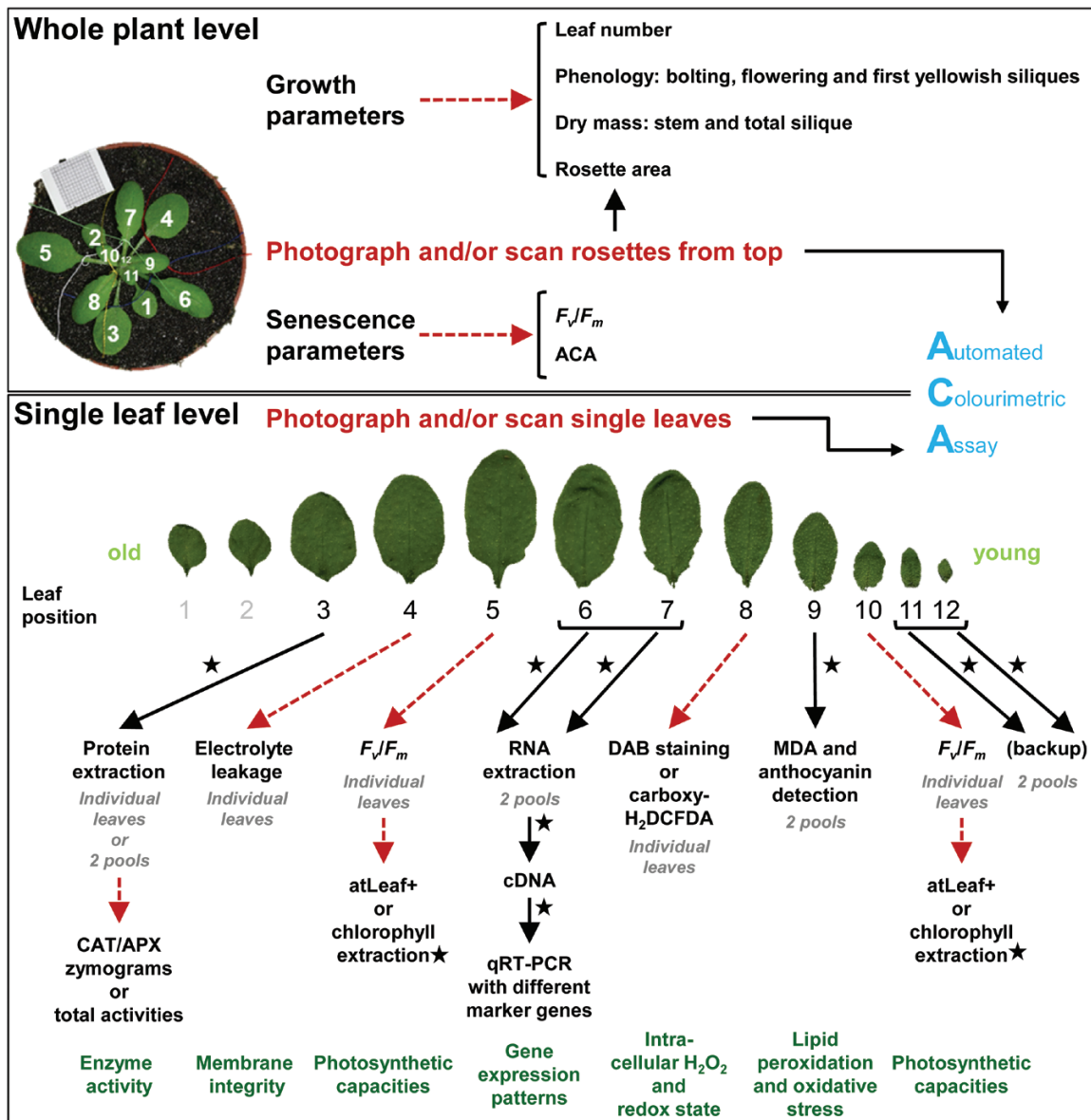


Fig. 1. Flow chart of the senescence phenotyping guideline. The upper part presents the analysis of growth and senescence at the whole-plant level with non-invasive and invasive measurements. The lower part represents the senescence phenotyping at the leaf level taking into account leaf position (age) within the rosette. Black lines and asterisks indicate that the processing can be done later and the plant material can be frozen and stored at -80 °C. Red dashed lines indicate immediate processing is required. ACA can be done at both the whole-rosette and leaf levels non-invasively from photographs or invasively from scans.

such as bolting, flowering, or first silique shattered. In our conditions, Col-0 plants started to bolt and flower at approximately 19 and 28 d, respectively (Fig. 2A–C). Sampling was started when the plants reached their maximal rosette area at bolting time (week 3) and was continued until rosette, stem, and silique walls were almost completely senescent at approximately 50 d after sowing (week 7; Fig. 2A–C). Sampling and measurements were done at the same time of the day to avoid circadian effects.

Senescence was evaluated at both the whole-rosette and leaf levels using different early and late markers involved in key senescence-related processes. Four plants were dissected each week to analyse senescence at the whole-rosette

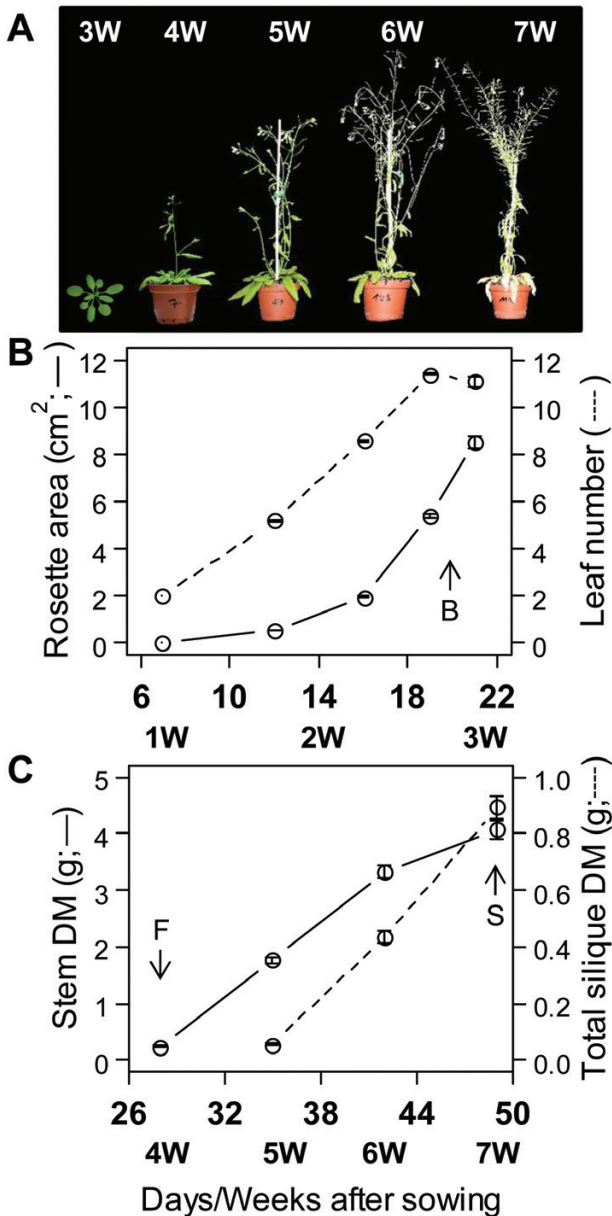


Fig. 2. Plant growth and development analyses. (A) A representative picture of Col-0 growth and senescence over 3–7 weeks after sowing. (B) Rosette area (solid line) and leaf number (dashed line), and (C) total stem (solid line) and silique dry mass (DM; dashed line) per d/week after sowing. Data are means (\pm SE) of 16–80 leaves. Arrows indicate bolting (B), flowering (F), and first yellowish siliques (S) stages.

level by using Chl fluorescence (ChlF; i.e. photosynthetic efficiency, F_v/F_m) and an automated colourimetric assay (ACA; Fig. 1). The other markers were assessed in individual leaves of 12 plants taking into account the leaf position (age) within the rosette (Fig. 1). Since old and young leaves also show extensive differences in gene expression (Hinderhofer and Zentgraf, 2001; Zentgraf *et al.*, 2004), using the same leaf position for distinct measurements is crucial for reliable, reproducible, and comparable data. The leaves emerging after the cotyledons were numbered continuously from old to young, starting at the two first leaves and ending before the emergence of the cauline leaves, which are recognizable by their small and pointed leaf blade and lack of petioles (Steynen *et al.*, 2001). Leaf positions were labelled when the first leaves were fully expanded by marking each leaf with a coloured thread following a colour-code (Fig. 1; Hinderhofer and Zentgraf, 2001). After growth cessation, Col-0 rosettes displayed 10 leaves on average (Fig. 2B), meaning that all senescence-markers could routinely be analysed in the same plant but in different detached leaves (Fig. 1). The decline of photosynthetic capacity, mainly occurring during the reorganization phase, was analysed by direct and indirect measurements of Chl levels via measurements relying on light transmittance through the leaves (atLeaf+ Chl meter), ChlF, and Chl extractions. These measurements were done consecutively in the same leaves but at two different leaf positions: position 5 and 10 (except for Chl extraction, only at leaf position 5). These young and middle-aged leaves allow the analysis of early and late effects of senescence on the photosynthetic capacity. Membrane deterioration was estimated by measuring electrolyte leakage (EL) and lipid peroxidation. For measuring EL, leaves at position 4 were used. These relatively old leaves were selected because membrane integrity is mainly affected during the termination phase of senescence. Membrane damage through lipid peroxidation is mostly driven by increased ROS production, which has been shown to be higher in young leaves than in old leaves (Bieker *et al.*, 2012). Hence, lipid peroxidation and total anthocyanin content were measured in two pools, each composed of six leaves at position 9. For the same reason, hydrogen peroxide (H_2O_2) was quantified in leaves at position 8 to determine changes in the redox status during senescence. Finally, developmental gene regulation was analysed in leaves at positions 6 and 7, through expression of key senescence-related genes by quantitative real-time polymerase chain reaction (qRT-PCR) in two distinct pools by leaf position (composed of six leaves each). Leaf positions were chosen here in order to have enough material and to be able to compare expression levels to the reference transcriptome provided for leaf seven by Breeze *et al.* (2011). Leaves at position 3 can be used to profile the activity of anti-oxidative enzymes such as catalases or ascorbate peroxidases. Leaves 11 and 12 were used as backups for other analyses. Methods and results are presented and explained in detail in the sections below. All protocols used are provided in the supplementary information.

Quantifying leaf senescence based on the breakdown of photosynthetic capacity

The different methods to analyse the breakdown of photosynthetic activity specified below are complementary and describe different aspects related to Chl degradation during senescence. Applying all of them gives the most holistic view of this process; however, if specific instruments are not at hand, e.g. atLeaf+ Chl meter or ChlF imaging, these measurements can be skipped in favour of Chl extraction and ACA.

Chlorophyll content through extraction and relative measurements

Photosynthesis is gradually inactivated during senescence and accompanied by degradation of Chl. Total leaf Chl content is the most popular trait for characterizing senescence progression related to the photosynthetic capacity. In higher plants, two forms of pigments prevail, Chl *a* and Chl *b*, which are differently involved in light harvesting. Chl *a* is linked to energy-processing centres of the photosystems (PS) whereas Chl *b* is considered an accessory pigment that transfers light energy to Chl *a* (Tanaka and Tanaka, 2006). During senescence, the Chl *a/b* ratio gives a valuable indication of the underlying process of chloroplast degradation (Pruzinská *et al.*, 2005; Sakuraba *et al.*, 2012). There are different methods to assess Chl levels in leaves. Traditionally, leaf Chl concentration is determined by spectrophotometric measurements of an 80% acetone extract. Absorbance is then converted to Chl concentration using standard equations derived from Arnon (1949; see Supplementary Protocol S1). In addition to the quantification of total Chl amount, this method allows Chl *a* and *b* levels to be distinguished based on their distinct absorption peaks, at 662.6 nm and 645.6 nm, respectively. Chl concentrations can be normalized by fresh weight (FW) or by leaf area (i.e. mg Chl g⁻¹ FW or mg Chl cm⁻²). Depending on plant growth conditions, Chl concentrations start to decrease at different time points during development. For example, decreased Chl levels have been shown at approx. 10 d after *A. thaliana* flowering under long days, 250 μmol m⁻² s⁻¹ light, 22 °C and 70% relative humidity (Breeze *et al.*, 2011). In our conditions, the total Chl concentration per unit FW was reduced by 27% one week after flowering (week 5 after sowing), parallel to an increased Chl *a/b* ratio (Fig. 3A). While Chl *a* level stayed almost constant, a decline in Chl *b* content was observed. This phenomenon mainly results from the conversion of Chl *b* to Chl *a* during degradation (Ito *et al.*, 1996). During silique maturation (week 7), the Chl *a/b* ratio was reduced and returned to values close to 1, due to equally low levels of Chl *a* and *b* in fully senescent leaves (Fig. 3A). In Arabidopsis, an increased Chl *a/b* ratio has also been shown during dark-induced senescence (Pruzinská *et al.*, 2005; Sakuraba *et al.*, 2012). However, senescence can affect the Chl *a/b* ratio differently depending on the species. An increase at late senescence stages was shown in barley (Krupinska *et al.*, 2012), whereas a decrease occurred in *Phaseolus vulgaris* and *Acer pseudoplatanus* (Jenkins *et al.*, 1981; Maunders and Brown, 1983).

A handheld Chl meter, relying on light transmittance through the leaf surface, provides a convenient and non-invasive method to measure relative Chl content. Optical values obtained from Chl meters are highly correlated to extractable leaf Chl levels (Novichonok *et al.*, 2016). In principle, optical values can be directly converted into Chl content. Here, we used the atLeaf+ Chl meter, which measures leaf absorbance of both 660 nm (red) and 940 nm (near-infrared) wavelengths. Red light is strongly absorbed by Chl, whilst near-infrared light is used as a reference wavelength to compensate for differences in leaf structure, notably leaf thicknesses (Markwell *et al.*, 1995). A single measurement takes only a few seconds and the measuring device is small enough to use on the small leaves of Arabidopsis (bigger than 0.2 cm²). As environmental and measurement conditions can substantially influence atLeaf+ readings, measurements should be standardized as far as possible. Moreover, the non-uniform Chl distribution that occurs in leaves during senescence also has to be considered. For reproducible measurements, the readings should be done with the same leaf orientation (i.e. abaxial side up) and repeated several times over the flattened surface of the whole leaf (e.g. from the tip to the base). The proportion of leaf veins in larger leaves has an influence on the light transmittance, and therefore primary and secondary veins should generally be excluded from the measurements (Uddling *et al.*, 2007). The timing of readings is also important as the diurnal chloroplast movements in response to light affect the degree of heterogeneity in the Chl distribution (Hoel and Solhaug, 1998). Over the course of our study, 12 samples of detached leaves of both young and middle-age (positions 10 and 5, respectively) were analysed, and the atLeaf+ values could be converted into total chlorophyll content in mg cm⁻² (<http://www.atleaf.com/SPAD.aspx>). As expected based on their position inside the rosette, leaf 5 globally presented lower atLeaf+ values compared to leaf 10 over the time course of the experiment (Fig. 3B). Leaf 5 displayed a significant decrease in atLeaf+ values one week after flowering, with reductions of 34% and 51% at weeks 5 and 6, respectively. Leaf 10 presented a lower decrease relatively to leaf 5, shown by a constant reduction (around 13%) until week 6 followed by a strong decline (Fig. 3B). atLeaf+ values for leaf 5 were linearly and positively correlated to the extracted total Chl concentration ($R^2=0.82$; $P\leq 0.001$). However, the relationship between atLeaf+ and the Chl *a/b* ratio was more complex and showed a curvilinear regression (data not shown). These two methods allow the time point of Chl breakdown to be defined as being during weeks 5 and 6 after sowing, and to schedule senescence initiation at flowering (week 4).

Chlorophyll fluorescence imaging

ChlF imaging, such as the pulse amplitude modulation (PAM) method, is also a widely used tool to assess photosynthetic status (Maxwell and Johnson, 2000). This method provides a non-invasive evaluation of the efficiency of PSII to supply electrons to the photosynthetic machinery. It also has the advantage of being applicable at the whole-rosette or leaf levels in various different plant species (Murchie and Lawson, 2013).

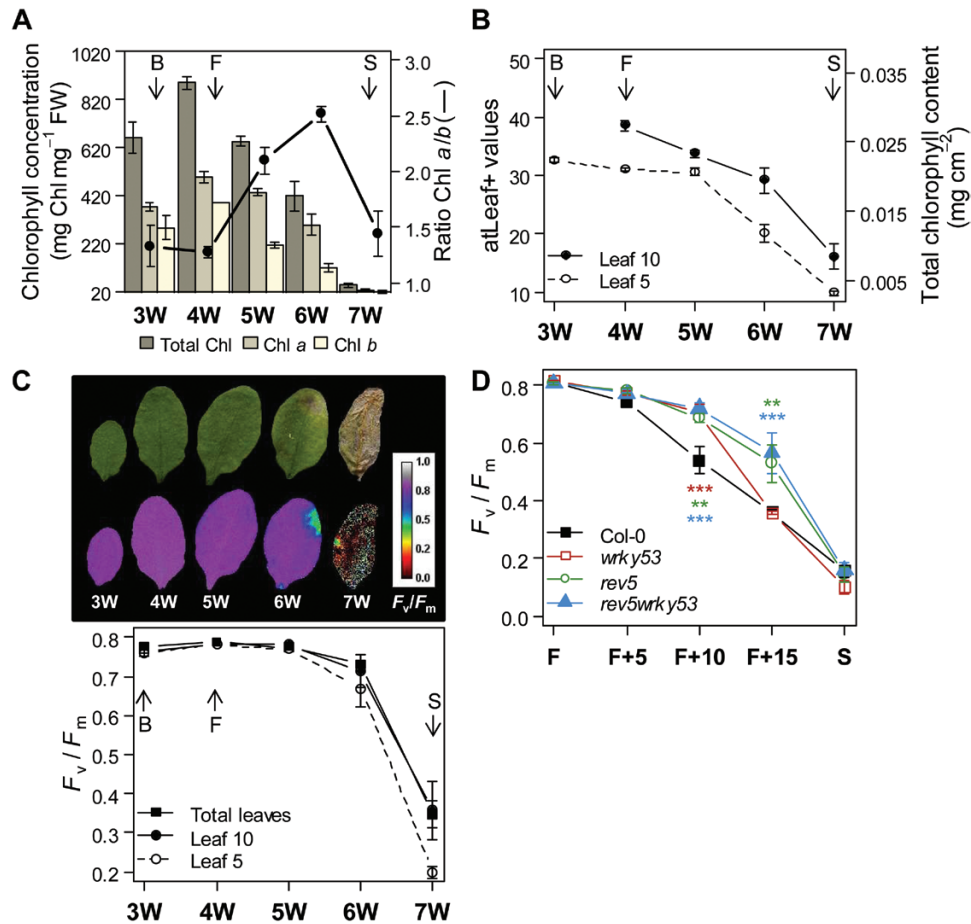


Fig. 3. Breakdown of photosynthetic capacity during leaf senescence. These measurements were taken consecutively on the same leaves at positions 5 and 10 (except for chlorophyll, Chl, content, only for leaf 5). (A) Total Chl, Chl a, and Chl b concentrations expressed by leaf fresh weight (FW) are indicated by the bars and the Chl a/b ratio by the black line. (B) Chl contents were measured using an atLeaf+ chlorophyll meter in Col-0 leaves over 3–7 weeks after sowing. Optical atLeaf+ values can be directly converted to total Chl content (right axis; <http://www.atleaf.com/SPAD.aspx>). (C) Top: representative leaves at position 5 in a false colour scale of photosynthetic efficiency (F_v/F_m), ranging from black (value 0) through red, yellow, green, blue to purple (ending at 1). Bottom: F_v/F_m values at the whole-rosette and leaf levels over time. Data are means (\pm SE) of 4–12 leaves. (D) Example of F_v/F_m measurements in knockout mutants delayed in senescence (*wrky53*, *rev5*, and *rev5wrky53*) from flowering (F) until the first siliques started yellowing (S). F+5, F+10, and F+15 indicate days after flowering. Data are means (\pm SE) of 5–8 plants per genotype. Significant differences were analysed using the Kruskal–Wallis test: * $P \leq 0.05$, ** $P \leq 0.001$, and *** $P \leq 0.0001$. Arrows in (A–C) indicate bolting (B), flowering (F), and first yellowish siliques (S) stages.

ChlF is based on the quantification of the light re-emitted in red wavebands by dark-adapted leaves, after having been subjected to a saturating flash. Amongst the ChlF parameters, the F_v/F_m ratio, reflecting the maximal quantum yield of PSII photochemistry, is used as a sensitive and rapid indicator of physiological status (Genty et al., 1989). Senescence- or stress-induced damage to the photosynthetic apparatus leads to a reduction of F_v/F_m values (Maxwell and Johnson, 2000; Bresson et al., 2015). F_v/F_m has been shown to be closely related to the leaf relative water content and the Chl a content (Woo et al., 2008; Filipovic et al., 2013). Measurement of F_v/F_m is initiated by exposing dark-adapted leaves to a low modulated light beam to elicit a minimum value of ChlF, F_0 . Dark-adaptation of leaves is a crucial step and should last 15–20 min for Arabidopsis. F_0 represents the basal fluorescence when excitation energy is not being transferred to the PSII reaction centres. After dark adaptation, the application of a brief saturating flash induces a maximum value of ChlF, F_m , which reflects the electron accumulation through PSII. The difference between F_0 and F_m is the variable fluorescence,

F_v , and F_v/F_m is given by $(F_m - F_0)/F_m$ (Genty et al., 1989). The settings for the light pulses are dependent on both growth conditions and the device used, and should be adjusted in order to reach F_v/F_m values of approximately 0.83 for healthy (fully green) plants. Values significantly under this threshold are indicative of an impaired physiological status, and under 0.3 the leaf tissues are considered as dead (Woo et al., 2008). Our ChlF measurements were performed using the Imaging-PAM chlorophyll fluorometer and ImagingWin software application (Maxi version; ver. 2-46i, Heinz Walz GmbH; see Supplementary Protocol S2). The plants were dissected and leaves were fixed on the abaxial side with increasing age from left to right on black paper using double-sided tape. Data extraction from the ChlF images was done with an ImageJ (1.47v, Rasband, Bethesda, Maryland, USA) macro modified from Bresson et al. (2015). False-colour images of F_v/F_m permit the visualization of the spatio-temporal progression of senescence in leaves (Fig. 3C).

Senescence is often described as progressing from the leaf tip to the base with a bleaching gradient, but this is not a fixed

rule. From our experience, senescence progression can be spatially heterogeneous within the leaf, starting for example from the margins or in some cases even from the base. When examining the mean F_v/F_m value of all detached leaves over time, it displayed a similar pattern as if only leaves at positions 5 and 10 were considered (Fig. 3C). F_v/F_m dropped rather suddenly 6 weeks after sowing when senescence was clearly visible and Chl levels and *atLeaf+* values were drastically reduced (Fig. 3A–C). In an independent experiment, ChlF was analysed in different lines delayed in their senescence progression, such as *wrky53*, *rev5*, and the double-knockout mutant *wrky53rev5* (Fig. 3D). WRKY53 is a well-known positive key regulator of age-induced leaf senescence (Zentgraf *et al.*, 2010) while REVOLUTA (REV) has been recently identified as a direct and positive regulator of WRKY53 expression (Xie *et al.*, 2014). The plants were harvested according to their developmental stages from flowering until the first siliques started yellowing. Fig. 3D shows that the different mutants exhibited a significantly slower decline of F_v/F_m 10 d after flowering and reached equal F_v/F_m levels compared to Col-0 only during maturation of siliques. *rev5* and *wrky53rev5* presented an even more pronounced delay of senescence than *wrky53*, as previously shown by Xie *et al.* (2014). Although ChlF is a powerful tool to discriminate senescence mutant lines, F_v/F_m appears to be a later marker during the reorganization phase compared to extracted Chl and *atLeaf+* values. However, ChlF imaging allows the easy analysis of the F_v/F_m patterns of the rosette in a dynamic manner and the estimation of the switch points of leaf senescence, as shown for example in *rev5* compared to Col-0 (see Supplementary Fig. S1).

Automated colourimetric assay (ACA)

Chl degradation is the earliest and most significant change that is visible to the naked eye. This is generally manifested by progressive leaf colour modifications from deep green to pale green, to yellow, and to brown (dry) as the final step. One of our former methods used to monitor senescence was to assign each leaf of the rosette to different categories according to its colour by visual inspection (e.g. green, green-yellow, yellow, and brown) and to calculate the proportion of each compared to the total leaf number (Miao and Zentgraf, 2010). Although this method can provide a reliable measure, it can be somewhat subjective due to the difficulties to assigning a general colour to leaves presenting colour heterogeneity. To avoid bias in leaf colour assignment, we have developed an automated colourimetric assay, which allows clustering each pixel within a leaf depending on its colour (see Supplementary Protocol S3 and <http://www.zmbp.uni-tuebingen.de/gen-genetics/research-groups/zentgraf.html>). ACA allows the single colour categorization by leaf to be ignored by instead giving an accurate quantification of each colour percentage within the leaf. ACA can be used in a non-invasive manner at the whole-rosette level, or in detached leaves. Non-invasive application on whole-rosettes also allows pre-screening of many plant lines before starting with detailed phenotyping of selected lines, or even the use of automated phenotyping platforms. Here, the *A. thaliana*

rosettes were dissected; leaf blades were separated from their petiole, sorted by age, stuck to black paper, and scanned. Zenithal photographs can be used but the image acquisition settings (especially the lighting) must be homogeneous within an image and constant over experiments. Scans of leaves usually offer the best homogeneity. Leaves were then individually separated in single images using a semi-automatic ImageJ macro (see Supplementary Protocol S3). After manual selection of the region of interest from the background and also the labelling of pictures by plant identification and leaf position number. Using R scripts (R Development Core Team, 2009), ACA was designed to automatically extract information such as genotype and plant age as well as leaf and plant number on the basis of the file name. ACA is based on grouping of each pixel of a picture depending on its position in the hue saturation value (HSV) colour-space. The three-dimensional representation of the HSV colour-space offers the opportunity to define ranges of colours taking into account three different channels (see Supplementary Protocol S3). We have defined six colour groups using Col-0 leaf pictures from four independent experiments with different growth conditions, notably with regard to light intensity (see Supplementary Fig. S2). The black background was first identified by filtering pixels based on both V and S channels, defined by $V \leq 15\%$ and $S \leq 10\%$. The remaining pixels were grouped into bins describing green, green-yellow, yellow, brown, purple, or unknown (Fig. 4A). To achieve that, H, S, and V distributions of pictures of green, yellow, and brown leaves (classified visually) were examined, thus allowing definition of thresholds for each colour (see Fig. 3 in Supplementary Protocol S3). The purple category comprises all pinkish-purplish colours that are related to anthocyanin production (Fig. 4A). Although in some cases anthocyanin accumulates during senescence, the purple colour did not only appear in the last stage of senescence progression (from green to brown) but was also found independent of leaf age (e.g. in fully green leaves). All pixels that did not belong to the five defined classes were categorized as unknown. The percentage of each class was then calculated by subtracting background from the total pixel count. Unknown pixels represented only 0.002% across the different experiments. Fig. 4A shows a comparison of colour assignments between ACA and visual inspection. For example, a leaf considered by eye as being globally yellow displayed colour heterogeneity, with 22.6, 75.8, and 1.6% of green-yellow, yellow, and brown colours, respectively.

Here, in long-day and low-light conditions, green-yellow colours reflecting the onset of Chl breakdown during the reorganization phase of senescence appeared 6 weeks after sowing at the whole-rosette level and in leaf 5, and 7 weeks after sowing in leaf 10 (Fig. 4B). This is one week after the first decrease in Chl content and in *atLeaf+* values, but in accordance with modifications observed in F_v/F_m values (Fig. 3). Indeed, green percentage was linearly and positively correlated to F_v/F_m values ($R^2=0.76$; $P \leq 0.001$), whereas green-yellow, yellow, and brown were negatively correlated ($R^2=0.18$, 0.17, and 0.68, respectively; $P \leq 0.001$). The purple class was represented only marginally over the experiment, reaching a

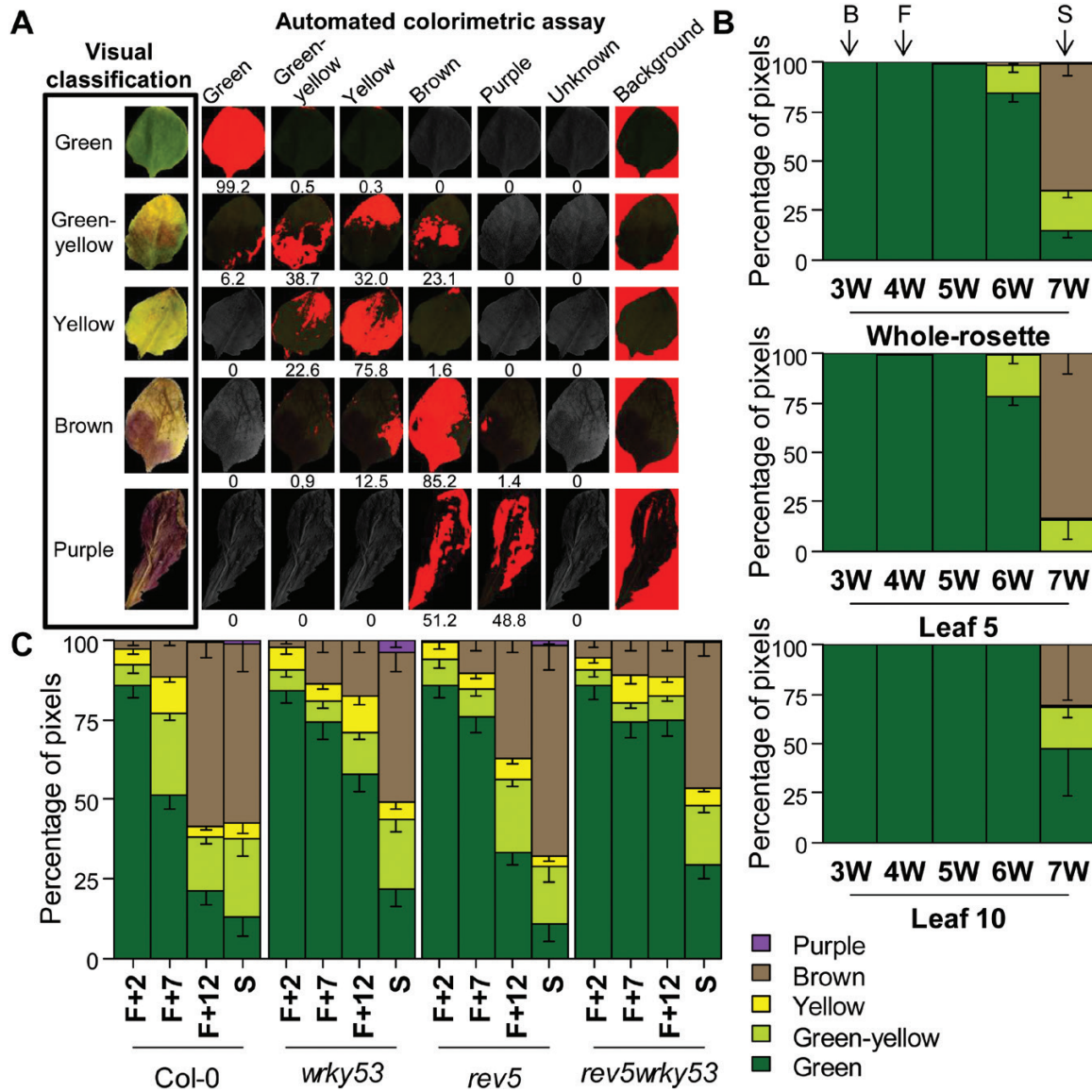


Fig. 4. Automated colourimetric assay (ACA). (A) Comparison of leaf colour assignment between visual inspection and ACA. Numbers indicate percentage of pixels of the respective colours. (B) ACA in Col-0 plants grown in long-day and low-light conditions, presented for the whole-rosette and in leaves 5 and 10 over 3–7 weeks after sowing. Data are means (\pm SE) of four plants. (C) Example of ACA in knockout mutants delayed in senescence (*wrky53*, *rev5*, and *rev5wrky53*) from flowering (F) until the first siliques started yellowing (S). F+2, F+7, and F+12 indicate days after flowering. Data are means (\pm SE) of 3–4 plants. Colour classes are organized from top to bottom: purple, brown, yellow, green-yellow, and green. Purple colours are related to anthocyanin production and do not reflect the last stage of senescence progression (from green to brown). Arrows indicate bolting (B), flowering (F), and first yellowish siliques (S) stages.

maximum of 0.9% in the termination phase (week 7). ACA was also performed on the *wrky53*, *rev5*, and *wrky53rev5* senescence-delayed lines over the period of development after flowering (Fig. 4C). While the different plants displayed a nearly similar whole-rosette pattern 2 d after flowering, Col-0 had a higher green-yellow percentage 7 d after flowering, resulting in a higher brown percentage 12 d after flowering. ACA thus validated the fact that senescence was delayed in these mutants. As for F_v/F_m values, the different mutants presented similar patterns compared to Col-0 during the maturation of the siliques (Fig. 4C). ACA thus permits quantification of senescence that is closely correlated to other Chl content-related measurements and can be robust across a variety of image samples.

Molecular and physiological investigations for analysing leaf senescence

Redox regulation: the case of hydrogen peroxide

Living cells constantly balance generation and scavenging of ROS in all cellular compartments to keep the redox status under tight control. In Arabidopsis, a network of at least 152 genes including ROS-scavenging and ROS-producing proteins is involved in managing ROS levels (Mittler et al., 2004). Throughout senescence ROS, especially H_2O_2 , play a pivotal role in signalling and molecule degradation (Zentgraf et al., 2012). Many senescence-associated TFs are highly responsive to H_2O_2 including, for example, *WRKY53* (Miao et al., 2004), *ORS1* (Balazadeh et al., 2011), *JUB1* (Wu et al., 2012), and

ATAF1 (Garapati *et al.*, 2015). Additionally, plants affected in H_2O_2 production or with changes in scavenging capacities show altered senescence phenotypes (Barth *et al.*, 2004; Bieker *et al.*, 2012). In Arabidopsis, the initiation of senescence coincides with an increase in intracellular H_2O_2 concentrations (Fig. 5A, B). This temporal loss of anti-oxidative capacity appears to be mainly achieved by a decrease in CATALASE2 (CAT2) and ASCORBATE PEROXIDASE1 (APX1) activities, two key H_2O_2 -scavenging enzymes (Ye *et al.*, 2000; Zimmermann *et al.*, 2006). Initially, transcriptional down-regulation of *CAT2* leads to increasing H_2O_2 levels, which in turn induce post-translational inactivation of APX1 (Panchuk *et al.*, 2005). The inhibition of APX1 activity creates a positive feedback loop driving the first H_2O_2 peak, which appears to be restricted to the bolting period.

As a consequence of high H_2O_2 levels, *CAT3* expression and activity are induced, which then lower the H_2O_2 levels and contribute to the recovery of APX1 activity. An even more substantial second H_2O_2 peak occurs during the termination phase of senescence, which most likely originates from degradation processes such as lipid degradation, membrane deterioration, and disruption of the electron transport chains.

Due to the inherent reactivity and instability of ROS, the specific and sensitive detection of intracellular ROS in a biological system is difficult and laborious. Here, we measured H_2O_2 contents in detached Col-0 leaves (Fig. 5B) using a semi-quantitative method according to Cathcart *et al.* (1983). This fluorescent assay uses 5(6)-carboxy-dichloro-fluorescein diacetate (carboxy- H_2DCFDA), which can react with several ROS including H_2O_2 , hydroxyl radicals, and peroxynitrite.

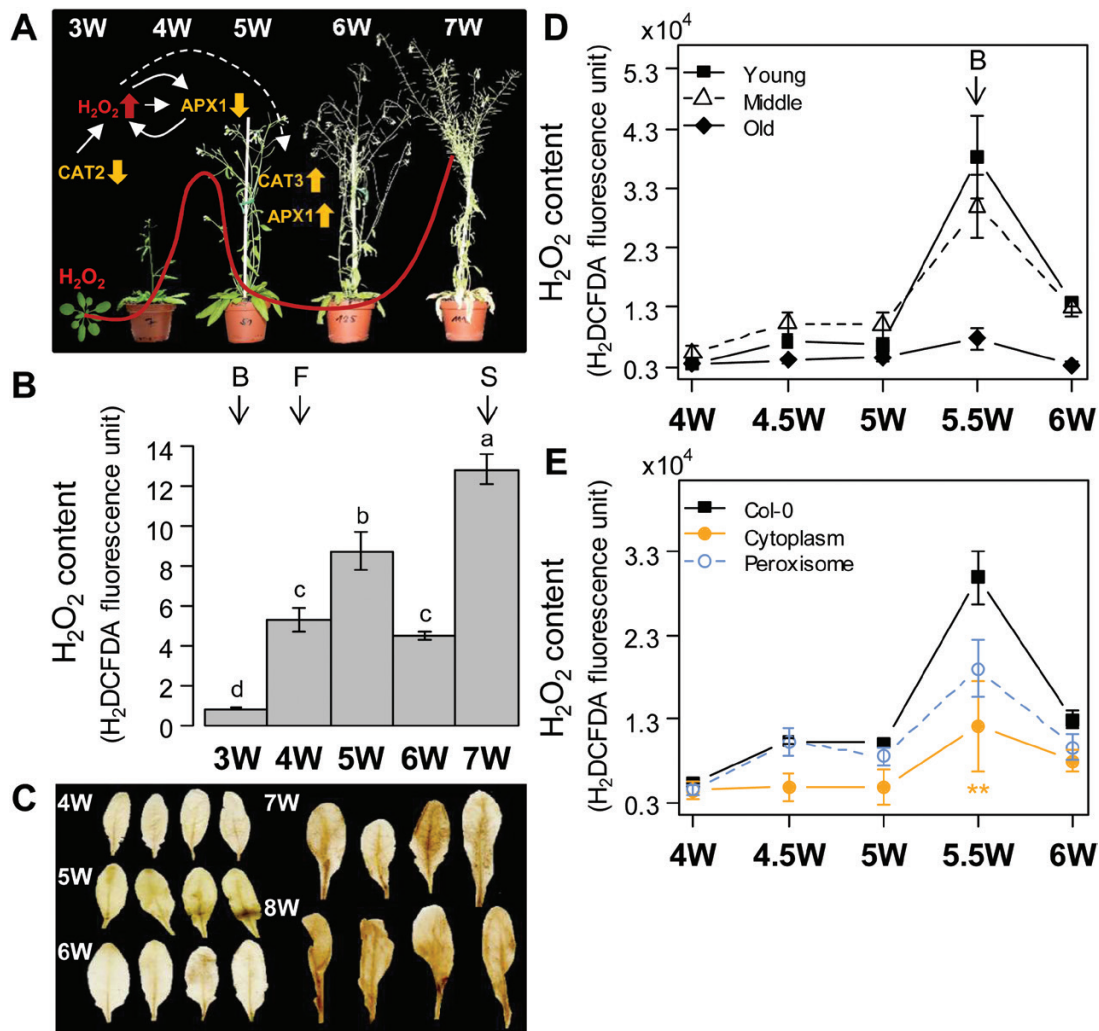


Fig. 5. Hydrogen peroxide plays a pivotal role during age-induced senescence initiation and progression. (A) Model of hydrogen peroxide (H_2O_2) regulation throughout senescence via H_2O_2 -scavenging enzyme activities, notably CATALASES (CATs) and ASCORBATE PEROXIDASE 1 (APX1; according to Zimmermann *et al.*, 2006). (B) H_2O_2 content in Col-0 leaves over 3–7 weeks after sowing. H_2O_2 content was measured using a carboxy- H_2DCFDA fluorescence assay in independent leaves at position 9. Data are means (\pm SE) of 12 leaves. Different letters indicate significant differences according to the Kruskal–Wallis test at $P \leq 0.05$. (C) Illustration of DAB staining in four independent Col-0 leaves from 4–8 weeks after sowing. (D) H_2O_2 content over 4–6 weeks after sowing depending on Col-0 leaf position: young (leaves 8–12), middle-aged (leaves 4–7), and old (leaves 1–3), according to Bieker *et al.* (2012). Data are means (\pm SE) of at least three replicates. (E) Example of changes in H_2O_2 pattern in middle-aged leaves using two different lines having altered H_2O_2 levels in either the peroxisome or cytoplasm, according to Bieker *et al.* (2012). Values are means (\pm SE) of 10–15 biological replicates. Significant differences were analysed according to the Kruskal–Wallis test ($*P \leq 0.05$). Arrows indicate bolting (B), flowering (F), and first yellowish siliques (S) stages.

Although more H₂O₂-specific dyes such as di-amino-benzidine exist, they are often highly toxic and thus not easy to handle. Furthermore, techniques such as cerium-chloride staining or spin trapping require special equipment such as an electron microscope or an electron paramagnetic resonance spectroscopy, respectively. Additionally, cerium chloride has a low cell-penetration efficiency, and thus requires relatively long incubation times. Carboxy-H₂DCFDA is a non-polar dye able to passively diffuse across cellular membranes. It is trapped inside the cells after deacetylation by an intracellular esterase, rendering the molecule polar. Deacetylated carboxy-H₂DCFDA can then be oxidized by ROS and is converted to highly fluorescent dichlorofluorescein (DCF). Only intracellular DCF is measured, as extracellular oxidized dye is not able to enter the cells and leaves are rinsed after incubation. In order to get comparable results with different dye stock solutions, calibration of the dye is required. Two options are given here, both include chemical deacetylation followed by oxidation of the dye via H₂O₂ (see Supplementary Protocol S4). H₂O₂ content can be expressed on a per leaf basis, or it can be normalized by leaf FW or area in cases of significant size differences between genotypes. For other plant species having larger leaves, a combination of FW and area (e.g. weighed leaf discs with the same diameter) usually gives the best results.

Another possibility to visualize *in situ* modifications in leaf H₂O₂ content during senescence is the 3,3'-diaminobenzidine (DAB) staining method, which has to be used with caution because of its toxicity (see Supplementary Protocol S4). Although this method can also be conducted quantitatively, we used it here to analyse the spatio-temporal H₂O₂ accumulation in leaves (Fig. 5C). DAB is oxidized by H₂O₂ in the presence of haem-containing proteins, such as peroxidases, leading to an easily visible dark brown precipitate. This is exploited as a stain to detect the presence and localization of H₂O₂ in plant cells (Daudi and O'Brien, 2012). Fig. 5C illustrates DAB staining of individual Col-0 leaves from 4 to 8 weeks after sowing, from an independent experiment. The variations of stain intensity were comparable with the measured fluctuations in leaf H₂O₂ content during plant development (Fig. 5B, C). It is also important to note that the leaf position for H₂O₂ measurement is crucial, because levels increase differently depending on age and position of the respective leaves. The youngest and middle-aged leaves (leaves 8–12 and 4–7, respectively) show a higher increase in H₂O₂ whereas the oldest leaves (1–3) present a poor and negligible H₂O₂ peak (Fig. 5D; Bieker *et al.*, 2012).

To illustrate the contribution of H₂O₂ measurement for senescence analyses, we present some examples of Arabidopsis lines affected in leaf senescence. Two prevalent changes in H₂O₂ pattern can be observed, mainly related to modifications in H₂O₂ peaks. Fig. 5E shows results of two different lines having an altered H₂O₂ level in either peroxisomes or cytoplasm by the overexpression of the fusion *Escherichia coli* protein OxyR-RD-cpYFP (Belousov *et al.*, 2006; Costa *et al.*, 2010) that consumes H₂O₂. Both transgenic lines have clearly shown a slower senescence progression (Bieker *et al.*, 2012). The H₂O₂ peak observed in wild-type plants at bolting

(here at 5.5 weeks after sowing) occurred at the same time point in both transgenic lines but with significantly reduced amplitudes (Fig. 5E). On the other hand, a delay in senescence can also translate into a delay of the H₂O₂ peak with equal amplitude compared to Col-0 plants, as it was shown for *wrky53* knockout lines, which are delayed in senescence initiation (see Supplementary Fig. S3).

As well as the intracellular H₂O₂ content, CAT and APX activities can also be used as early physiological markers of senescence. Their activities decrease in Arabidopsis at a very early stage during bolting time and before the beginning of Chl breakdown (Supplementary Fig. S4; Zimmermann *et al.*, 2006). This has also been observed in other plant species, for example oilseed rape and sun flowers (Agüera *et al.*, 2010; Bieker *et al.*, 2012). Here, we give two different protocols to monitor the activity of these enzymes (see Supplementary Protocol S5). Native PAGE followed by in-gel activity staining allows the visualization of changes at the isoform level, but quantification is not easily feasible in a reproducible manner. In contrast to in-gel activity profiling, photometric assays can easily quantify total enzyme activities, but isoform-specific alterations cannot be detected.

Genetic regulation of age-induced leaf senescence markers

Identifying the dynamic changes in transcript levels gives helpful clues about key switch points in the different leaf senescence phases. Transcriptome studies using expressed sequence tag libraries and *A. thaliana* genomic arrays have revealed that senescence involves the expression of thousands of genes and many signalling pathways (Zentgraf *et al.*, 2004; Buchanan-Wollaston *et al.*, 2005; Breeze *et al.*, 2011). Genes up- or down-regulated in expression are grouped into two categories: senescence-associated genes (SAGs; Lohman *et al.*, 1994) and senescence down-regulated genes (SDGs). Among these genes, many TFs have been identified as key regulators in the control of senescence and can be used for characterizing senescence progression, such as *NAC*, *WKRY*, *MYB*, *bZIP*, and *bHLH* family members (Liu *et al.*, 2010; Li *et al.*, 2012). In this large network, we have chosen some *A. thaliana* key SAG and SDG markers at both early and late senescence stages, which we recommend as a basic set (Table 1, Fig. 6). However, other marker genes might also be suitable if specific functional aspects of senescence need to be analysed in detail. Gene expression levels were followed by qRT-PCR of Col-0 leaves over four consecutive weeks (Fig. 6; see Supplementary Protocol S6). Samples harvested in the last week (week 7) were removed from the analyses because leaves were almost completely senescent and dead, and hence only very low amounts of RNA could be isolated and no reliable transcript levels were detected. Transcriptional changes were calculated based on the comparative C_T method (Pfaffl, 2001) and normalized to *ACTIN2* levels (Panchuk *et al.*, 2005).

SAGs are up-regulated during senescence but their expression patterns in the course of plant development are quite variable due to the large spectrum of their functions (Lohman *et al.*, 1994; Weaver *et al.*, 1998). Many SAGs also respond

Table 1. List of key genes involved in age-induced senescence

Name	Locus	Description	Relevant papers
Senescence-associated genes (SAGs): up-regulated during senescence			
<i>SAG12</i>	At5g45890	Encodes a cysteine protease	Lohman <i>et al.</i> , 1994; Weaver <i>et al.</i> , 1998; Noh and Amasino, 1999
<i>SAG13</i>	At2g29350	Encodes a short-chain alcohol dehydrogenase	Gan, 1995; Weaver <i>et al.</i> , 1998
<i>WRKY53</i>	At4g23810	Member of WRKY transcription factor family (group III)	Hinderhofer and Zentgraf, 2001; Miao <i>et al.</i> , 2004; Zentgraf <i>et al.</i> , 2010
<i>ANAC092</i>	At5g39610	Encodes a NAC-domain transcription factor (also called <i>AtNAC2</i> , <i>ORE1</i>)	Balazadeh <i>et al.</i> , 2008, 2010; Kim <i>et al.</i> , 2009
<i>ATG7</i>	At5g45900	Encodes an E1 enzyme for the ubiquitin-like autophagy proteins (also called <i>APG7</i> and <i>AtAPG7</i>)	Doelling <i>et al.</i> , 2002; Thompson and Vierstra, 2005; Breeze <i>et al.</i> , 2011
<i>ZAT12</i>	At5g59820	Encodes a zinc finger protein	Rizhsky <i>et al.</i> , 2004a; Davletova <i>et al.</i> , 2005; Miller <i>et al.</i> , 2008
<i>CAT3</i>	At1g20620	Encodes a heme-containing enzyme with catalase activity to detoxify H ₂ O ₂	Orendi <i>et al.</i> , 2001; Zimmermann <i>et al.</i> , 2006; Du <i>et al.</i> , 2008
Senescence down-regulated (SDGs): down-regulated during senescence			
<i>CAT2</i>	At1g58030	Encodes a heme-containing enzyme with catalase activity to detoxify H ₂ O ₂	Orendi <i>et al.</i> , 2001; Zimmermann <i>et al.</i> , 2006; Du <i>et al.</i> , 2008
<i>RBCS1A</i>	At1g67090	Encodes a member of the Rubisco small subunit (RBCS) multigene family	Mae <i>et al.</i> , 1984; Izumi <i>et al.</i> , 2012
<i>CAB1</i>	At1g29930	Encodes a subunit of light-harvesting complex II (also called <i>LHCB1.3</i>)	Green <i>et al.</i> , 1991; Weaver <i>et al.</i> , 1998

to environmental stresses and can be considered as integrators of the different signalling pathways controlling stress responses and/or age-dependent senescence (Weaver *et al.*, 1998). Generally, *SAG12* and *SAG13* expression are the most extensively used SAG markers, reflecting late and early status of senescence, respectively. *SAG12* has been strictly associated with naturally induced senescence (Noh and Amasino, 1999). It encodes a putative cysteine protease, located predominantly in senescence-associated vacuoles involved in protein degradation (Carrion *et al.*, 2013). In oilseed rape, the *SAG12/Cab* expression pattern has been shown to reflect the transition from sink to source tissue for nitrogen (Gombert *et al.*, 2006). Although *SAG12* is involved in the massive proteolytic processes in later senescence stages, its specific targets and functions in Arabidopsis senescence are still unclear as mutants have shown no altered senescence phenotype and display normal growth and development (Otegui *et al.*, 2005; Masclaux-Daubresse *et al.*, 2010). Nevertheless, its expression is regulated in a developmentally controlled, senescence-specific manner (Noh and Amasino, 1999). *SAG12* is highly up-regulated at the mRNA level only in senescent tissues (week 6; Fig. 6A). *SAG13* encodes a protein related to a short-chain alcohol dehydrogenase and/or oxidoreductase (Gan, 1995) and is quite differently regulated from *SAG12*. Expression rose slightly before senescence initiation (week 4) and then progressively increased (Fig. 6B). Modifications in the dynamics of *SAG12* and *SAG13* expression have been shown in various mutants affected in senescence (e.g. He and Gan, 2002; Miao *et al.*, 2004).

In addition, the *NAC* and *WRKY* families constitute the two largest groups of TFs in the senescence transcriptome (Guo *et al.*, 2004). They represent valuable markers playing central roles in senescence (Guo and Gan, 2006; Zentgraf *et al.*, 2010). As key senescence-related TFs, *WRKY53* and *ANAC092* have been shown to affect the expression of many

known senescence-regulated genes involved in, for example, reallocation of nutrients, cell wall modifications, and amino acid and hormone metabolism (Balazadeh *et al.*, 2010). Here, qRT-PCR analyses revealed that *WRKY53* expression can be used as a very early senescence marker, showing a strong increase at 4 weeks after sowing, when plants started to flower but no visible signs of senescence and no significant increase in *SAG12* and *SAG13* expression were observed (Figs 3, 4, 6A–C). *ANAC092* expression also increased with senescence initiation, but reached its maximum expression levels at later stages in senescent leaves (week 6; Fig. 6D), as previously determined by Balazadeh *et al.* (2008).

Some other SAGs involved in senescence-related processes were chosen to complete the overall picture. *ATG7* belongs to the autophagy-associated gene family, composed of 30 genes identified in yeast and *A. thaliana* (Bassham *et al.*, 2006). Extensive cell death and early yellowing have been shown in leaves of a number of *atg*-defective Arabidopsis mutants such as *apg7-1* (Doelling *et al.*, 2002), *atg5* (Sakuraba *et al.*, 2014), *apg9-1* (Hanaoka *et al.*, 2002), and *atg4a4b-1* (Yoshimoto *et al.*, 2004). *ATG7* encodes an E1 enzyme, which is a ubiquitin-like autophagy protein involved in intracellular protein degradation (Thompson and Vierstra, 2005). It has been shown to be required for proper nutrient recycling and senescence (Doelling *et al.*, 2002). The timing of *ATG7* expression might be a control point for autophagy activation in senescing leaf cells. Moreover, its expression is heavily enhanced in parallel with the breakdown of photosynthetic capacity during the reorganization phase (Breeze *et al.*, 2011). In our growth conditions, *ATG7* expression showed a slight initial up-regulation 5 weeks after sowing, indicating the first step of the degradative processes while photosynthetic capacity did not appear to be affected. The latter started to decline when *ATG7* expression was maximal (Figs 3C, 6E).

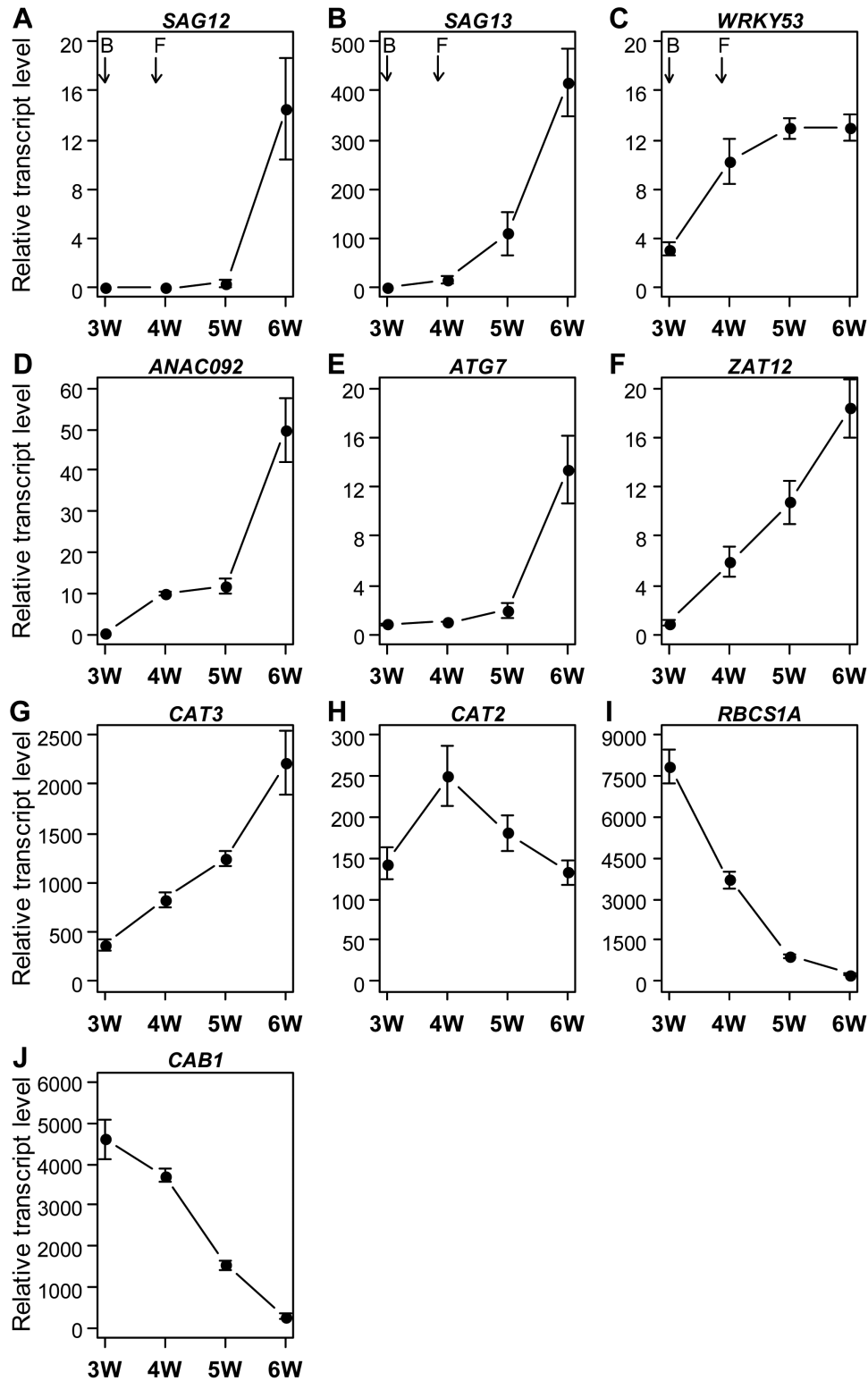


Fig. 6. Genetic regulation of senescence-related genes. qRT-PCR of different key markers in Col-0 leaves (positions 6 and 7) over 3–6 weeks after sowing: (A) *SAG12*, (B) *SAG13*, (C) *WRKY53*, (D) *ANAC092*, (E) *ATG7*, (F) *ZAT12*, (G) *CAT3*, (H) *CAT2*, (I) *RBCS1A*, and (J) *CAB1*. qRT-PCR was performed in two distinct pools by leaf position, each comprising six independent leaves. Transcriptional levels were calculated based on the comparative $\Delta\Delta C_T$ method and normalized to *ACTIN2* levels. Arrows indicate the bolting (B) and flowering (F) stages. Data are means (\pm SE) of four biological replicates with 1–2 technical replicates.

The TF *ZAT12* responds at transcript levels to a plethora of abiotic and biotic stresses and is notably involved in cold and oxidative stress signalling in *Arabidopsis* (Rizhsky et al., 2004b; Vogel et al., 2005). *ZAT12* might be related to leaf

senescence by its strong implication in ROS signal transduction (Miller et al., 2008). *ZAT12* expression is notably induced by H_2O_2 (Davletova et al., 2005), which accumulates in *A. thaliana* cells during senescence initiation at bolting

(Fig. 5A–C). In addition, during oxidative stress, *ZAT12* was shown to be required for *APX1* expression (Rizhsky *et al.*, 2004a). In our experiment, *ZAT12* transcript abundance showed a strong rise at very early stages (week 4), which is concomitant with an increase in H₂O₂ content at this time point. However, the *ZAT12* expression increased steadily during senescence progression, not following the H₂O₂ leaf content dynamics (Figs 5, 6F). Furthermore, *APX1* expression is also not induced during senescence progression (Panchuk *et al.*, 2005), indicating a more complex function of *ZAT12* in the senescence regulatory network.

CAT2 and *CAT3* also play a key role in H₂O₂ metabolism (Fig. 5A), as they catalyse the decomposition of H₂O₂ to water and oxygen without need of reducing equivalents (Du *et al.*, 2008). The Arabidopsis CAT family is a good example of a gene family containing SAGs as well as SDGs. While two members, *CAT3* and *CAT1*, are SAGs with different dynamics, *CAT2* belongs to the group of SDGs. Their role during leaf senescence is well documented (e.g. Orendi *et al.*, 2001; Zimmermann *et al.*, 2006). The development of senescence symptoms is correlated with modifications of CAT activities: *CAT2* activity decreases at an early stage during bolting, whereas *CAT3* activity increases with plant age (Zimmermann *et al.*, 2006). Consistent with this, *CAT3* expression started to increase with senescence initiation and reached maximal expression in senescent leaves. In contrast, *CAT2* is down-regulated during leaf senescence (Fig. 6G, H).

In contrast to SAGs, SDGs are not generally assumed to actively participate in the senescence regulatory network itself but instead they reflect a more general reduction of the leaf maintenance machinery. Interestingly, using multi-parallel qRT-PCR, Balazadeh *et al.* (2008) have found more TF genes being down-regulated than up-regulated during senescence. Here, we have chosen two key SDGs that are often used as senescence-markers and that reflect the breakdown of photosynthetic capacity (Table 1, Fig. 6I, J). The *RBCS1A* and *CABI* genes both have important roles in photosynthetic CO₂ fixation (Izumi *et al.*, 2012). Senescence-correlated losses in photosynthetic capacity are usually associated with alterations in their protein activities. Rubisco is a critical enzyme of the Calvin cycle and the most abundant chloroplast protein, comprising approximately 50% of soluble proteins (Wittenbach, 1978). Rubisco content changes greatly during a leaf's life span and is one of the proteins broken down early during senescence. Fragmentation of the Rubisco large subunits is notably induced by ROS (Desimone *et al.*, 1996). Rubisco is transported from chloroplasts to the vacuole by autophagy for degradation (Ishida *et al.*, 2008). It has been shown in wheat that the amount of Rubisco decreases rapidly in the early leaf senescence stages, although more slowly in the later stages (Mae *et al.*, 1984). Moreover, Rubisco subunits were found to be controlled at the translational levels during rice leaf senescence (Suzuki and Makino, 2013). Here, *RBCS1A* in Col-0 leaves showed a reduction of 50% of its transcript levels at 4 weeks after sowing, which appears to be early compared to the breakdown of photosynthetic capacity. Its expression then gradually decreased during senescence progression (Figs 3C, 6I). *CABI* belongs to the *LHC* gene

family and encodes for a subunit of the light-harvesting complex II (Green *et al.*, 1991). It has been shown that *LHCB* gene expression is tightly regulated by developmental cues as well as by multiple environmental signals, particularly including light or oxidative stresses (see references in Liu *et al.*, 2013). Decreased *CABI* expression is also associated with reduced photosynthetic activity as plants senesce (Li *et al.*, 2013). Fig. 6J shows that *CABI* presented a similar pattern to *RBCS1A*, but with a weaker decrease at 4 weeks after sowing.

All these markers acting in various key senescence-related processes give a global picture that includes the initiation, reorganization, and termination phases of leaf senescence. Moreover, they do not act individually but in a complex network with many possible interconnections.

Membrane integrity

During senescence, the membrane undergoes biochemical and biophysical changes leading to the final collapse of the cell. The plasma membrane of senescing cells becomes fragile and permeable. Membrane proteins and lipids are oxidized and degraded. This leads to dramatic modifications in lipid composition and a decrease in solute retention (Dhindsa *et al.*, 1981). We suggest estimating cell membrane integrity during senescence through measurements of EL and lipid peroxidation. EL is a well-established method to analyse disruption of cell membranes manifested by the leaking of solutes out of leaves that occurs under various stresses (e.g. Debrunner and Feller, 1995; Campos *et al.*, 2003) or ageing (e.g. Rolny *et al.*, 2011). An increase of EL reflects an extensive disruption of plasma membranes during leaf senescence (Lim *et al.*, 2007). During the reorganization phase, although cell membranes exhibit no massive degradation, EL can also increase due to the accumulation of leaf ammonium resulting from protein degradation (Rolny *et al.*, 2011). Slower increases in EL indicate a delayed senescence phenotype, as shown for example in *ore1* mutants affected in ageing-induced cell death (Kim *et al.*, 2009). EL is often quantified in detached leaves by measuring conductivity of a bathing solution (e.g. Saltveit, 2002; Campos *et al.*, 2003; Rolny *et al.*, 2011). Here, we present senescence-induced effects on EL for single detached leaves of Col-0 measured by a conductivity meter (CM100-2, Reid & Associates, Durban, South Africa; Fig. 7A, B). Leaves were first washed in deionized water to remove solutes from the surface. The conductivity of the bathing solution (deionized water) was measured every hour for 20 h. The slope of a fitted linear curve was then used to quantify the EL velocity, which can be normalized by leaf FW or area (see Supplementary Protocol S7). EL expressed by FW showed an initial increase during senescence initiation at flowering (week 4), which also coincides with the first increase in H₂O₂ content (Figs 5B, 7A). EL then showed a slight but still constant increase during the reorganization phase (weeks 5–6) and a strong peak in fully senescent leaves in the termination phase (week 7), which reflects cell death (Fig. 7A).

Lipid peroxidation can also be used as an indicator of membrane deterioration during senescence (Dhindsa *et al.*, 1981; Ahmad and Tahir, 2016). Lipid peroxidation is the

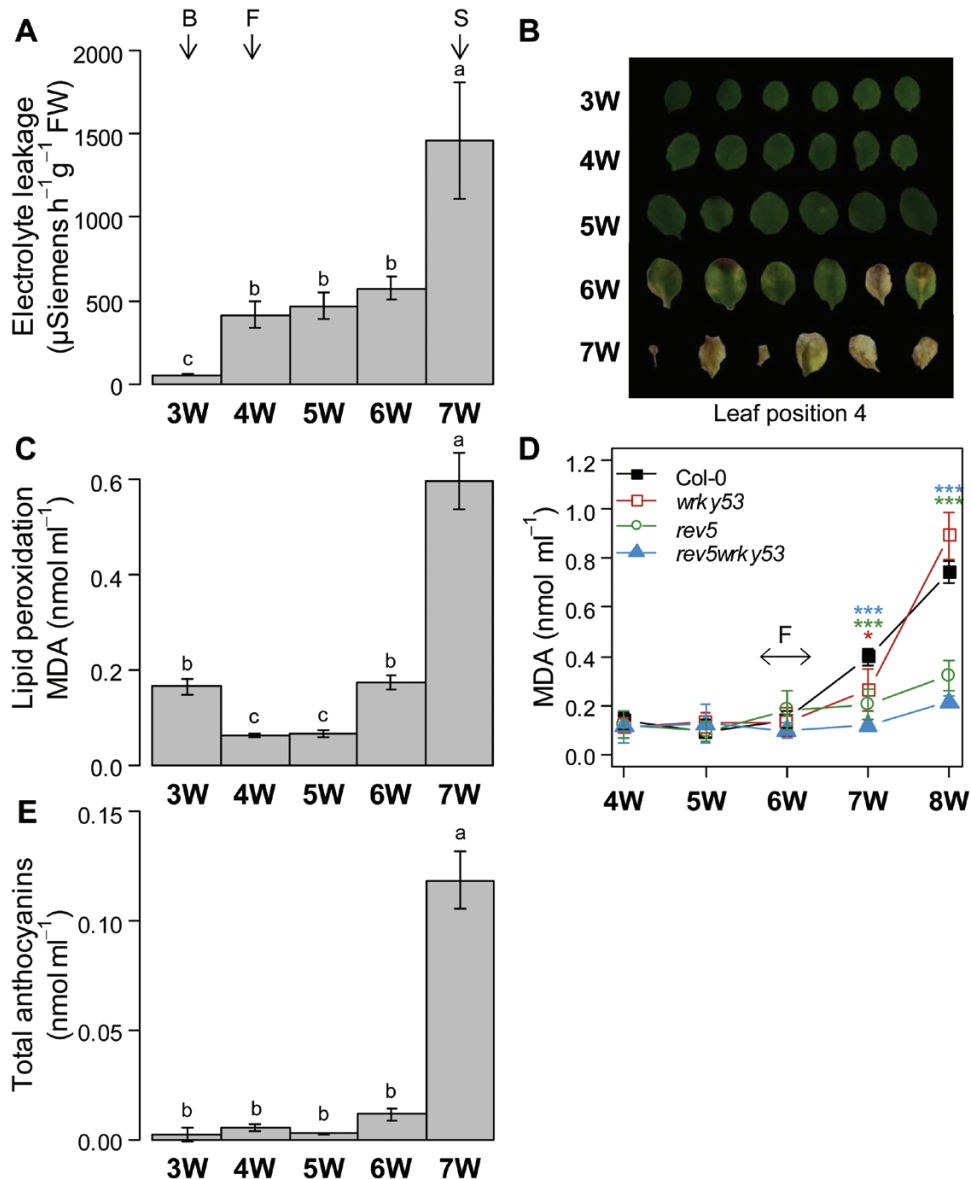


Fig. 7. Loss of membrane integrity during leaf senescence. (A) Electrolyte leakage (EL) in Col-0 leaves over 3–7 weeks after sowing. EL was measured in single detached leaves (position 4) using a conductivity meter (CM100-2, Reid & Associates, Durban, South Africa) and normalized to leaf fresh weight (FW). Data are means (\pm SE) of 12 leaves. (B) A representative picture of leaves used for EL. (C) Lipid peroxidation in Col-0 leaves over 3–7 weeks after sowing. Lipid peroxidation was measured using two distinct pools each of six independent leaves (position 9). Data are means (\pm SE) of two biological and two technical replicates. Different letters indicate significant differences according to the Kruskal–Wallis test at $P \leq 0.05$. (D) Example of lipid peroxidation measurements in knockout mutants delayed in senescence (*wrky53*, *rev5*, and *rev5wrky53*) according to Xie *et al.* (2014). Data are means (\pm SD) of at least three biological replicates. Comparison of means and determination of statistical differences was carried out using Student's *t*-test ($*P \leq 0.05$, $**P \leq 0.005$, and $***P \leq 0.0005$). (E) Total anthocyanin content in Col-0 leaves over 3–7 weeks after sowing, measured during lipid peroxidation determination. Arrows in (A, C–E) indicate bolting (B), flowering (F), and first yellowish siliques (S) stages.

consequence of the oxidative degradation of polyunsaturated fatty acids, through auto-oxidation or ROS, occurring during ageing. This induces the production of a large variety of oxidation products such as malondialdehyde (MDA), propanal, hexanal, and 4-hydroxynonenal (Ayala *et al.*, 2014). MDA concentration is one of the most widespread and reliable markers of lipid peroxidation in plant tissues (Del Rio *et al.*, 2005). Here, we utilized an improved thiobarbituric acid-reactive-substances assay (TBARS) developed by Hodges *et al.* (1999). This method is based on spectrophotometric measurement of a pinkish-red adduct between MDA and two molecules of TBA with a maximum absorbance at 532 nm

(Janero, 1990; Hodges *et al.*, 1999). Certain compounds, such as anthocyanin and carbohydrates, may interfere with the measurements at this wavelength and thus could lead to an over-estimation of MDA levels. To estimate and correct for the interference of non TBA-complexes, another reaction with the same plant extracts but without TBA is used and the values are subtracted from the corresponding reaction containing TBA. Total anthocyanin levels are determined as the difference between absorbance at 532 and 600 nm (Hodges and Nozzolillo, 1995), which is also used as a physiological parameter of senescence progression. Furthermore, in addition to lipid peroxides, sugars can also bind to TBA,

and therefore a further measurement at 440 nm is made. The MDA concentration is then corrected using these three measurements according to Hodges *et al.* (1999). For senescence analyses, corrections for interfering compounds are indispensable as plants can accumulate anthocyanin and sugars in their leaves during senescence. Normalization of MDA levels is not normally necessary as the same amount of sample is used for extraction (see Supplementary Protocol S8). If this is not the case, normalization to allow for differing amounts of sample is still possible. Here, MDA levels measured in Col-0 leaves showed a global increase over the time course, which was highly correlated with increased EL (Fig. 7A, C; $R^2=0.81$; $P\leq 0.001$). This illustrated the age-dependent degradation of cell membranes, which showed a progressive loss of integrity from flowering until irreversible and fatal damage occurred in fully senescent leaves during the termination phase. As an example, we have compared Col-0 plants to *wrky53*, *rev5*, and *wrky53rev5* mutants that are delayed in senescence. Lipid peroxidation showed an accelerated increase in Col-0 leaves at 7 weeks after sowing compared to the mutants. As shown for the results for F_v/F_m and ACA, *wrky53* recovered to Col-0 values in the termination phase of senescence (Figs 3D, 4C, 7D; Xie *et al.*, 2014). Interestingly, it could be shown that levels of lipid peroxidation were related to levels of senescence (via Chl content) in the different mutants (Xie *et al.*, 2014). As for lipid peroxidation, total anthocyanin levels started to increase in week 6 and reached very high levels during the terminal phase in week 7. This also correlated with the results obtained from the ACA (Figs 4, 7E).

Conclusion and perspectives

This paper proposes a guideline for analysing senescence in a dynamic manner using different early and late markers in key senescence-related processes involved during the initiation, reorganization, and termination phases. We provide a novel simple and automated quantification of leaf senescence, which also allows the quantification of anthocyanin in senescing leaves. We did not want to make an exhaustive list of all the methods that exist, but rather give a simple directive for starting analysis of different plants and/or abiotic and biotic stresses, which could affect leaf senescence. This can serve as a basis for identifying senescence-associated genes as well as natural diversity that can then be extended to a deeper analysis to answer specific questions depending on the study. For example, amongst the different key markers, hormone and sugar signalling can be investigated for senescence analyses.

We also wanted to emphasize that a clear distinction must be made between plant development and the onset or progression of leaf senescence. Bolting/flowering time (and by extension stem length) is often considered as a marker of the onset of senescence in annual plants; however, although senescence usually starts at bolting, it is not correlated to the progression of senescence across leaves. For instance, Koornneef *et al.* (1991) have shown that two *A. thaliana* mutants (*co-2* and *fca*) exhibit a delay in flowering but have a normal progression of

leaf senescence. This clearly illustrates that leaf senescence and reproductive development should be considered as dissectible processes.

All the methods presented here were described for Arabidopsis but can easily be adapted to other plant species, for example as already shown for oilseed rape (Bieker *et al.*, 2012). As senescence is an important trait in agriculture, analysing senescence in crop plants is already a significant issue and will become more and more important. Therefore, a detailed analysis as described here but applied to crop plants showing altered senescence will lead to a better understanding as to which part of the senescence program is actually affected by specific genome changes. This would give early hints on whether the modifications in senescence might interfere with yield stability and stress resistance of high-performance crop plant lines.

Supplementary Data

Supplementary data are available at JXB online.

Table S1. Composition of the soil used in our experiments.

Fig. S1. F_v/F_m rosette patterns of Col-0 and of the delayed-senescence mutant *rev5* over the course of plant development.

Fig. S2. Automated colourimetric assays in different experiments with varying light conditions.

Fig. S3. Hydrogen peroxide content in the delayed-senescence mutant *wrky53* over the course of plant development.

Fig. S4. Activity zymograms for catalases and ascorbate peroxidase over the course of development.

Protocol S1. Chlorophyll extraction.

Protocol S2. Chlorophyll fluorescence imaging.

Protocol S3. Automated colourimetric assay.

Protocol S4. Hydrogen peroxide measurement.

Protocol S5. Anti-oxidative enzyme activities.

Protocol S6. Quantitative real-time polymerase chain reaction (qRT-PCR).

Protocol S7. Electrolyte leakage.

Protocol S8. Lipid peroxidation.

Acknowledgments

We thank Gesine Seibold and Manuela Freund for their technical support. We also thank François Vasseur for comments on previous versions of the present paper. The authors' research was supported by grants from the Deutsche Forschungsgemeinschaft (FOR948 ZE 313/8-2, ZE 313/9-1, and the CRC1101, B06). JB was funded by the Alexander von Humboldt Foundation.

References

- Agüera E, Cabello P, de la Haba P. 2010. Induction of leaf senescence by low nitrogen nutrition in sunflower (*Helianthus annuus*) plants. *Physiologia Plantarum* **138**, 256–267.
- Ahmad SS, Tahir I. 2016. Increased oxidative stress, lipid peroxidation and protein degradation trigger senescence in *Iris versicolor* L. flowers. *Physiology and Molecular Biology of Plants* **22**, 507–514.
- Arnon DI. 1949. Copper enzymes in isolated chloroplasts. polyphenoloxidase in *Beta vulgaris*. *Plant Physiology* **24**, 1–15.
- Ayala A, Muñoz MF, Argüelles S. 2014. Lipid peroxidation: production, metabolism, and signaling mechanisms of malondialdehyde and

4-hydroxy-2-nonenal. *Oxidative Medicine and Cellular Longevity* **2014**, 360438.

Balazadeh S, Kwasniewski M, Caldana C, Mehrnia M, Zanon MI, Xue GP, Mueller-Roeber B. 2011. ORS1, an H₂O₂-responsive NAC transcription factor, controls senescence in *Arabidopsis thaliana*. *Molecular Plant* **4**, 346–360.

Balazadeh S, Riaño-Pachón DM, Mueller-Roeber B. 2008. Transcription factors regulating leaf senescence in *Arabidopsis thaliana*. *Plant Biology* **10**(Suppl 1), 63–75.

Balazadeh S, Siddiqui H, Allu AD, Matallana-Ramirez LP, Caldana C, Mehrnia M, Zanon MI, Köhler B, Mueller-Roeber B. 2010. A gene regulatory network controlled by the NAC transcription factor ANAC092/AtNAC2/ORE1 during salt-promoted senescence. *The Plant Journal* **62**, 250–264.

Barth C, Moeder W, Klessig DF, Conklin PL. 2004. The timing of senescence and response to pathogens is altered in the ascorbate-deficient *Arabidopsis* mutant *vitamin c-1*. *Plant Physiology* **134**, 1784–1792.

Bassham DC, Laporte M, Marty F, Moriyasu Y, Ohsumi Y, Olsen LJ, Yoshimoto K. 2006. Autophagy in development and stress responses of plants. *Autophagy* **2**, 2–11.

Belousov VV, Fradkov AF, Lukyanov KA, Staroverov DB, Shakhbazov KS, Terskikh AV, Lukyanov S. 2006. Genetically encoded fluorescent indicator for intracellular hydrogen peroxide. *Nature Methods* **3**, 281–286.

Bieker S, Riestler L, Stahl M, Franzaring J, Zentgraf U. 2012. Senescence-specific alteration of hydrogen peroxide levels in *Arabidopsis thaliana* and oilseed rape spring variety *Brassica napus* L. cv. Mozart. *Journal of Integrative Plant Biology* **54**, 540–554.

Biswal U, Biswal B. 1984. Photocontrol of leaf senescence. *Photochemistry and Photobiology* **39**, 875–879.

Breeze E, Harrison E, McHattie S, et al. 2011. High-resolution temporal profiling of transcripts during *Arabidopsis* leaf senescence reveals a distinct chronology of processes and regulation. *The Plant Cell* **23**, 873–894.

Bresson J, Vasseur F, Dauzat M, Koch G, Granier C, Vile D. 2015. Quantifying spatial heterogeneity of chlorophyll fluorescence during plant growth and in response to water stress. *Plant Methods* **11**, 23.

Buchanan-Wollaston V, Earl S, Harrison E, Mathas E, Navabpour S, Page T, Pink D. 2003. The molecular analysis of leaf senescence—a genomics approach. *Plant Biotechnology Journal* **1**, 3–22.

Buchanan-Wollaston V, Page T, Harrison E, et al. 2005. Comparative transcriptome analysis reveals significant differences in gene expression and signalling pathways between developmental and dark/starvation-induced senescence in *Arabidopsis*. *The Plant Journal* **42**, 567–585.

Campos PS, Quartín V, Ramalho JC, Nunes MA. 2003. Electrolyte leakage and lipid degradation account for cold sensitivity in leaves of *Coffea* sp. plants. *Journal of Plant Physiology* **160**, 283–292.

Carrión CA, Costa ML, Martínez DE, Mohr C, Humbeck K, Guamet JJ. 2013. *In vivo* inhibition of cysteine proteases provides evidence for the involvement of ‘senescence-associated vacuoles’ in chloroplast protein degradation during dark-induced senescence of tobacco leaves. *Journal of Experimental Botany* **64**, 4967–4980.

Cathcart R, Schwiers E, Ames BN. 1983. Detection of picomole levels of hydroperoxides using a fluorescent dichlorofluorescein assay. *Analytical Biochemistry* **134**, 111–116.

Costa A, Drago I, Behera S, Zottini M, Pizzo P, Schroeder JI, Pozzan T, Lo Schiavo F. 2010. H₂O₂ in plant peroxisomes: an *in vivo* analysis uncovers a Ca²⁺-dependent scavenging system. *The Plant Journal* **62**, 760–772.

Daudi A, O’Brien JA. 2012. Detection of hydrogen peroxide by DAB staining in *Arabidopsis* leaves. *Bio-protocol* **2**, e263.

Davletova S, Schlauch K, Coutu J, Mittler R. 2005. The zinc-finger protein Zat12 plays a central role in reactive oxygen and abiotic stress signaling in *Arabidopsis*. *Plant Physiology* **139**, 847–856.

Debrunner N, Feller U. 1995. Solute leakage from detached plant parts of winter wheat: influence of maturation stage and incubation temperature. *Journal of Plant Physiology* **145**, 257–260.

Del Rio D, Stewart AJ, Pellegrini N. 2005. A review of recent studies on malondialdehyde as toxic molecule and biological marker of oxidative stress. *Nutrition, Metabolism, and Cardiovascular Diseases* **15**, 316–328.

Desimone M, Henke A, Wagner E. 1996. Oxidative stress induces partial degradation of the large subunit of ribulose-1,5-bisphosphate carboxylase/oxygenase in isolated chloroplasts of barley. *Plant Physiology* **111**, 789–796.

Dhindsa RS, Plumb-Dhindsa P, Thorpe TA. 1981. Leaf senescence: correlated with increased levels of membrane permeability and lipid peroxidation, and decreased levels of superoxide dismutase and catalase. *Journal of Experimental Botany* **32**, 93–101.

Díaz-Mendoza M, Velasco-Arroyo B, Santamaria ME, González-Melendi P, Martínez M, Díaz I. 2016. Plant senescence and proteolysis: two processes with one destiny. *Genetics and Molecular Biology* **39**, 329–338.

Doelling JH, Walker JM, Friedman EM, Thompson AR, Vierstra RD. 2002. The APG8/12-activating enzyme APG7 is required for proper nutrient recycling and senescence in *Arabidopsis thaliana*. *The Journal of Biological Chemistry* **277**, 33105–33114.

Du YY, Wang PC, Chen J, Song CP. 2008. Comprehensive functional analysis of the catalase gene family in *Arabidopsis thaliana*. *Journal of Integrative Plant Biology* **50**, 1318–1326.

Filipovic A, Poljak M, Skobic D. 2013. Response of chlorophyll *a*, SPAD values and chlorophyll fluorescence parameters in leaves of apricot affected some abiotic factors. *Journal of Food Science and Engineering* **3**, 19.

Gan S. 1995. Molecular characterization and genetic manipulation of plant senescence. Doctoral dissertation, Madison: University of Wisconsin.

Garapati P, Xue GP, Munné-Bosch S, Balazadeh S. 2015. Transcription factor ATAF1 in *Arabidopsis* promotes senescence by direct regulation of key chloroplast maintenance and senescence transcriptional cascades. *Plant Physiology* **168**, 1122–1139.

Genty B, Briantais J-M, Baker NR. 1989. The relationship between the quantum yield of photosynthetic electron transport and quenching of chlorophyll fluorescence. *Biochimica et Biophysica Acta (BBA) - General Subjects* **990**, 87–92.

Gombert J, Etienne P, Ourry A, Le Dily F. 2006. The expression patterns of *SAG12/Cab* genes reveal the spatial and temporal progression of leaf senescence in *Brassica napus* L. with sensitivity to the environment. *Journal of Experimental Botany* **57**, 1949–1956.

Green BR, Pichersky E, Klopstech K. 1991. Chlorophyll *a/b*-binding proteins: an extended family. *Trends in Biochemical Sciences* **16**, 181–186.

Guo Y, Cai Z, Gan S. 2004. Transcriptome of *Arabidopsis* leaf senescence. *Plant, Cell & Environment* **27**, 521–549.

Guo Y, Gan S. 2006. AtNAP, a NAC family transcription factor, has an important role in leaf senescence. *The Plant Journal* **46**, 601–612.

Hanaoka H, Noda T, Shirano Y, Kato T, Hayashi H, Shibata D, Tabata S, Ohsumi Y. 2002. Leaf senescence and starvation-induced chlorosis are accelerated by the disruption of an *Arabidopsis* autophagy gene. *Plant Physiology* **129**, 1181–1193.

He J, Giusti MM. 2010. Anthocyanins: natural colorants with health-promoting properties. *Annual Review of Food Science and Technology* **1**, 163–187.

He Y, Gan S. 2002. A gene encoding an acyl hydrolase is involved in leaf senescence in *Arabidopsis*. *The Plant Cell* **14**, 805–815.

Hensel LL, Grbić V, Baumgarten DA, Bleecker AB. 1993. Developmental and age-related processes that influence the longevity and senescence of photosynthetic tissues in *Arabidopsis*. *The Plant Cell* **5**, 553–564.

Hinderhofer K, Zentgraf U. 2001. Identification of a transcription factor specifically expressed at the onset of leaf senescence. *Planta* **213**, 469–473.

Hodges DM, DeLong JM, Forney CF, Prange RK. 1999. Improving the thiobarbituric acid-reactive-substances assay for estimating lipid peroxidation in plant tissues containing anthocyanin and other interfering compounds. *Planta* **207**, 604–611.

Hodges DM, Nozzolillo C. 1995. Anthocyanin and anthocyanoplast content of cruciferous seedlings subjected to mineral nutrient deficiencies. *Journal of Plant Physiology* **147**, 749–754.

Hoel BO, Solhaug KA. 1998. Effect of irradiance on chlorophyll estimation with the Minolta SPAD-502 leaf chlorophyll meter. *Annals of Botany* **82**, 389–392.

Ishida H, Yoshimoto K, Izumi M, Reisen D, Yano Y, Makino A, Ohsumi Y, Hanson MR, Mae T. 2008. Mobilization of rubisco and

- stroma-localized fluorescent proteins of chloroplasts to the vacuole by an *ATG* gene-dependent autophagic process. *Plant Physiology* **148**, 142–155.
- Ito H, Ohtsuka T, Tanaka A.** 1996. Conversion of chlorophyll *b* to chlorophyll *a* via 7-hydroxymethyl chlorophyll. *The Journal of Biological Chemistry* **271**, 1475–1479.
- Izumi M, Tsunoda H, Suzuki Y, Makino A, Ishida H.** 2012. *RBCS1A* and *RBCS3B*, two major members within the Arabidopsis *RBCS* multigene family, function to yield sufficient Rubisco content for leaf photosynthetic capacity. *Journal of Experimental Botany* **63**, 2159–2170.
- Janero DR.** 1990. Malondialdehyde and thiobarbituric acid-reactivity as diagnostic indices of lipid peroxidation and peroxidative tissue injury. *Free Radical Biology & Medicine* **9**, 515–540.
- Jansson S, Thomas H.** 2008. Senescence: developmental program or timetable? *New Phytologist* **179**, 575–579.
- Jenkins GI, Baker NR, Woolhouse HW.** 1981. Changes in chlorophyll content and organization during senescence of the primary leaves of *Phaseolus vulgaris* L. in relation to photosynthetic electron transport. *Journal of Experimental Botany* **32**, 1009–1020.
- Johansson E, Olsson O, Nyström T.** 2004. Progression and specificity of protein oxidation in the life cycle of *Arabidopsis thaliana*. *The Journal of Biological Chemistry* **279**, 22204–22208.
- Kim JH, Woo HR, Kim J, Lim PO, Lee IC, Choi SH, Hwang D, Nam HG.** 2009. Trifurcate feed-forward regulation of age-dependent cell death involving miR164 in Arabidopsis. *Science* **323**, 1053–1057.
- Koornneef M, Hanhart CJ, van der Veen JH.** 1991. A genetic and physiological analysis of late flowering mutants in *Arabidopsis thaliana*. *Molecular & General Genetics* **229**, 57–66.
- Krupinska K, Mulisch M, Hollmann J, Tokarz K, Zschiesche W, Kage H, Humbeck K, Bilger W.** 2012. An alternative strategy of dismantling of the chloroplasts during leaf senescence observed in a high-yield variety of barley. *Physiologia Plantarum* **144**, 189–200.
- Kuriyama H, Fukuda H.** 2002. Developmental programmed cell death in plants. *Current Opinion in Plant Biology* **5**, 568–573.
- Li Z, Peng J, Wen X, Guo H.** 2012. Gene network analysis and functional studies of senescence-associated genes reveal novel regulators of Arabidopsis leaf senescence. *Journal of Integrative Plant Biology* **54**, 526–539.
- Li Z, Peng J, Wen X, Guo H.** 2013. ETHYLENE-INSENSITIVE3 is a senescence-associated gene that accelerates age-dependent leaf senescence by directly repressing miR164 transcription in Arabidopsis. *The Plant Cell* **25**, 3311–3328.
- Lim PO, Kim HJ, Nam HG.** 2007. Leaf senescence. *Annual Review of Plant Biology* **58**, 115–136.
- Liu R, Xu Y-H, Jiang S-C, et al.** 2013. Light-harvesting chlorophyll *a/b*-binding proteins, positively involved in abscisic acid signalling, require a transcription repressor, WRKY40, to balance their function. *Journal of Experimental Botany* **64**, 5443–5456.
- Liu X, Li Z, Jiang Z, Zhao Y, Peng J, Jin J, Guo H, Luo J.** 2010. LSD: a leaf senescence database. *Nucleic Acids Research* **39**, D1103–D1107.
- Lohman KN, Gan S, John MC, Amasino RM.** 1994. Molecular analysis of natural leaf senescence in *Arabidopsis thaliana*. *Physiologia Plantarum* **92**, 322–328.
- Mae T, Kai N, Makino A, Ohira K.** 1984. Relation between ribulose biphosphate carboxylase content and chloroplast number in naturally senescing primary leaves of wheat. *Plant and Cell Physiology* **25**, 333–336.
- Malagoli P, Lainé P, Le Deunff E, Rossato L, Ney B, Ourry A.** 2004. Modeling nitrogen uptake in oilseed rape cv Capitol during a growth cycle using influx kinetics of root nitrate transport systems and field experimental data. *Plant Physiology* **134**, 388–400.
- Markwell J, Osterman JC, Mitchell JL.** 1995. Calibration of the Minolta SPAD-502 leaf chlorophyll meter. *Photosynthesis Research* **46**, 467–472.
- Masclaux-Daubresse C, Daniel-Vedele F, Dechorgnat J, Chardon F, Gaufichon L, Suzuki A.** 2010. Nitrogen uptake, assimilation and remobilization in plants: challenges for sustainable and productive agriculture. *Annals of Botany* **105**, 1141–1157.
- Maunder MJ, Brown SB.** 1983. The effect of light on chlorophyll loss in senescing leaves of sycamore (*Acer pseudoplatanus* L.). *Planta* **158**, 309–311.
- Maxwell K, Johnson GN.** 2000. Chlorophyll fluorescence—a practical guide. *Journal of Experimental Botany* **51**, 659–668.
- Miao Y, Laun T, Zimmermann P, Zentgraf U.** 2004. Targets of the WRKY53 transcription factor and its role during leaf senescence in Arabidopsis. *Plant Molecular Biology* **55**, 853–867.
- Miao Y, Zentgraf U.** 2010. A HECT E3 ubiquitin ligase negatively regulates Arabidopsis leaf senescence through degradation of the transcription factor WRKY53. *The Plant Journal* **63**, 179–188.
- Miller G, Shulaev V, Mittler R.** 2008. Reactive oxygen signaling and abiotic stress. *Physiologia Plantarum* **133**, 481–489.
- Mittler R, Vanderauwera S, Gollery M, Van Breusegem F.** 2004. Reactive oxygen gene network of plants. *Trends in Plant Science* **9**, 490–498.
- Murchie EH, Lawson T.** 2013. Chlorophyll fluorescence analysis: a guide to good practice and understanding some new applications. *Journal of Experimental Botany* **64**, 3983–3998.
- Noh YS, Amasino RM.** 1999. Identification of a promoter region responsible for the senescence-specific expression of SAG12. *Plant Molecular Biology* **41**, 181–194.
- Nooden LD, Hillsberg JW, Schneider MJ.** 1996. Induction of leaf senescence in *Arabidopsis thaliana* by long days through a light-dosage effect. *Physiologia Plantarum* **96**, 491–495.
- Novichonok E, Novichonok A, Kurbatova J, Markovskaya E.** 2016. Use of the atLEAF+ chlorophyll meter for a nondestructive estimate of chlorophyll content. *Photosynthetica* **54**, 130–137.
- Ondzighi CA, Christopher DA, Cho EJ, Chang SC, Staehelin LA.** 2008. Arabidopsis protein disulfide isomerase-5 inhibits cysteine proteases during trafficking to vacuoles before programmed cell death of the endothelium in developing seeds. *The Plant Cell* **20**, 2205–2220.
- Orendi G, Zimmermann P, Baar C, Zentgraf U.** 2001. Loss of stress-induced expression of *catalase3* during leaf senescence in *Arabidopsis thaliana* is restricted to oxidative stress. *Plant Science* **161**, 301–314.
- Otegui MS, Noh YS, Martínez DE, Vila Petroff MG, Staehelin LA, Amasino RM, Guimmet JJ.** 2005. Senescence-associated vacuoles with intense proteolytic activity develop in leaves of Arabidopsis and soybean. *The Plant Journal* **41**, 831–844.
- Panchuk II, Zentgraf U, Volkov RA.** 2005. Expression of the *Apx* gene family during leaf senescence of *Arabidopsis thaliana*. *Planta* **222**, 926–932.
- Pfaffl MW.** 2001. A new mathematical model for relative quantification in real-time RT-PCR. *Nucleic Acids Research* **29**, e45.
- Pruzinska A, Tanner G, Aubry S, et al.** 2005. Chlorophyll breakdown in senescent Arabidopsis leaves. Characterization of chlorophyll catabolites and of chlorophyll catabolic enzymes involved in the degreening reaction. *Plant Physiology* **139**, 52–63.
- R Development Core Team.** 2009. *R: a language and environment for statistical computing*. Vienna, Austria: R Foundation for Statistical Computing, www.r-project.org.
- Rizhsky L, Davletova S, Liang H, Mittler R.** 2004a. The zinc finger protein Zat12 is required for cytosolic ascorbate peroxidase 1 expression during oxidative stress in Arabidopsis. *The Journal of Biological Chemistry* **279**, 11736–11743.
- Rizhsky L, Liang H, Shuman J, Shulaev V, Davletova S, Mittler R.** 2004b. When defense pathways collide. The response of Arabidopsis to a combination of drought and heat stress. *Plant Physiology* **134**, 1683–1696.
- Rolny N, Costa L, Carrión C, Guimmet JJ.** 2011. Is the electrolyte leakage assay an unequivocal test of membrane deterioration during leaf senescence? *Plant Physiology and Biochemistry* **49**, 1220–1227.
- Sakuraba Y, Balazadeh S, Tanaka R, Mueller-Roeber B, Tanaka A.** 2012. Overproduction of Chl *b* retards senescence through transcriptional reprogramming in Arabidopsis. *Plant & Cell Physiology* **53**, 505–517.
- Sakuraba Y, Lee SH, Kim YS, Park OK, Hörtensteiner S, Paek NC.** 2014. Delayed degradation of chlorophylls and photosynthetic proteins in Arabidopsis autophagy mutants during stress-induced leaf yellowing. *Journal of Experimental Botany* **65**, 3915–3925.
- Saltveit ME.** 2002. The rate of ion leakage from chilling-sensitive tissue does not immediately increase upon exposure to chilling temperatures. *Postharvest Biology and Technology* **26**, 295–304.

- Steynen QJ, Bolokoski DA, Schultz EA.** 2001. Alteration in flowering time causes accelerated or decelerated progression through *Arabidopsis* vegetative phases. *Canadian Journal of Botany* **79**, 657–665.
- Suzuki Y, Makino A.** 2013. Translational downregulation of RBCL is operative in the coordinated expression of Rubisco genes in senescent leaves in rice. *Journal of Experimental Botany* **64**, 1145–1152.
- Tanaka A, Tanaka R.** 2006. Chlorophyll metabolism. *Current Opinion in Plant Biology* **9**, 248–255.
- Thomas H.** 2013. Senescence, ageing and death of the whole plant. *New Phytologist* **197**, 696–711.
- Thompson AR, Vierstra RD.** 2005. Autophagic recycling: lessons from yeast help define the process in plants. *Current Opinion in Plant Biology* **8**, 165–173.
- Uddling J, Gelang-Alfredsson J, Piikki K, Pleijel H.** 2007. Evaluating the relationship between leaf chlorophyll concentration and SPAD-502 chlorophyll meter readings. *Photosynthesis Research* **91**, 37–46.
- Vasseur F, Pantin F, Vile D.** 2011. Changes in light intensity reveal a major role for carbon balance in *Arabidopsis* responses to high temperature. *Plant, Cell & Environment* **34**, 1563–1576.
- Vogel JT, Zarka DG, Van Buskirk HA, Fowler SG, Thomashow MF.** 2005. Roles of the CBF2 and ZAT12 transcription factors in configuring the low temperature transcriptome of *Arabidopsis*. *The Plant Journal* **41**, 195–211.
- Weaver LM, Gan S, Quirino B, Amasino RM.** 1998. A comparison of the expression patterns of several senescence-associated genes in response to stress and hormone treatment. *Plant Molecular Biology* **37**, 455–469.
- Wittenbach VA.** 1978. Breakdown of ribulose biphosphate carboxylase and change in proteolytic activity during dark-induced senescence of wheat seedlings. *Plant Physiology* **62**, 604–608.
- Woo NS, Badger MR, Pogson BJ.** 2008. A rapid, non-invasive procedure for quantitative assessment of drought survival using chlorophyll fluorescence. *Plant Methods* **4**, 27.
- Wu A, Allu AD, Garapati P, et al.** 2012. JUNGBRUNNEN1, a reactive oxygen species-responsive NAC transcription factor, regulates longevity in *Arabidopsis*. *The Plant Cell* **24**, 482–506.
- Xie Y, Huhn K, Brandt R, et al.** 2014. REVOLUTA and WRKY53 connect early and late leaf development in *Arabidopsis*. *Development* **141**, 4772–4783.
- Ye Z, Rodriguez R, Tran A, Hoang H, de los Santos D, Brown S, Vellanoweth RL.** 2000. The developmental transition to flowering represses ascorbate peroxidase activity and induces enzymatic lipid peroxidation in leaf tissue in *Arabidopsis thaliana*. *Plant Science* **158**, 115–127.
- Yoshimoto K, Hanaoka H, Sato S, Kato T, Tabata S, Noda T, Ohsumi Y.** 2004. Processing of ATG8s, ubiquitin-like proteins, and their deconjugation by ATG4s are essential for plant autophagy. *The Plant Cell* **16**, 2967–2983.
- Zentgraf U, Jobst J, Kolb D, Rentsch D.** 2004. Senescence-related gene expression profiles of rosette leaves of *Arabidopsis thaliana*: leaf age versus plant age. *Plant Biology* **6**, 178–183.
- Zentgraf U, Laun T, Miao Y.** 2010. The complex regulation of WRKY53 during leaf senescence of *Arabidopsis thaliana*. *European Journal of Cell Biology* **89**, 133–137.
- Zentgraf U, Smykowski A, Zimmermann P.** 2012. Role of intracellular hydrogen peroxide as signalling molecule for plant senescence. In: Nagata T, ed. *Senescence*. Rijeka, Croatia: INTECH, 31–50, doi:10.5772/34576.
- Zimmermann P, Heinlein C, Orendi G, Zentgraf U.** 2006. Senescence-specific regulation of catalases in *Arabidopsis thaliana* (L.) Heynh. *Plant, Cell & Environment* **29**, 1049–1060.
- Zimmermann P, Zentgraf U.** 2005. The correlation between oxidative stress and leaf senescence during plant development. *Cellular & Molecular Biology Letters* **10**, 515–534.

A guideline for leaf senescence analyses: from senescence quantification to physiological and molecular investigations

Justine Bresson^{1†*}, Stefan Bieker^{1†}, Lena Riester^{1†}, Jasmin Doll^{1†} and Ulrike Zentgraf¹
¹ZMBP, General Genetics, University of Tübingen, Auf der Morgenstelle 32, 72076 Tübingen
[†]Equal contributors

Supplementary Figure S1

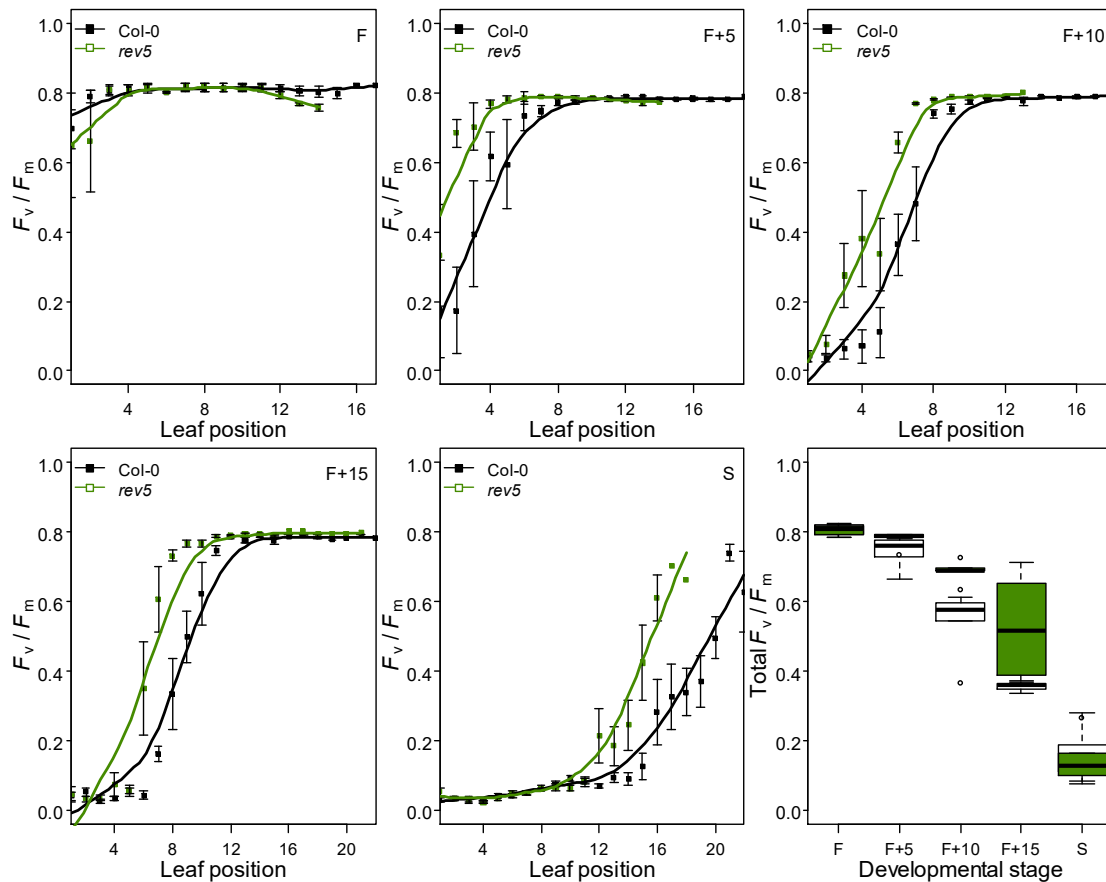


Fig. S1. F_v/F_m rosette patterns of Col-0 and of the delayed senescence mutant *rev5* over plant development. The five first panels present F_v/F_m values in the different leaves composing the rosette from flowering (F) until the first siliques started yellowing (S). F+5, F+10 and F+15 indicate days after flowering. Last panel shows the total F_v/F_m mean of the rosette during developmental stages (white boxes = Col-0 and green boxes = *rev5*). Data are means (\pm SE) of 6-8 plants.

Supplementary Figure S2

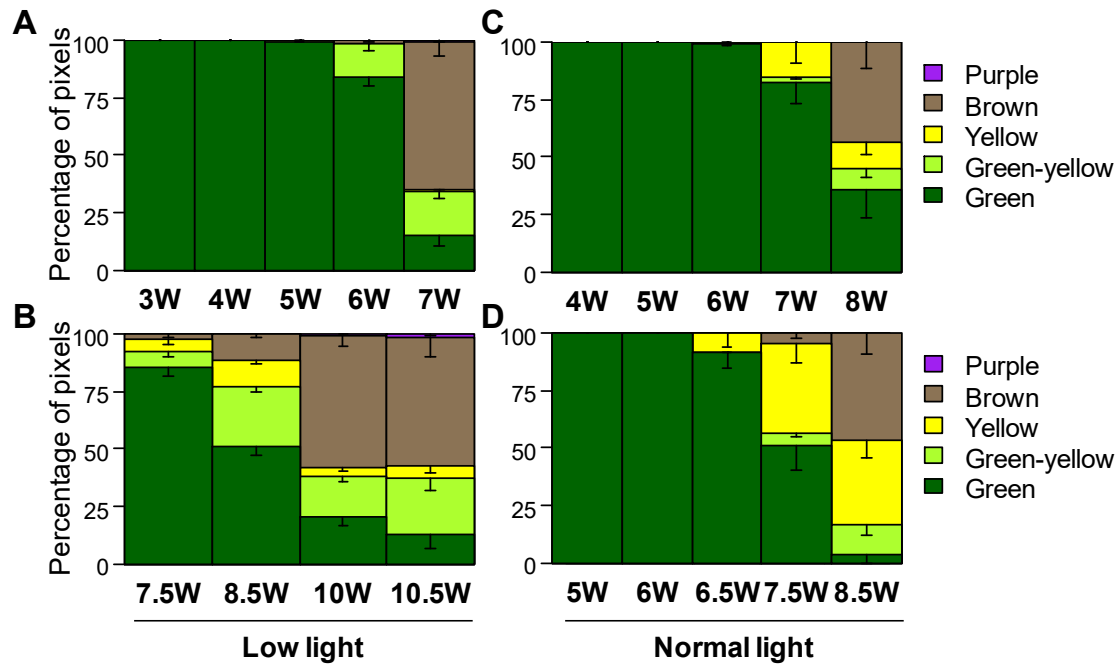


Fig. S2. Automated colourimetric assays (ACA) in different experiments depending on light conditions. ACA in Col-0 plants grew under long days and low light (A-B) ($\sim 70\text{-}80 \mu\text{E m}^{-2} \text{s}^{-1}$ at plant height) and normal light (C-D) ($\sim 120\text{-}140 \mu\text{E m}^{-2} \text{s}^{-1}$) conditions. ACA is analysed weekly after sowing. Colour classes are organised from top to bottom: purple, brown, yellow, green-yellow and green. Purple colours are related to anthocyanin production and not reflect the last stage of senescence progression (from green to brown). Data are means (\pm SE) of colour percentages calculated for each leaf composing the rosette of 4 (A), 5 (B), and 1 (C-D) plant(s).

Supplementary Figure S3

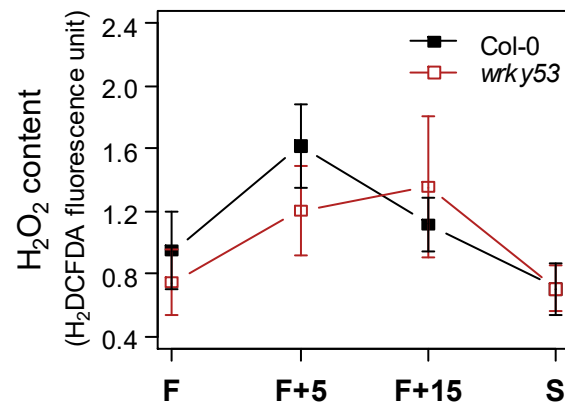


Fig. S3. Hydrogen peroxide (H₂O₂) content in the delayed senescence mutant *wrky53* over plant development starting with flowering (F) until first siliques yellowing (S). F+5 and F+15 indicate days after flowering. Data are means (\pm SE) of 5 plants.

Supplementary Figure S4

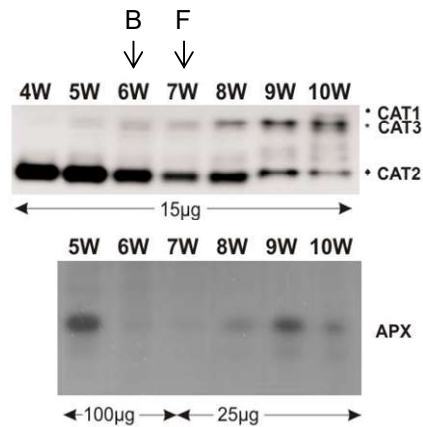


Fig. S4. Catalases (CAT; top) and Ascorbate Peroxidase (APX; bottom) activity zymograms over development of *A. thaliana*. CAT and APX activity staining after native PAGE modified after Zimmermann *et al.*, 2006. Plant age is indicated in weeks after sowing. Amount of loaded raw protein extracts are indicated below the lanes.

Live and Let Die: The Core Circadian Oscillator Coordinates Plant Life History and Pilots Leaf Senescence

For a long time, many scientists were keen on discovering “the master regulator” of plant senescence. However, in the last two decades, it became very clear that this “master regulator” does not exist, but an extremely complex regulatory network controls all aspects and phases of senescence. Temporal transcript profiling of a defined leaf of *Arabidopsis* with high resolution, which covered 22 time points during onset and progression of leaf senescence, revealed expression changes of more than 6500 genes and disclosed a distinct chronology of events (Breeze et al., 2011). Besides autophagy and transport, transcriptional response to reactive oxygen species (ROS), jasmonic acid (JA), and salicylic acid (SA) are activated at early time points. All three signaling molecules are also part of the stress responses to biotic as well as abiotic stresses, indicating a strong cross-talk between the senescence process and stress control. Incoming environmental signals are constantly integrated throughout life history and, if stress conditions produce long-term unfavorable conditions for the plant, premature senescence is initiated as an exit strategy to produce offspring. However, premature senescence often correlates with diminished seed quantity and quality.

As almost one fourth of the *Arabidopsis* genes change their expression during senescence, and transcription factors play a pivotal role in senescence regulation. Especially, the NAC and WRKY transcription factor families, which largely expanded during evolution of land plants, are overrepresented in the senescence transcriptomes, and many members of these families are part of the complex regulatory network, in many cases at hub positions. Nevertheless, members of all transcription factor families participate in the senescence regulatory network. Multi-layer feedback regulatory cues are in place to control senescence and transcriptional, post-transcriptional, post-translational regulatory mechanisms are realized for one and the same gene e.g., *WRKY53*. Moreover, we are just beginning to understand the dynamic changes in chromatin structure and nuclear architecture during senescence. Here also, multi-layer feedback regulation can be observed, and again the same players are involved. *WRKY53* expression, for example, is on the one hand activated by senescence-associated chromatin modifications (Ay et al., 2009), whereas, on the other hand, the *WRKY53* protein is part of the powerdress/HDA9 complex and directs chromatin modifications to promoters of senescence-regulating genes (Chen et al., 2016).

Moreover, early developmental processes are closely linked to leaf senescence so that a kind of “leaf developmental memory” appears to exist, meaning if early leaf development is perturbed, leaf senescence is affected. Evidence for this hypothesis is provided by detailed analyses of the transcription factor *REVOLUTA*

(*REV*), which is involved in early developmental processes such as establishment of leaf polarity, lateral meristem initiation, or vascular development and directly regulates the expression of the senescence-promoting transcription factors *WRKY53* in a redox-dependent manner during early senescence (Xie et al., 2014). More and more examples of this cross-talk between early and late leaf development have become apparent in recent years. Following the same lines of evidence, cell proliferation activity and leaf senescence are interconnected, as low cell proliferation activity is associated with accelerated leaf senescence and vice versa (for review, see Kim et al., 2018). This also points to the existence to a “leaf developmental memory”. Taken together, our current view on senescence regulation necessitates regulatory factors that co-ordinate not only environmental signals but also developmental events throughout the life history of a plant.

Very recently, Zhang et al. (2018) added a new piece to the puzzle. One good candidate for this coordinator function is the circadian clock. First, the circadian rhythm is affected by leaf age. The circadian periods of clock-regulated genes as well as the periods of the core clock genes are shorter in older leaves compared with young leaves and appear to be regulated through the clock oscillator *TOC1* (Kim et al., 2016). By the way, disruption of the circadian clock in animal systems can also affect senescence and age-related disorders. Second, Ezer et al. (2017) analyzed in detail that the circadian evening complex (EC) coordinates environmental and endogenous signals in *Arabidopsis*. Zhang et al. (2018) have disclosed a molecular mechanism how EC interferes with JA-induced leaf senescence in *Arabidopsis*. EC is a critical component of the core oscillator regulating circadian outputs and consists of three proteins: *EARLY FLOWERING3* (*ELF3*), *EARLY FLOWERING4* (*ELF4*), and *LUX ARRHYTHMO* (*LUX*). *LUX* is a GARP transcription factor mediating DNA-binding activity, while *ELF3* functions as an adaptor between *LUX* and *ELF4* to form a ternary transcriptional repression complex. Plants with mutations in the EC components all showed accelerated natural as well as more pronounced JA-induced leaf senescence. This indicates that the core component of the circadian clock, EC, negatively regulates senescence induction. In agreement, EC component overexpression led to stay-green phenotypes after JA treatment. Moreover, transcriptome analyses revealed that EC is involved in JA signaling and response reactions but also controls senescence regulators, such as *WRKY53* or *WRKY70* or the NAC factors *ORE1* or *NAP*. The EC component *LUX* directly interacts with the promoter of the *MYC2* transcription factor gene, which encodes a key

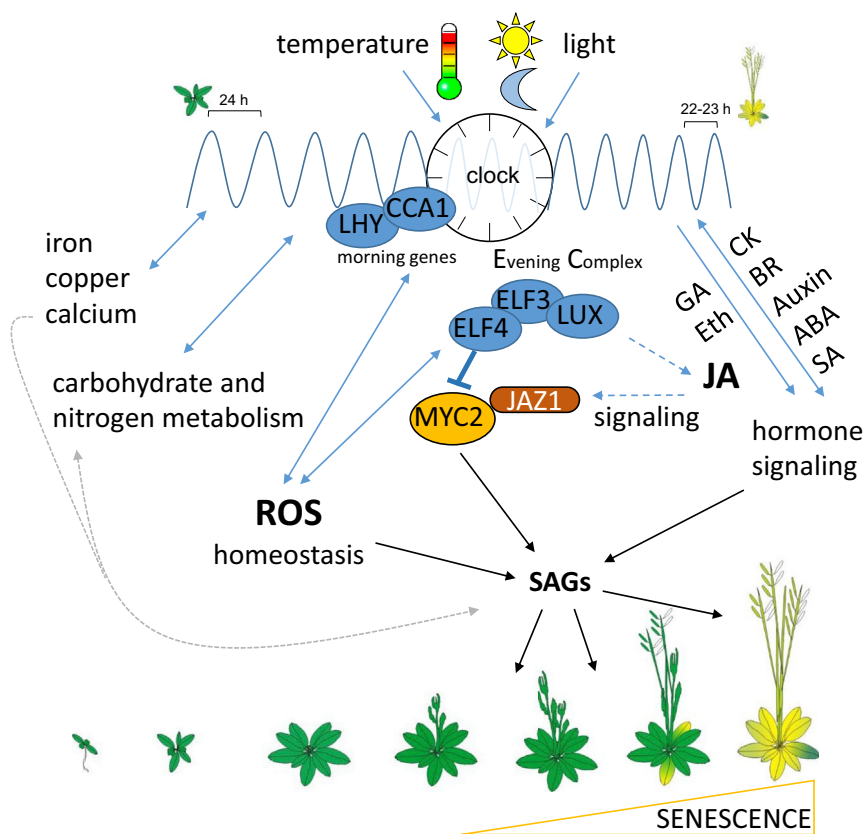


Figure 1. The Circadian Clock Shares Many Modulators with the Senescence Regulatory Network.

The central circadian oscillators are entrained by temperature and light, leading to diurnal rhythm of gene expression of a plethora of genes resulting in very diverse outputs. The period of the diurnal rhythm shortens from 24 h in young plants to 22–23 h in old plants (Kim et al., 2016). The central clock modulates carbohydrate and nitrogen metabolism, calcium, iron, and copper homeostasis as well as almost all hormone-signaling pathways. In turn, all metabolic processes involving these nutrients and hormones feed back to the core oscillator except GA, ethylene, and JA. Moreover, ROS homeostasis is triggered by CCA1 and EC (Lai et al., 2012). JA production as well as JA signaling is modulated by EC, in which JA production is reduced in EC mutants and LUX directly binds to the promoter of *MYC2* to repress its expression. In turn, *MYC2* regulates the expression of many SAGs. All actions related to the circadian clock are illustrated with blue arrows; black and gray arrows illustrate all actions related to senescence regulation; dashed lines indicate indirect effects. ABA, abscisic acid auxin; BR, brassinosteroids; CK, cytokinin; EC, evening complex; GA, gibberellin; JA, jasmonic acid; SA, salicylic acid; SAGs, senescence-associated genes.

activator of JA-induced leaf senescence, but not with the promoter of other JA signaling components such as *COI1* or *JAZ1*. LUX interaction with the *MYC2* promoter represses *MYC2* expression. When plants with mutations in the components of EC were crossed with the *myc2* mutant or the triple *myc2 myc3 myc4* mutant plants, the homozygous offspring abrogated the accelerated JA-induced leaf senescence observed in EC mutants. This confirms that a core component of the circadian clock controls JA signaling via MYC transcription factors to regulate leaf senescence. Moreover, all plants with mutations in the components of EC contained lower JA levels, suggesting further involvement of EC in JA production (Zhang et al., 2018). Remarkably, ELF3 can affect dark-induced leaf senescence also in an EC-independent manner. ELF3 and red light-activated phytochrome B can repress the senescence-promoting activity of PIF4/PIF5 at the transcriptional and the post-translational levels, respectively. These two PIFs activate the expression of *ORE1* through multiple feed-forward loops, thus connecting a clock component and the classical light signaling component to leaf senescence (Sakuraba et al., 2014).

Sanchez and Kay (2016) already entitled the circadian clock as the “mastermind” of plant life modulating a myriad of plant responses. Carbohydrate and nitrogen metabolism, calcium, iron, and copper as well as hormone homeostasis are modulated by the central clock but in turn, all these components feed back to the core oscillator except JA, gibberellic acid, and ethylene (for review see Sanchez and Kay, 2016). CCA1 was already disclosed as a master regulator of ROS homeostasis through association with

the EC in promoters of ROS-responsive genes *in vivo*; on the other hand, ROS also functions as an input signal that affects the transcriptional output of the clock (Lai et al., 2012). As carbohydrate and nitrogen metabolism, ROS as well as almost all hormone signaling pathways are also integral parts of the regulatory network of senescence, senescence and circadian regulatory circuits appear to have huge overlaps. Thus, plant senescence can definitely be added to the developmental steps governed by this pacemaker (Figure 1).

FUNDING

L.R. and J.D. were supported by the Deutsche Forschungsgemeinschaft (SFB1101, B06).

ACKNOWLEDGMENTS

We apologize for not being able to cite all relevant work due to space restrictions. No conflict of interest declared.

Received: January 29, 2018

Revised: February 9, 2018

Accepted: February 10, 2018

Published: February 16, 2018

Ulrike Zentgraf*, Jasmin Doll and Lena Riester

Centre of Molecular Biology of Plants (ZMBP), University of Tübingen, Auf der Morgenstelle 32, 72076 Tübingen, Germany

*Correspondence: Ulrike Zentgraf (ulrike.zentgraf@zmbp.uni-tuebingen.de)

<https://doi.org/10.1016/j.molp.2018.02.001>

REFERENCES

- Ay, N., Irmiler, K., Fischer, A., Uhlemann, R., Reuter, G., and Humbeck, K.** (2009). Epigenetic programming via histone methylation at *WRKY53* controls leaf senescence in *Arabidopsis thaliana*. *Plant J.* **58**:333–346.
- Breeze, E., Harrison, E., McHattie, S., Hughes, L., Hickman, R., Hill, C., Kiddle, S., Kim, Y.S., Penfold, C.A., Jenkins, D., et al.** (2011). High-resolution temporal profiling of transcripts during *Arabidopsis* leaf senescence reveals a distinct chronology of processes and regulation. *Plant Cell* **23**:873–894.
- Chen, X., Lu, L., Mayer, K.S., Scalf, M., Qian, S., Lomax, A., Smith, L.M., and Zhong, X.** (2016). POWERDRESS interacts with HISTONE DEACETYLASE 9 to promote aging in *Arabidopsis*. *Elife* **5**:e17214.
- Ezer, D., Jung, J.H., Lan, H., Biswas, S., Gregoire, L., Box, M.S., Charoensawan, V., Cortijo, S., Lai, X., Stöckle, D., et al.** (2017). The evening complex coordinates environmental and endogenous signals in *Arabidopsis*. *Nat. Plants* **3**:17087.
- Kim, H., Kim, Y., Yeom, M., Lim, J., and Nam, H.G.** (2016). Age-associated circadian period changes in *Arabidopsis* leaves. *J. Exp. Bot.* **67**:2665–2673.
- Kim, J., Kim, J.H., Lyu, J.I., Woo, H.R., and Lim, P.O.** (2018). New insights into the regulation of leaf senescence in *Arabidopsis*. *J. Exp. Bot.* **69**:787–799.
- Lai, A.G., Doherty, C.J., Mueller-Roeber, B., Kay, S.A., Schippers, J.H., and Dijkwel, P.P.** (2012). CIRCADIAN CLOCK-ASSOCIATED 1 regulates ROS homeostasis and oxidative stress responses. *Proc. Natl. Acad. Sci. USA* **109**:17129–17134.
- Sanchez, S.E., and Kay, S.A.** (2016). The plant circadian clock: from a simple timekeeper to a complex developmental manager. *Cold Spring Harb. Perspect. Biol.* **8**:a027748.
- Sakuraba, Y., Jeong, J., Kang, M.Y., Kim, J., Paek, N.C., and Choi, G.** (2014). Phytochrome-interacting transcription factors PIF4 and PIF5 induce leaf senescence in *Arabidopsis*. *Nat. Commun.* **5**:4636.
- Xie, Y., Huhn, K., Brandt, R., Potschin, M., Bieker, S., Straub, D., Doll, J., Drechsler, T., Zentgraf, U., and Wenkel, S.** (2014). REVOLUTA and WRKY53 connect early and late leaf development in *Arabidopsis*. *Development* **141**:4772–4783.
- Zhang, Y., Wang, Y., Wei, H., Li, N., Tian, W., Chong, K., and Wang, L.** (2018). Circadian evening complex represses jasmonate-induced leaf senescence in *Arabidopsis*. *Mol. Plant* **11**:326–337.